

**THE EFFECT OF OPENINGS ON THE CYCLIC BEHAVIOR  
OF REINFORCED CONCRETE INFILLED  
SHEAR WALLS**

**APPROVED:**

---

---

**To Mom and Dad**

**THE EFFECT OF OPENINGS ON THE CYCLIC BEHAVIOR  
OF REINFORCED CONCRETE INFILLED  
SHEAR WALLS**

by

Patricia Jean Gaynor, B.S.C.E

THESIS

Presented to the Faculty of the Graduate School of  
The University of Texas at Austin  
in Partial Fulfillment  
of the Requirements  
for the Degree of  
MASTER OF SCIENCE IN ENGINEERING

THE UNIVERSITY OF TEXAS AT AUSTIN

August 1988

## ACKNOWLEDGEMENTS

This research project was funded by National Science Foundation Grant ECE-8416147, "Strengthening of Reinforced Concrete Frame Structures." The author wishes to express her sincere gratitude to Dr. James O. Jirsa for his direction and counsel in all phases of this project. My personal and professional growth over the last two years are a direct product of my interaction with him. Special thanks go to Dr. Michael E. Kreger for providing advice and support at the neediest of times. Appreciation is also expressed for the contributions of Dr. Ramon Carrasquillo and Dr. Richard Klingner during the design phase. Thanks also go to Loring Wyllie, Jr. and David Bonneville of H. J. Degenkolb Associates, San Francisco, California, for their participation in the design and testing phases.

I would like to give special thanks to the members of the project team, Sanjeev Shah, Jorge Quiros, Larry Jimenez, Amador Teran and Enrique Martinez, without whose diligent efforts, the construction of this project would not have been possible. Thanks also go to Bob MacGregor and Richard Beaupre for their cooperation during construction and testing. Special thanks go to Gilson Guimares and David Hartmann for the laughs and encouragement and for the fine examples to follow.

Implementation of this project would not have been possible without the dedicated staff at Ferguson Lab. Special thanks go to Blake Stassney, Pat Ball, Robert Gracia, Laurie Golding, Alec Tahmessebi, Sharon Cunningham and Jean Gerkhe.

I would like to express my gratitude to Dr. Kyle A. Woodward for directing me to the University of Texas. A better choice could not have been made. Thanks also goes to David Yates for his patient instruction and significant contributions over the last two years. Finally, my accomplishments here and elsewhere are made possible by the love and support of my sister and brothers. Most of all, I owe it to Mom and Dad, who gave me the wings to fly.

Patti Gaynor  
May 1988  
Austin, Texas

## ABSTRACT

The response of reinforced concrete frames strengthened with infilled shear walls was investigated. Three one-bay, one-story reinforced concrete frames were constructed and retrofitted with shotcrete walls. One frame had no openings, the second had a door opening and the third had a window opening. The two-thirds scale specimens were subjected to in-plane, reversed lateral load to simulate the effects of earthquake ground motions. The frames represented a structure originally designed for lower lateral forces and less stringent detailing requirements.

The initial elastic stiffness of the retrofitted frames with openings was about 60% of the solid wall. In subsequent cycles, the stiffness of the specimen (measured at the peak of the cycle) with a window opening was consistently less than that of the specimen with a door. The strength of the full infill and the infill with a door were controlled by anchorage failure of splices of dowels at the base of the wall. In the full infill, failure was initiated by loss of anchorage in tension in the column splices at the bottom of the column. In the infill with the door, anchorage failure was initiated in the column splices and the trim bars at the face of the door. The wall with a window failed in shear. Various approaches for estimating the strength of the retrofitted frames were examined.

## TABLE OF CONTENTS

Chapter	Page
1. INTRODUCTION . . . . .	1
1.1 Purpose and Scope . . . . .	1
1.2 Background . . . . .	1
1.2.1 Repair and Retrofit of Structures . . . . .	1
1.2.2 Infilled Shear Walls . . . . .	2
1.2.3 Related Research . . . . .	3
2. EXPERIMENTAL PROGRAM . . . . .	19
2.1 Test Specimens . . . . .	19
2.1.1 Specimen Geometry . . . . .	19
2.1.2 Materials . . . . .	24
2.1.3 Construction Procedures . . . . .	32
2.2 Test Set Up . . . . .	48
2.2.1 Loading . . . . .	48
2.2.2 Data Acquisition . . . . .	54
3. EXPERIMENTAL RESULTS . . . . .	60
3.1 Full Infill Specimen . . . . .	60
3.1.1 Condition of Specimen Before Testing . . . . .	60
3.1.2 Cyclic Response . . . . .	60
3.2 Infill with Window . . . . .	81
3.2.1 Condition Prior to Testing . . . . .	81
3.2.2 Response Under Cyclic Loading . . . . .	81
3.3 Infill with Door . . . . .	110
3.3.1 Condition Prior to Testing . . . . .	110
3.3.2 Response to Cyclic Loading . . . . .	118

3.4	Behavior of Epoxied Voids . . . . .	155
4.	ANALYSIS . . . . .	170
4.1	Linear Elastic Response . . . . .	170
4.1.1	Measured Elastic Stiffness . . . . .	170
4.1.2	Classical Theory . . . . .	175
4.1.3	Finite Element Analysis . . . . .	180
4.1.4	Comparisons of Measured and Theoretical Stiffnesses . . . . .	184
4.2	Inelastic Response . . . . .	192
4.2.1	Stiffness . . . . .	192
4.2.2	Deflection Components . . . . .	202
4.2.3	Coupled Wall Behavior . . . . .	211
4.3	Strength . . . . .	215
4.3.1	Comparative Strength and Deformation Capacity . . . . .	215
4.3.2	Flexural Strength . . . . .	216
4.3.3	Shear Strength . . . . .	219
4.3.4	Anchorage of Reinforcement . . . . .	227
4.4	Strength of Low Rise Infilled Systems with Openings . . . . .	228
4.4.1	Strength Analysis Using the Strut Model . . . . .	231
4.4.2	Design Techniques Using the Strut Model . . . . .	234
4.4.3	Conclusions . . . . .	237
5.	SUMMARY, CONCLUSIONS AND RECOMMENDATIONS . . . . .	239
5.1	Summary . . . . .	239
5.2	Conclusions and Recommendations . . . . .	239
5.2.1	Behavior of Shear Walls . . . . .	239
5.2.2	Construction of Reinforced Concrete Infilled Shear Walls . . . . .	240
5.2.3	Detailing of Shear Walls . . . . .	240
5.2.4	Design Procedures for Infilled Shear Walls with Openings . . . . .	241
5.3	Research Recommendations . . . . .	241
	REFERENCES . . . . .	243

## LIST OF TABLES

Table		Page
2.1	Concrete Mix and Batch Proportions for Frame Concrete . . . . .	27
2.2	Frame Concrete Compressive Strengths . . . . .	27
2.3	Wall Shotcrete Compressive Strengths . . . . .	31
2.4	Shotcrete Mix Design . . . . .	31
2.5	Epoxy Grouted Bar Pullout Results . . . . .	35
4.1	Initial Stiffnesses . . . . .	174
4.2	Deflections Under Unit Load . . . . .	179
4.3	Member Moments of Inertia, Coupling Beam Analogy . . . . .	212
4.4	Alpha Parameters and Values, Infills with Openings . . . . .	214
4.5	Flexural Strength of Infilled Walls from Interaction Analyses and Experimental Data . . . . .	218
4.6	Shear Strength Predictions and Experimental Values . . . . .	220
4.7	Strength Analysis Using Strut Model . . . . .	233



## LIST OF FIGURES

Figure	Page
1.1 Cast-In-Place Infilled Walls . . . . .	4
1.2 Equilibrium of a Cracked Squat Shear Wall Under Lateral Load . . . . .	6
1.3 Strut Model for Infilled Walls . . . . .	8
1.4 Reinforcement Layout for Coupling Beams . . . . .	12
1.5 Positioning of Openings in a Shear Wall Building . . . . .	13
1.6 Laminar Method Idealization . . . . .	15
1.7 Idealized Structure for Frame Analogies . . . . .	17
1.8 Braced Wide Column Modules . . . . .	18
2.1 Frame Member Cross Sections . . . . .	21
2.2 Loading Block Reinforcement . . . . .	23
2.3 Cross Section for Flexural Analysis, Full Infill and Infill with Window . . . . .	25
2.4 Cross Section for Flexural Analysis, Infill with Door . . . . .	26
2.5 Shotcreting Process . . . . .	28
2.6 Shotcrete Test Panel . . . . .	30
2.7 Dowel Insertion in Pull Out Test Specimen . . . . .	33
2.8 Pull Out Test Set Up . . . . .	34
2.9 Pull Out Failure . . . . .	36
2.10 Frame Formwork . . . . .	37
2.11 Tilt Up of Bounding Frame . . . . .	39
2.12 Dowel Hole Drilling Operation . . . . .	40
2.13 Support of Overhead Dowels for Curing . . . . .	41
2.14 Roughened Frame-Wall Interface . . . . .	42
2.15 Reinforcement Layout, Full Infill . . . . .	44

2.16	Reinforcement Layout, Infill with Window . . . . .	45
2.17	Reinforcement Layout, Infill with Door . . . . .	46
2.18	Shotcrete Wall Voids . . . . .	47
2.19	Epoxy Injection of Crack . . . . .	49
2.20	Epoxy Injected Surface . . . . .	50
2.21	Patching Operation with Epoxy Grout . . . . .	51
2.22	Finished Epoxied Joint . . . . .	52
2.23	Thermal Cracking . . . . .	53
2.24	Loading Frame and Reaction Assemblage . . . . .	55
2.25	Instrumentation, Full Infill . . . . .	57
2.26	Instrumentation, Infill with Window . . . . .	58
2.27	Instrumentation, Infill with Door . . . . .	59
3.1	Load History, Full Infill . . . . .	61
3.2	Load-Deflection History, Full Infill . . . . .	62
3.3	Definition of Specimen End under Load . . . . .	63
3.4	Load-Deflection Response, Cycles to 120 K . . . . .	64
3.5	Crack Patterns, Cycles to 120 K . . . . .	65
3.6	Strain Profile, Cycles to 120 K, Positive Load . . . . .	67
3.7	Strain Profile, Cycles to 120 K, Negative Load . . . . .	68
3.8	Load-Deflection Response, Cycles to 180 K . . . . .	70
3.9	Crack Patterns, Cycles to 180 K . . . . .	71
3.10	Strain Profile, Cycles to 180 K, Positive Load . . . . .	73
3.11	Strain Profile, Cycles to 180 K, Negative Load . . . . .	74
3.12	Load-Deflection Response, Cycles to 240 K . . . . .	75
3.13	Crack Patterns, Cycles to 240 K . . . . .	76
3.14	Load-Deflection Response, Cycles to 0.50% Drift . . . . .	77
3.15	Full Infill at Failure, Elevation . . . . .	78

3.16	Full Infill at Failure, Splice Region . . . . .	79
3.17	Full Infill at Failure, Bar Slip . . . . .	80
3.18	Load History, Infill with Window . . . . .	82
3.19	Load-Deflection History, Infill with Window . . . . .	83
3.20	Load-Deflection Response, Cycles to 0.07% Drift . . . . .	84
3.21	Crack Pattern, Cycles to 0.07% Drift . . . . .	85
3.22	Strain Profiles, Cycles to 0.07% Drift, Base of Wall . . . . .	87
3.23	Strain Profiles, Cycles to 0.07% Drift, Top of Opening . . . . .	88
3.24	Strain Profiles, Cycles to 0.07% Drift, Bottom of Opening . . . . .	89
3.25	Load-Deflection Response, Cycles to 120 K . . . . .	90
3.26	Crack Patterns, Cycles to 120 K . . . . .	92
3.27	Wall Splitting in Window Opening, Cycles to 120 K . . . . .	93
3.28	Load-Deflection Response, Cycles to 0.17% Drift . . . . .	95
3.29	Strain Profiles, Cycles to 0.17% Drift, Base of Wall . . . . .	96
3.30	Strain Profiles, Cycles to 0.17% Drift, Top of Opening . . . . .	97
3.31	Strain Profiles, Cycles to 0.17% Drift, Bottom of Opening . . . . .	98
3.32	Load-Deflection Response, Cycles to 0.27% Drift . . . . .	99
3.33	Load-Deflection Response, Cycles to 180 K . . . . .	101
3.34	Crack Patterns, Cycles to 180 K . . . . .	102
3.35	Strain Profiles, Cycles to 180 K, Base of Wall . . . . .	104
3.36	Strain Profiles, Cycles to 180 K, Top of Opening . . . . .	105
3.37	Strain Profiles, Cycles to 180 K, Bottom of Opening . . . . .	106
3.38	Load-Deflection Response, Cycles to 0.50% Drift . . . . .	107
3.39	Crack Patterns, Cycles to 0.50% Drift . . . . .	108
3.40	Load-Deflection Response, Cycles to 200 K . . . . .	109
3.41	Infill with Window at Failure, Elevation . . . . .	111
3.42	Upload Column at Failure . . . . .	112

3.43	Failure Plane in Infill . . . . .	113
3.44	Download Column at Failure . . . . .	114
3.45	Wall Splitting in Window Opening . . . . .	115
3.46	Strut Crushing at Failure . . . . .	116
3.47	Load History, Infill with Door . . . . .	117
3.48	Load-Deflection History, Infill with Door . . . . .	119
3.49	Load-Deflection Response, Cycles to 0.07% Drift . . . . .	120
3.50	Crack Patterns, Cycles to 0.07% Drift . . . . .	121
3.51	Strain Profiles, Cycles to 0.07% Drift, Base of Wall . . . . .	122
3.52	Strain Profiles, Cycles to 0.07% Drift, Top of Opening . . . . .	123
3.53	Load-Deflection Response, Cycles to 80 K . . . . .	125
3.54	Strain Profiles, Cycles to 80 K, Base of Wall . . . . .	127
3.55	Strain Profiles, Cycles to 80 K, Top of Opening . . . . .	128
3.56	Load-Deflection Response, Cycles to 100 K . . . . .	129
3.57	Load-Deflection Response, Cycles to 120 K . . . . .	131
3.58	Load-Deflection Response, Cycles to 0.17% Drift . . . . .	133
3.59	Crack Patterns, Cycles to 0.17% Drift, North Pier . . . . .	134
3.60	Crack Patterns, Cycles to 0.17% Drift, South Pier . . . . .	135
3.61	Load-Deflection Response, Cycles to 0.27% Drift . . . . .	136
3.62	Crack Patterns, Cycles to 0.27% Drift . . . . .	138
3.63	Strain Profiles, Cycles to 0.27% Drift, Base of Wall . . . . .	139
3.64	Strain Profiles, Cycles to 0.27% Drift, Top of Opening . . . . .	140
3.65	Load-Deflection Response, Cycles to 180 K . . . . .	141
3.66	Load-Deflection Response, Cycles to 34 D . . . . .	143
3.67	Load-Deflection Response, Cycles to 50 D . . . . .	145
3.68	Crack Patterns, Cycles to 0.50% Drift, South Pier . . . . .	146
3.69	Crack Patterns, Cycles to 0.50% Drift, North Pier . . . . .	147

3.70	Anchorage Failure of Vertical Trim Steel . . . . .	148
3.71	Strain Profiles, Cycles to 0.50% Drift, Base of Wall . . . . .	149
3.72	Strain Profiles, Cycles to 0.50% Drift, Top of Opening . . . . .	150
3.73	Load-Deflection Response, Cycles to 0.55% Drift . . . . .	152
3.74	Crack Patterns, Cycles to 0.55% Drift . . . . .	153
3.75	Load-Deflection Response, Cycles to 0.60% Drift . . . . .	154
3.76	Upload Pier Under Load at Failure . . . . .	156
3.77	Vertical Trim Steel at Failure . . . . .	157
3.78	Splice Failure in Upload Column . . . . .	158
3.79	Load-Slip Behavior, Positive Potentiometer . . . . .	159
3.80	Load-Slip Behavior, Center . . . . .	160
3.81	Load-Slip Behavior, Negative Potentiometer . . . . .	161
3.82	Load-Slip Behavior, Center Potentiometer . . . . .	162
3.83	Load-Slip Behavior, Positive Potentiometer . . . . .	163
3.84	Load-Slip Behavior, Center Potentiometer . . . . .	164
3.85	Load-Slip Behavior, Negative Potentiometer . . . . .	165
3.86	Cracked Epoxy Under Load . . . . .	166
3.87	Crushing of Plain Epoxy . . . . .	168
4.1	Load-Deflection Response, Initial Cycle, Full Infill . . . . .	171
4.2	Load-Deflection Response, Initial Cycle, Infill with Window . . . . .	172
4.3	Load-Deflection Response, Initial Cycle, Infill with Door . . . . .	173
4.4	Classical Deflections, Infill with Window . . . . .	177
4.5	Classical Deflections, Infill with Door . . . . .	178
4.6	Finite Element Model, Full Infill . . . . .	181
4.7	Finite Element Model, Infill with Window . . . . .	182
4.8	Finite Element Model, Infill with Door . . . . .	183
4.9	Strain Profile, Finite Element Model, Infill with Window . . . . .	185

4.10	Strain Profiles, Finite Element Model, Infill with Door . . . . .	186
4.11	Superimposed Finite Element Profiles . . . . .	187
4.12	Lateral Deflection Profile, Finite Element Model, Full Infill . . . . .	188
4.13	Lateral Deflection Profile, Finite Element Model, Infill with Window	189
4.14	Lateral Deflection Profile, Finite Element Model, Infill with Door . .	190
4.15	Superimposed Lateral Deflection Profile, Finite Element Models . . .	191
4.16	Load-Deflection Response, 120 K . . . . .	193
4.17	Load-Deflection Response, 180 K . . . . .	194
4.18	Load-Deflection Response, 0.17% . . . . .	195
4.19	Load-Deflection Response, 0.27% . . . . .	196
4.20	Load-Deflection Response, 0.50% . . . . .	197
4.21	Superimposed Half-Cycles, Infill with Door . . . . .	199
4.22	Measured Relative Stiffness . . . . .	200
4.23	Measured Relative Stiffness vs. Drift . . . . .	201
4.24	Theoretical Relative Stiffness vs. Drift . . . . .	203
4.25	Shear Deformations in Walls . . . . .	204
4.26	Load-Shear Component Ratio Envelopes . . . . .	206
4.27	Lateral Deflection Profile, Full Infill . . . . .	208
4.28	Lateral Deflection Profile, Infill with Window . . . . .	209
4.29	Lateral Deflection Profile, Infill with Door . . . . .	210
4.30	Geometric Parameters for Coupling Factor . . . . .	213
4.31	Stress-Strain Relationship for Concrete and Steel . . . . .	217
4.32	Geometric Parameters for AIJ Standard . . . . .	224
4.33	Strut Models for Infills . . . . .	230
4.34	Download Pier Mechanism, Infill with Window . . . . .	235

# CHAPTER 1

## INTRODUCTION

### 1.1 Purpose and Scope

The purpose of this study was to investigate the behavior of reinforced concrete infilled frames with openings under cyclic lateral loads. Three large scale specimens were constructed. One infill had a door opening, one infill had a window opening and one infill was constructed with no openings. The infill without openings, hereafter referred to as the "full infill," was used as a reference for quantifying the behavior of the other two specimens.

Behavior was evaluated in terms of deflection characteristics, interface shear transfer between the bounding frame and the infilled wall, anchorage of reinforcement (splices and dowels) and the load carrying characteristics of the repaired sections in the undamaged shear walls. These areas will be fully developed in subsequent chapters.

Design engineers from H. J. Degenkolb Associates provided the details of the prototype building and the infill walls. The construction and testing of the specimens was carried out at Ferguson Structural Engineering Laboratory.

### 1.2 Background

**1.2.1 Repair and Retrofit of Structures.** Problems faced by owners of buildings located in seismic regions include providing occupants with a safe environment and protecting the building against costly damage due to earthquakes. In a few municipalities in the United States, owners of certain types of buildings (unreinforced masonry) in regions of high seismicity are legally obligated to upgrade their structures to comply with requirements for a minimum level of safety or to destroy the structure. Thus, undamaged buildings may need to be strengthened to prevent collapse or stiffened to prevent damage to nonstructural elements such as glass, cladding, mechanical equipment and walls. Often buildings are damaged in an earthquake but do not collapse. Damaged buildings may either be demolished and rebuilt or repaired. It is frequently cost

effective to repair the damage and return the building to its original condition or to repair and strengthen the building beyond its original capacity. These needs have given rise to structural retrofitting operations.

The repair/strengthening process has several phases. The first phase consists of a thorough evaluation of the damage incurred in a building and an evaluation of the existing lateral force resisting system. In formulating a repair/strengthening scheme, the engineer must not create new areas of weakness. The repair must be economical. Often retrofit operations must be undertaken while the building is still occupied. Finally, the repair must be aesthetically pleasing. Once the owner and engineer have agreed on the project scope and details, implementation of the repair may proceed.

**1.2.2 Infilled Shear Walls.** Infilling is a strengthening technique used for frames. The frames may be made of either concrete or steel. This technique has several advantages, including substantial increases in strength and dissipation of significant amounts of energy through deformations of the infill panel. Infills increase the effective viscous damping ratio for a building. Shear walls may be located on the perimeter of a building which permits occupation during the repair. Often, shear walls are infilled against an existing masonry wall and do not alter the appearance of a building. Some of the difficulties in effecting this type of repair include a significant increase in the vertical loads transferred to the foundation and an increase in inertial forces associated with the increase of mass to the building system. The latter is offset by the beneficial structural effects of infilling.

Construction of infilled walls presents problems in some cases. When retrofitting a frame with a cast in place concrete wall, a problem is encountered in placing concrete. Typically, concrete is placed through an opening in the formwork at the top of the wall. This technique leaves a gap in the top of the wall which must be filled. Gaps on the boundaries of infills have been drypacked with mortar or have utilized mechanical connectors without notable success. These operations have resulted in shear failure of the frame elements [1]. One solution to this problem is to use shotcrete. The often questionable quality of concrete



obtained from shotcreting may render this technique less attractive than a cast in place system. Another solution that utilizes cast concrete is to construct the formwork with a lip in the form as pictured in Figure 1.1. Concrete is then cast above the level of the bottom of the beam and allowed to set. After the forms have been removed, the lip of concrete may be removed with a concrete saw or chipped away.

### 1.2.3 Related Research.

*1.2.3.1 Shear Walls.* Shear walls offer advantages particularly in areas where lateral loads resulting from wind loading or earthquake ground motions are significant. Various types of shear wall systems are employed in buildings of all heights. In one type of structural system, shear walls are used in conjunction with a frame and are proportioned to withstand a majority, if not all of the lateral load. The interaction of frames and shear walls is a complex problem. One source of analytical difficulty lies in the different deflection modes of the two systems under lateral load. Columns in frames deform in primarily a double curvature shape or sidesway mode while shear walls generally deform as deep cantilever beams. Investigations have been undertaken to determine the nature of interaction between the two systems and to present analysis techniques for designers to use. These techniques are detailed in References 2-4 and will not be repeated here. An excellent summary of methods of analysis of wall-frame interaction is presented in Reference 5.

Shear walls are classified on the basis of their height and width. "Tall" shear walls have aspect ratios (wall height divided by wall width) of 2 or more. "Short" or "squat" shear walls have aspect ratios less than 2. Shear walls may have rectangular cross sections, or they may be flanged or even channel shaped. The shape of the cross section, coupled with the distribution of steel in the section influences the flexural capacity of the system. In the design of shear walls for seismic application, a ductile failure mode is advanced by providing a shear capacity that is greater than the shear associated with the flexural capacity of the wall.

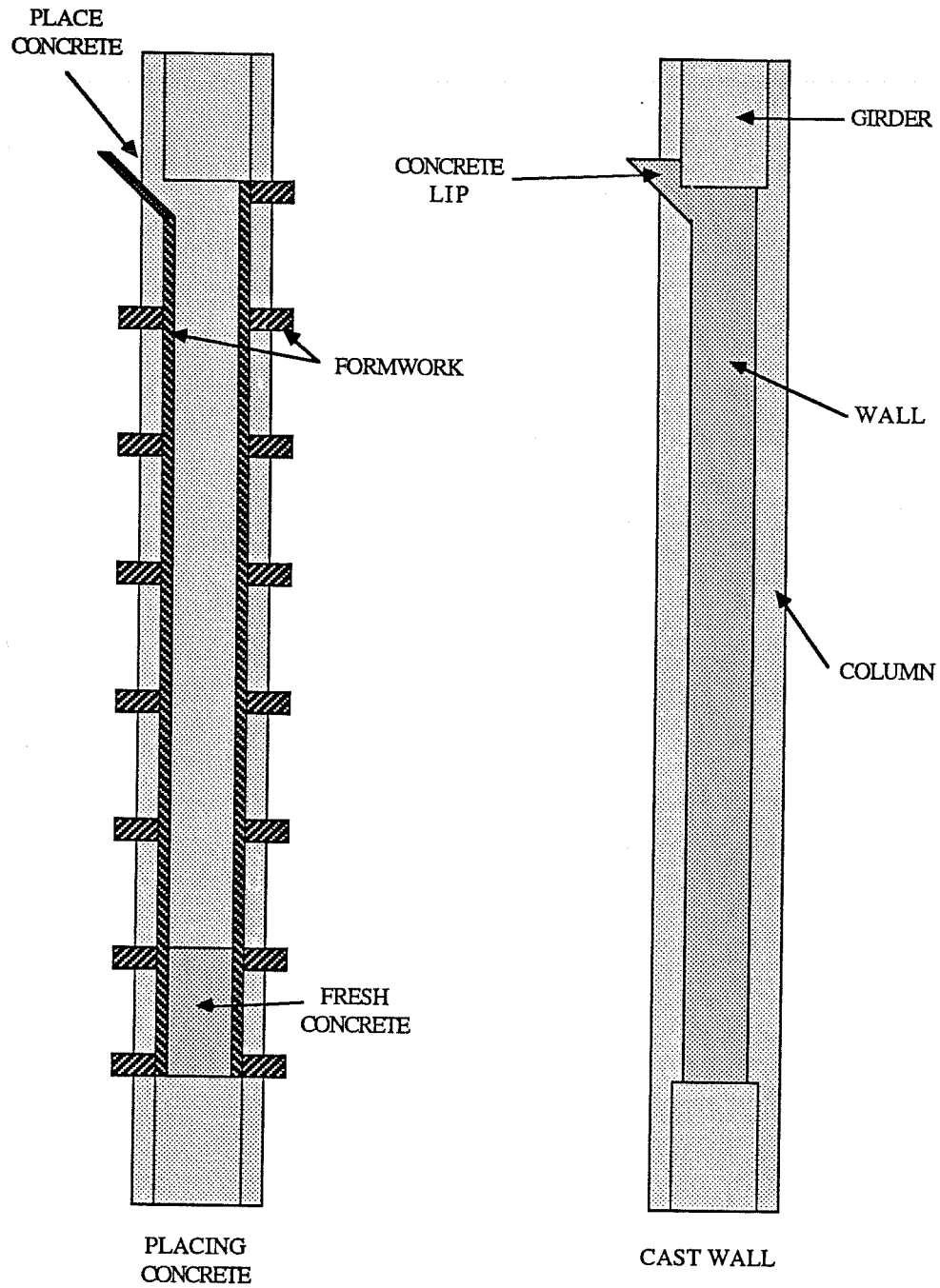


Fig. 1.1 Cast-In-Place Infilled Wall

Typically, tall shear walls are analyzed as cantilevered reinforced concrete beams subjected to moments and shears that result from lateral loads. The flexural capacity of these walls can be determined from a moment-axial force interaction diagram. The reinforcing steel in the boundary columns and the vertical steel in the wall contribute to the flexural capacity of the assemblage. Since gravity loads on these members are usually small with respect to their areas, shear walls axially loaded usually fail below the balance point. Floor diaphragms in a building act as lateral support for the thin webs of a shear wall, preventing buckling of the member. Floors also distribute the shear to the wall system. The shear capacity of a wall may be determined as in a reinforced concrete beam. For seismic applications where ductility is desired, the contribution of the concrete to shear capacity may be neglected at the critical hinging section if axial stress is low [6]. Hinging typically occurs at the base of the wall.

In squat shear walls, applied lateral load is transferred through the formation of compression struts. The behavior coincides with the behavior of geometrically similar deep beams. The inclination of the struts is dependent on the aspect ratio of the wall. Early studies of squat shear walls conducted by Benjamin and Williams indicated that the shear capacity of the walls is related to the aspect ratio of the wall [7]. In this investigation, as the aspect ratio of the wall decreased, the load at which the wall cracked approached the ultimate load of the specimen. The influence of vertical reinforcement on strength was shown to be greater than that of the horizontal wall reinforcement. Vertical and horizontal reinforcement for shear is required for equilibrium of a cracked section as illustrated in Figure 1.2. For squat shear walls, the vertical steel is required for development of compression struts in the center portions of the wall. The horizontal reinforcement is required for equilibrium of the corner elements. The maximum amount of vertical reinforcement that is required is equal to the amount of horizontal reinforcement. For squat shear walls, current specifications indicate the amount of vertical web reinforcement required is a function of the aspect ratio of the wall [8]. The designer is urged to neglect the concrete contribution to shear capacity in critical regions where ductile hinging is to occur and where the concrete may be damaged [6]. The flexural capacity of

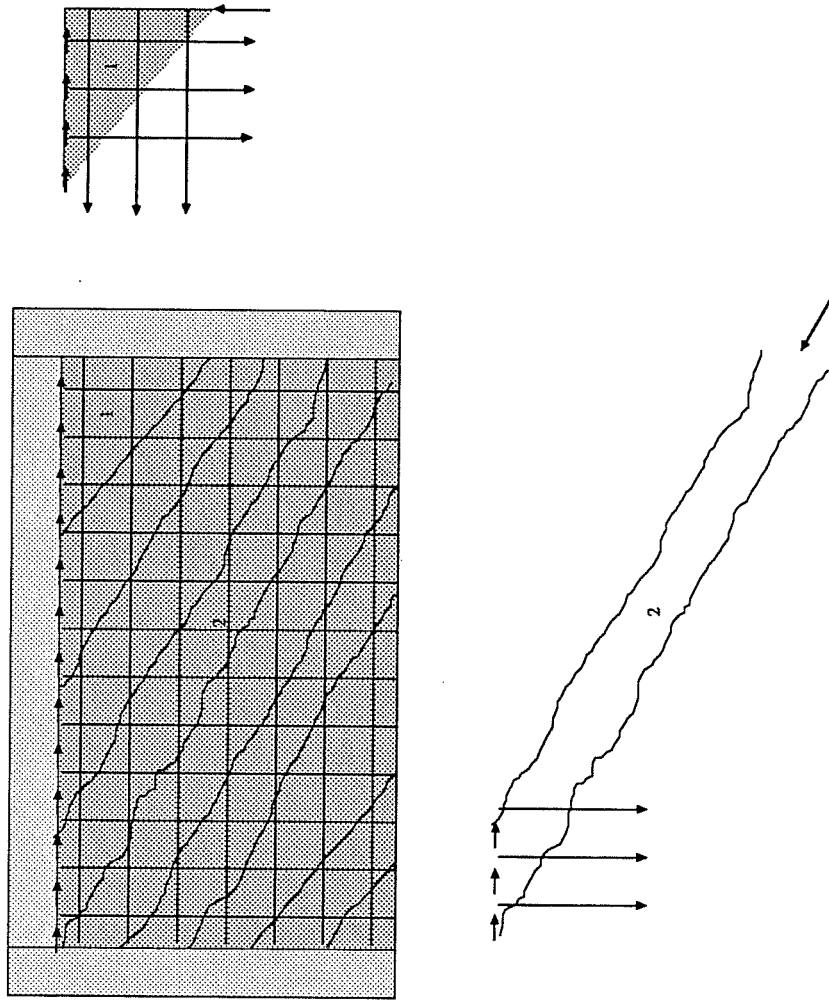


Fig. 1.2 Equilibrium of a Cracked Squat Shear Wall Under Lateral Load

squat walls may be assessed through the use of a moment-axial force interaction diagram.

There are several modes of failure in squat shear walls. Crushing of one or both of the corners of the wall can cause failure of the system. Diagonal compression failures result when the shear associated with the wall flexural capacity is greater than the shear strength and adequate horizontal reinforcement is provided. Diagonal tension failures result when an insufficient amount of horizontal steel is provided to transfer the shear force at which ductile flexural yielding occurs. Sliding shear failures occur when flexural cracks that originate due to reversed loading connect and form a horizontal plane that extends across the entire width of the wall. Shear is transferred across this plane through dowel action of vertical reinforcement and shear friction. Diagonal reinforcement is recommended to help control sliding shear failures [9].

**1.2.3.2 Infilled Frames.** Infilling frames with shear walls produces a combined system with stiffness greater than the sum of the stiffnesses of the frame and the infill taken separately. The behavior of the assemblage is primarily determined by the aspect ratio of the assemblage and by the frame to wall connection. In an assemblage with a low aspect ratio, struts will develop in the infill irrespective of the frame to wall connection. In a high rise assemblage where the frame to wall connection is maintained and shear can be transferred across that boundary, as in a monolithically cast system, the assemblage will bend. The stiffness and strength of the system is determined by the composite section at the critical location for flexure and shear. This is the most efficient behavior that can be achieved for infilled systems. In a high rise assemblage where the frame to wall connection is not maintained, the assemblage will act as a braced frame, with the infill acting as a compression strut. Strut development has been found to have adverse impact on a bounding frame. The force that the strut carries is transferred to the column ends through shear and tension as illustrated in Figure 1.3. The diagonal struts may produce premature failure of the columns or beams in shear. In several cases, crushing of one or both of the corners of the strut have caused failure of the infill.

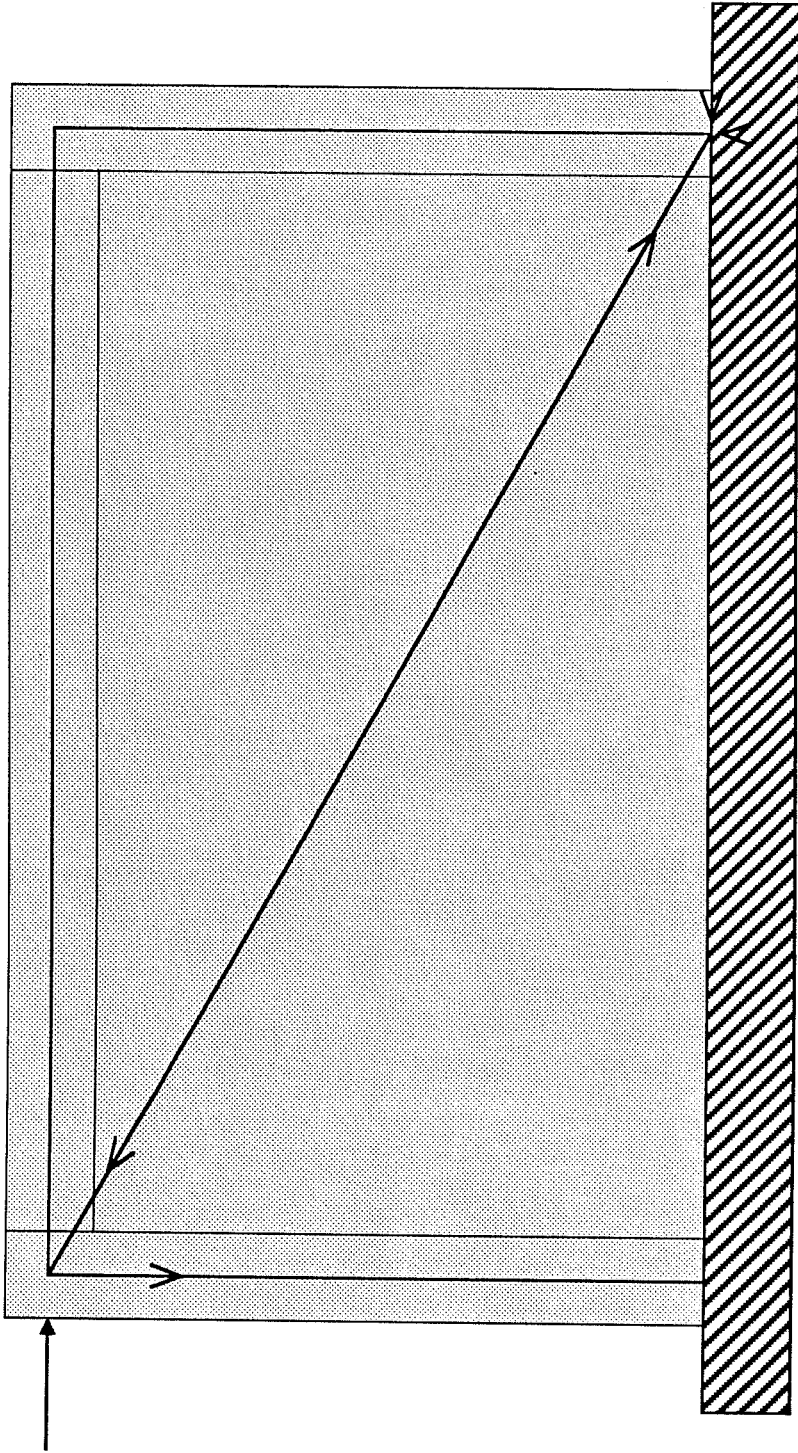


Fig. 1.3 Strut Model for Infilled Walls

There have been several studies on infilled walls both with and without a mechanism for shear transfer between the bounding frame and the infill [10,11]. Masonry infills often are employed without the use of shear connectors. Such systems do not exhibit large energy dissipation characteristics. However, good behavior obtained with the use of shear connectors in masonry infilled walls [12,13]. In infills without shear connectors, behavior is characterized by cracks that open along the boundary and increase in width with increasing load. These cracks extend over the entire boundary except in the vicinity of the loaded corners of the infill. Cracking of the infill is limited. Failure in these specimens occurs due to crushing along the diagonal. In cases where ineffective shear connectors are used, shear failures of boundary frame elements are common [1].

Several types of shear connectors have been studied for use with both concrete and masonry infills. Good results have been obtained through the use of dowelled reinforcement [1,13,15], and through the use of wedge anchors and shear keys [15,16]. In infills with effective shear connectors, separation of the wall and frame is controlled and the entire infill is mobilized to transfer lateral forces. Significant increases in strength and stiffness have been noted in specimens with shear connectors due to the composite action of the frame and the infill. Failure modes in these specimens are similar to failure modes of monolithically cast specimens [12]. Behavior of infilled assemblages with effective shear connectors is dependent on the aspect ratio of the assemblage.

Techniques have been developed to predict the stiffness and strength of infilled walls. In one method, the infill is modelled as a diagonal compression strut. The properties of the strut are established using energy principles. The system may be modelled as a pin ended truss or a braced frame. Hand computation or standard frame analyses may then be used to assess the response to lateral loads. Failure is governed by the strength of the bounding frame members, crushing of the infill strut or diagonal tension failure of the infill. Use of this method is justified where struts may be expected to form due to a lack of connectors or a low aspect ratio is provided [1,13,15,17,18]. An equivalent frame method for analyzing infilled systems may be employed where composite action

of the bounding frame and infill can be expected. Transformed sections are derived from the modular ratio of the infill and bounding frame materials. Wide columns and beams are the result. The shear stiffness of equivalent members are included in what is an otherwise typical frame analysis [16]. Finite element analyses have also been used to determine infilled frame behavior and dynamic properties [10,11]. More accurate representations of degrading material properties and of boundary conditions may be achieved, however, the cost of these analyses is often substantial. Some investigators make use of elastic stress functions to describe the state of stress in infilled walls. The limiting stress is taken as the maximum stress obtained experimentally [19].

*1.2.3.3 Shear Walls with Openings.* Experimental data on infills with openings is limited. Researchers have used both masonry and concrete infills with and without bounding frames made of steel and concrete. Mallick and Garg [25] used steel frames with concrete infills and dowelled connectors. The size and location of the openings was varied to determine which had the highest capacity under monotonic load. The results indicated that the best results can be obtained when openings are located far from the paths of compression struts. A centrally located window opening had a capacity that was exceeded only by the capacity of the infill with an opening in the loaded corner of the infill. All specimens failed by diagonal tensile cracking in the infill.

Liauw and Lee [16] investigated the effect of door openings in concrete infills bounded by steel frames spanning four stories. In specimens with shear connectors, the capacity of the infill decreased as the width of the door opening increased. As the aspect ratio of the assemblage decreased, the ultimate load increased. This tendency is surprising in that the decreasing aspect ratio will force struts to pass through openings, which were of a constant height. Thus, the infills with openings must form a different mechanism for handling lateral load because the formation of a large strut that spans the entire panel is precluded. The failure of these specimens occurred in the lowest story and consisted of diagonal cracking in the infill and compression failures in the bottom of the coupling beam and at the base of the download wall (see Figure 3.3).



Benjamin and Williams [14] conducted a study of single story concrete shear walls with window and door openings, most of which had boundary elements. The specimens were cast monolithically with no shear connectors between the boundary elements and the wall. However, horizontal and vertical panel steel was developed the boundary elements although it was not designed to transfer the applied shear across the interface. Single openings and multiple openings of the same and both types of openings were studied. Monotonic in-plane lateral load was applied to failure. The primary mode of failure was shear failure in the panel elements. One conclusion of the study was that diagonal reinforcement in the corners of the openings was effective in controlling cracking. The investigators also determined that the shear capacity of a wall with openings is determined by the capacity of the horizontal sections on either side of the opening. Cracking in the panels usually consisted of a set of large inclined cracks that ultimately formed the failure plane of the panel. Splitting along the horizontal boundaries was evident. In several cases, the boundary elements failed in shear.

Adachi, Shirai and Nakanishi [27] conducted an investigation into the effect of window openings on the cyclic behavior of three story, reinforced concrete shear walls with boundary elements. Four models were constructed, three of which had openings that were of various sizes and a fourth with no openings. The openings were centrally located in the wall panel and were reinforced with horizontal, vertical and diagonal reinforcement in a layout similar to that pictured in Figure 1.4. The assemblages were monolithically cast. The investigation indicated that as the size of a window opening increased, the strength decreased, the ductility increased, and the rate of degradation with cycling increased. Also, as the size of the openings increased, the specimens tended to deflect more as a frame than as a vertical cantilever. Failure in three of the specimens occurred due to diagonal compression failure in the wall. In the specimen with the largest window openings, the girder at the top of the second story failed in shear.

Recommendations for the placement of openings indicate that vertical rows of openings are better than staggering openings in a wall, as illustrated in Figure 1.5. When openings are placed in a vertical row, the system becomes a "coupled" shear wall system consisting of two shear walls and deep coupling

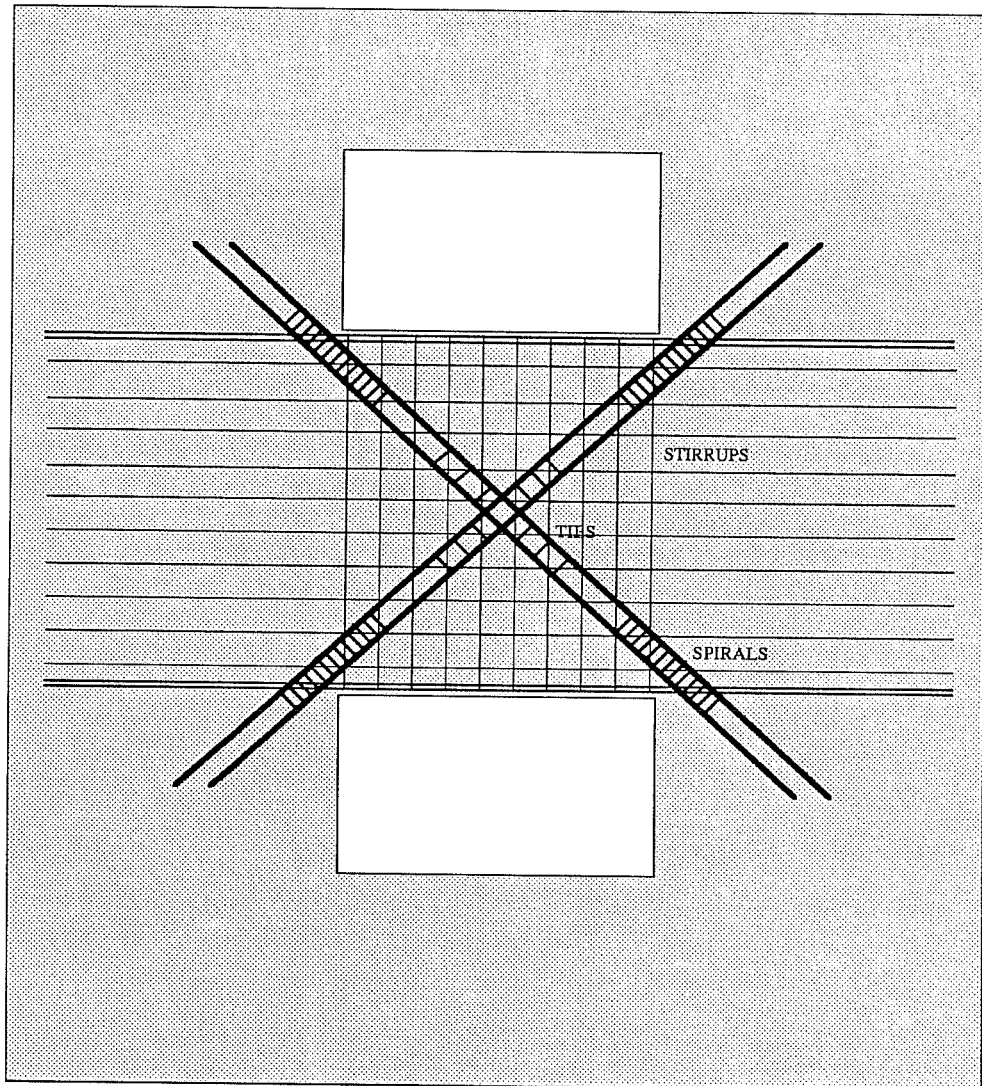


Fig. 1.4 Reinforcement Layout for Coupling Beams

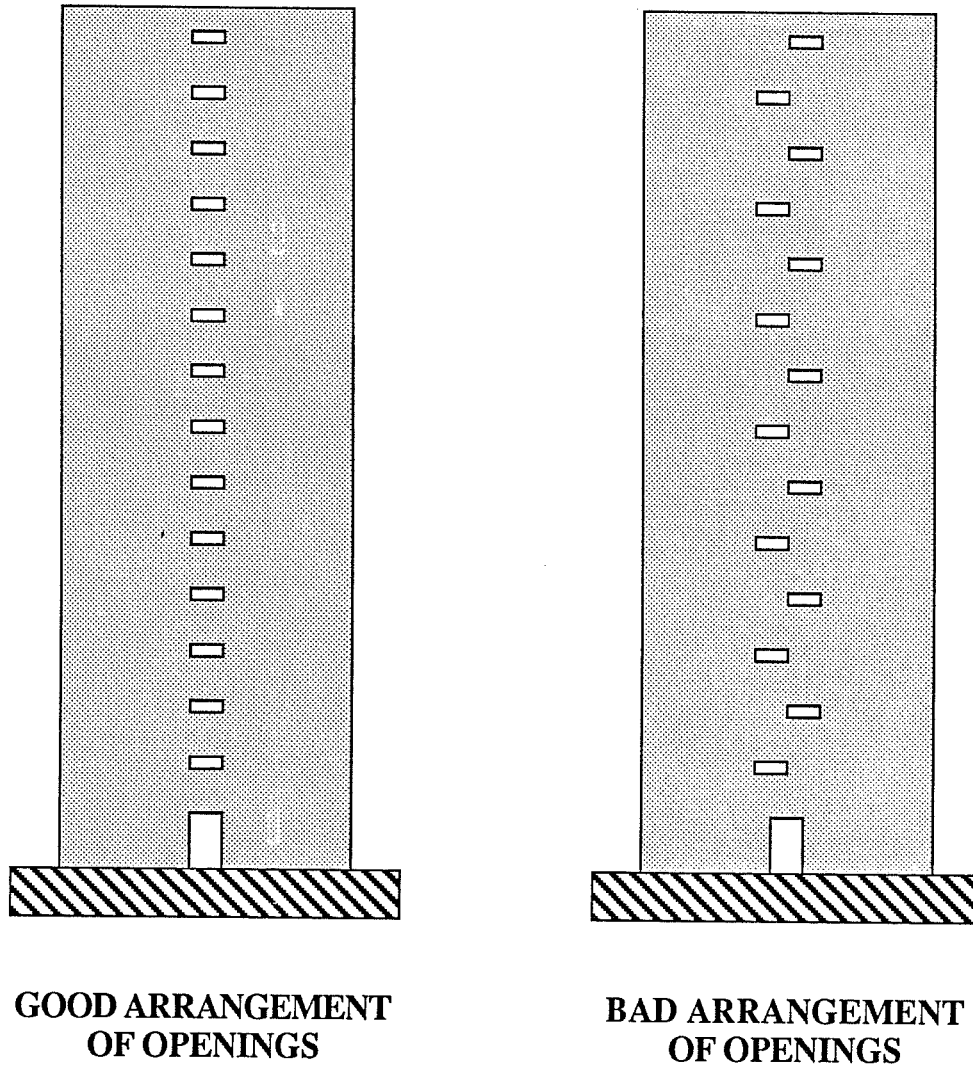


Fig. 1.5 Positioning of Openings in a Shear Wall Building

beams. This system may be engineered for ductile behavior. The coupling beams require careful detailing, as they are subjected to very high shears resulting from large deformations of the shear walls.

In “lightly coupled” shear wall systems, coupling beams are relatively flexible and weak. Experimental studies indicate that the weak beams will yield well in advance of yielding of the wall elements and will suffer extensive damage by the time wall elements have yielded. This can reduce a coupled system to a linked system in which the wall elements behave as isolated walls. In a linked system, the coupling beams cannot provide for redistribution of shear between the walls. The stiffness of this system is equal to the stiffness of two uncoupled walls as opposed to the substantially higher stiffness of a coupled system. The lightly coupled system is similar to the geometry of shear walls with a vertical row of door openings [20].

In “heavily coupled” shear walls, coupling beams are stronger and stiffer. These beams will yield before yielding of the wall elements, but will maintain enough integrity to allow for redistribution of shear between the two wall elements. The behavior of this system is that of a single vertical cantilever. Experimental studies show failure is categorized as diagonal compression in the wall elements. As this mode of failure is unacceptable for seismic applications, it is recommended that the designer implement a weak beam, strong wall concept, where flexure governs the failure of the wall elements. The geometry inherent in shear walls with a vertical row of window openings suggests that a heavily coupled system may result.

There are several analysis techniques available for coupled shear walls. In the laminae method, the vertical row of openings is replaced by a continuous laminae that connects the two shear walls, as pictured in Figure 1.6. The shear forces in the laminae are determined from a differential equation, which, in turn, can be integrated to yield the shear in the coupling beams. Bending moments and lateral deflections of the two shear walls may then be determined [21]. Use of this theory is limited to precracking stages of load and to buildings with regular stiffness in walls and beams. The technique has been updated to account for

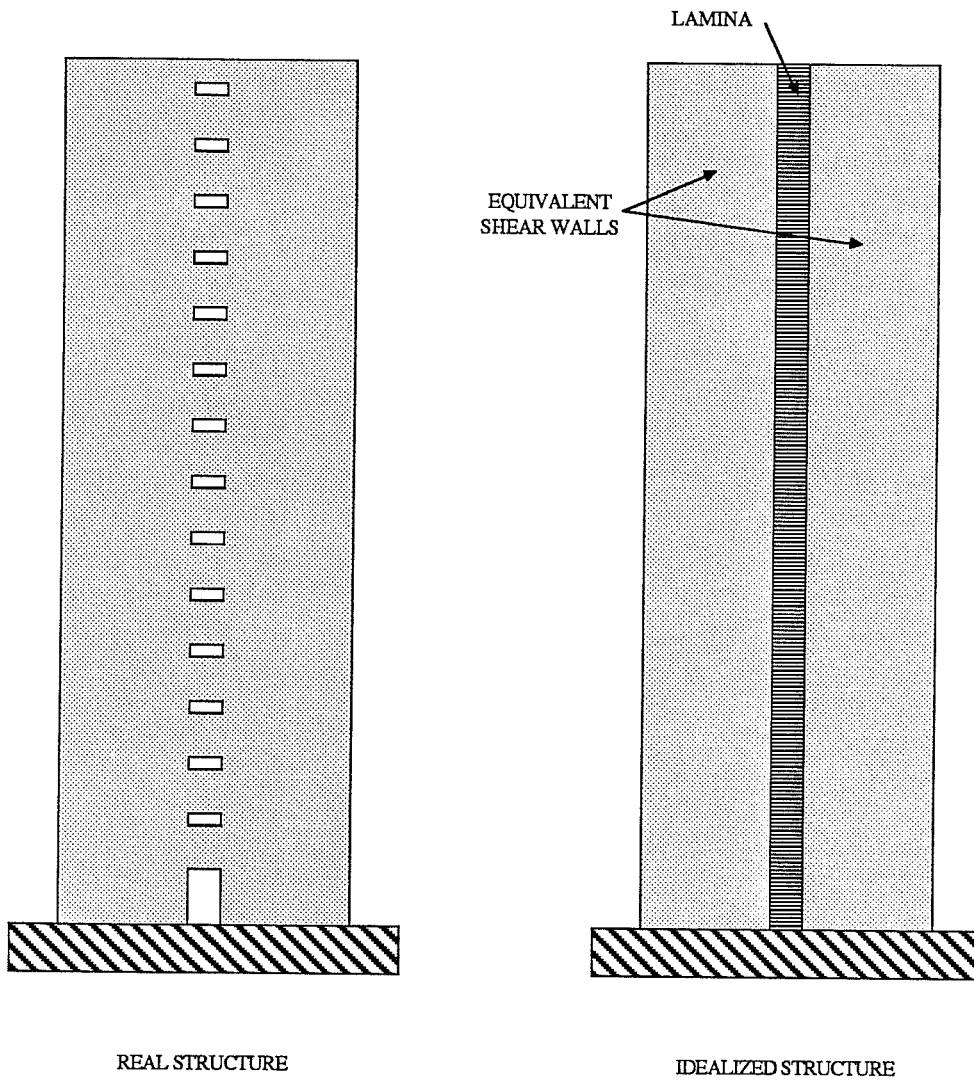


Fig. 1.6 Laminar Method Idealization

non-linear behavior in coupled shear walls [26]. Standard frame analyses may be used to analyze shear walls with openings using an equivalent frame technique or a wide column frame analogy previously mentioned.

In the wide column frame method, the rotations of the columns induce deflections in the coupling beams through the use of fully rigid beam ends that extend to the centerlines of the two shear walls (called "columns" in this method) [22]. This approach better predicts deflections than an equivalent frame analogy, which tends to overestimate deflections. The idealized structures for these two methods are pictured in Figure 1.7. Derivatives of the wide column frame analogy include the braced wide column frame [23]. In this idealization, wall elements are reduced to an assemblage of rigid beams and a single column with two pin-ended diagonal braces connecting beam ends. The braces correct problems in the wide column frame analogy with shear and bending deformations. A number of similar arrangements of members in a module have been proposed for use with various arrangements of walls. The idealizations are presented in Figure 1.8. A finite element approach may be used for analyzing shear walls with openings. It is most useful for walls with arrangements of openings that do not lend themselves readily to the laminar approach or to any of the frame approaches.

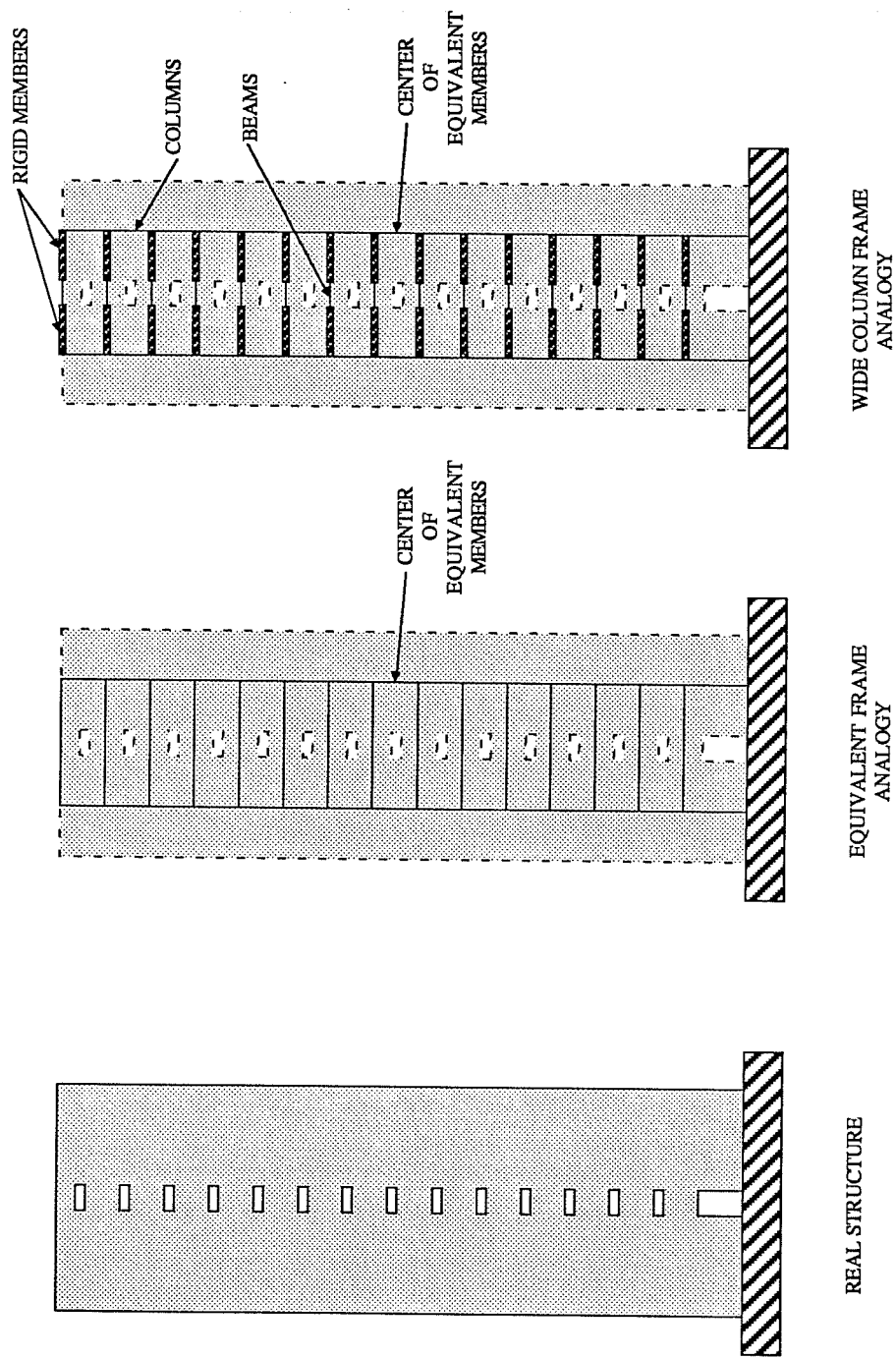


Fig. 1.7 Idealized Structure for Frame Analogies

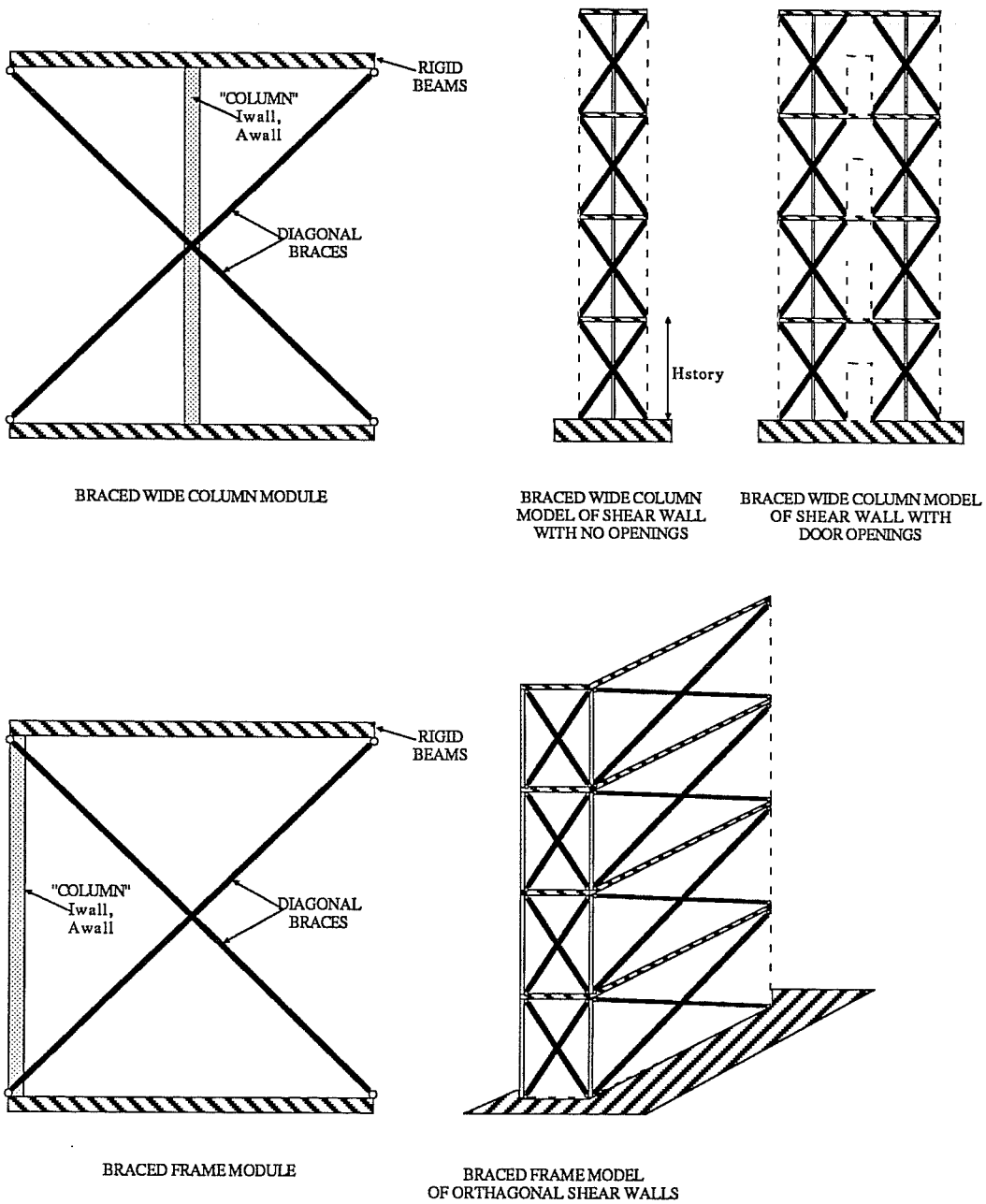


Fig. 1.8 Braced Wide Column Modules



## CHAPTER 2

### EXPERIMENTAL PROGRAM

#### 2.1 Test Specimens

##### 2.1.1 Specimen Geometry

*2.1.1.1 Design Philosophy and Procedures.* The test specimen consisted of two types of elements from a design standpoint. The prototype building, ultimately realized in the test specimen as the bounding frame, represented the "existing element." The infilled wall represented the "new element." The prototype building was selected as a four story reinforced concrete frame with 12 ft. story height and 20 ft. square bays. Preliminary member sizes were 18 in. square columns, 12 in. by 18 in. deep beams and a 6 in. thick slab. The reinforcement ratio for the columns was 1.5% based on modelling constraints discussed later. Dead load on the frame included self weight, a 20 psf partition load and 10 psf miscellaneous load. Live load was taken as 50 psf. In accordance with the 1955 edition of the Uniform Building Code (UBC), loads were factored and moment coefficients used to establish maximum positive and negative beam moments. Column axial load for a typical interior, first story column at ultimate was determined and compared with UBC capacity. Column ties were #4 bars at the designated maximum spacing of 12 in. Concrete strength was 4000 psi and Grade 40 steel was chosen.

In selecting the scale of the test specimen, a balance was reached between laboratory space constraints and realistic element dimensions. A two-thirds scale model with one bay and one story was selected. A one story model was selected assuming that the failure of an infill with openings would involve only one story.

There were several weaknesses of the prototype frame in a seismic area. One such weakness was the compression splice at the floor level which was typical of the 1950's construction. The splice detail did not meet current specifications for a splice in new construction in seismic areas. While the detail was acknowledged as being marginal, it was maintained in the test structures.

Another deficiency is the low column ductility. If the frame is to dissipate energy during ground motion, plastic hinges must be developed. Column ductility is related to the amount of confinement of the core by ties or stirrups. With larger ties and closer spacings, the confinement and therefore, the ductility improves. The column ties in the prototype classify the structure as "non-ductile." Column details for the test specimens are shown in Figure 2.1.

The infill wall was designed using Appendix A of ACI 318-83, Building Code Requirements for Reinforced Concrete. Size and spacing of wall reinforcement was chosen for ease of shotcreting. It was determined that a single curtain of reinforcement is often used in shotcreting construction and would allow for better consolidation than two curtains (one in each face). The resulting panel strength in shear was used to design, by shear friction, the dowels between the existing frame and infill wall.

The infills with openings had vertical and horizontal trim steel surrounding the openings. The horizontal trim steel was designed to serve as collectors transferring one-half of the shear to the each pier. The vertical trim steel was designed assuming frame action of the piers in the wall section on either side of the opening. In this analysis, the lintel and foundation beams were assumed to be stiff enough to prevent rotation of the pier ends. The shear capacity of the infills with openings was assumed to be proportional to the relative rigidity of the infill with an opening to the rigidity of the full infill. The stiffness of infills with openings was established using classical mechanics by summing flexural and shear displacements in each section of constant properties. Infills with openings were assumed to be coupled. Details of this analysis are presented in Chapter 4. The stiffness of the full infill was determined using both shear and flexural displacements. The capacity of the full infill in shear was established as described above. The area of curtain reinforcement for the infills with openings the same as that of the full infill. Steel terminated at the opening was replaced by trim bars. The area of dowel reinforcement was held constant for all specimens. Wall reinforcement details are given in Figs. 2.15, 2.16 and 2.17.

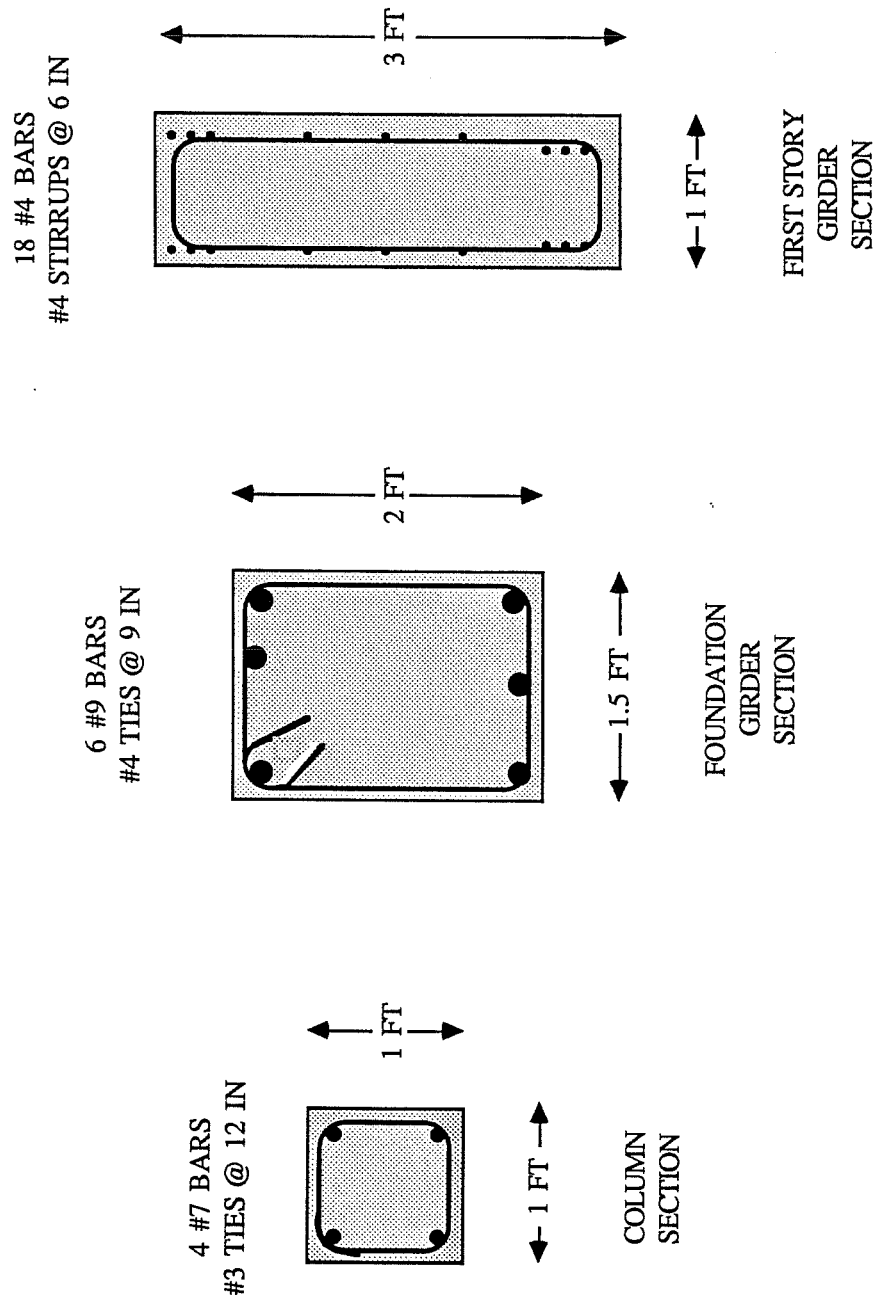


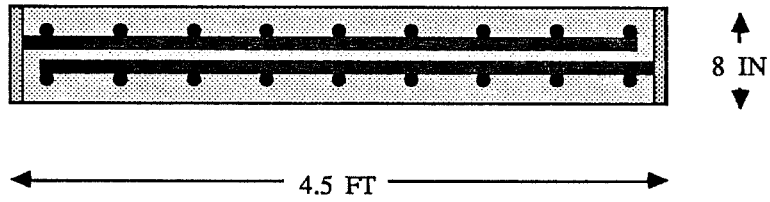
Fig. 2.1 Frame Member Cross Sections

*2.1.1.2 Modelling Considerations.* The frame was built on a foundation girder that was intended to provide continuity similar to that of the story below or that of a stiff foundation. In designing this element, it was assumed that it would be anchored to the floor. Dimensions were based on anchorage requirements for the column steel and minimum longitudinal and transverse reinforcement was provided (see Figure 2.1).

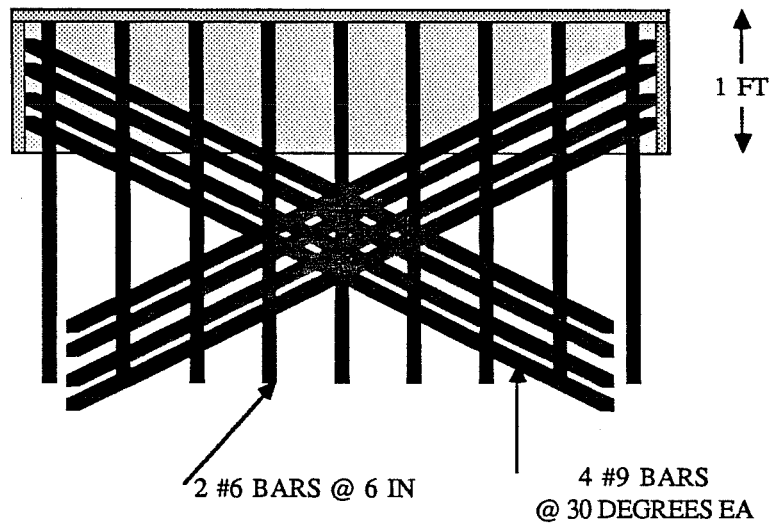
The first story girder was designed to transfer shear to the full infill with a considerable margin of strength. It also served to distribute the applied lateral load to the wall. Typically, rigid floor diaphragms distribute shear to columns and shear walls under lateral load. Concentrated point loads applied to a beam proportioned for gravity loads would probably not approach the even distribution of load anticipated in real structures under extreme lateral load. An attempt was made to provide a uniform distribution of shear to the wall through the use of two points to apply load and the use of a deep first story beam. The depth was selected to increase the moment at the base of the wall for a given applied force. The bottom of the beam at the top of the infill wall represented the girder design in the prototype building (see Figure 2.1).

Each specimen had two loading blocks on the top designed for load application. Each block was designed to transfer one half of the maximum shear (in either direction) expected in the full infill specimen. The blocks were designed with enough concrete to transfer the entire shear force without cracking and twice the steel necessary to transfer that same amount of shear. The steel was welded to plates on one end and anchored into the concrete below. The unusual reinforcement layout pictured in Figure 2.2 is the result of the large amount of steel in these loading blocks and in the first story girder.

The low aspect ratio of the model was expected to have a significant effect on the behavior of the specimen and on the shear strength. In a tall structure with a relatively large aspect ratio, lateral loads applied well above the base of the wall result in a large moment at the base of the wall. Since a ductile failure mode was desired in this investigation, analyses were undertaken to determine the moment shear relationship. Moment curvature response was



A) PLAN SECTION THROUGH  
LOADING BLOCK



B) ELEVATION

Fig. 2.2 Loading Block Reinforcement

determined for the full infill and the infill with the window opening (Figure 2.3). It was assumed that the infill with the window and the trim steel around the opening would carry moments in a manner similar to that of the full infill. The infill with the door opening was analyzed as two piers, each consisting of one column and the section of the wall on that side of the specimen. The piers were joined by a deep spandrel beam. Frame action of these two piers was analyzed considering the ends fixed. The length of the piers was assumed to be the distance from the base of the piers to the centroid of the deep beam. The section and the frame components are pictured in Figure 2.4.

Using the test specimen geometry, the force required to produce initial yield of the extreme column longitudinal bars of the full infill and the infill with the window opening was compared with the shear capacity of the wall (without the use of understrength factors) and the flexural strength was adjusted so that flexural failure would occur first. In the infill with the door opening, the shear required to produce yielding of the piers was compared against the strength in shear of those piers.

### **2.1.2 Materials**

**2.1.2.1 Concrete.** The material properties used in this investigation were chosen to be representative of construction of both the 1950's (for the frame) and current shotcreting practice (for the walls). The nominal concrete strength for the bounding frame was 4000 psi. Mix and batch proportions are listed in Table 2.1. The maximum size of the coarse aggregate was the size equal to or smaller than the smallest scaled bar spacing. The results of seven day, twenty-eight day and at test compressive strengths of the concrete in the bounding frames are listed in Table 2.2. These cylinders were cured under the same condition as the frames.

The nominal concrete strength for the shotcrete walls was 4000 psi. Since "wet process" shotcreting was used, the concrete was unloaded from a ready mix truck into the hopper of the pump and discharged through a nozzle. The shotcreting process is pictured in Figure 2.5. Standard cylinders were cast from the concrete dispatched from the ready mix truck at the beginning of the

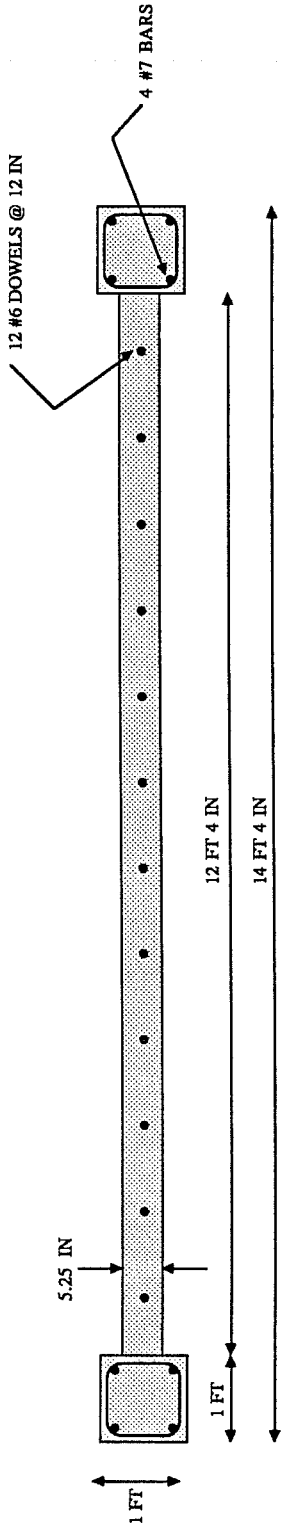


Fig. 2.3 Cross Section for Flexural Analysis, Full Infill & Infill with Window

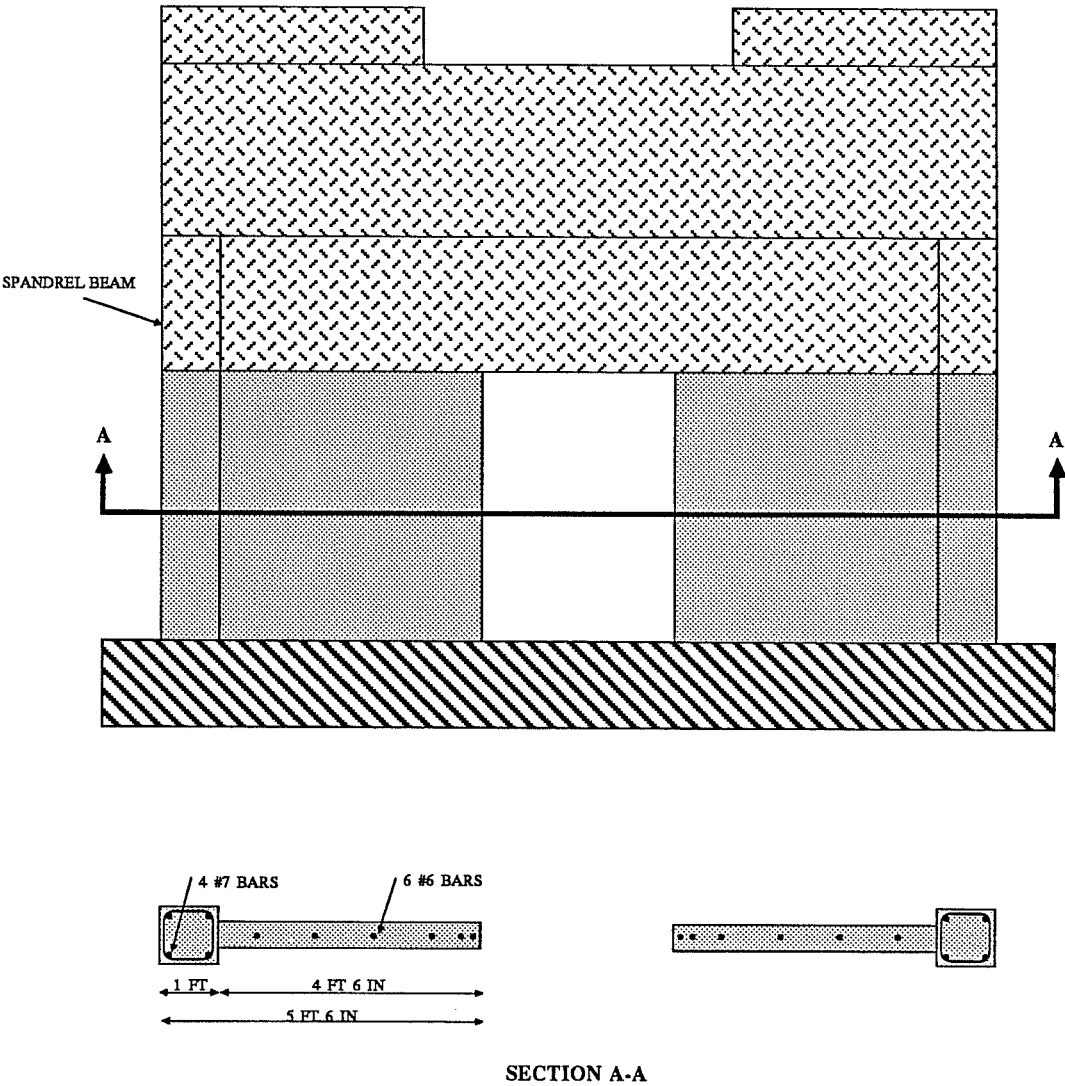


Fig. 2.4 Cross Section for Flexural Analysis, Infill with Door



**TABLE 2.1**  
**Concrete Mix and Batch Proportions for Frame Concrete**

Item	Mix Weight (lbs.)	Full Batch Weight (lbs.)	Window Batch Weight (lbs.)	Door Batch Weight (lbs.)
Cement	471	471	471	470
Sand	1655	1751	1751	1756
Water	250	279	287	250
Rock	1625	1625	1625	1625

**TABLE 2.2**  
**Frame Concrete Compressive Strengths (psi)**

Specimen	#1	#2	#3	Average
Full:				
7-D	3050	2930	2890	2950
28-D	3500	3660	3480	3550
@ Test	4380	3970	4100	4150
Window:				
7-D	4110	3730	4140	3990
28-D	5210	5340	5230	5260
@ Test	5470	5570	5710	5580
Door:				
7-D	3580	3490	3380	3480
28-D	4280	4150	4220	4220
@ Test	4770	4800	4820	4800

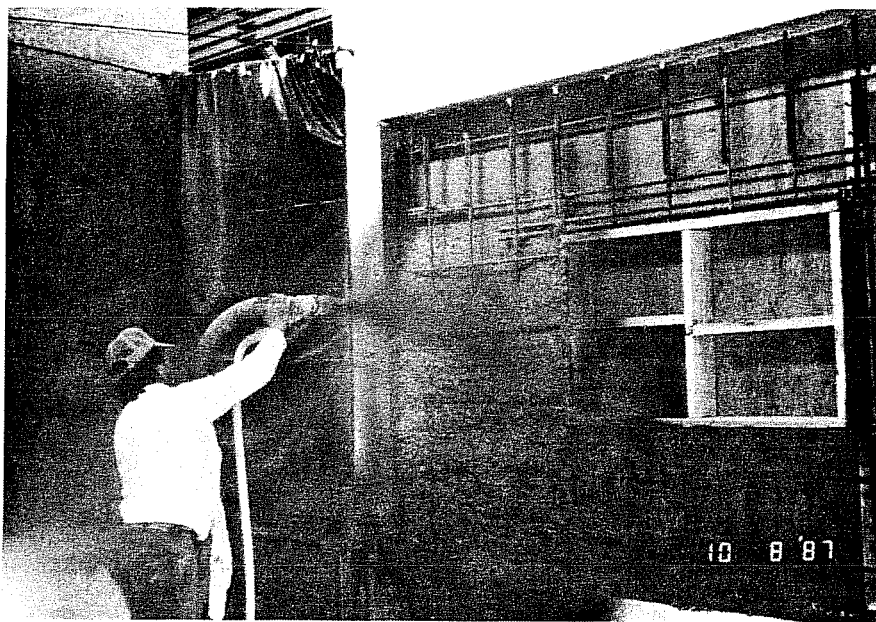


Fig. 2.5 Shotcreting Process

operation. Five test panels were constructed to obtain concrete cores for testing in compression. These panels were shot at various intervals during the shotcreting to reflect changes in strength as water was added. Reinforcement was placed in three of the test panels with the same reinforcement pattern as the walls. The test panels provided a means for determining the degree of consolidation achieved in the walls. Accordingly, the thickness of these test panels was 6 in., similar to the nominal value of 5.25 in. for the walls and almost equal to the actual wall thickness achieved in the specimens. The test panel is pictured in Figure 2.6. Seven day, twenty-eight day and at test compressive strengths are listed for both cores and standard cylinders in Table 2.3. The mix design specified by the shotcrete contractor is listed in Table 2.4. Actual proportions for the shotcrete were not made available. Inspection of the panels indicated that excellent consolidation was obtained in the shotcreting operation. However, visual inspection of the completed walls indicated voids in some critical locations. The repair of these voids is discussed later.

**2.1.2.2 Steel.** Reinforcement used commonly in the 1950's was Grade 40. Attempts were made to obtain Grade 40 reinforcement for column longitudinal steel and for column ties. However, it was not possible to procure steel with actual yield values near 40 ksi in bar sizes needed for the columns. For that reason, Grade 60 bars were used throughout. Grade 60 steel was specified for the design of the walls and the dowels.

**2.1.2.3 Epoxy.** The epoxy used to grout the dowels into the bounding frame was a two component, non-sag epoxy gel produced by Adhesive Engineering (Concresive 1411). The material was the same as that used in an earlier study of embedment of grouted dowels. However, in the earlier study, the epoxy contained a different filler. The change in filler altered the sag characteristics and pot life of the epoxy gel. Both variables were critical to the grouting operation. High temperatures in the lab were in excess of 95 ° and shortened the pot life significantly. Therefore, a series of pullout tests were conducted to verify the suitability of the epoxy and the grouting techniques for the test specimens.

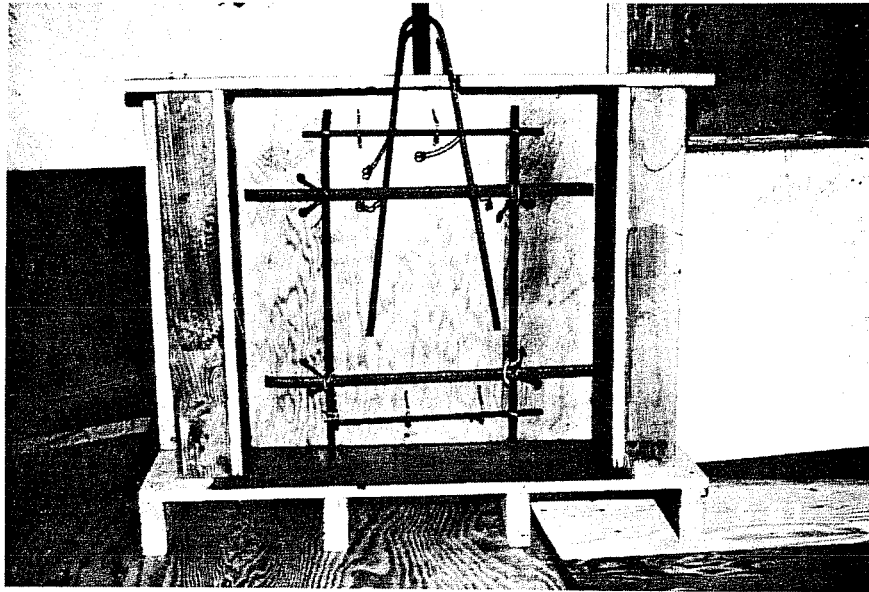


Fig. 2.6 Shotcrete Test Panel

Nine plain concrete blocks were utilized for the pullout tests. One inch diameter holes were drilled with a rotary drill to a depth of 9 in. The holes were vacuumed, brushed with a bottle brush to loosen dust clinging to the sides of the hole and vacuumed again. This was repeated until the holes were virtually dust free. Blocks were then placed so that grouting orientations simulating those required in the frames would be represented. Specifically, three blocks had horizontal hole orientations, three blocks had overhead holes and three had vertical (downward) holes. Epoxy was placed into the holes with a resealable caulking gun. The #6 bars were inserted into the holes with a twisting motion to remove entrapped air (Figure 2.7). Spacers (golf tees) were inserted as needed to position the bars while the epoxy was curing. Specimens were allowed to cure for six days before testing. The test set up is shown in Figure 2.8. A 30 ton center hole hydraulic ram was used to pull the bars.

Results from the tests are listed in Table 2.5. In all specimens, the reinforcement yielded before pull out failure. The failure cones were very shallow as illustrated in Figure 2.9. It was interesting to note that the reinforcement continued to hold a very large portion of the yield load as the bar pulled out. It was determined that the epoxy and the grouting procedure was satisfactory for grouting the dowels into the bounding frame.

Concresive 1411 was also used, following the manufacturer's advice, to patch cracks and voids in the shotcrete walls. Graded and colored sand filler was supplied by the manufacturer. This process is discussed later.

### 2.1.3 Construction Procedures

*2.1.3.1 Frame Construction.* The frames were cast horizontally for ease of forming and placing concrete. It was decided that the variation in concrete strength over the height of a column cast vertically was not enough to significantly affect behavior. The formwork consisted of three platforms forming one side of the frame and removable side forms that bolted to these platforms as illustrated in Figure 2.10. Because the temperatures during casting were high (greater than 90 °), the concrete was covered with wet burlap and plastic to

**TABLE 2.3**  
**Wall Shotcrete Compressive Strengths (psi)**

Specimen	#1	#2	#3	Average
7 - Day				
Cylinders	2330	2330	2260	2300
3x6-in. Cores	2370	2310	2010	2230
28 - Day				
Cylinders	2950	2620	2910	2830
3x6-in. Cores	3370	2730	3230	3110
@ Test: Full				
6x12-in. Cylinders	3100	3300	3240	3230
3x6-in. Cores	3523	3150	3450	3380
@ Test: Window				
6x12-in. Cylinders	3360	3430	3410	3410
3x6-in. Cores	3110	3080	-	3100
@ Test: Door				
6x12-in. Cylinders	3750	3500	3570	3610
3x6-in. Cores	3060	3360	3400	3270

**TABLE 2.4**  
**Shotcrete Mix Design**

Item	Mix Weight (lbs.)
Cement	658
Sand	2560
Water	308
Coarse Aggregate	495

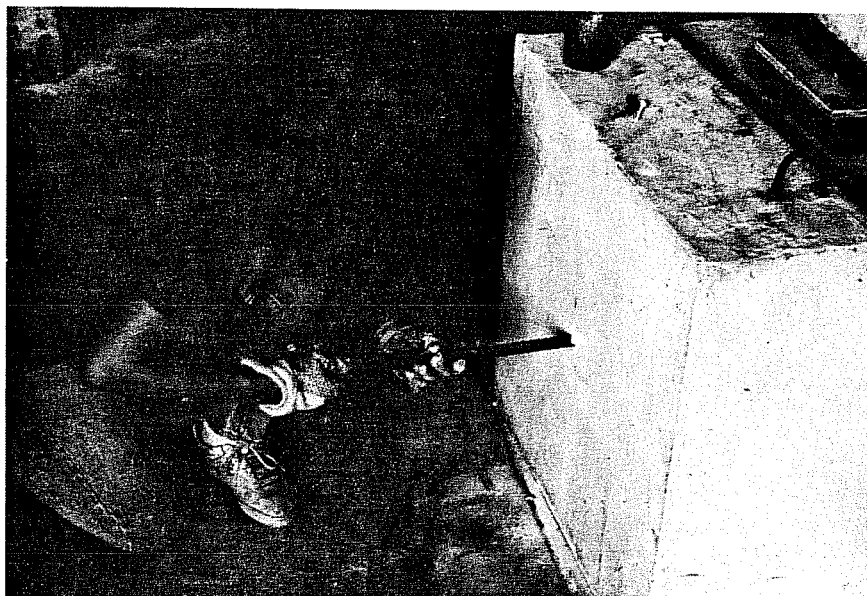


Fig. 2.7 Dowel Insertion in Pull Out Test Specimen

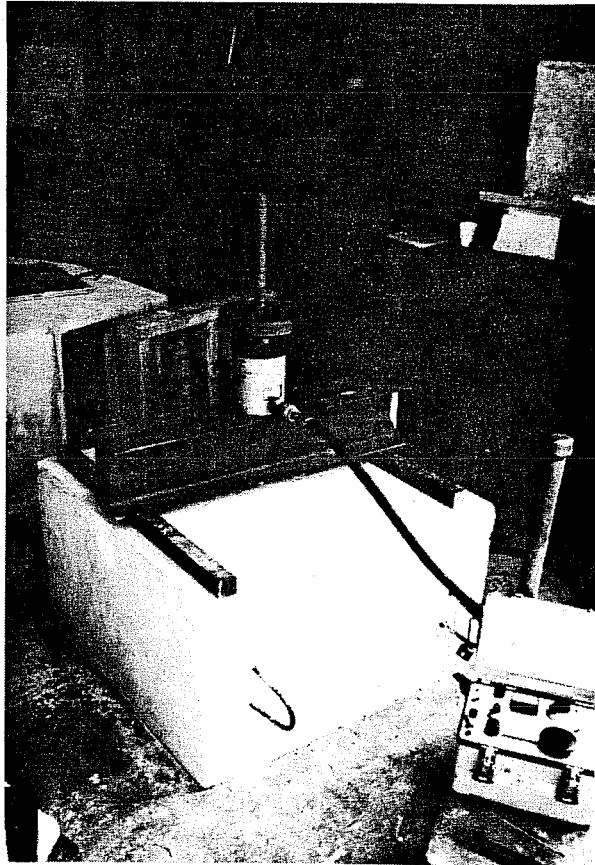


Fig. 2.8 Pull Out Test Set Up



**TABLE 2.5**  
**Epoxy Grouted Bar Pullout Results**

Grouting Orientation	Test Number	Maximum Load (kips)
Overhead	1	41
	2	39
	3	54
Horizontal	1	38
	2	33
	3	36
Down	1	30
	2	29
	3	33

NOTE: Nominal force to yield bar = 26.5 kips

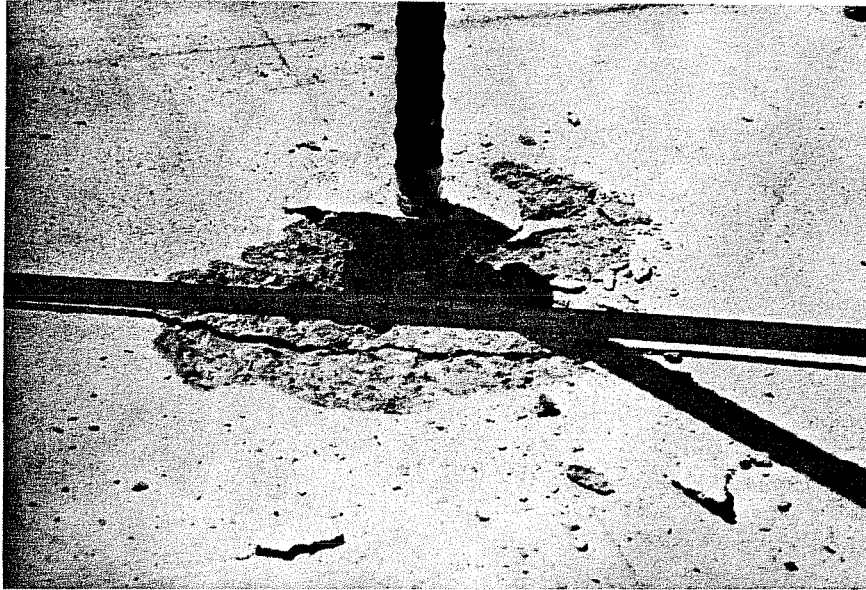


Fig. 2.9 Pull Out Failure

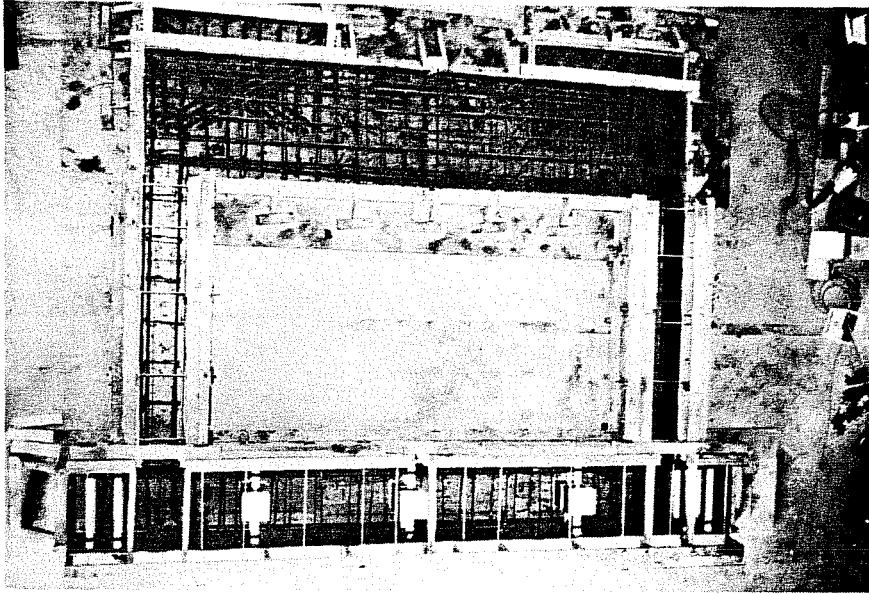


Fig. 2.10 Frame Formwork

provide proper curing conditions. After the concrete cured, side forms were removed and the frame was lifted off the platforms with the overhead crane. The specimens were rotated into their upright positions as illustrated in Figure 2.11. Frames were cast one at a time and all three frames were cast before the walls were built.

*2.1.3.2 Wall Construction.* Preparation of the bounding frames for the wall shotcreting involved several operations. First, one inch diameter holes for anchoring the reinforcing bar dowels were drilled to the specified embedment depth of 9 in. with a rotary drill, as illustrated in Figure 2.12. The cleaning operation was repeated until the hole was virtually free of dust. The holes were then sealed with tape until the dowels were grouted.

In the grouting operation, epoxy was injected into the holes with a caulking gun. The tip of the nozzle was placed at the back of the hole and epoxy was expelled. The caulking gun was slowly removed as the epoxy was placed. Dowel reinforcement was then placed into the hole with a twisting motion to expel any entrapped air. Dowels were positioned with golf tees for horizontal and vertical grouting orientations. Overhead bars were supported on a shelf, as illustrated in Figure 2.13. Grouted dowels were allowed to cure for several days before further construction proceeded.

Shear transfer across the column-wall and beam wall interfaces was enhanced by chipping the surface of the bounding frame to roughness with an amplitude of about 1/4 inch. Hand held and electric chipping hammers were used for this purpose. The resulting surface is shown in Figure 2.14.

The formwork for the infilled walls consisted of a panel of 3/4 in. plywood backed by 2 by 4 in. studs on 1 ft. centers. The studs were supported by walers on 2 ft. centers that were tied through the forms to the dowel reinforcement. Blockouts for the window and door openings were constructed of 2 by 6 in. studs cut to the wall thickness of 5- 1/4 in. and attached to the panels with screws. Forms were oiled prior to the shotcreting operation.

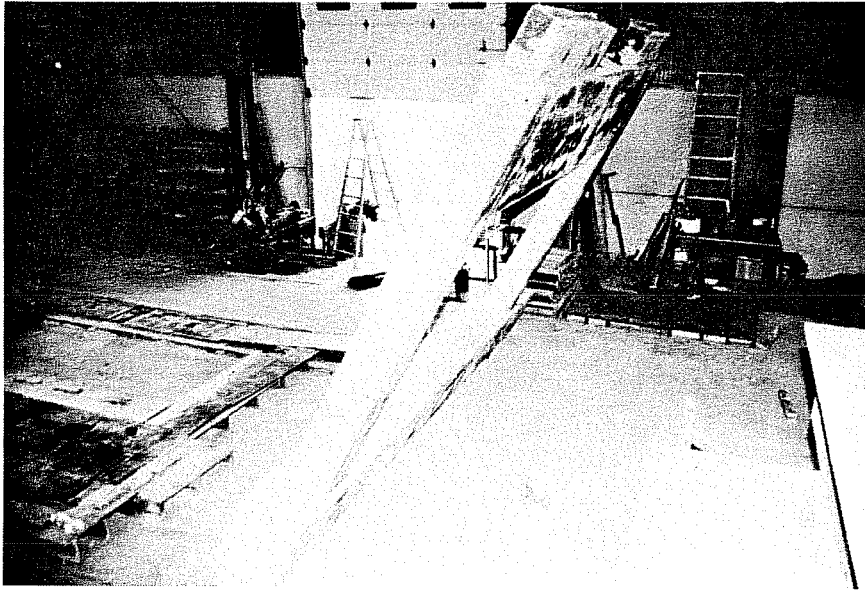


Fig. 2.11 Tilt Up of Bounding Frame

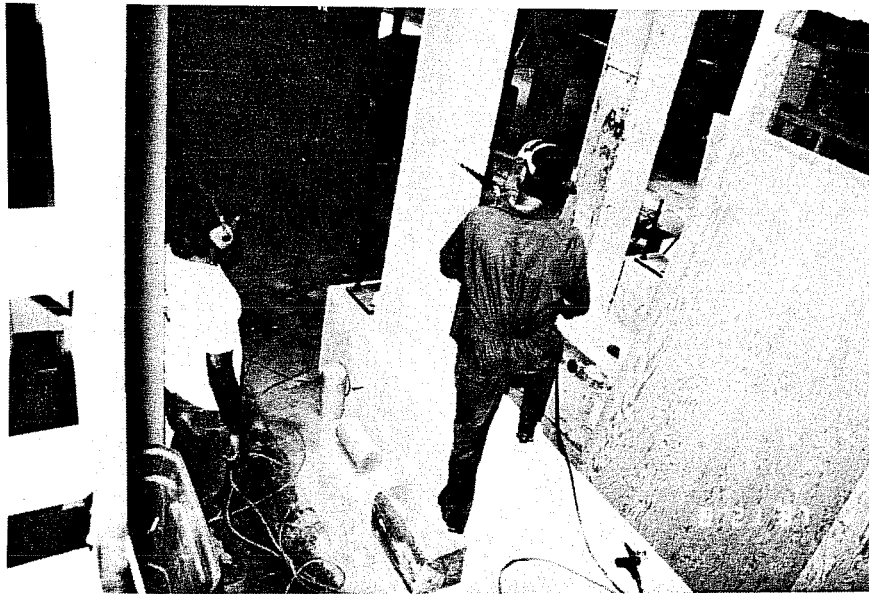


Fig. 2.12 Dowel Hole Drilling Operation

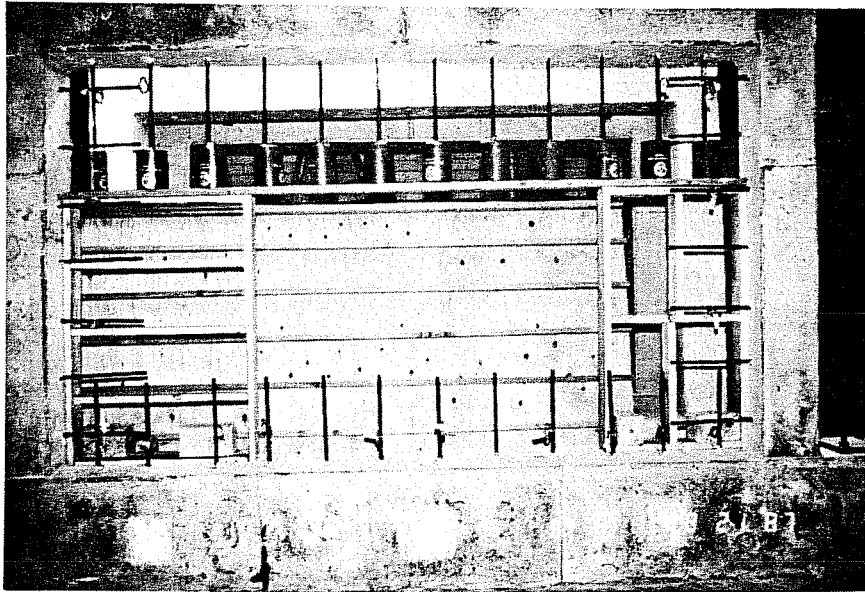


Fig. 2.13 Support of Overhead Dowels for Curing

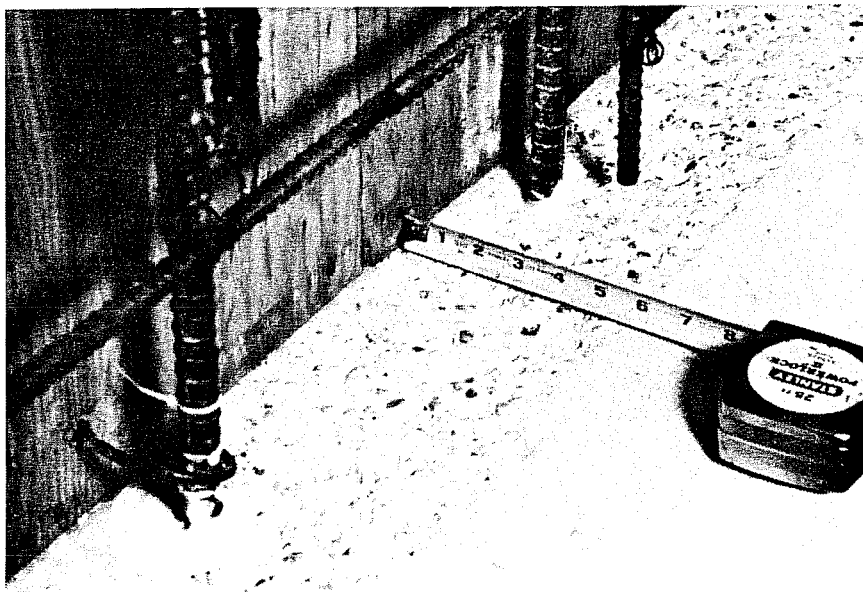


Fig. 2.14 Roughened Frame-Wall Interface



The wall reinforcement was tied to the dowels. The resulting layouts are pictured in Figures 2.15, 2.16, and 2.17. The three walls were shotcreted in an upright position at the same time by the same operator.

**2.1.3.3 Wall Repair.** One common problem in using shotcrete construction is the tendency for the shotcrete to “slump away” from the girder at the top of the wall. Crack widths of up to 1/2 in. have been noted in practice. These cracks are usually not repaired. It was anticipated that this might occur in the construction of the walls.

Visual inspection of the top boundary of the walls from the finished side following the shotcreting operation revealed minimal concrete slumping on this interface. More severe problems were revealed several days later when, upon removal of the formwork, large cracks and voids located at the top of the wall were found. Typical voids are pictured in Figure 2.18. The location of the voids was generally in areas where it was difficult to place concrete, behind dowels and wall reinforcement.

In many projects of this type, walls are shot against an existing masonry wall. Thus, the voids on the formed side are not visible and no further attention is given to the problem. However, it is assumed that the lack of consolidation on the formed side is typical in many infill walls.

The voids were found at locations critical to wall response. It was anticipated that large strut forces could not be transferred across sections with voids without local crushing. Several options were considered for repair of the top interface to eliminate the voids as a factor in wall behavior. It was decided that the best technique was epoxy gel injection with a caulking gun to fill the cracks and an epoxy grout applied with a trowel to fill the larger voids. The primary disadvantage of this type of repair in the field is the high cost of epoxy. A sand filler was added to the epoxy to more closely match the modulus of concrete and to reduce the amount of epoxy needed for patching.

Prior to placing the epoxy, loose concrete and aggregate was removed with a chipping hammer. In chipping loose material, additional voids were exposed. The cracks and voids were then cleaned with a vacuum with a flexible

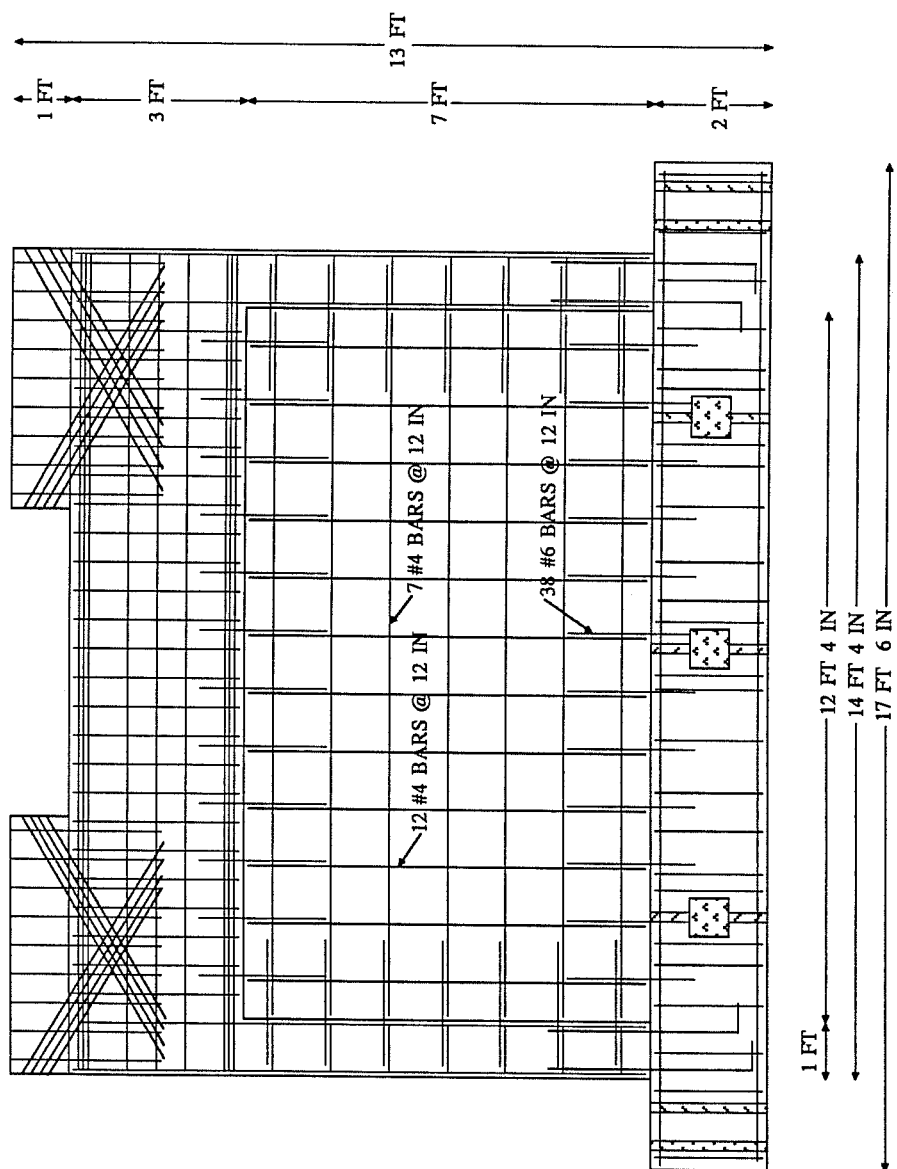


Fig. 2.15 Reinforcement Layout, Full Infill

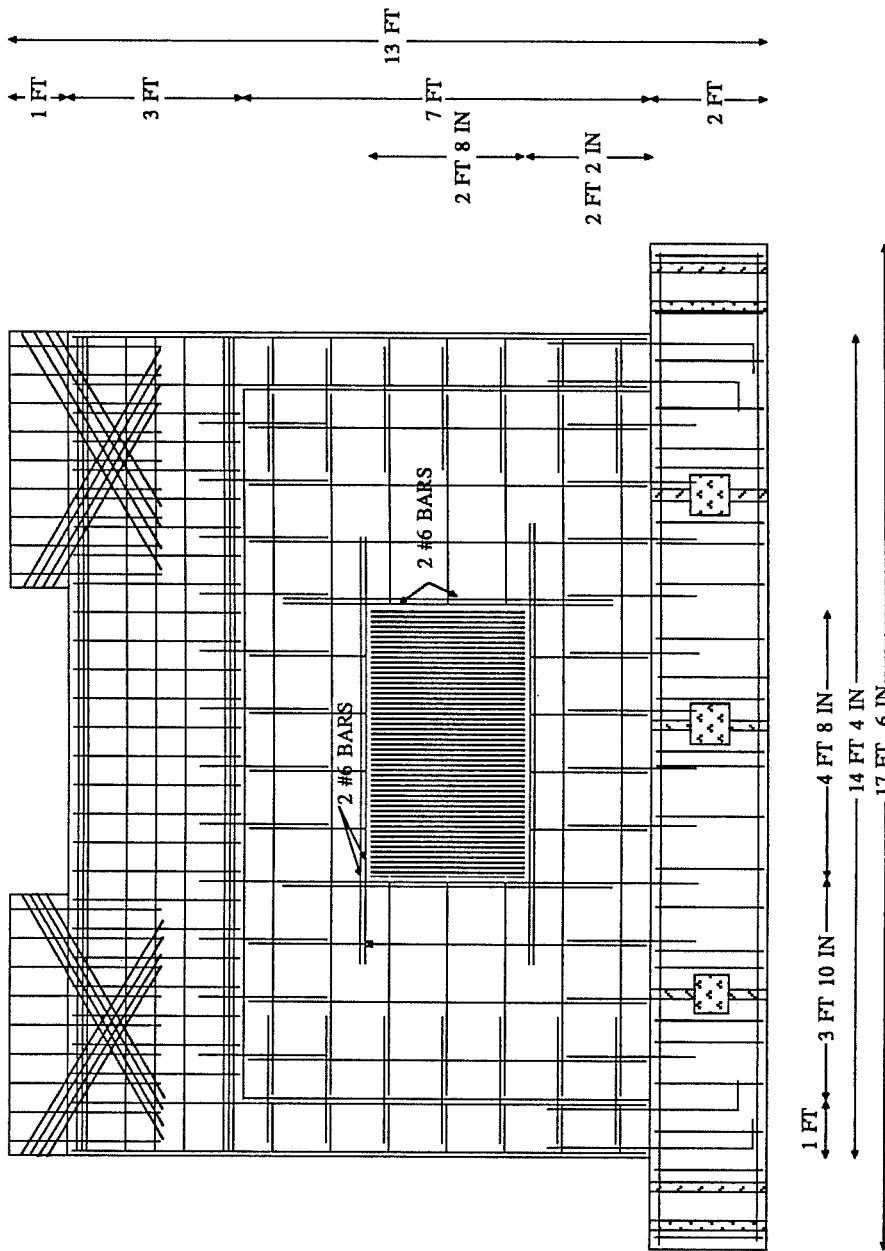


Fig. 2.16 Reinforcement Layout, Infill With Window

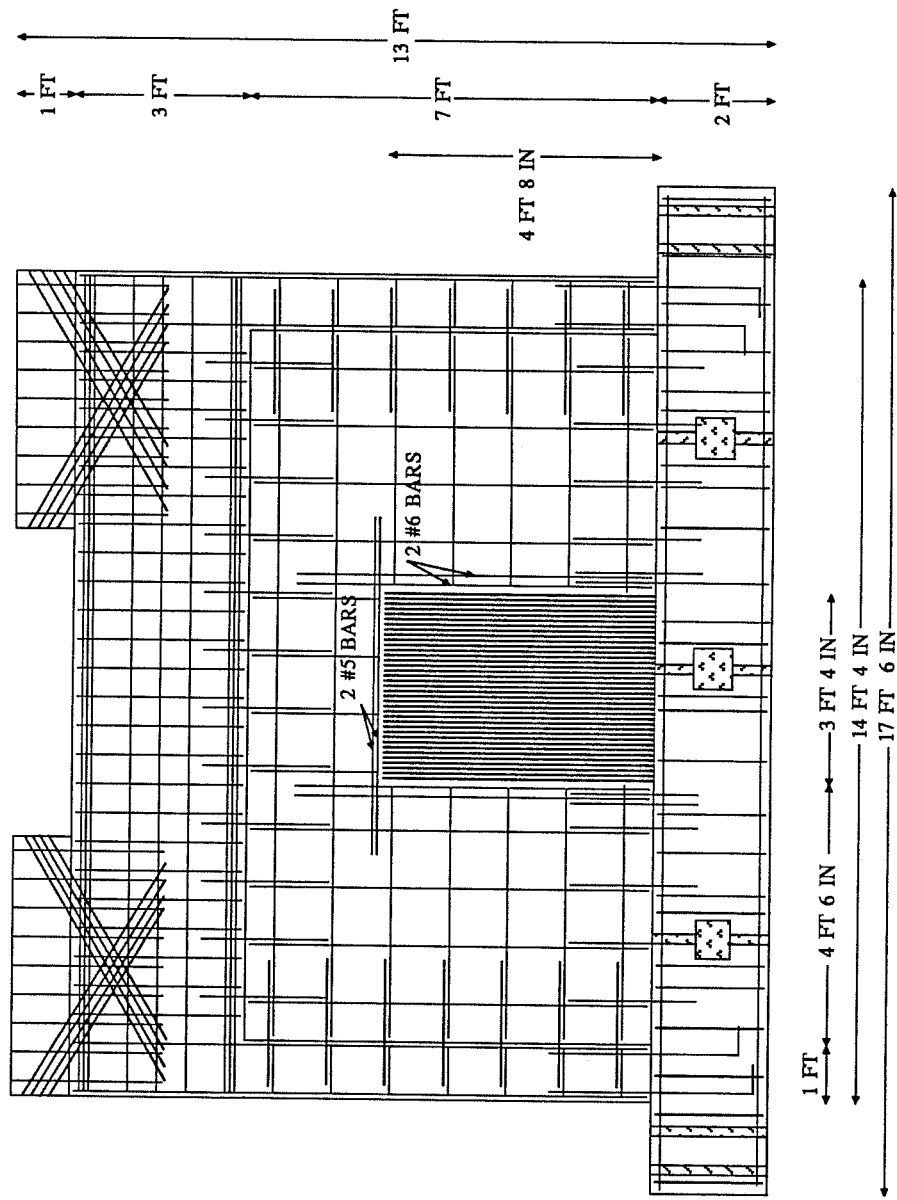


Fig. 2.17 Reinforcement Layout, Infill With Door

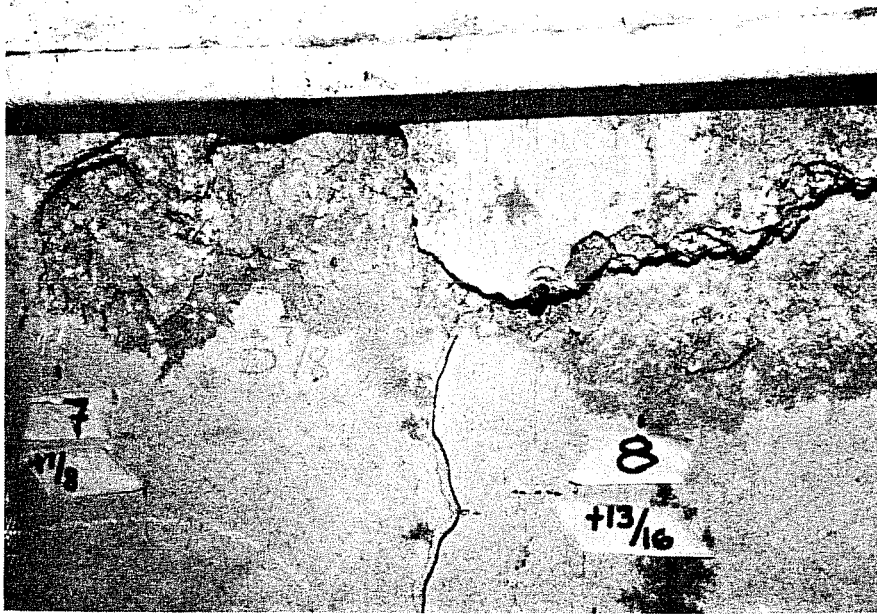


Fig. 2.18 Shotcrete Wall Voids

plastic hose extension on the end. The cleaning process was continued until the surfaces were relatively free of loose materials and sound concrete was left.

A resealable caulking gun was filled with epoxy and fitted with flexible plastic hose. The hose was then advanced into the narrow cracks and epoxy was injected as pictured in Figure 2.19. The gun was slowly backed out of the opening as the epoxy filled in around the tip. Using this process, the narrow cracks were entirely filled with the epoxy. The appearance of the interface upon completion of this step is pictured in Figure 2.20.

Patching the large voids with epoxy grout (sand filled) produced the best results when the plain epoxy in the cracks hardened. The grout was then placed with a trowel, as illustrated in Figure 2.21. Very deep holes had to be grouted in two steps to eliminate air pockets. The resulting surface is pictured in Figure 2.22.

Prior to testing, the specimens were checked for cracking and a network of hairline cracks were found in the shotcrete walls at dowel locations and at locations close to the voids that resulted from the shotcreting operation. The cracks are highlighted in Figure 2.23. The cracks likely were the result of thermal strains developed during curing. Cracks were initiated at the frame-wall boundary and ran toward the center of the specimen. Bonding between the bounding frame and the wall restricted expansion of the wall. The dowel locations were also a point of restraint. The voids constituted areas of weakness. A large temperature rise in the walls during hydration was driven by high ambient temperatures at the time of placement and the insulating effect of the formwork. The walls contracted upon cooling and tensile strains that developed resulted in cracking at the weakest sections and at points of restraint.

## 2.2 Test Set Up

**2.2.1 Loading.** Reversed cyclic lateral in-plane loading was used to simulate the effects of earthquake ground motions. Axial loads were not applied to the columns or the walls. Loads were applied statically. One cycle at low load level was applied to each specimen in order to verify instrumentation and



Fig. 2.19 Epoxy Injection of Crack



Fig. 2.20 Epoxy Injected Surface





Fig. 2.21 Patching Operation with Epoxy Grout

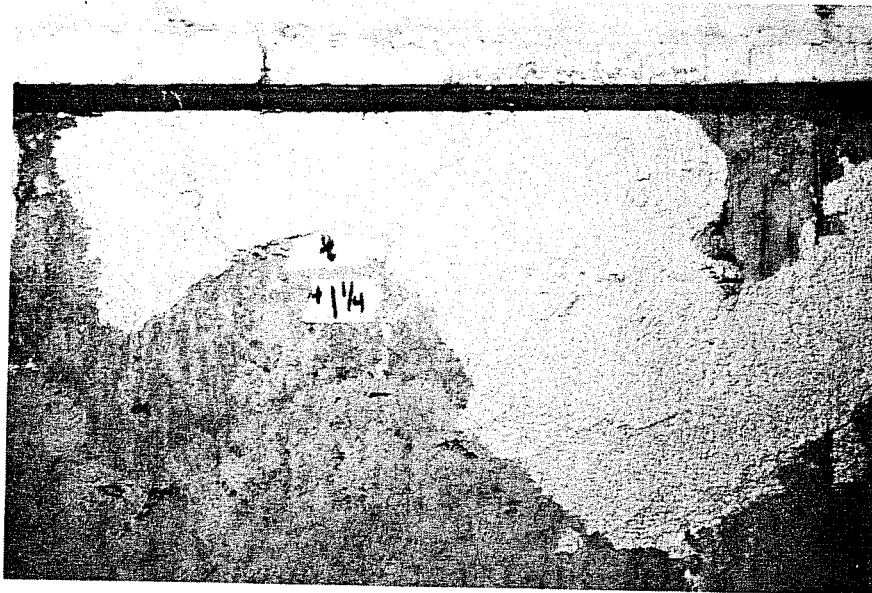


Fig. 2.22 Finished Epoxyed Joint

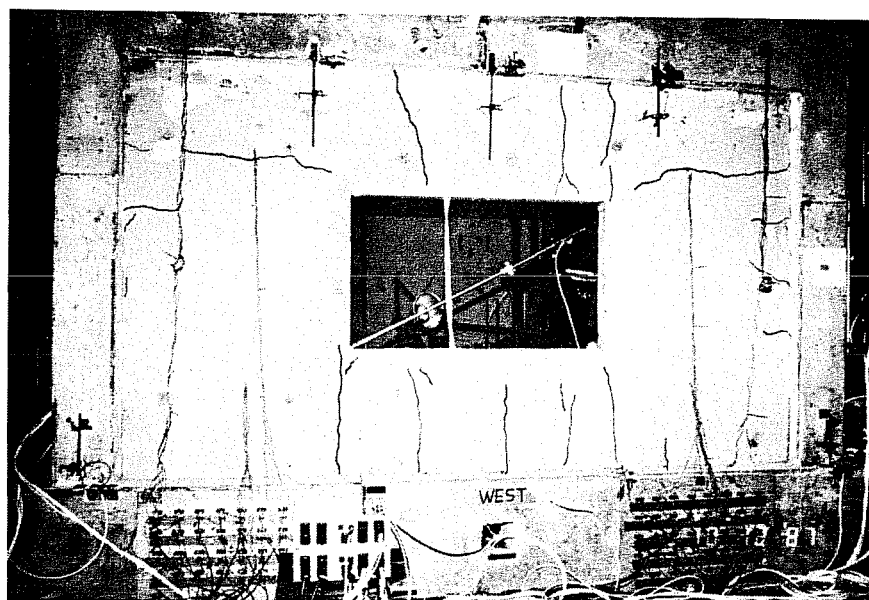


Fig. 2.23 Thermal Cracking

test procedure. Test specimens were then subjected to selected load or deflection levels. Load and drift levels were a function of the behavior of the specimen and the load-deflection histories of previously tested specimens. Specimens were subjected to several reversed cycles to the same level of load or deflection in order to quantify the cyclic degradation. In all cases, the applied load or deflection was monitored and controlled continuously by an X-Y plotter.

Loads were applied to the top of the specimens through the loading blocks. Four 100 ton hydraulic rams were used to apply load. Only two rams were activated for loading in a given direction. The idle rams were retracted. The rams were held in a loading frame that was attached to the reaction wall. Details of the assemblage are provided in Figure 2.24.

The base of the test specimens was set in cement grout. The grout provided uniform contact on the bottom surface of the specimens. After the grout cured, the specimens were then bolted to the reaction floor at five locations. Tie locations were spaced at four foot intervals. On either end of the test specimen, four 1-1/4 in. diameter bolts were stressed to provide a clamping force of 200 kips on each end. Intermediate ties utilized two bolts which were stressed to provide 40 kips of clamping force at each location. This arrangement provided fixity at the base of the walls.

*2.2.2 Data Acquisition.* Strain gages were placed on the reinforcement at critical sections of the specimens. Linear potentiometers were used to measure displacements at various locations.

The approach taken in gaging the steel in the frames was to concentrate on the areas that were expected to have the highest damage, namely the joints of the frame. The number and location of strain gages in the bounding frames was the same for all specimens. Gages in the wall reinforcement were placed to provide strain distributions along horizontal and vertical critical sections at openings and at the base of the specimen. Consequently, the number and location of gages in the specimens varied. The total number of strain gages placed in each specimen was about 70. A total of 59 quarter bridge channels were read during

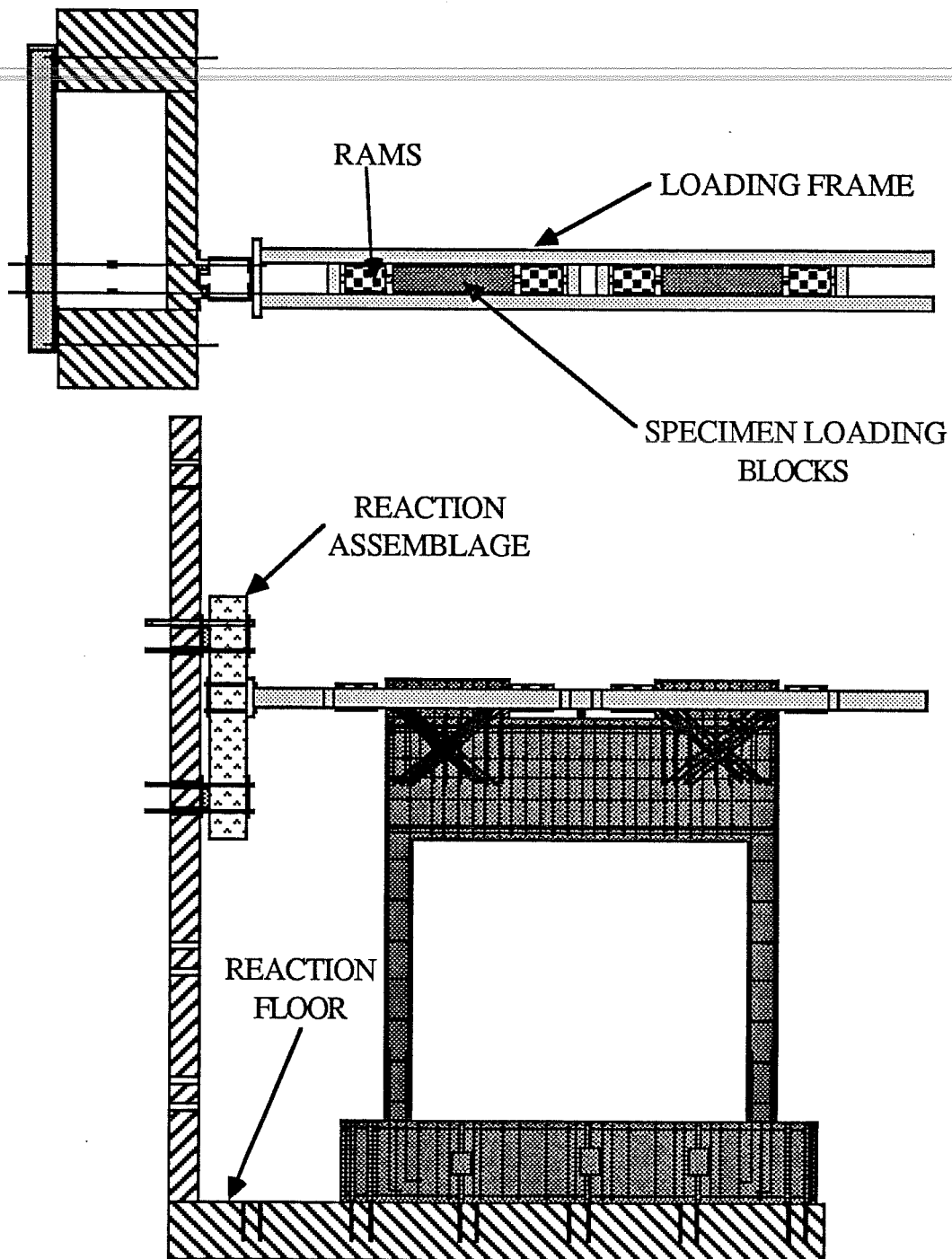


Fig. 2.24 Loading Frame and Reaction Assemblage

the test as some of these gages were intended as back up gages in case critical gages were lost during casting or testing.

Potentiometers were utilized to establish the lateral and shear deformations of the test specimen, the slip between the top of the wall and the bottom of the first story girder, and column extensions. The number and arrangement of the potentiometers varied for each specimen. The potentiometers were checked against a dial gage mounted at the same elevation as one of the linear potentiometers. Illustrations of the instrumentation schemes are found in Figures 2.25, 2.26 and 2.27.

A pressure transducer was used to monitor the applied load. The load was determined from the hydraulic line pressure and the ram area. The output of the transducer was verified by a pressure gage.

A microcomputer was used to acquire and reduce the data. This system read the status of the instrumentation at each load stage and converted it to digital format. Voltages were reduced to engineering units. Hard copies of the results were printed at the test site.

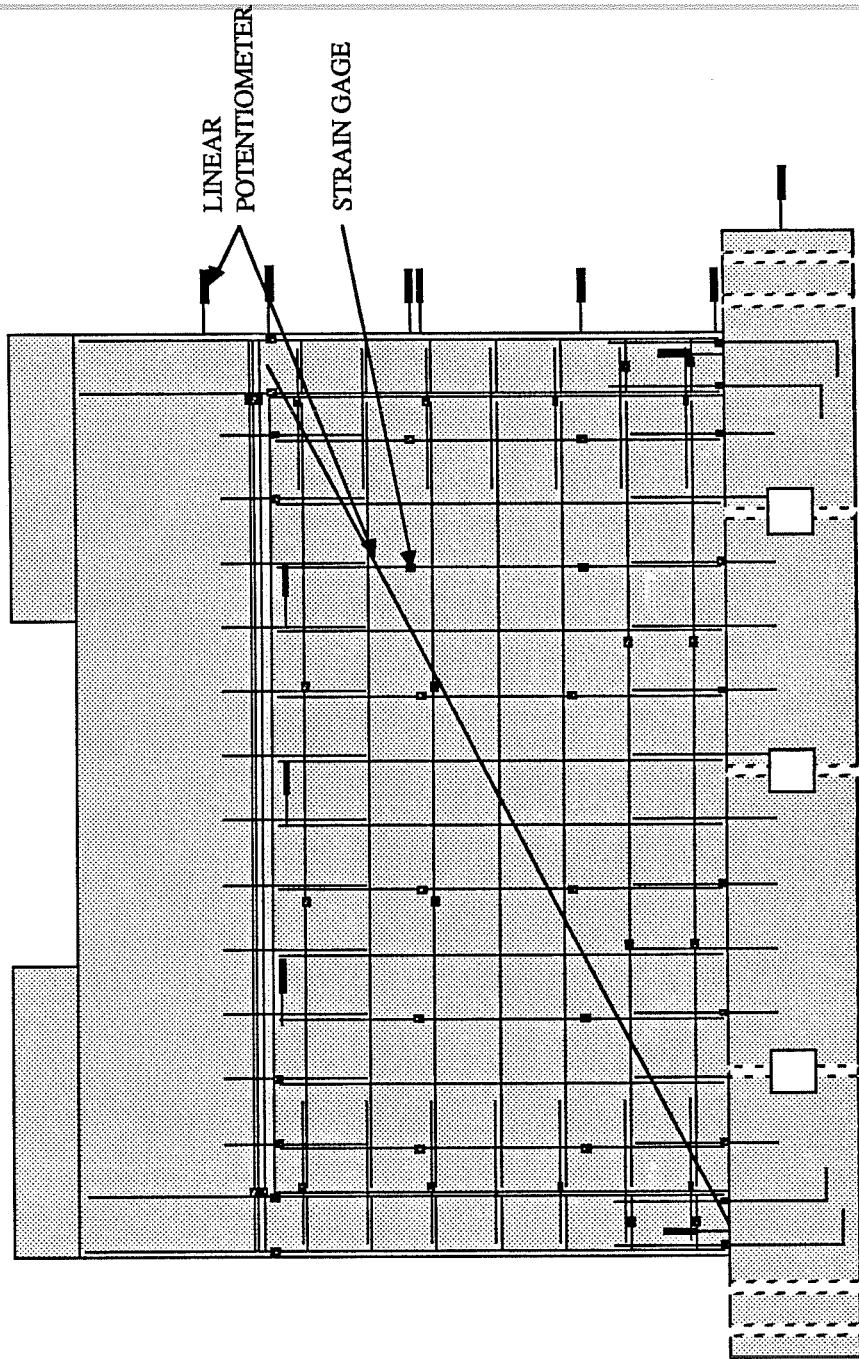


Fig. 2.25 Instrumentation, Full Infill

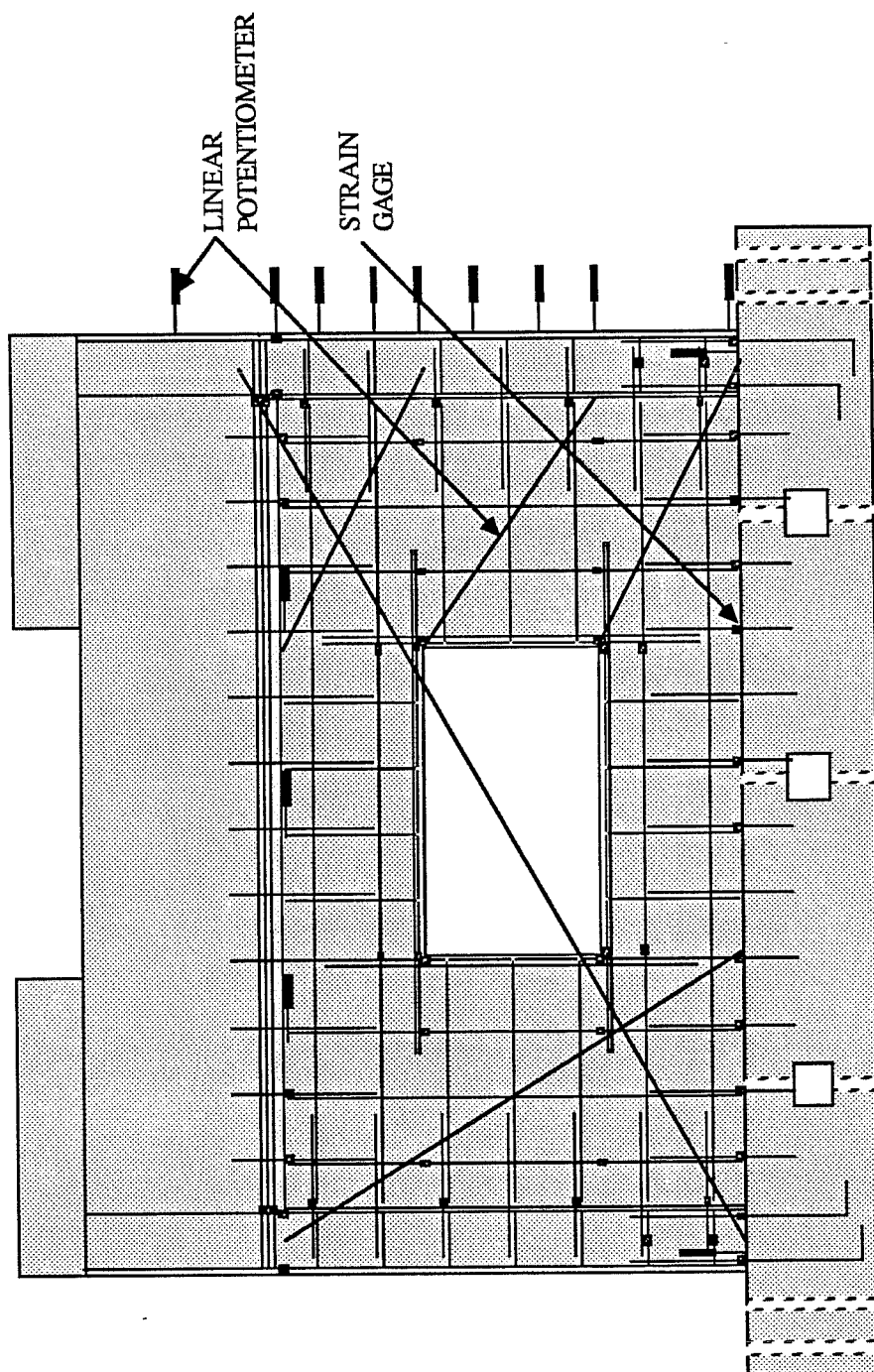


Fig. 2.26 Instrumentation, Infill with Window



## CHAPTER 3

### EXPERIMENTAL RESULTS

---

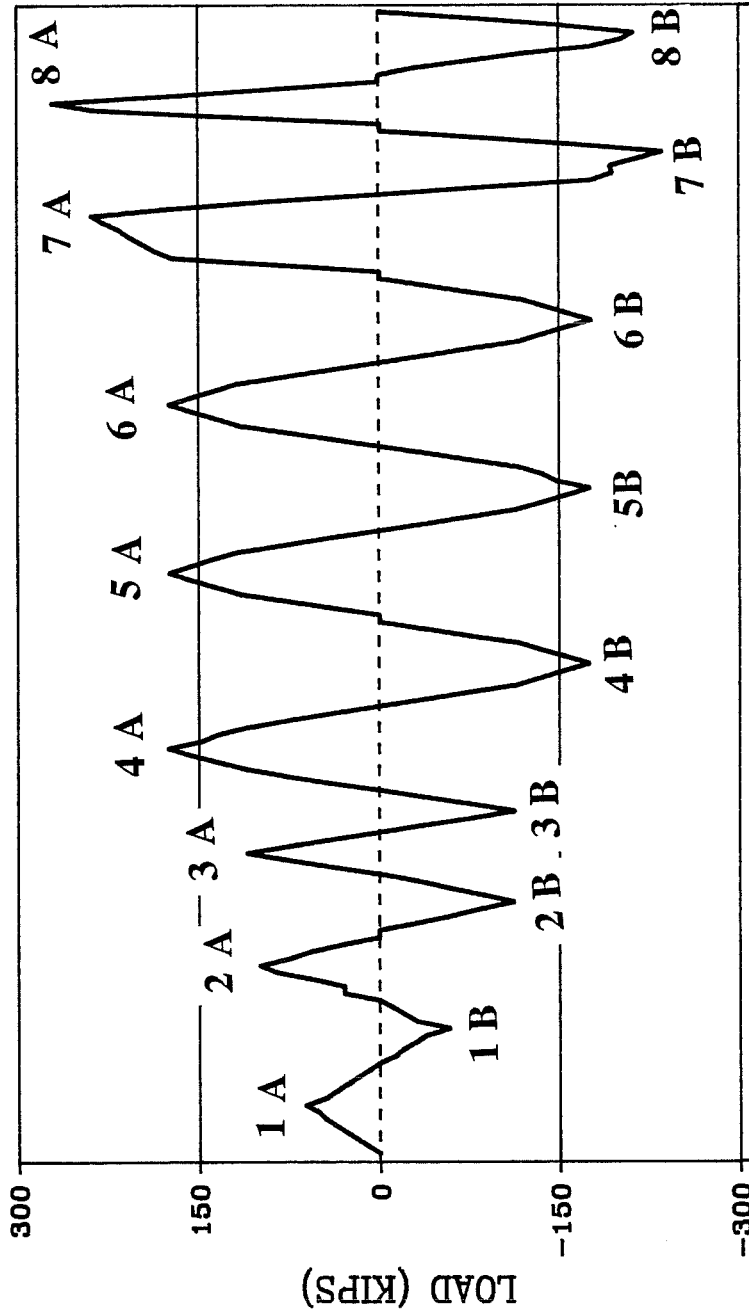
#### 3.1 Full Infill Specimen

**3.1.1. Condition of Specimen Before Testing.** The full infill specimen was tested first and formed the basis for the loading histories for the other two specimens. It was anticipated that the full infill would present the best behavior in terms of load and deformation capacity. It was subjected to two cycles of load to 120 kips, three cycles of load to 180 kips, one cycle at 240 kips and one cycle to a drift of 0.5%. The load history is presented in Figure 3.1. The load-deflection history is presented in Figure 3.2. In all load-deflection curves presented in this paper, positive load and positive deflection correspond to loads and drifts in what will be hereafter referred to as the “positive direction.” The positive direction is the direction of first loading for a specimen. The direction of first loading was chosen to be the direction least affected by the location of the epoxied voids. The letters “A” and “B” refer to the first and second half cycles of one full reversed cycle. In general, the half cycle in the positive direction is labelled “A” and the half cycle in the negative direction is labelled “B”. The cycles are numbered for reference. Cycle 1 is the cycle in which instrumentation was verified, and so is not presented here. However, the first cycles are discussed in Chapter 4. In referring to the two ends of the specimen under loads in a given direction, the terms “upload” and “download” refer to the ends of the specimen as labelled in Figure 3.3.

#### 3.1.2 Cyclic Response.

*Cycles to 120K.* The infill without openings was subjected to two full reversed cycles to 120 kips. “Drift” refers to the lateral deflection at the top of the wall divided by the height of the wall. The load-deflection history for these two cycles is presented in Figure 3.4. The cracking after loading to 120 kips is shown in Figure 3.5.

In the first cycle to 120 kips, horizontal cracks formed across the upload column at the second, third, fourth and fifth column ties from the bottom of the



LOAD STAGE

Fig. 3.1 Load History, Full Infill

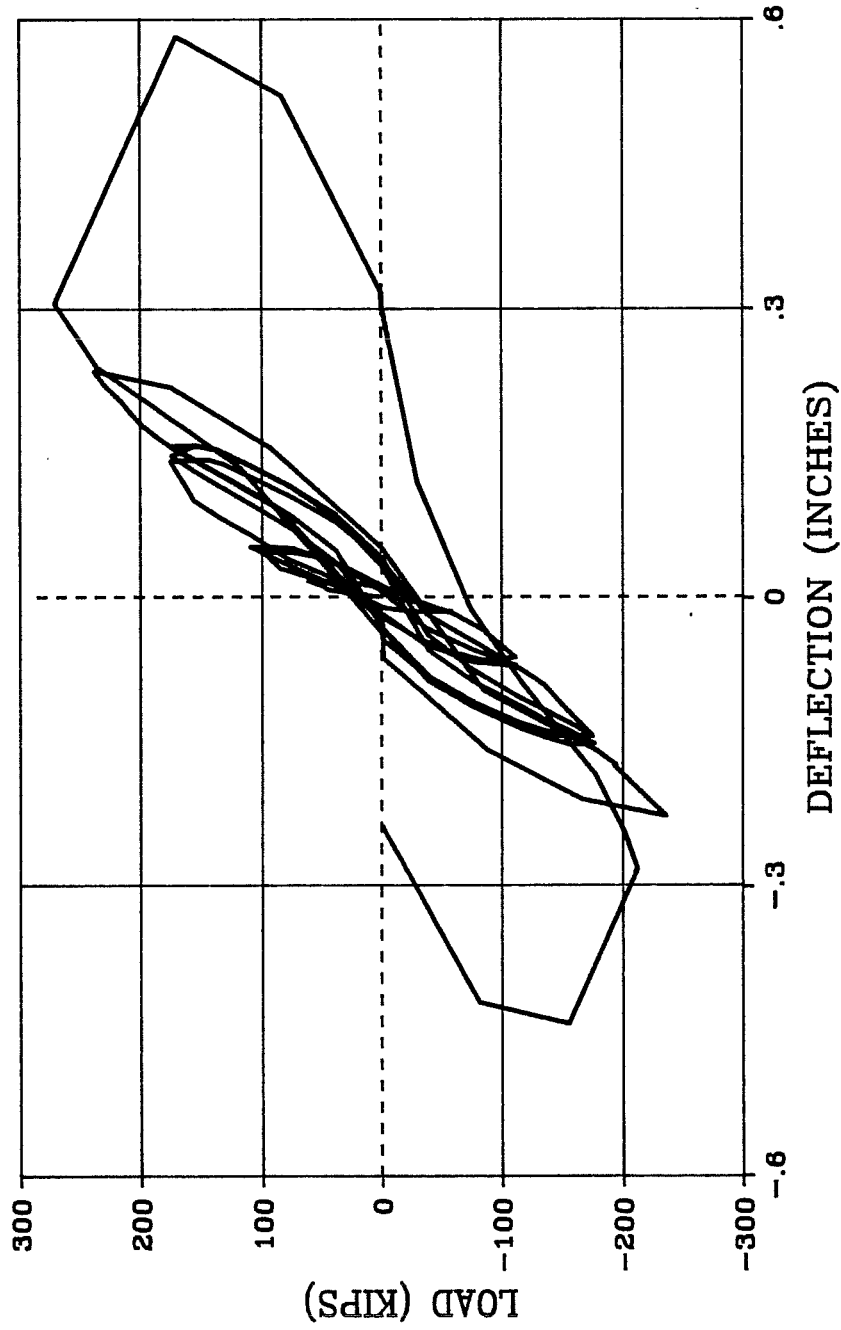


Fig. 3.2 Load-Deflection History, Full Infill

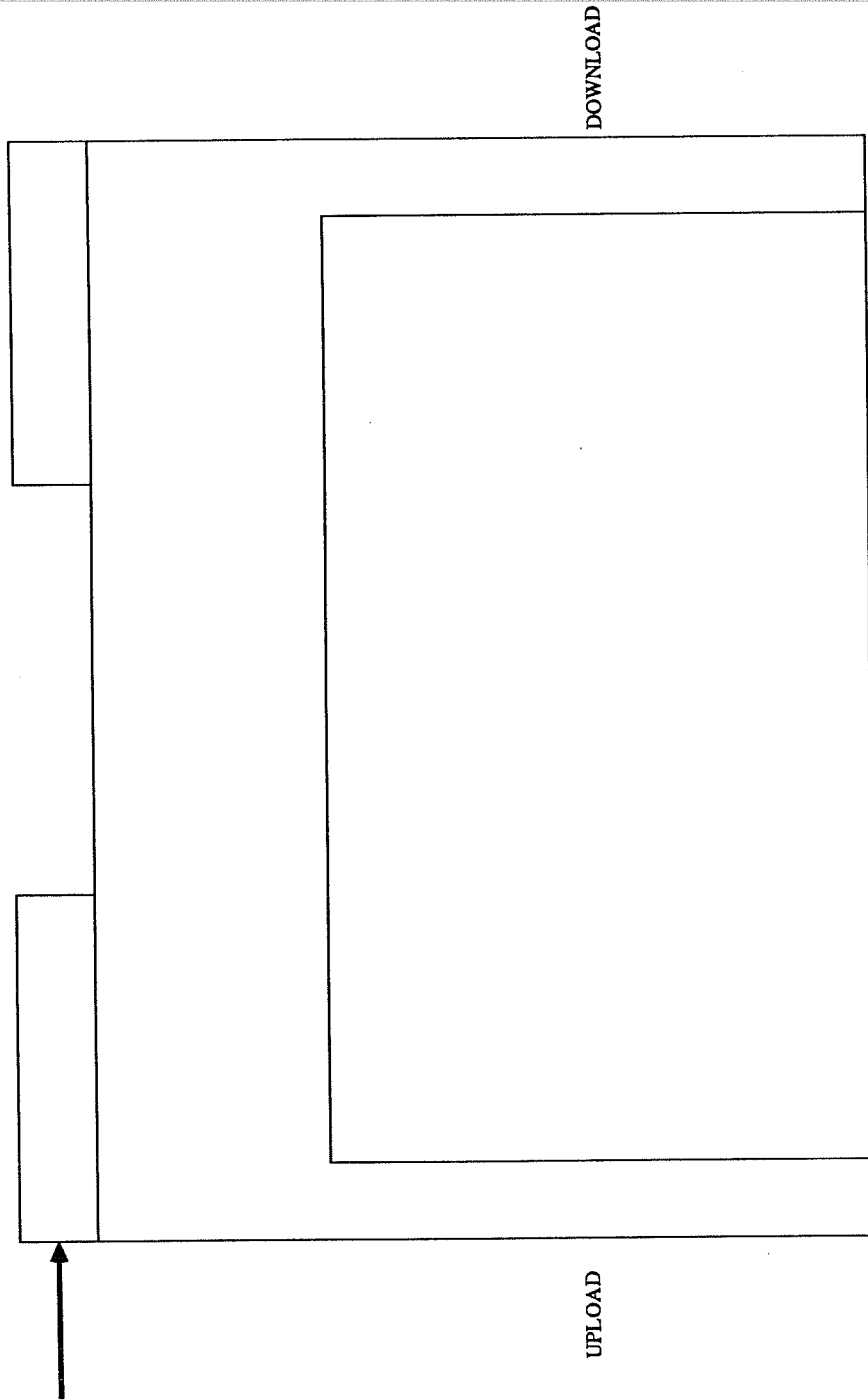


Fig. 3.3 Definition of Specimen End Under Load

# FULL INFILL

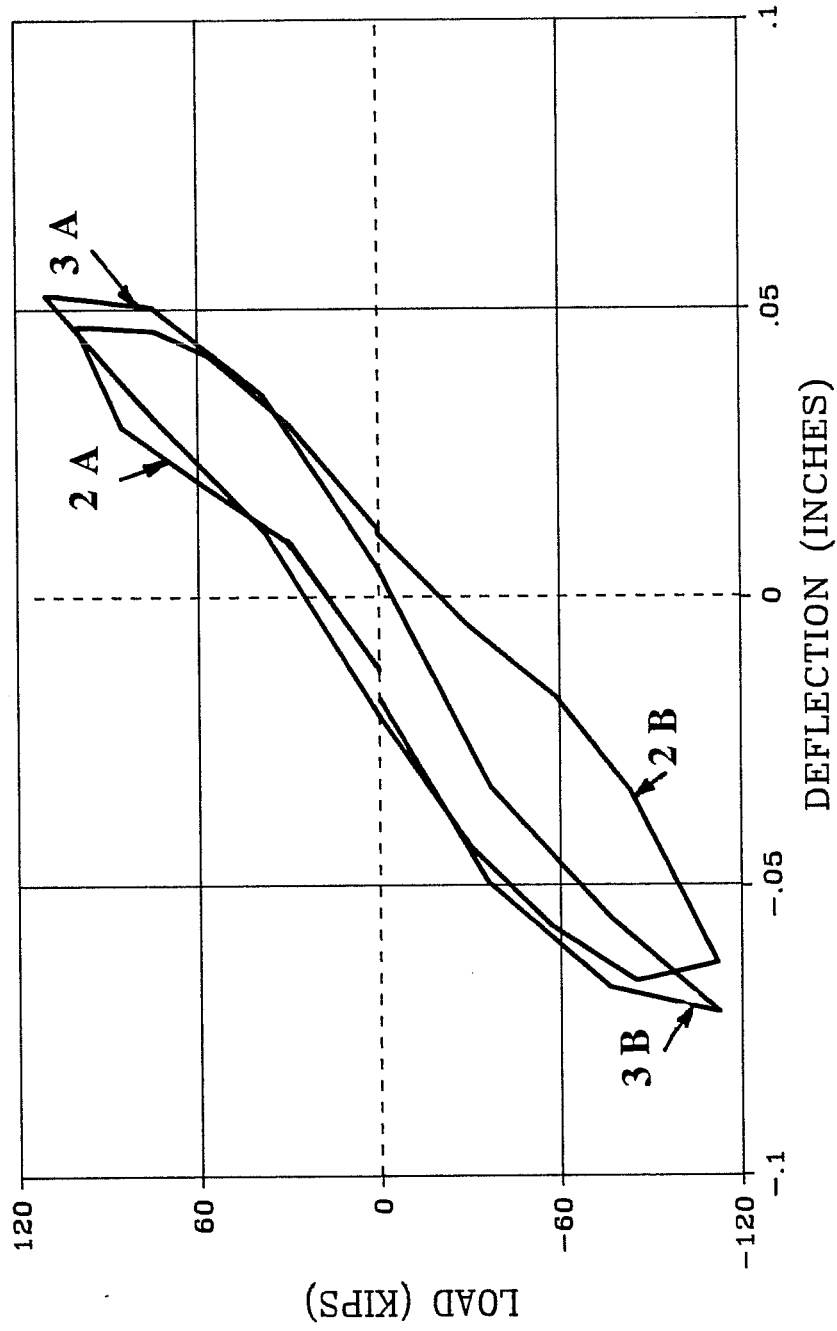


Fig. 3.4 Load-Deflection Response, Cycles to 120 K

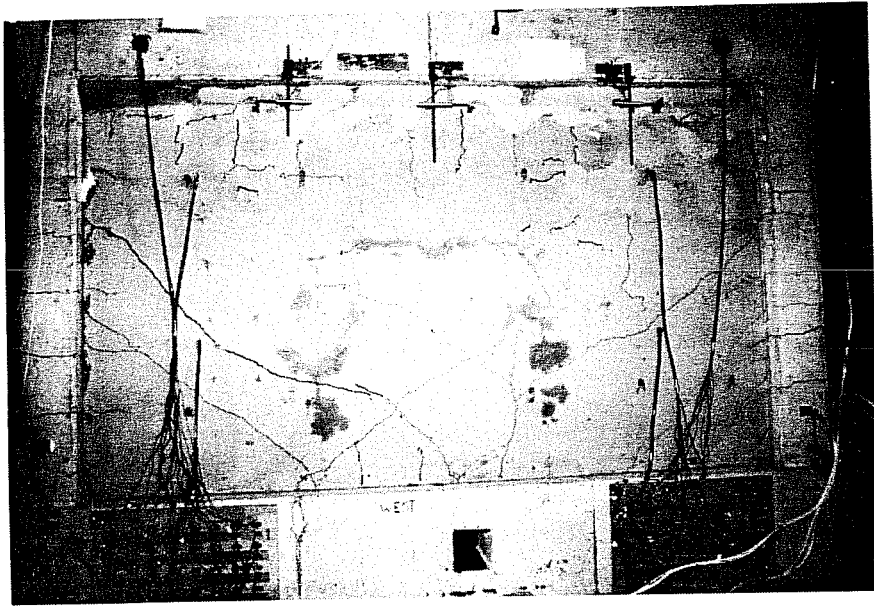


Fig. 3.5 Crack Patterns, Cycles to 120 K

wall. Cracks also appeared at the base on the exterior of the upload column and at the base on the interior (the side in contact with the wall) of the download column. Inclined cracks appeared in the wall panel that, in some cases, appeared to be flexure-shear cracking, extending from the horizontal cracks in the column on the frame-wall boundary. The inclination of these cracks was about  $45^\circ$  from horizontal. Stiffness in the negative direction was 71% of the stiffness in the positive direction. "Stiffness" refers to the peak load attained divided by the sum of the lateral deflection at the top of the wall and the residual deflection present at zero load. This difference in stiffness in the two directions occurred in each of the specimens during initial cycles and was attributed to cracking which occurred under loading in the negative direction. Average drift in this cycle was 0.07%.

Strains in the dowels at the base of the wall and in the column bars are shown in Figures 3.6 and 3.7. Note that the entire wall-column section is acting as a cantilever with the upload column and portion of wall in tension and the download wall in compression. The download column appeared to deform independently of the infilled wall with tension on the inside face and compression on the outside face. There was no apparent degradation of the wall-column interface which would have enabled the wall to slip relative to the column. This effect was more pronounced when loading in the negative direction (Figure 3.7) than in the positive direction (Figure 3.6). Throughout the test, dowels embedded in columns exhibited very low strains, as did instrumentation on panel steel except where cracking was close to or over a gage location.

In the second cycle to 120 kips, some cracks formed in the joint between the girder and the top of the upload column. Inclined cracks appeared in the wall at mid-height and mid-width. In this cycle, the wall stiffness in the two directions was nearly equal. The average stiffness in this cycle was 82% of the average stiffness in the first cycle to 120 kips.

*Cycles to 180K.* Three reversed cycles of load to 180 kips were applied. During these cycles, the deflections in the negative and positive directions were remarkably symmetric. The drifts noted in these cycles averaged 0.17% in the

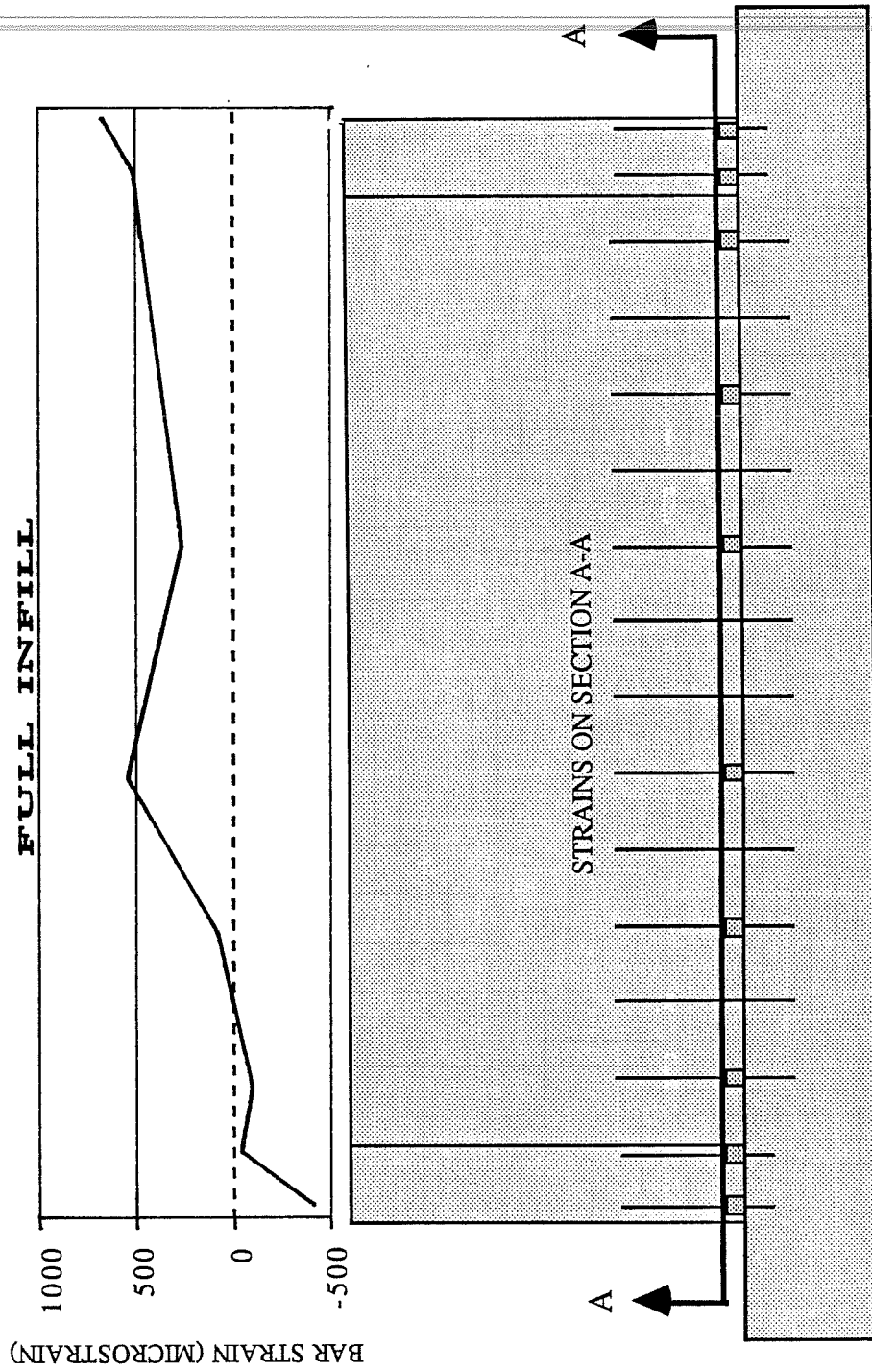


Fig. 3.6 Strain Profile, Cycles to 120 K, Positive Load



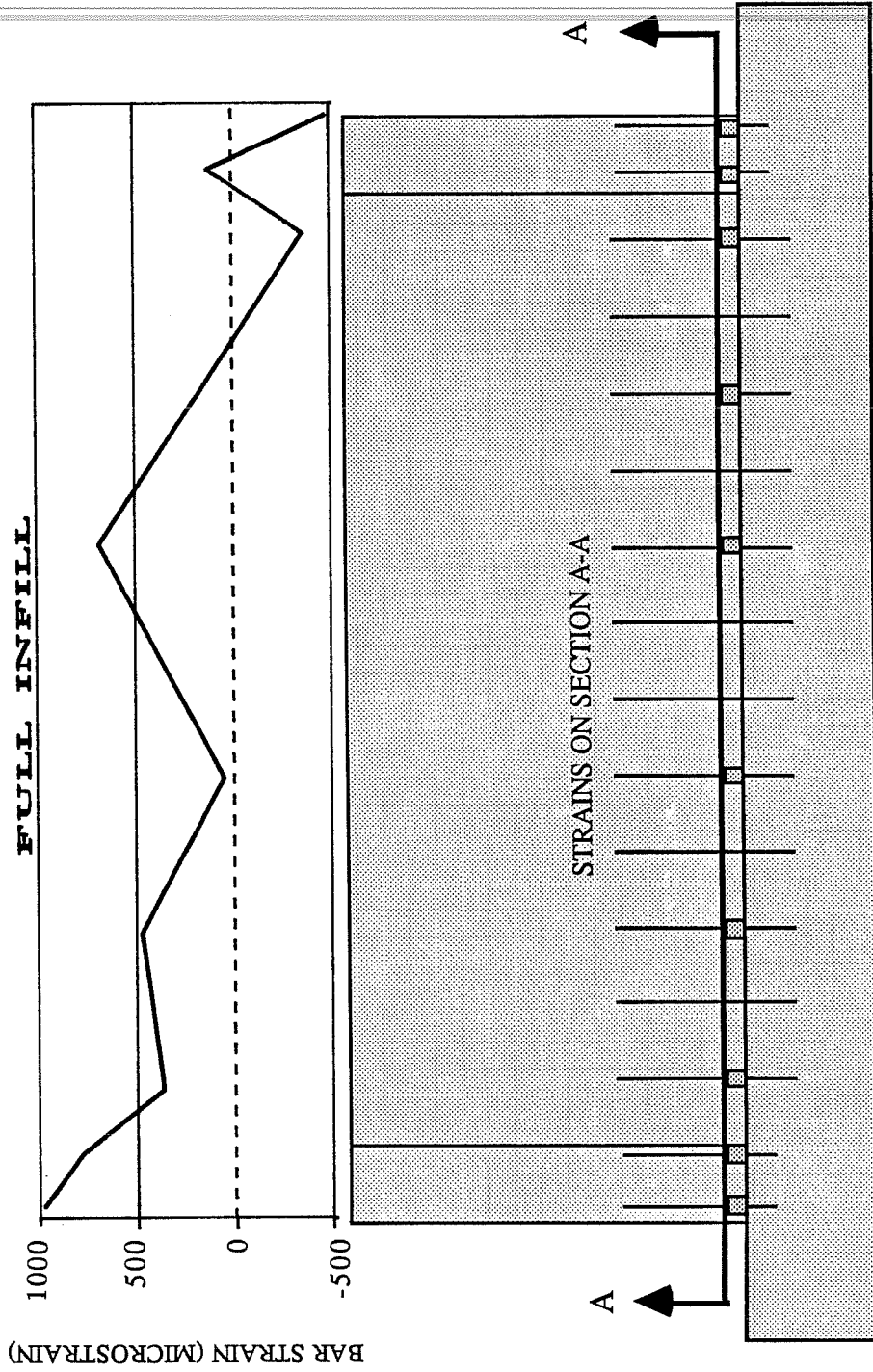


Fig. 3.7 Strain Profile, Cycles to 120 K, Negative Load

first cycle to 180 kips, 0.17% in the second cycle and 0.18% in the third cycle. The load-deflection curves for the three cycles to 180 kips are presented in Figure 3.8. The load-deflection curves showed the typical pinching of the loops which indicated advanced degradation of the specimen and decreasing energy dissipation. On the loading part of the curve, the initial stiffness from zero load to the first load stage was very low. As cracks closed under reversed loads, stiffness increased significantly from this initial value. Crack patterns in the specimen after cycles to 180 kips are pictured in Figure 3.9. During the first cycle to 180 kips, new inclined cracks extended from corner to corner of the wall at roughly an inclination of  $35^\circ$ . Some large extensions of previously formed inclined panel cracks were found. The crack patterns indicate that large compression struts were forming in the wall. Additional horizontal cracks were found high in the columns and in the top column-beam joint of the frame. The average stiffness of the wall in this cycle was 70% of that exhibited in the second cycle to 120 kips. The "average" stiffness in a cycle is the average of the stiffness as defined previously for two half cycles. This was a significant loss of stiffness. The stiffness in the negative direction was 88% of the stiffness in the positive direction. Strains at the base were nearly constant over about half the width of the wall. The extreme column bar on the upload side was nearly 75% of the yield strain in tension. This distribution did not vary appreciably for additional cycles at the same load.

During the second cycle to 180 kips, new horizontal cracks appeared near the bottom of the upload column. Small vertical cracks formed in the corners of the columns approximately two feet from the base. New cracks formed in the wall again indicating mobilization of previously undamaged sections of the wall. Some large extensions of inclined panel cracks were also noted. The stiffness of the wall in this cycle was 95% of the stiffness exhibited in the first cycle to 180 kips.

During the last cycle to 180 kips, no new major cracks were noted. Some inclined cracks appeared in the upper joint on the upload side of the specimen. Small extensions of inclined cracks in the panel were found. The stiffness of the wall in this cycle was 95% of the stiffness in the second cycle and

# FULL INFILL

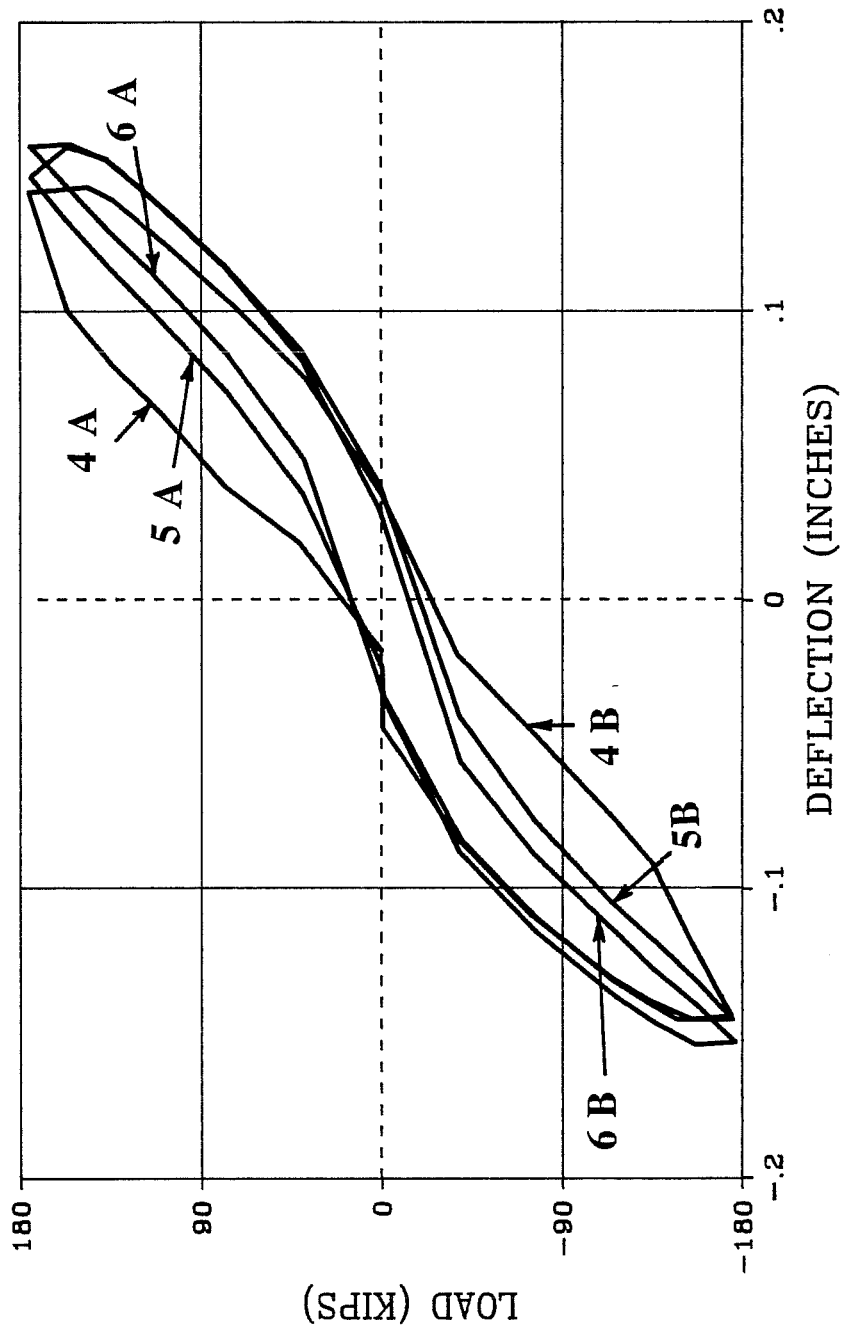


Fig. 3.8 Load-Deflection Response, Cycles to 180 K

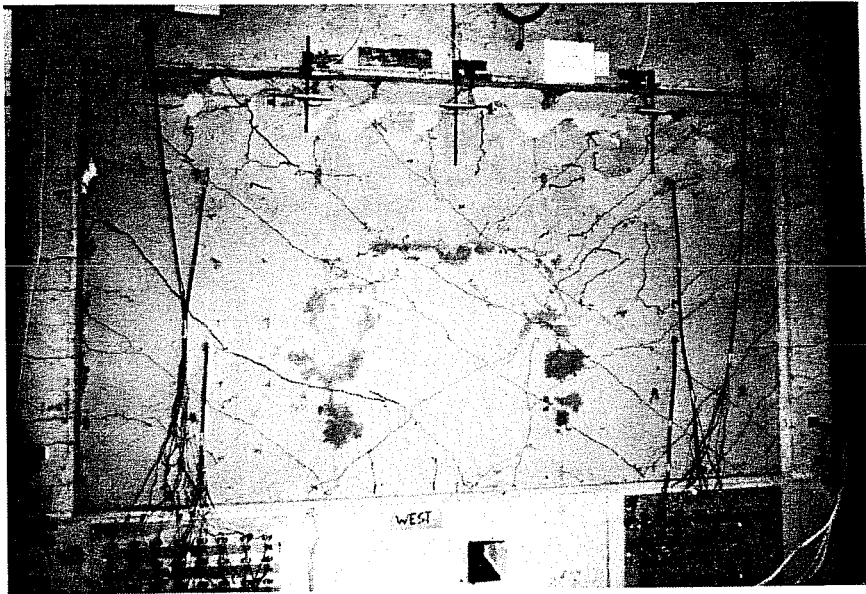


Fig. 3.9 Crack Patterns, Cycles to 180 K

91% of the stiffness in the first cycle to 180 kips. Stiffnesses in the two directions of loading were essentially the same.

The strain distribution at the base of the wall under loading in the positive direction indicates that the download column no longer exhibited bending independent of the wall (Figure 3.10). This was not the case when loading in the positive direction. The positive column continued to bend independently of the infilled wall throughout the test (Figure 3.11)

*Cycle to 240K.* One cycle of load to 240 kips was applied to the full infill. The response was nearly the same in both directions. The load-deflection plot for this cycle is pictured in Figure 3.12.

During this cycle, small extensions in many wall cracks were noted. An additional large inclined wall crack formed between two existing cracks. Wall crack widths were in excess of 1 mm. New horizontal cracks formed in the upload column. New vertical cracks formed in the corners of the column. Some relative slip was noted between the wall and the upload column. The damaged specimen is pictured in Figure 3.13. The stiffness of the wall in this cycle was 93% of the stiffness in the last cycle to 180 kips. The strain profile on the horizontal section at the base of the specimen showed that the extreme column bar in the upload column and the interior column bar in the download column yielded in tension while the magnitude and distribution of strains over the rest of the base were virtually unchanged.

*Cycle to 0.5% Drift.* During loading to a drift of 0.5%, the full infill failed. The load-deflection plot is shown in Figure 3.14. The failure was initiated by failure of the column compression splice. It was apparent that vertical cracks in the corners of the upload column indicated relative slip between the spliced bars and provided a warning of impending failure. A failure plane developed at a level 21 in. above the base (point where splice terminates) and extended nearly halfway across the wall just above the dowels into the base which extended 18 in. into the wall. The crack was about 1/2 in. wide. The failure pattern is pictured in Figure 3.15, 3.16 and 3.17. The peak load at failure was 271 kips in the positive direction and 212 kips in the negative direction. The failure occurred

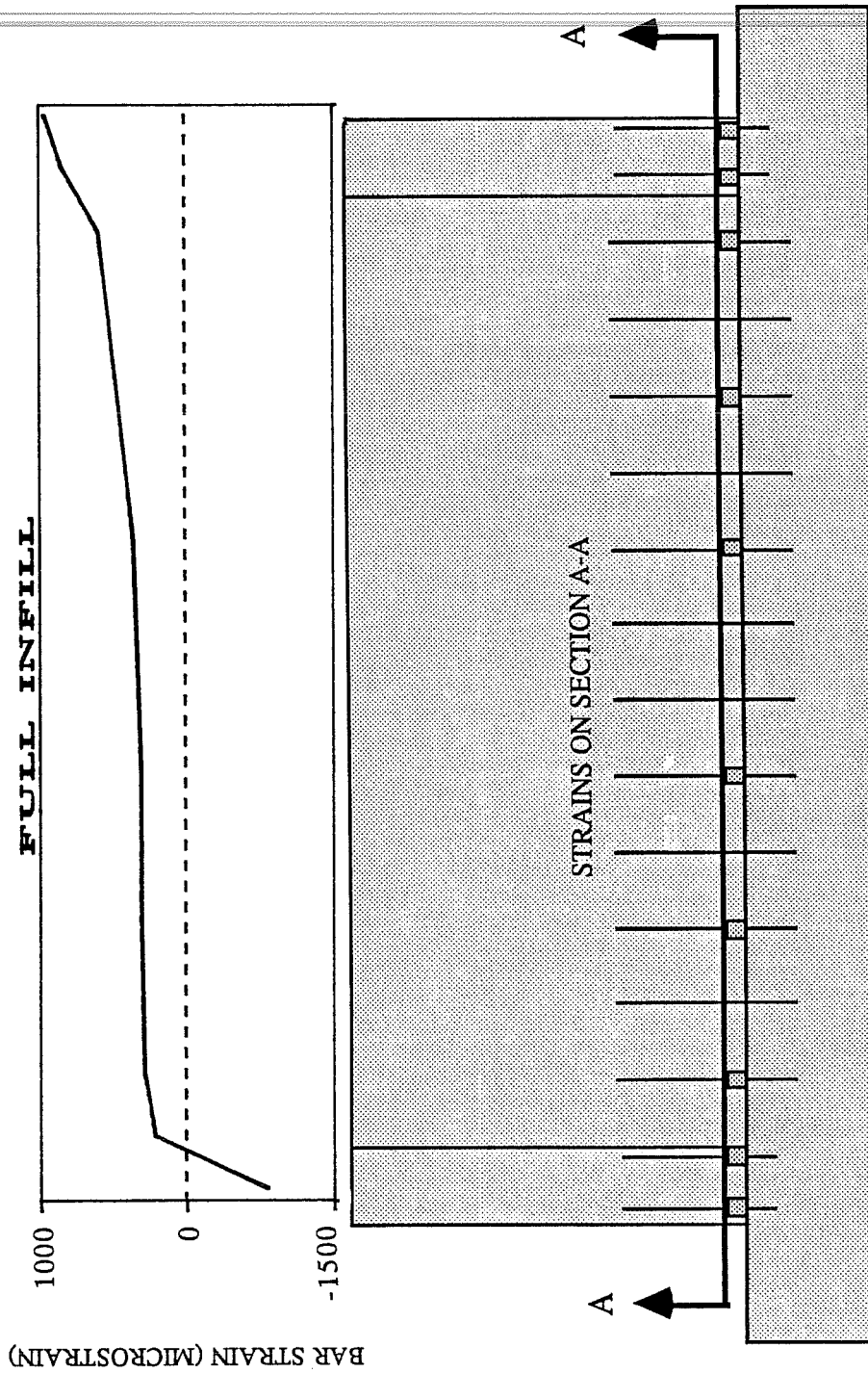


Fig. 3.10 Strain Profile, Cycles to 180 K, Positive Load

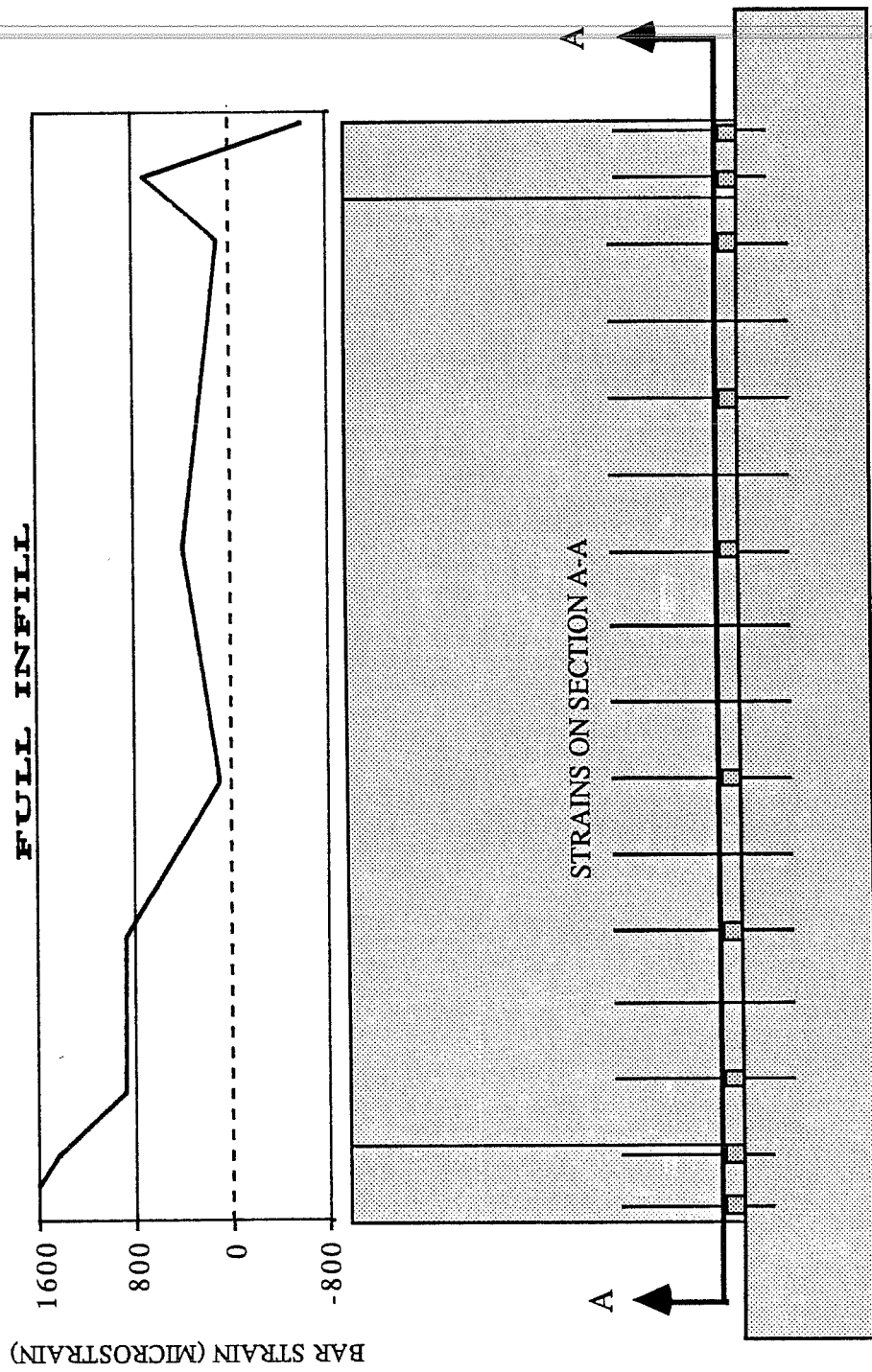


Fig. 3.11 Strain Profile, Cycles to 180 K, Negative Load

# FULL INFILL

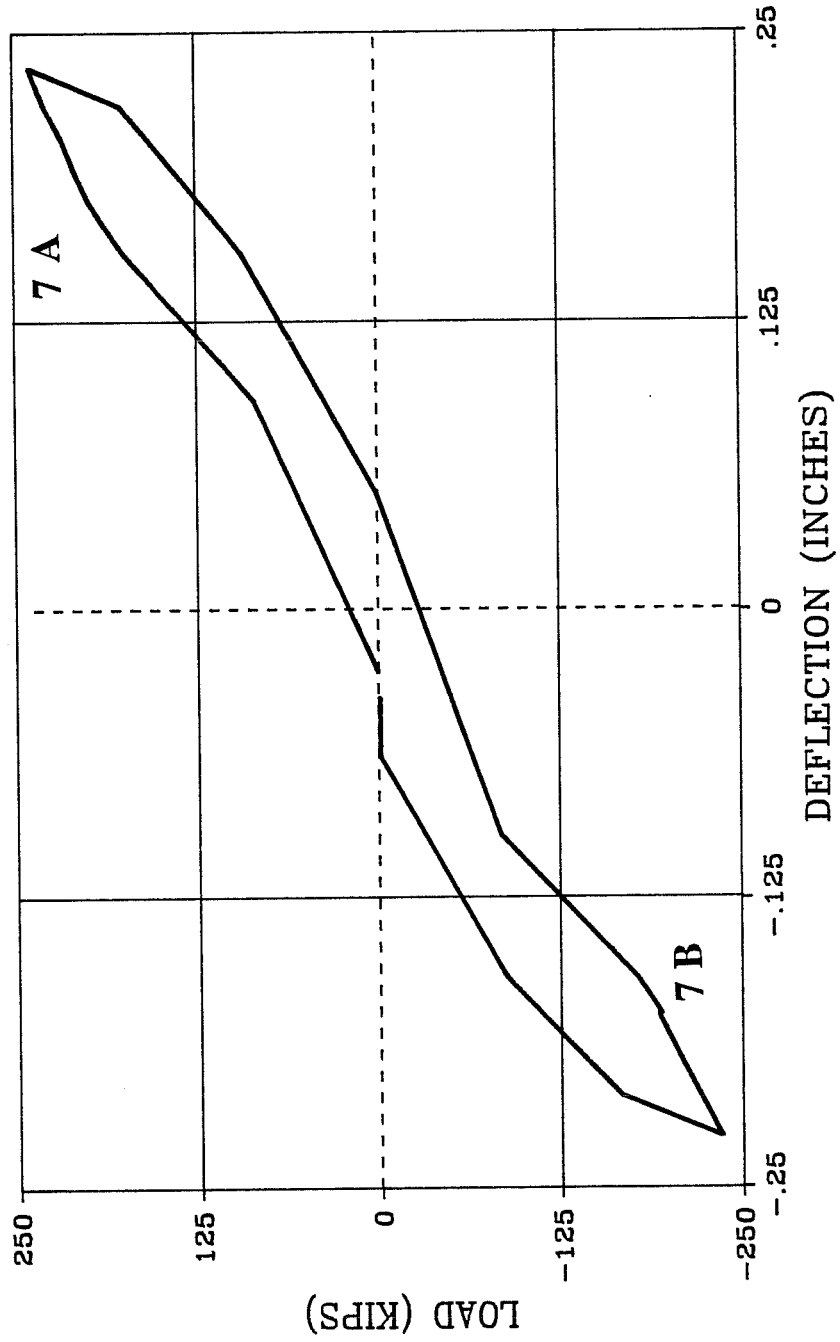


Fig. 3.12 Load-Deflection Response, Cycles to 240 K



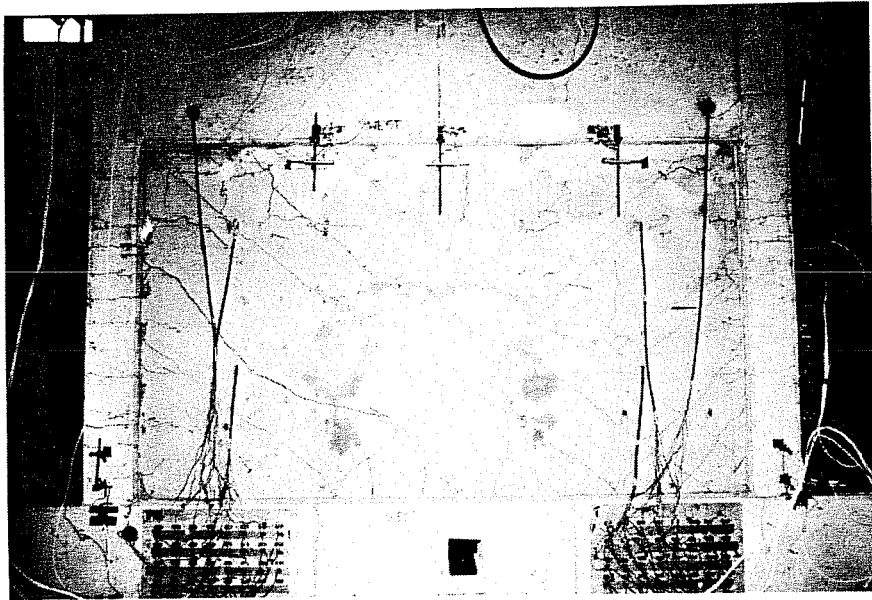


Fig. 3.13 Crack Patterns, Cycle to 240 K

# FULL INFILL

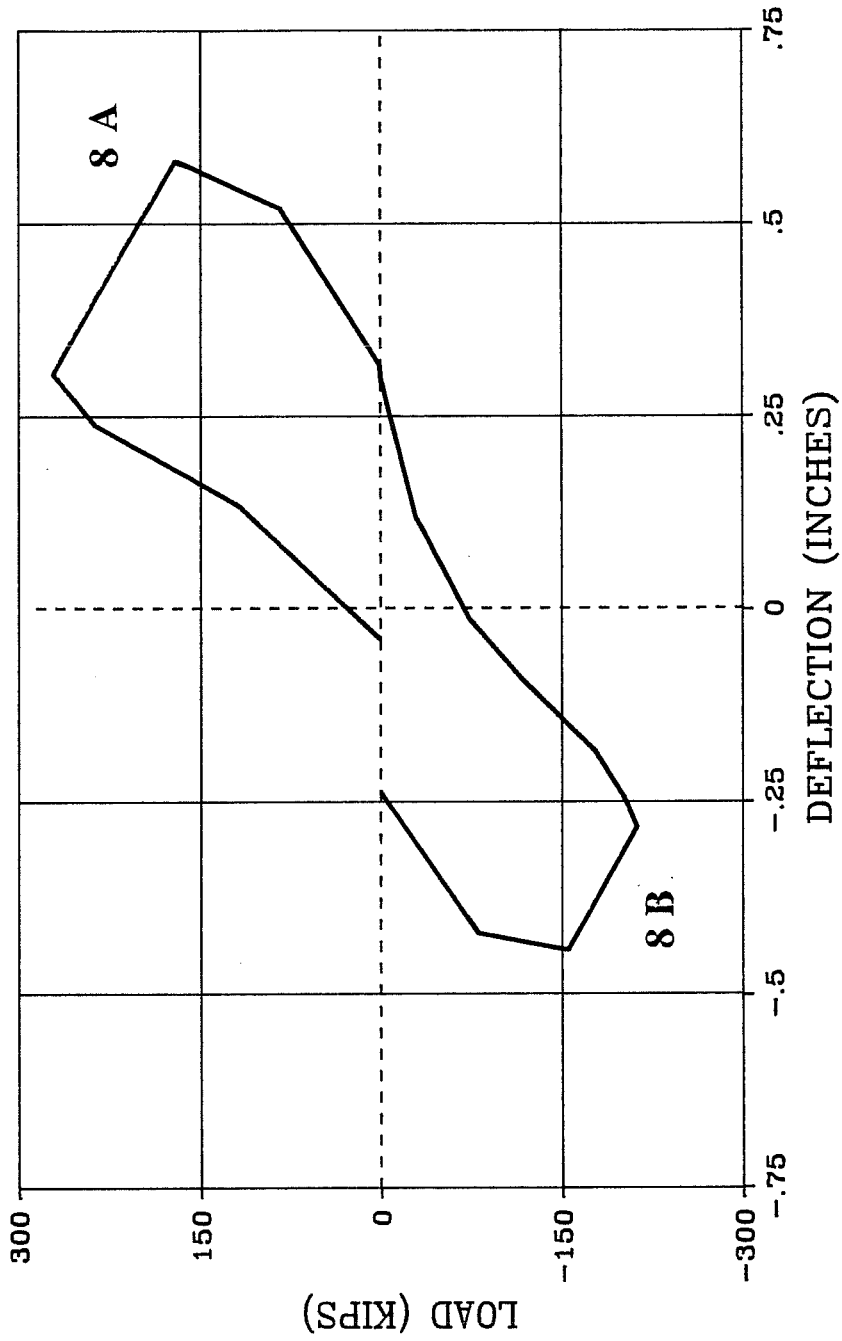


Fig. 3.14 Load-Deflection Response, Cycles to 0.50% Drift

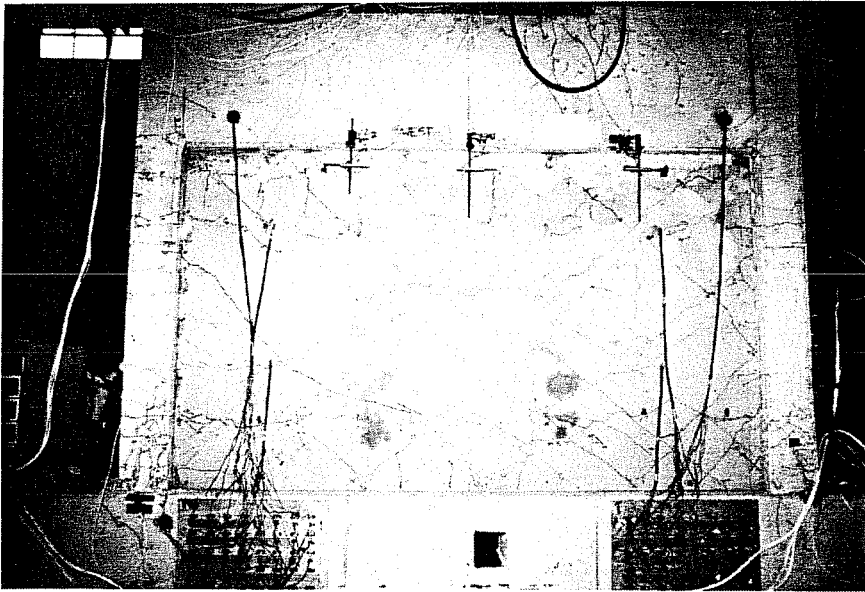


Fig. 3.15 Full Infill at Failure, Elevation

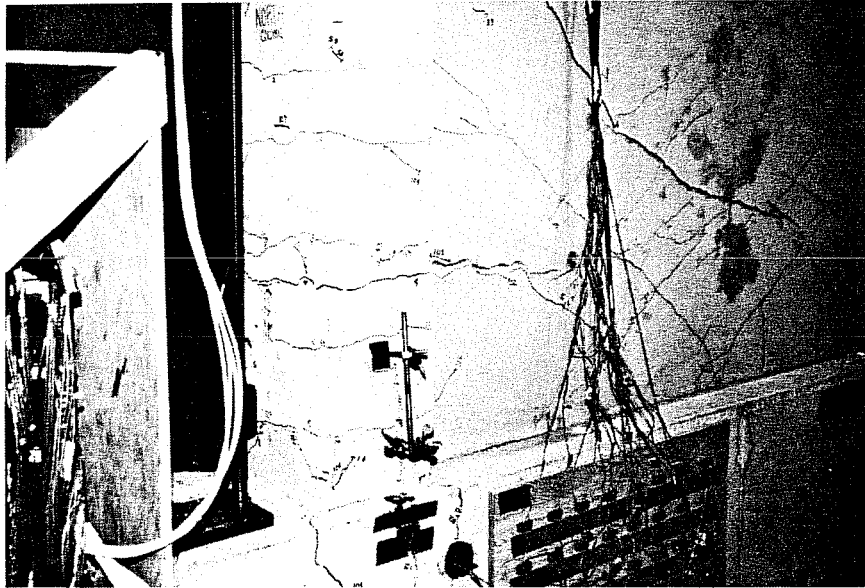


Fig. 3.16 Full Infill at Failure, Splice Region

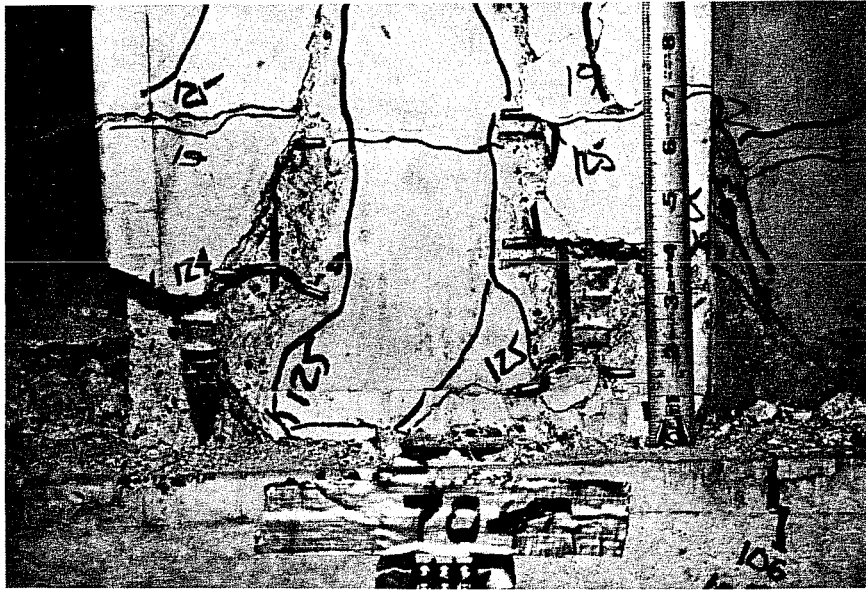


Fig. 3.17 Full Infill at Failure, Bar Slip

while the load was held for data collection. Before failure, new wall cracks formed near the top of the wall toward the download end where little previous damage was noted. The strain profile at the base of the specimen indicated that the longitudinal bars in the upload column reached a maximum strain of 0.7% in tension.

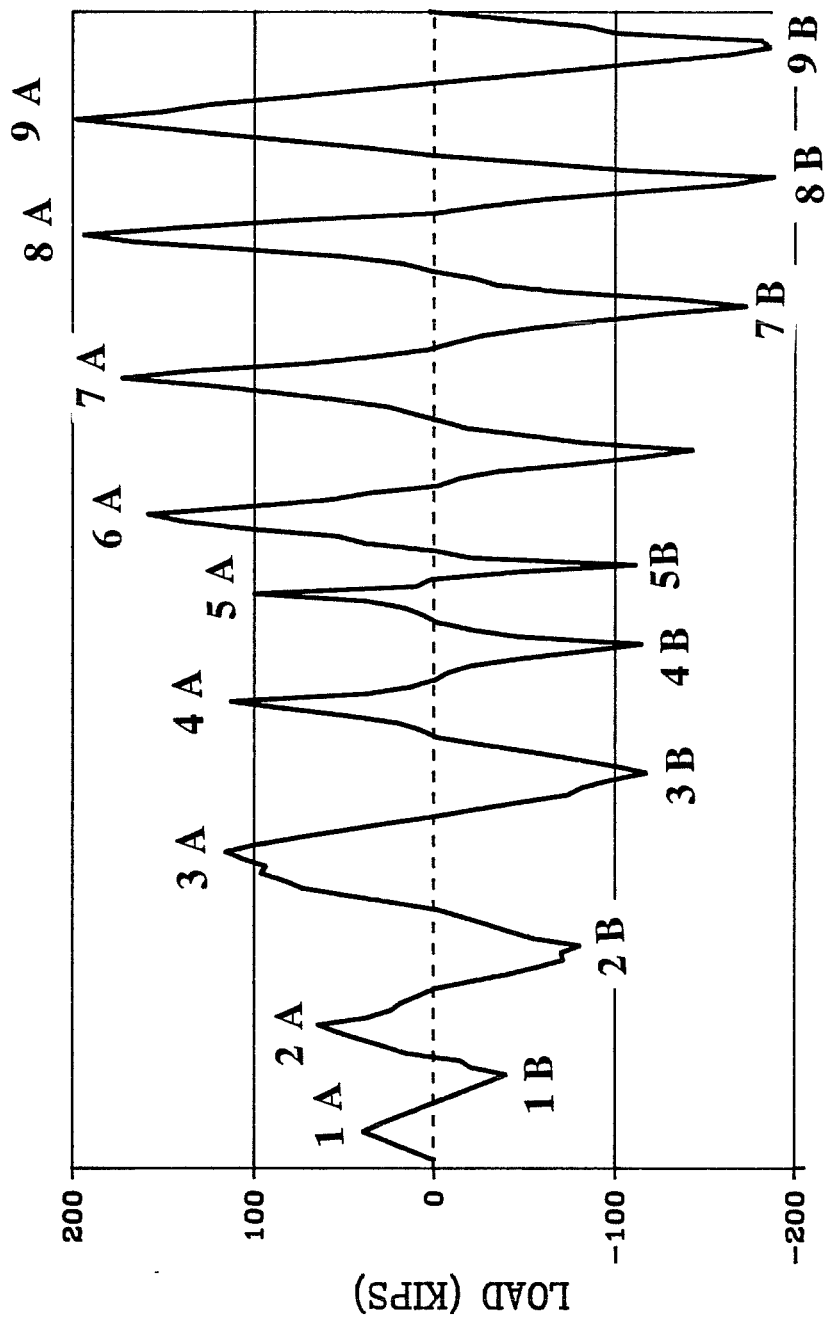
## 3.2 Infill with Window

**3.2.1 Condition Prior to Testing.** The shotcreted wall had a rather extensive pattern of cracking prior to loading. Thermal and shrinkage cracks were found at all corners, along dowels and window trim steel and in the vicinity of the voids formed during shotcreting. Cracks initiated at the frame-wall boundary and extended into the panel toward the opening. The infill with a window was subjected to one full reversed cycle to 0.07% drift, one cycle to 120 kips, two cycles to 0.17% drift, one cycle to 0.27% drift, one cycle to 180 kips, one cycle to 0.5% drift and one cycle to 200 kips. The load history is illustrated in Figure 3.18. The entire load-deflection history is illustrated in Figure 3.19.

### 3.2.2 Response Under Cyclic Loading.

*Cycle to 0.07% Drift.* One cycle to a drift of 0.07% was applied to permit a comparison with the response of the full infill specimen under the first loading to 120 kips. The load-deflection plot for this cycle is shown in Figure 3.20. The hysteresis curves in both directions were similar. The stiffness in the negative direction was 82% of the stiffness in the positive direction. Hairline cracks opened up at the base of the upload column. Inclined wall cracks appeared near the bottom of the window on the download side of the specimen and extended down the lower corner of the wall. Inclined cracks appeared on the upload side of the specimen at about the same height and also at the top of the window opening. Figure 3.21 shows the crack pattern.

Strain profiles at the base of the specimen and on the horizontal sections at the top and bottom of the window opening indicated that initially the two short "piers" consisting of the column and the wall section on either side of the window opening developed a strut and tie mechanism. The upload end of



LOAD STAGE

Fig. 3.18 Load History, Infill with Window

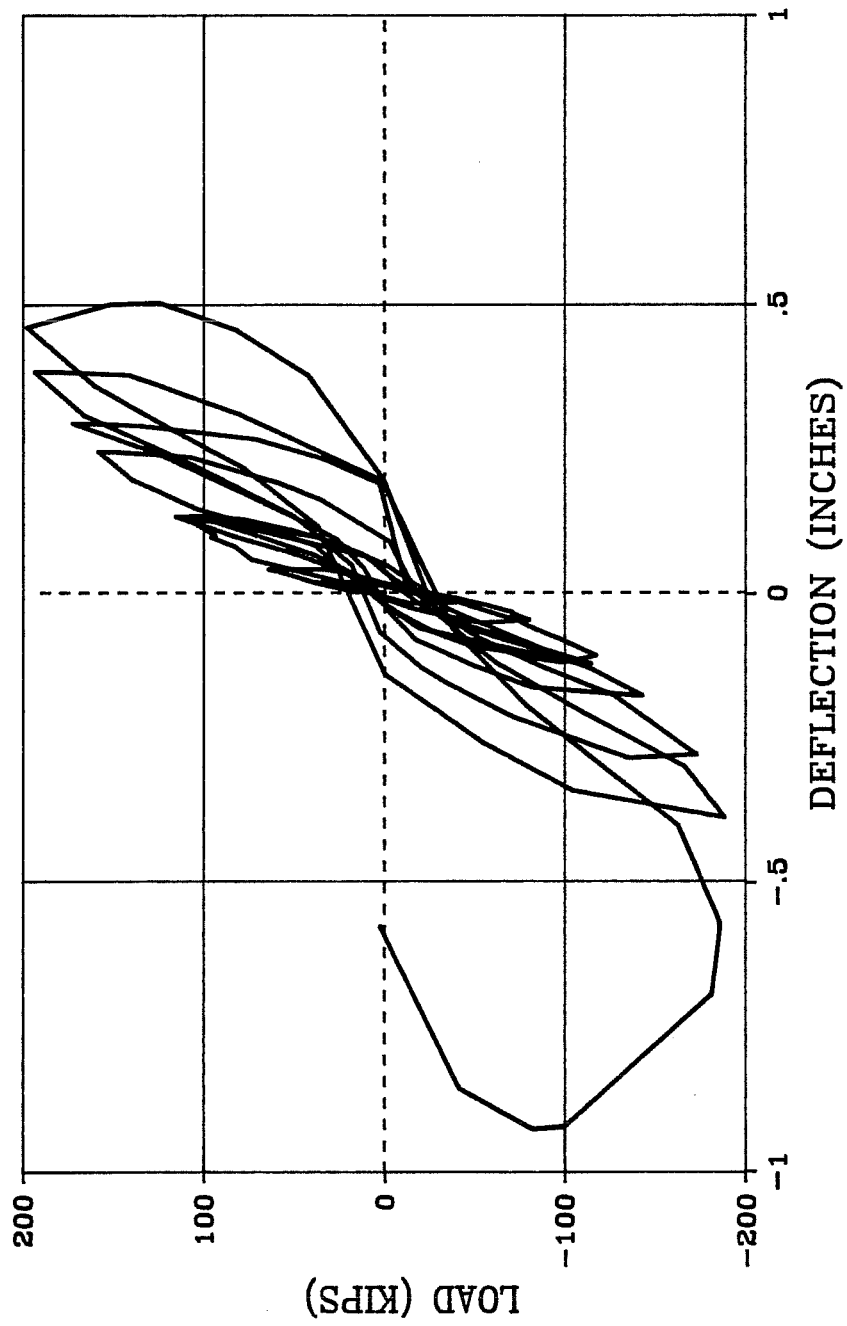


Fig. 3.19 Load-Deflection History, Infill with Window



# INFILL WITH WINDOW

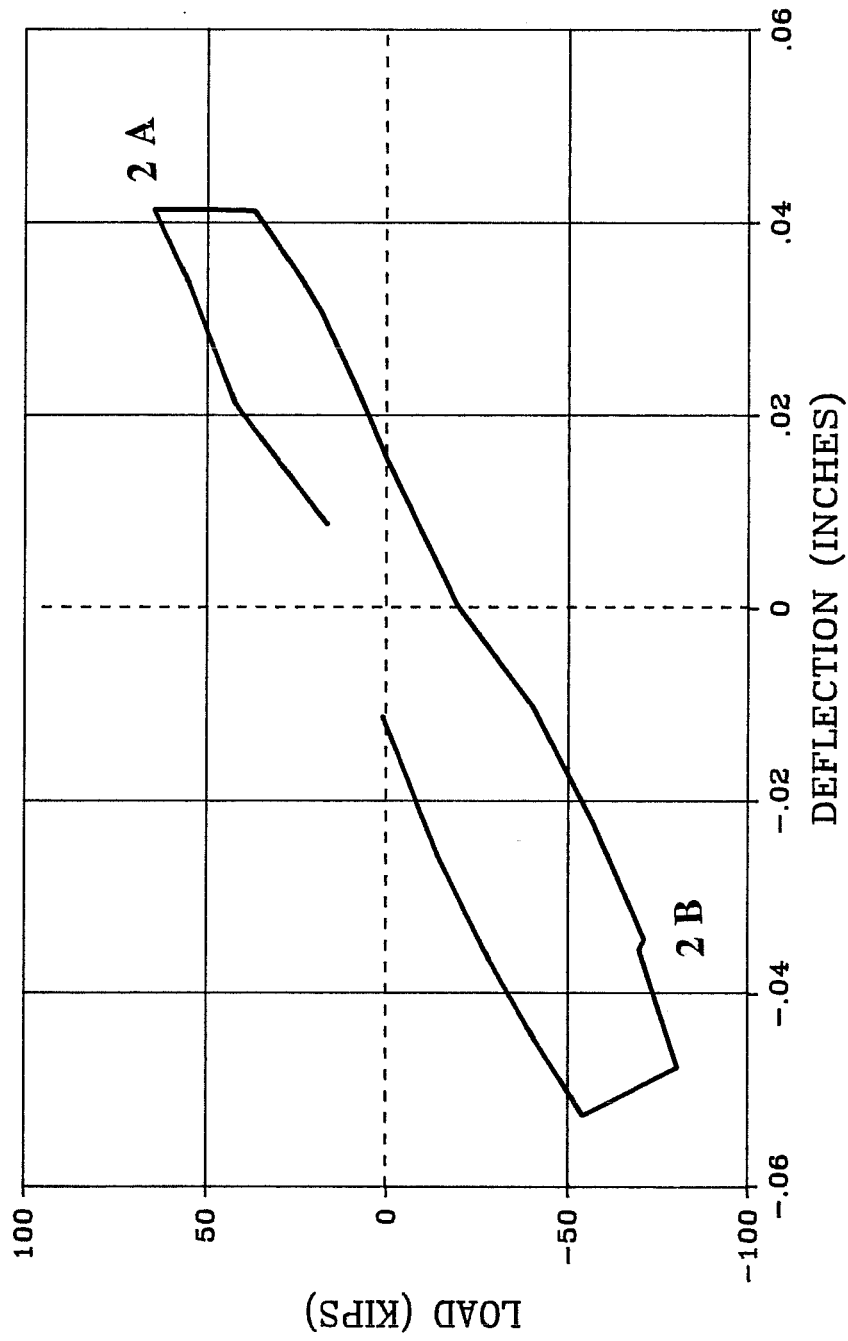


Fig. 3.20 Load-Deflection Response, Cycles to 0.07% Drift

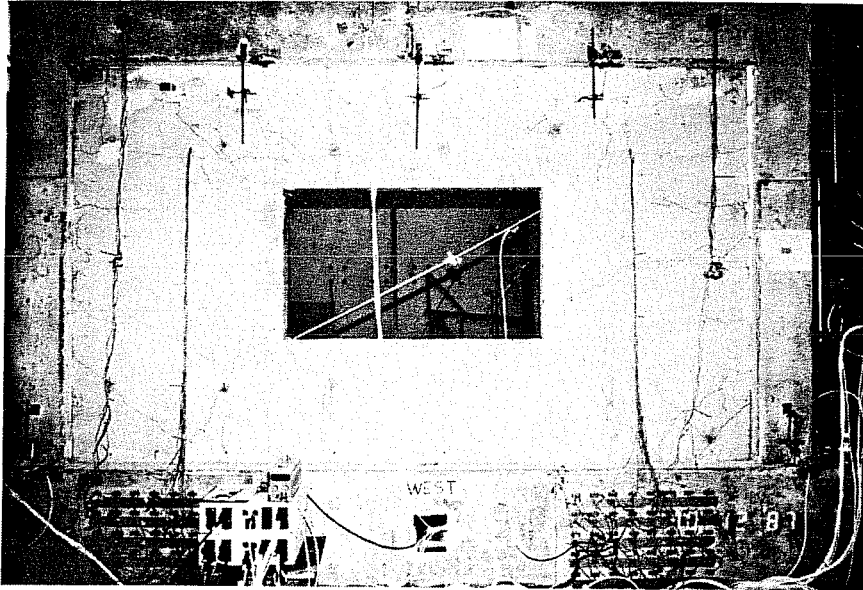


Fig. 3.21 Crack Pattern, Cycles to 0.07% Drift

the specimen carried considerable tension and the strain distribution over this section was linear. The strain distribution at the base of download pier was less uniform and indicated that the download column bent independently of the remainder of that pier. These profiles on horizontal sections at the base of the specimen and at the elevations of the top and bottom of the window opening for this cycle for loading in the negative direction are presented in Figures 3.22, 3.23 and 3.24. Strain histories on the horizontal section at the top of the wall revealed the extreme column bar on the upload side ultimately yielded at failure. The other column bars and dowels at this elevation showed no significant strains. Review of strain distributions on vertical sections revealed few locations of distress. For the duration of the test of the infill with the window opening, the dowels grouted into the upload column exhibited no significant strains. This conclusion applied to the dowels grouted into the top of the download columns as well. The two dowels located closest to the bottom of the column showed increasing tensile strains with a maximum value of about one half of the yield strain at the peak load. Gages on the horizontal trim bars indicated no significant strains for the duration of the test under the opening on the download side of the opening. Horizontal panel steel under the window opening on the download side reached one half of the yield strain in tension in the cycle prior to the failure cycle. The horizontal trim and panel steel over the door opening on the upload side exhibited increasing tensile strains that exceeded the yield strain in the last two cycles.

*Cycle to 120K.* The infill with the window was subjected to one load controlled cycle to 120 kips. This limit was chosen to form a comparison with the full infill. The average drift level was 0.14%.

The load-deflection plot for this cycle is pictured in Figure 3.25. The stiffnesses were equivalent in the two directions with the stiffness in the negative direction 93% of that in the positive. The stiffness in this cycle was 56% of the stiffness in the previous cycle, a considerable loss of stiffness. Horizontal cracks appeared in the upload column at the second through seventh column ties from the bottom of the column and at the frame joint with the first story girder. Extensive inclined cracking of the panel on the upload side was found. Smaller

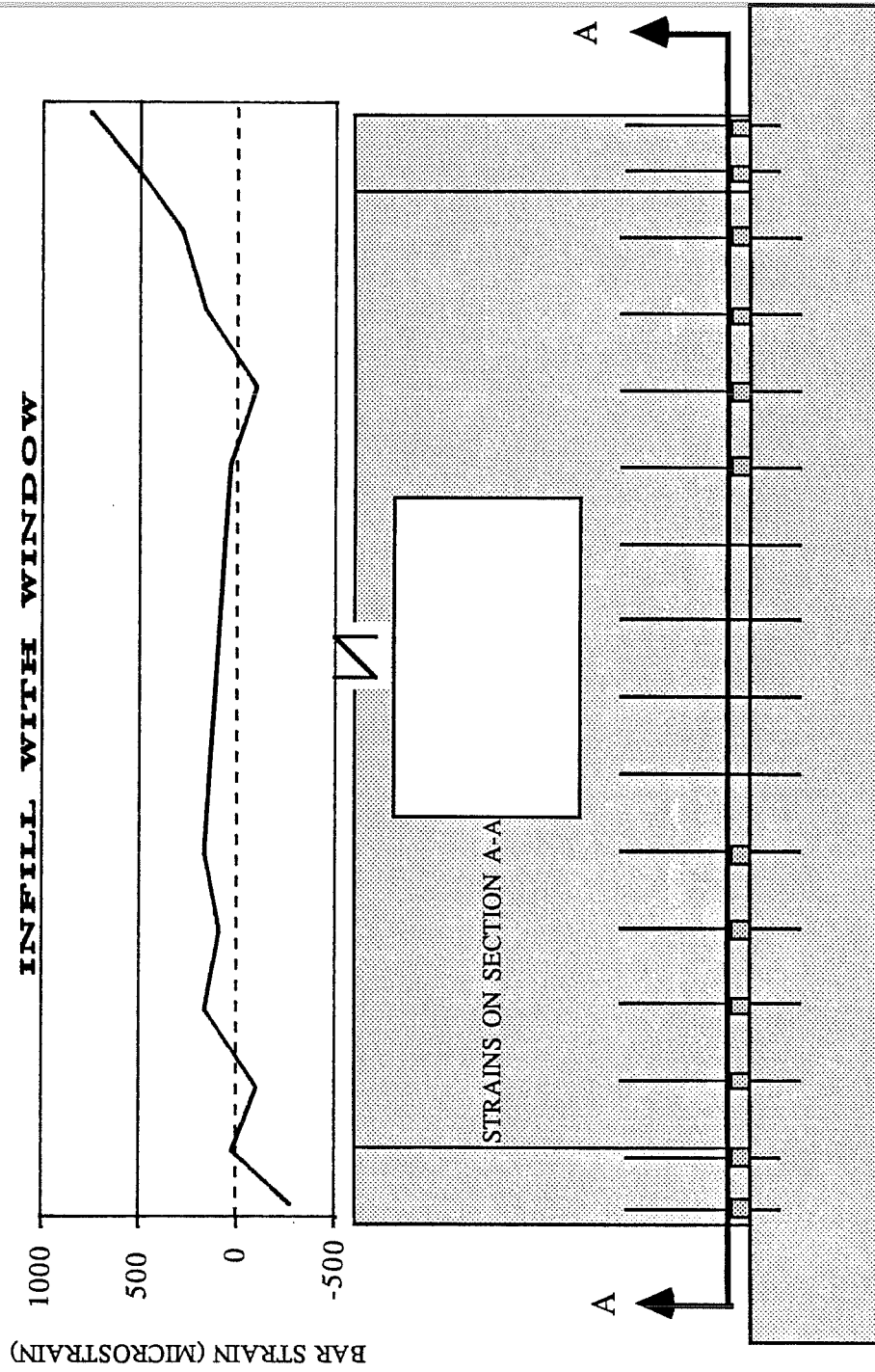


Fig. 3.22 Strain Profile, Cycles to 0.07% Drift, Base of Wall

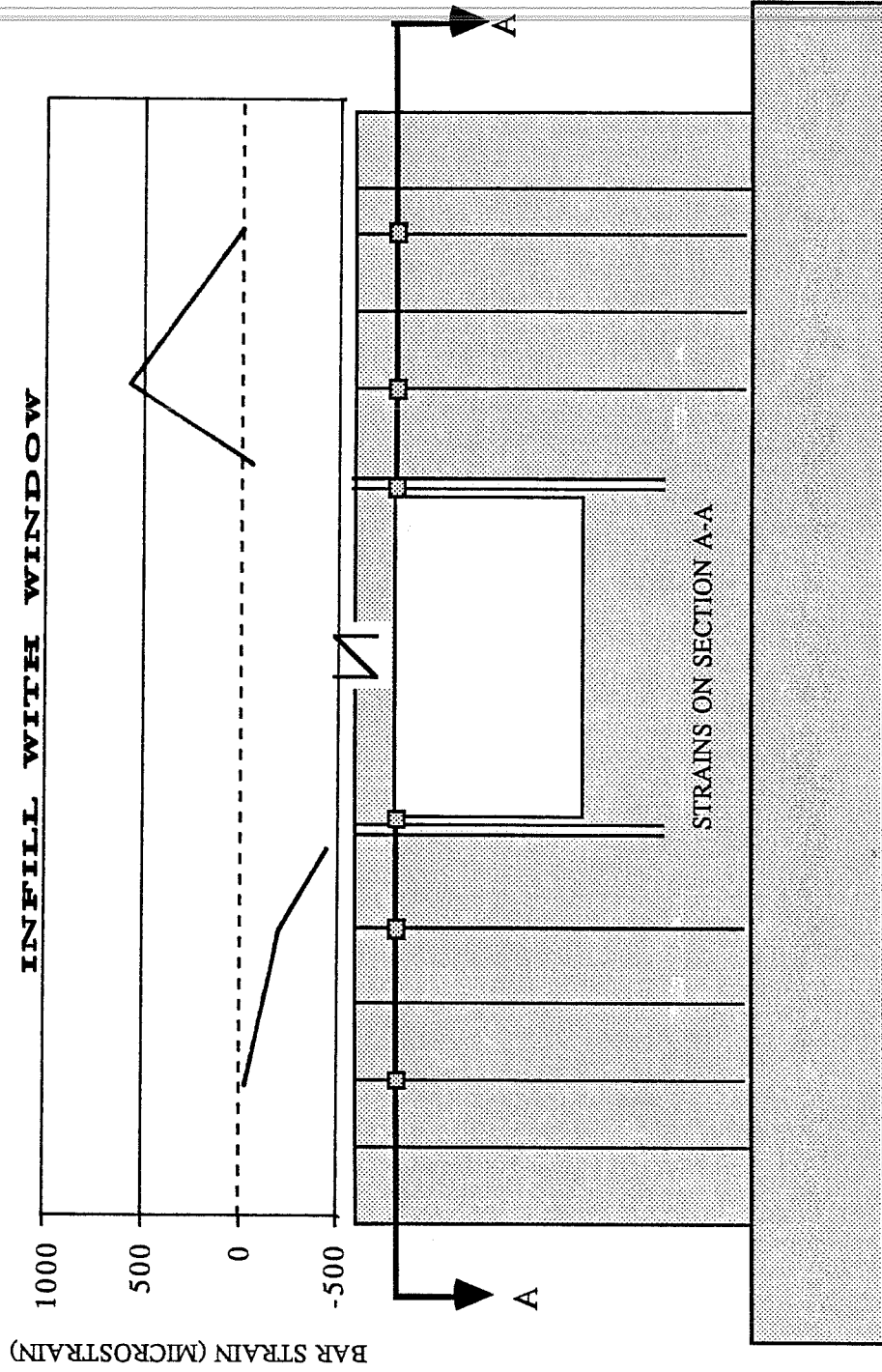


Fig. 3.23 Strain Profiles, Cycles to 0.07% Drift, Top of Opening

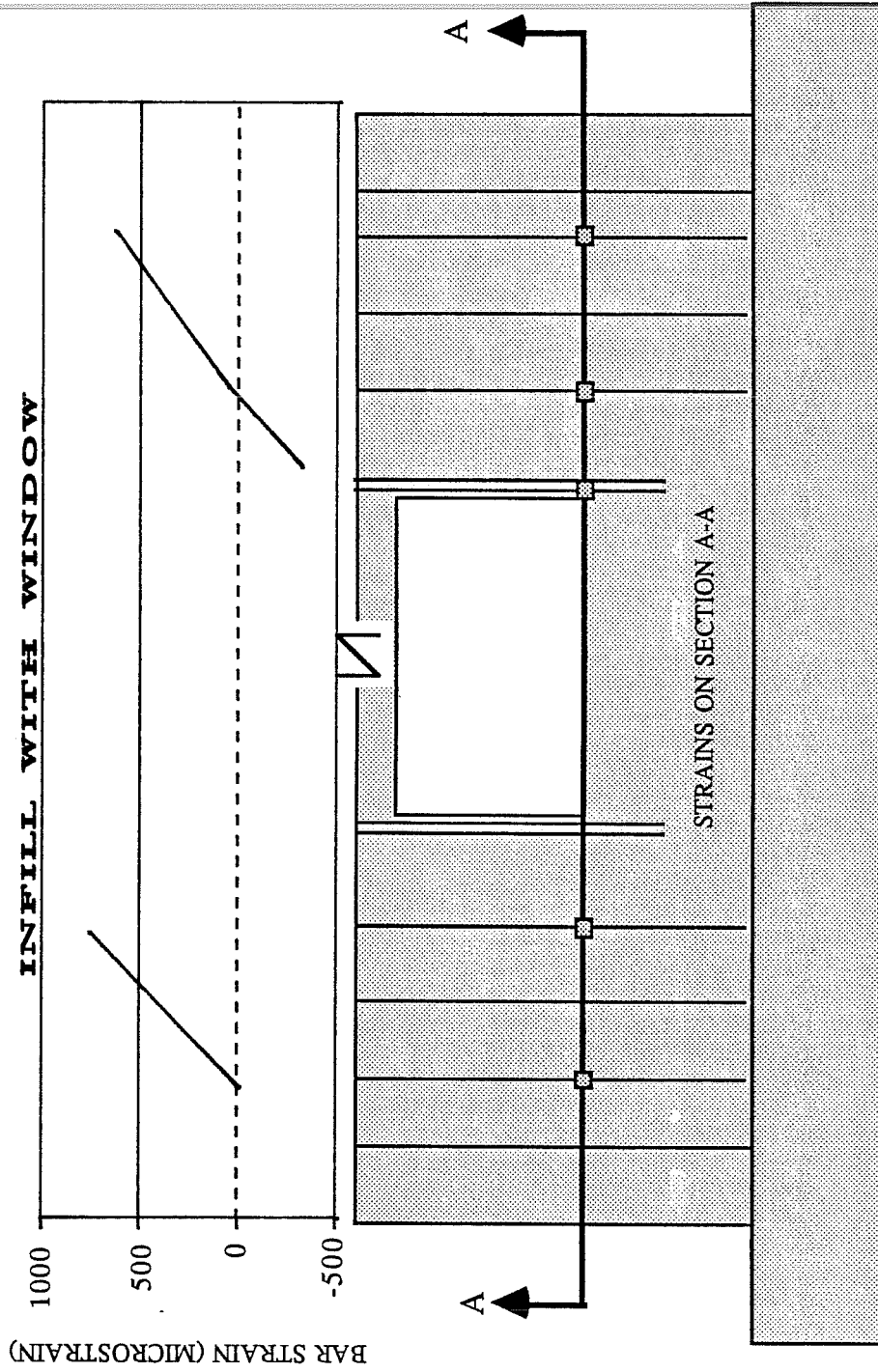


Fig. 3.24 Strain Profiles, Cycles to 0.07% Drift, Bottom of Opening

# INFILL WITH WINDOW

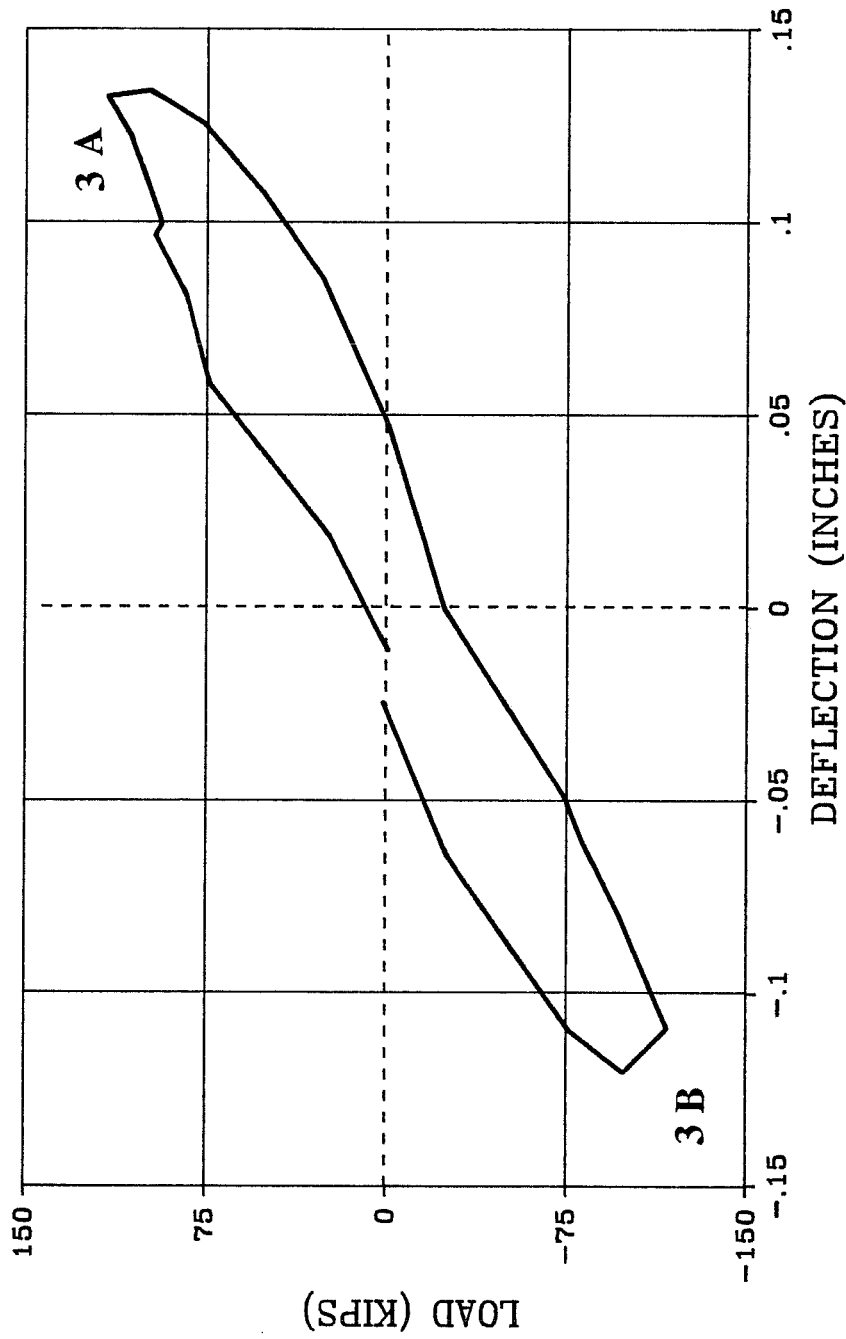


Fig. 3.25 Load-Deflection Response, Cycles to 120 K

cracks were found at the window opening. A large inclined crack formed in the download section of the panel at the window opening as well. One of the most unusual cracks appeared on the bottom download corner of the window opening and was inclined at roughly  $90^\circ$  to all other cracks that appeared when loading in this direction. This crack resulted primarily from the shear deformations imposed on the infilled wall. As the wall strained to assume the typical trapezoidal shape of an element under shear only, the bottom download corner of the window is pulled upward and toward the opposite diagonal corner of the window opening. These deformations resulted in tensile strains oriented at  $90^\circ$  to the rest of the inclined cracks found in the panel under load in a given direction. This theory was further supported by similar cracks found in later cycles in the upload pier at the top of the window opening at the same orientation. These cracks were then expected to occur in the wall panel in the vicinity of the two corners of an opening where the corner to corner diagonal of the opening shortens under applied shear. Cracks at these orientations can be arrested by orthogonal trim reinforcement only. Also during this cycle, a large vertical crack appeared on the vertical face inside the window opening indicating splitting was taking place on the download side of the opening. This splitting of the infill was caused by buckling of the unconfined trim steel, which was in compression at the top of the opening at this load stage. Some of the damage is pictured in Figure 3.26 and 3.27. The strain distribution at the base of the specimen changed very little from the previous cycle with most of the difference being increases in tensile strain in the column bars on the upload side of the specimen and increases in compressive strain in the extreme download column bar. Strain profiles on a section across the bottom of the window opening showed very large tensile strains at the download end of the opening. This result corresponded with the location of cracks that form there. Cracks that appeared in the panel near the upload column at the bottom of the window were responsible for the tensile strains noted in bars located on this section.

*Cycles to 0.17% Drift.* Two cycles of drift to 0.17% were applied to the infill with the window. This drift limit was the drift exhibited by the full infill



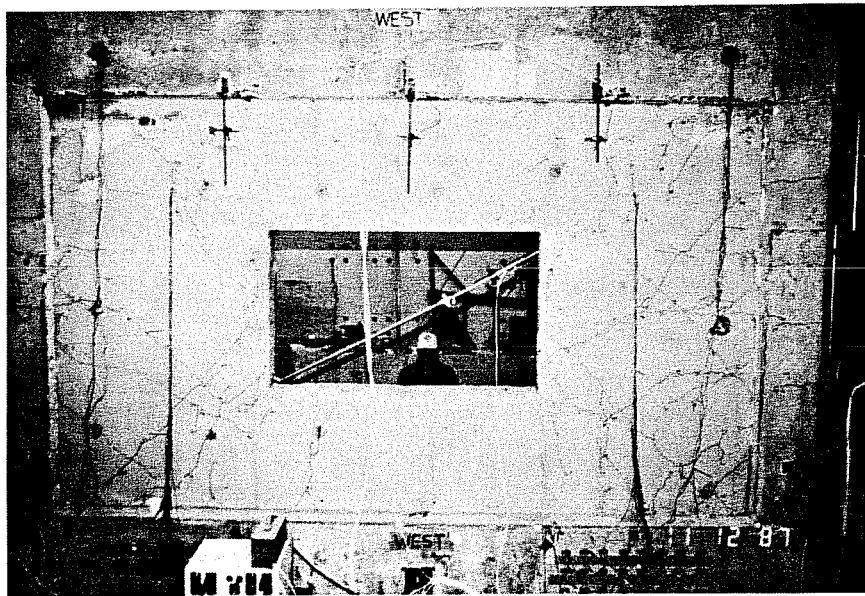


Fig. 3.26 Crack Patterns, Cycles to 120 K

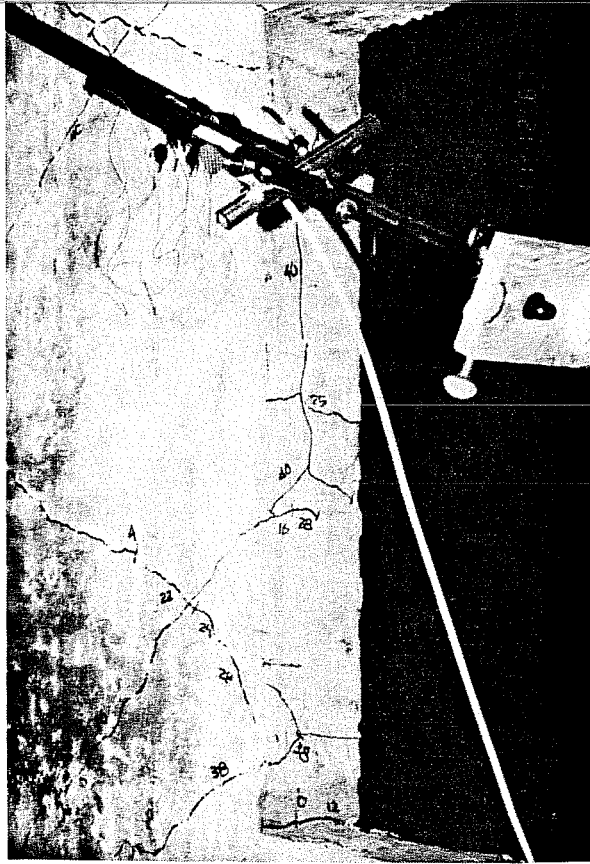


Fig. 3.27 Wall Splitting in Window Opening, Cycles to 120 K

specimen in its first cycle to 180 kips. The load-deflection plot for these cycles is contained in Figure 3.28.

In the first cycle to 0.17% drift, the wall averaged 0.15% drift at an average load of 115 kips. The behavior in the positive and negative directions was symmetric, with the average stiffness in this cycle constituting 93% of the stiffness exhibited in the previous cycle to 120 kips. In these cycles, the shape of the load-deflection curve indicated that the specimen began the cycle with a low stiffness that increased with increasing load. This increase in stiffness was due to the closing of cracks that opened under loading in the opposite direction. Damage during this cycle was minimal. Crack extensions were formed in columns and in the upper joint. Some new inclined cracks formed in the upload and download piers and over the window opening on the upload side.

The only noteworthy change in strain profile at the base of the specimen was the appearance of independent download column bending. The base of the specimen was virtually unstressed over an 8 foot length. The profiles for this cycle for loading in the negative direction are presented in Figures 3.29, 3.30 and 3.31. The distributions at the base of the specimen did not change significantly for the second cycle to this drift level.

In the second cycle to 0.17% drift numerous inclined cracks appeared in the download side of the wall passing near the top of the window. These cracks indicated that a major strut formed with nodes at the top of the wall at mid width and at the download column about 24 inches up from the base. These cracks ultimately formed the failure plane in that direction of loading. New horizontal cracks appeared in the columns over the height of the window opening. More vertical cracks appeared in the window opening. The stiffness in this cycle was 93% of the stiffness in the previous cycle to this deflection.

*Cycle to 0.27% Drift.* One cycle of drift to 0.27% was applied to the infill with the window as a comparison to the behavior of the full infill specimen in a cycle to 240 kips and the same deflection. The average drift in this cycle was 0.25% at an average load of 151 kips. The load-deflection plot for this cycle is illustrated in Figure 3.32. The stiffness was similar in the two directions, with

# INFILL WITH WINDOW

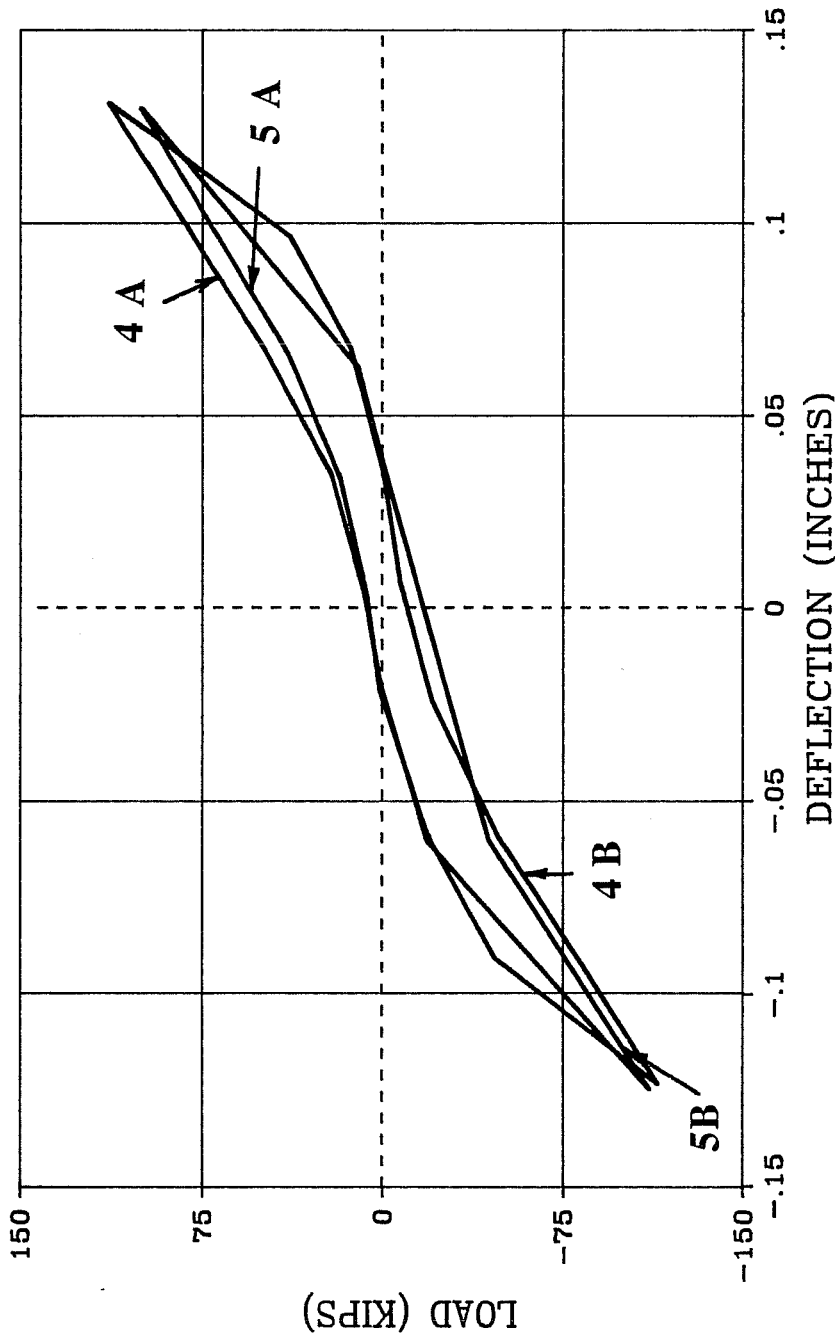


Fig. 3.28 Load-Deflection Response, Cycles to 0.17% Drift

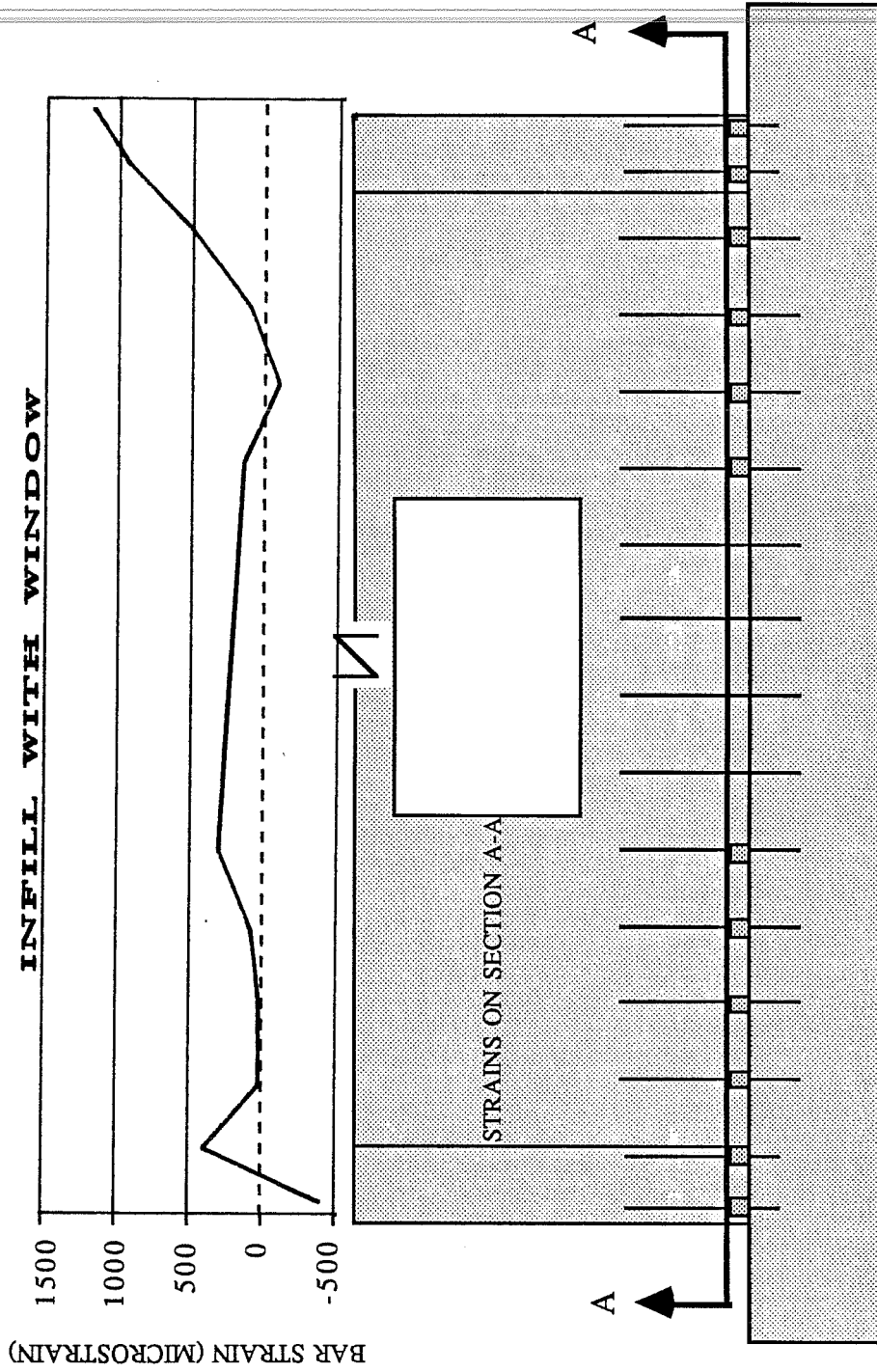


Fig. 3.29 Strain Profile, Cycles to 0.17% Drift, Base of Wall

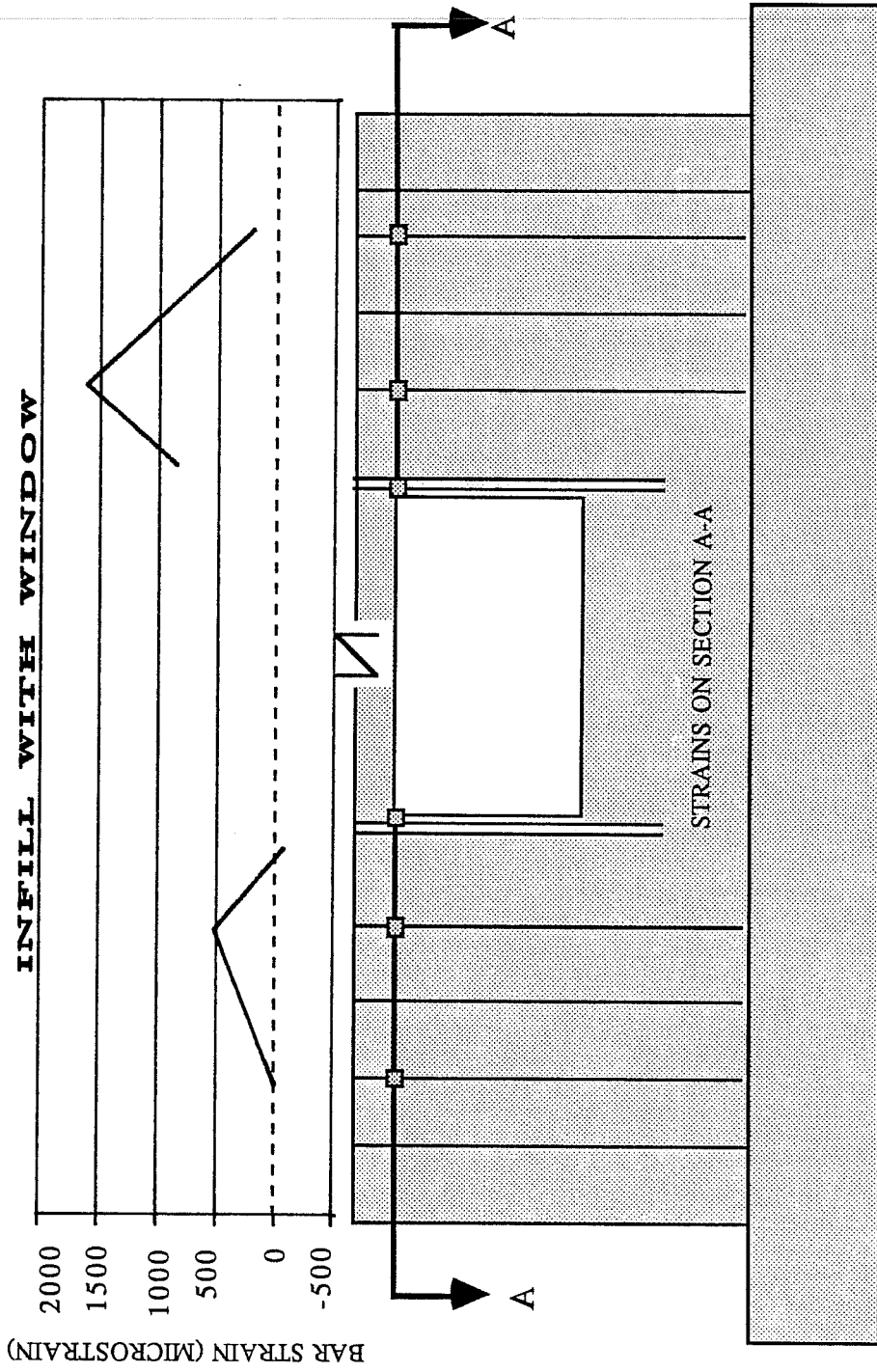


Fig. 3.30 Strain Profile, Cycles to 0.17% Drift, Top of Opening

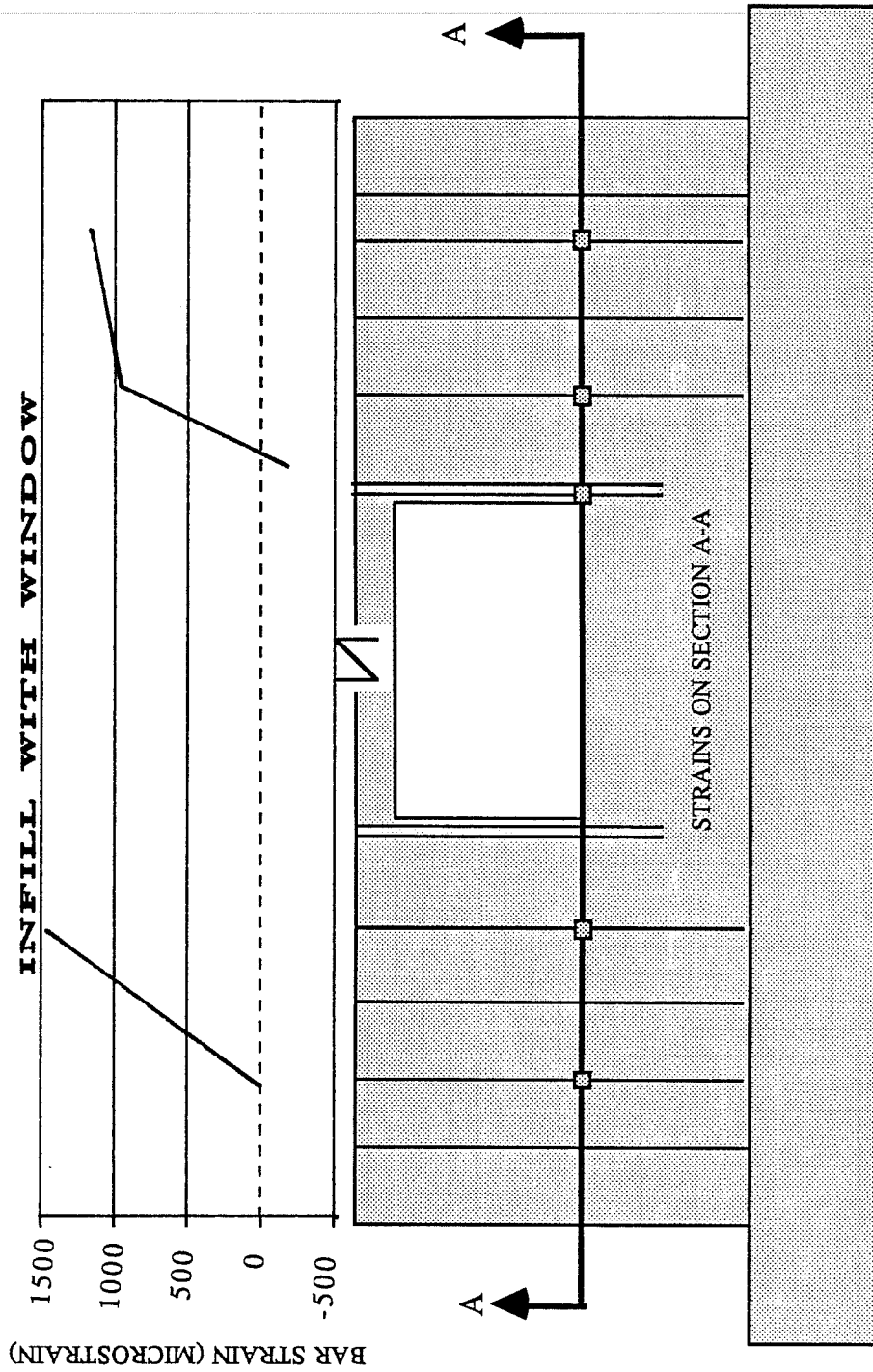


Fig. 3.31 Strain Profile, Cycles to 0.17% Drift, Bottom of Opening

# INFILL WITH WINDOW

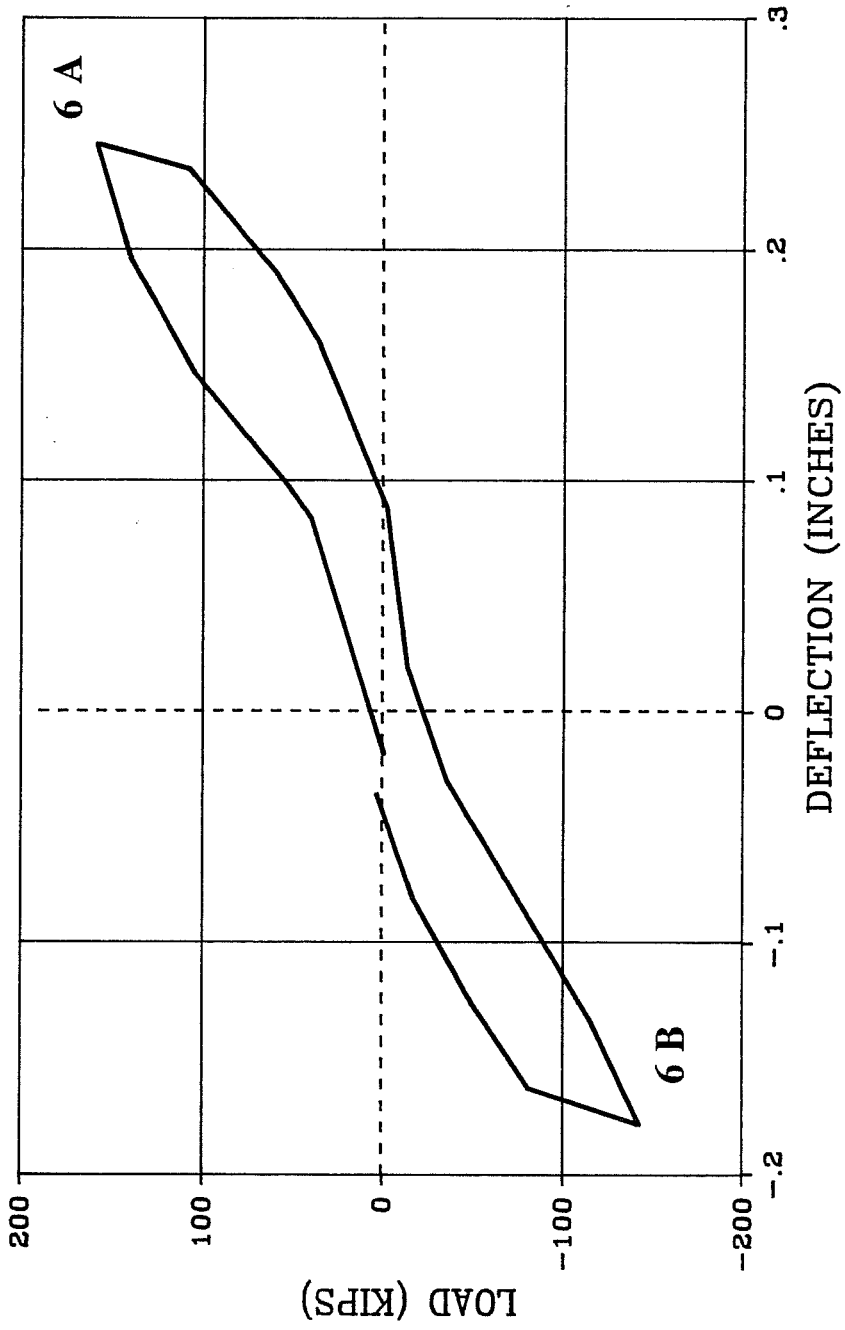


Fig. 3.32 Load-Deflection Response, Cycles to 0.27% Drift



the stiffness in the negative direction constituting 89% of that in the positive direction. The stiffness in this cycle was 84% of the stiffness in the previous cycle to 0.17% drift. In this cycle, major cracks formed in the download end of the panel over the window opening as in the previous cycle. This cracking indicated the formation of a strut that had initiated in the top of the wall and extended past the upper download corner of the window to the lower download corner of the wall. In the upload side of the panel, cracks gave clear evidence that a strut that had formed passing directly under the window. New inclined cracks formed directly over and under the window. Several horizontal cracks appeared in the upload columns. Extensions of the vertical cracks on the vertical surfaces of the window opening on the download side were noted. Crack widths in panel cracks were in excess of 1.0 mm.

Strain profiles on sections at the top and bottom of the window opening showed a drop in the download panel strains. Upload panel strains at the bottom of the opening increased near the opening with the formation of a crack there.

*Cycle to 180K.* One cycle of load to 180 kips was applied to the infill with the window. This cycle was to form a basis for comparison with the full infill at the same load. The drift exhibited in the cycle averaged 0.34%. The stiffnesses in the two directions were different, with the stiffness in the negative direction totalling 70% of the stiffness in the positive direction. The stiffness in this cycle was 78% of the stiffness in the previous cycle to 0.27% drift. The load-deflection plot for this cycle is contained in Figure 3.33. New inclined panel cracks were relatively small and concentrated in the upload side of the specimen. Small extensions of inclined cracks were formed under the window opening and at the base of the download column. New horizontal cracks were formed in the upload column at about mid height. The width of inclined cracks in the panel at the level of the opening were in excess of 1.5 mm. Some crushing of concrete was noted during this cycle in struts on the download side of the specimen. Crack patterns for this cycle are pictured in Figure 3.34.

Strain distributions at the base of the wall for this cycle indicated that the entire section was in tension up to the neutral axis of the download column.

# INFILL WITH WINDOW

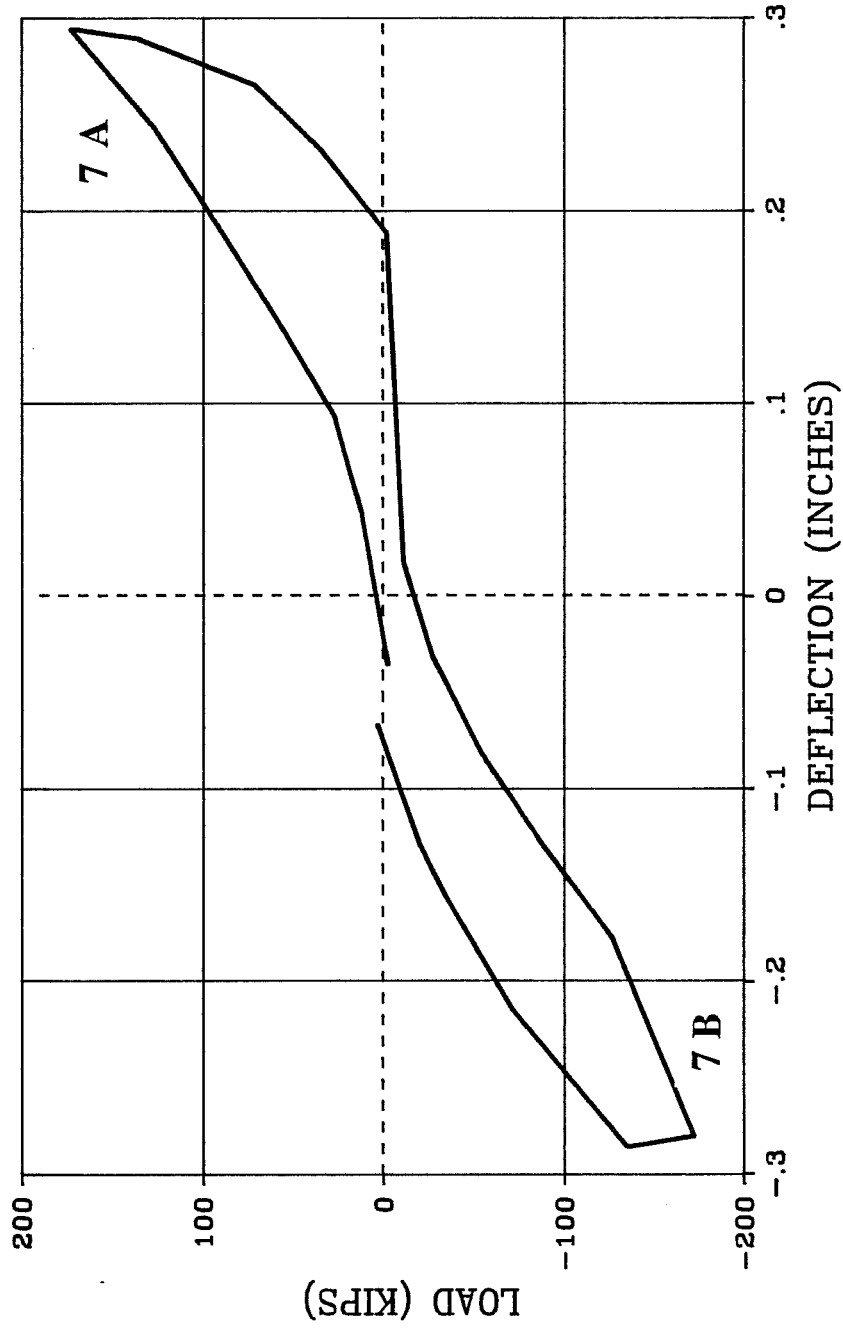


Fig. 3.33 Load-Deflection Response, Cycles to 180 K



Fig. 3.34 Crack Patterns, Cycles to 180 K

Strains in extreme column bars in tension were about 80% of the yield strain. The tensile strain in the download column's interior bar was about one-half of the yield strain. Strains in curtain steel reached yield on the section at the bottom of the window on the download side as more new cracks formed there. Strains in curtain steel at the top of the window opening indicated bars had yielded or were near yield on the upload side of the panel and in one of the bars on the download side that bridges an old crack. The profiles for this cycle for loading in the negative direction are presented in Figures 3.35, 3.36 and 3.37.

*Cycle to 0.5% Drift.* One cycle of drift to 0.5% was applied to the infill with the window. This was the drift that the full infill failed to sustain. The average drift attained in this cycle was 0.46% at an average load of 191 kips. The load-deflection plot for this cycle is pictured in Figure 3.38. The stiffnesses in the two directions were different with the stiffness in the negative direction constituting 75% of the stiffness in the positive direction. The stiffness in this cycle was 86% of the stiffness in the previous cycle. Damage in the panel was concentrated under the window opening. Inclined cracks formed in the upload column near the top of the wall. A few extensions of inclined panel cracks were noted in the upload and download side of the wall. In this cycle, crack widths in inclined panel cracks that resided over the height of the window opening were 2.5 mm. A picture of the specimen after this cycle was applied is contained in Figure 3.39.

Strain distributions at the base of the specimen indicated yield of the column bar in tension on the upload side of the specimen. The interior column bar on the download side of the specimen deformed to roughly 60% of yield. Sections at the top and bottom of the window opening continued to show the most distress in the upload side of the wall.

*Cycle to 200K.* One cycle of load to 200 kips was applied to the infill with the window. The infill failed under this load while take readings at the peak. The load-deflection plot for this cycle is listed in Figure 3.40. The mechanism by which it failed was inclined shear cracking through the top of the upload column, through the upload panel and through the bottom of the download

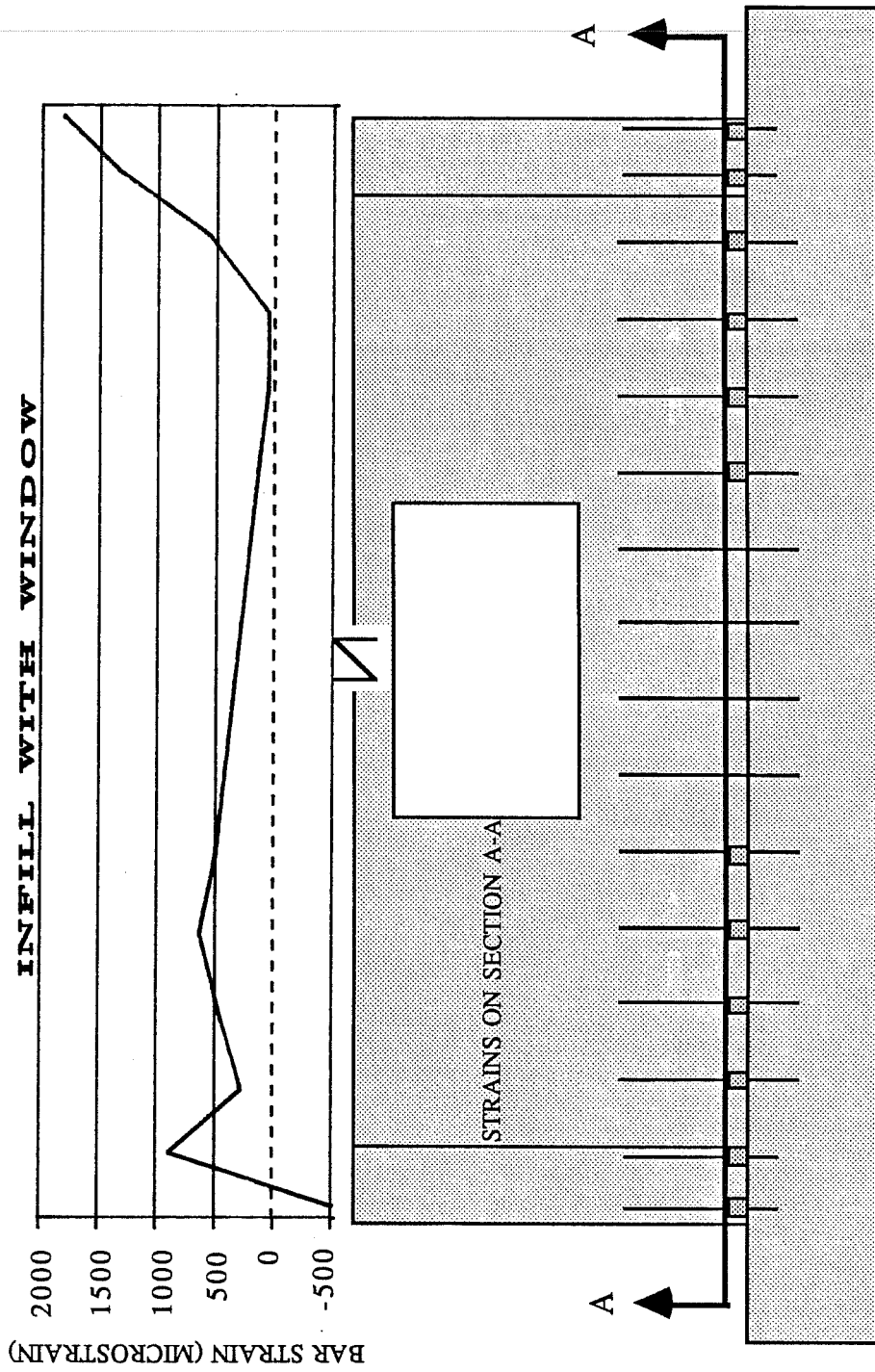


Fig. 3.35 Strain Profiles, Cycles to 180 K, Base of Wall

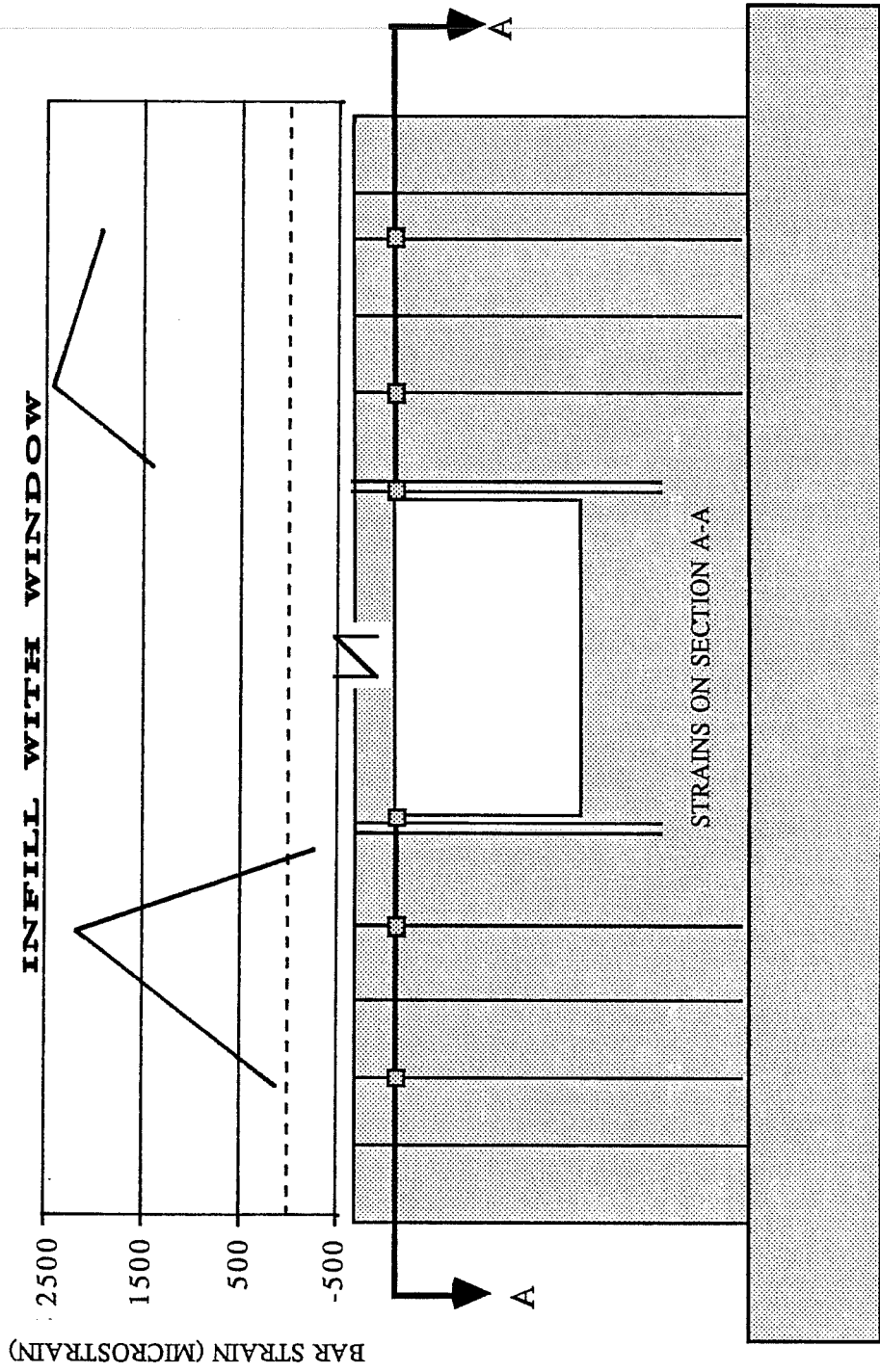


Fig. 3.36 Strain Profiles, Cycles to 180 K, Top of Opening

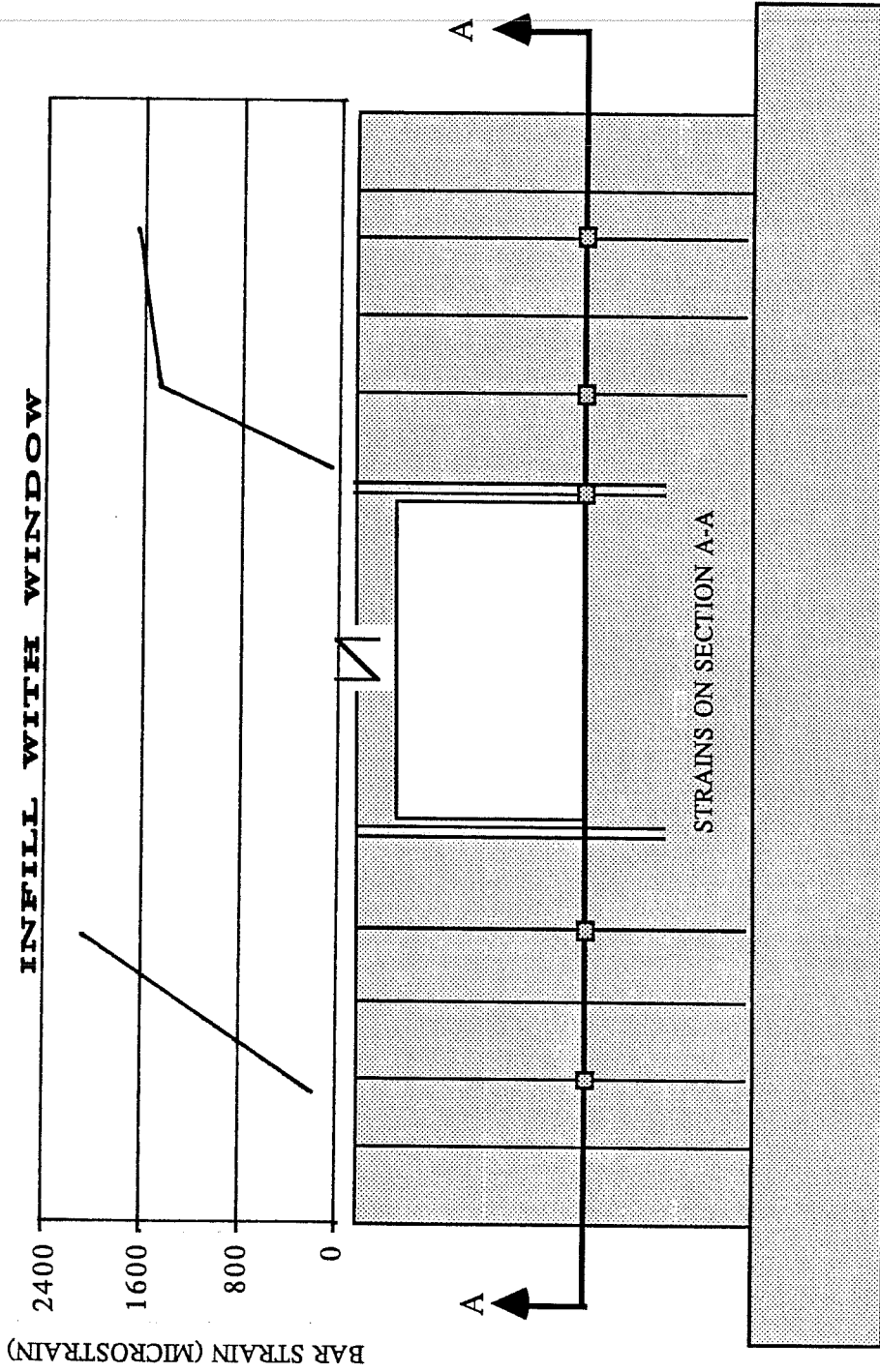


Fig. 3.37 Strain Profile, Cycles to 180 K, Bottom of Opening

# INFILL WITH WINDOW

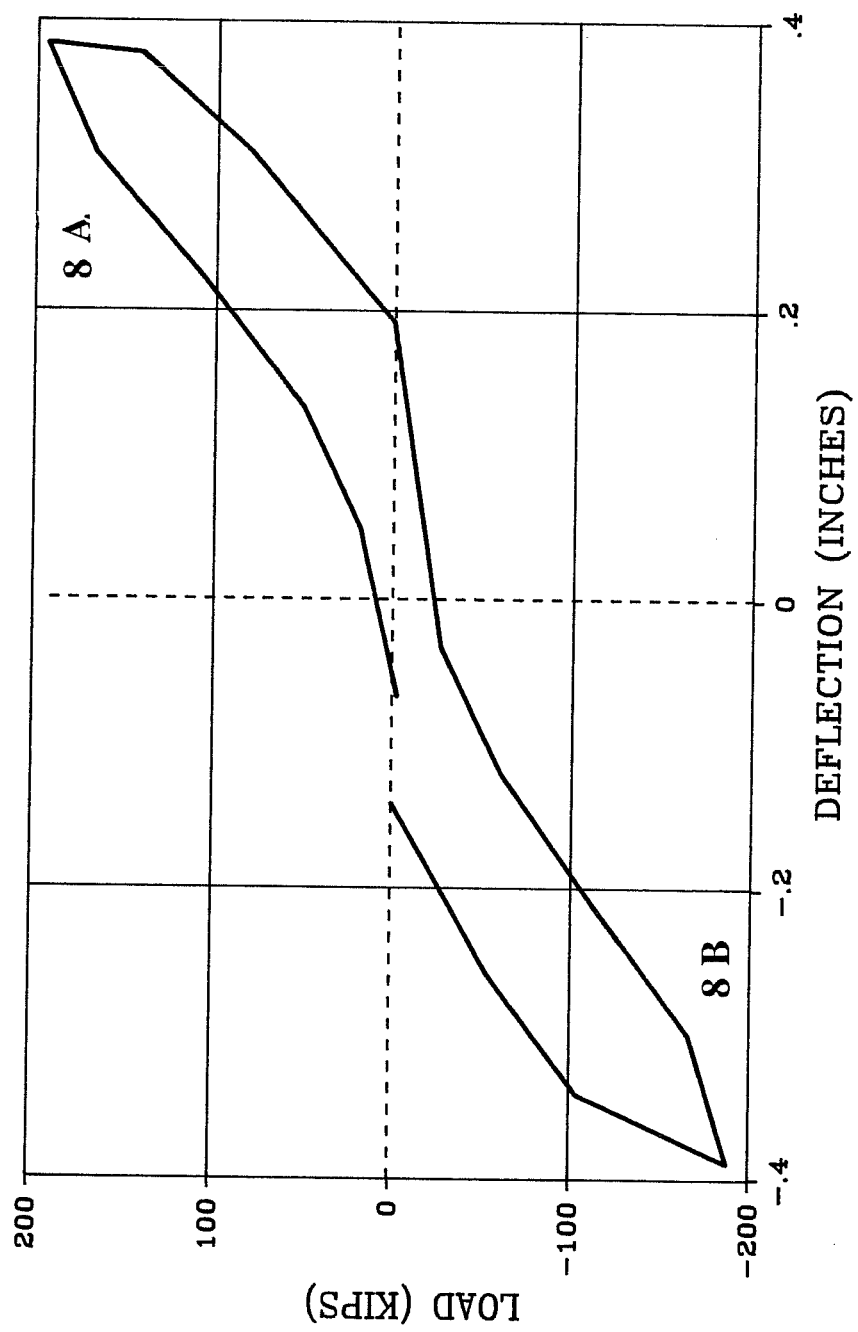


Fig. 3.38 Load-Deflection Response, Cycles to 0.50% Drift



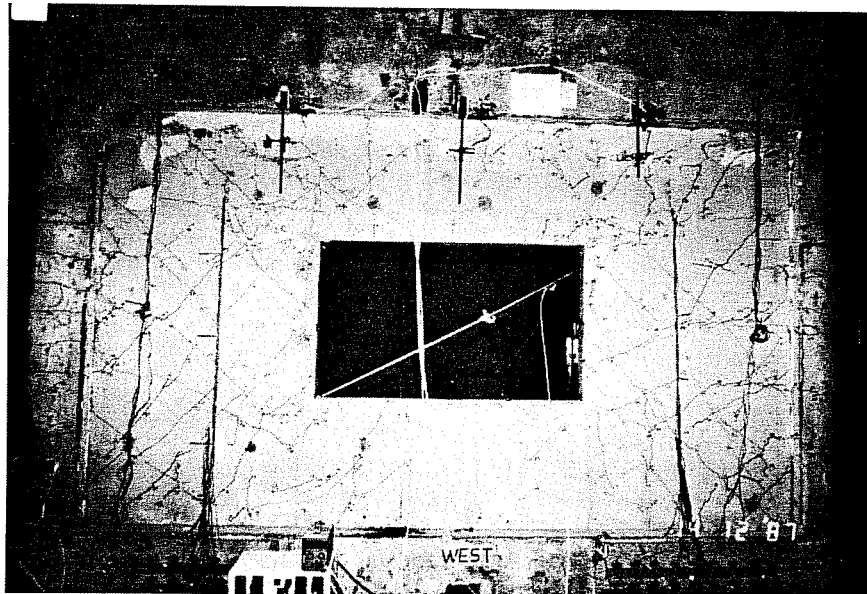


Fig. 3.39 Crack Patterns, Cycles to 0.50% Drift

# INFILL WITH WINDOW

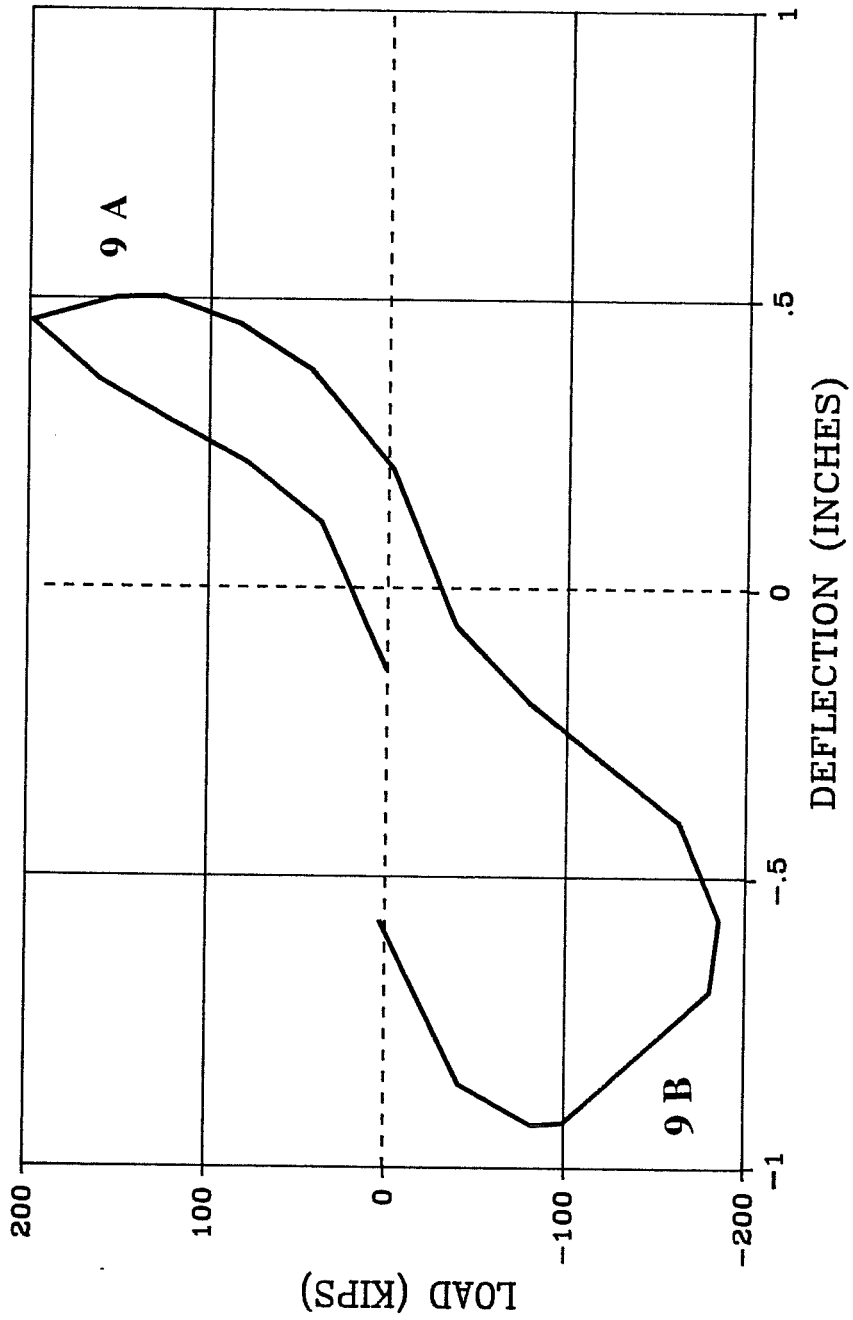


Fig. 3.40 Load-Deflection Response, Cycles to 200 K

column and wall section. Very large inclined cracks appeared on the upload side of the specimen in the wall and through the top of the column. These cracks were very wide under load. Considerable crushing of concrete in the upper, download corner of the window opening was noted in the negative direction, indicating a concentration of compression in this area. More crushing of the strut on the download side occurred under positive loads. At the top positive corner of the wall, crushing was noted at failure under negative loads. Splitting of the wall was evident in the window opening, with crack widths in excess of 1/4 in. Some of the damage observed during this cycle is pictured in Figures 3.41, 3.42, 3.43, 3.44, 3.45 and 3.46. The maximum drifts reached by the specimen were 0.55% in the positive direction and 0.68% in the negative. The maximum load reached was 198 kips in the positive direction and 186 kips in the negative.

Strain distributions at the base of the specimen indicated that the extreme column bar on the upload side of the specimen carried very little load, possibly from an anchorage failure created upon failure in the other direction. The interior column bar on the upload side of the specimen yielded as did the interior column bar on the download side of the specimen. The remainder of the specimen showed virtually no change from the magnitude and distribution of strains found on this section in the previous cycle. Strains on horizontal sections at the bottom of the window opening showed an overall decrease in net tension on both sides of the specimen compared with the previous cycle. Strains on the horizontal section at the top of the window opening showed tensile spikes at the middle of both piers as those bars bridged large cracks there.

### 3.3 Infill With Door

**3.3.1 Condition Prior to Testing.** The infill with the door was the last specimen to be tested. It was subjected to many cycles of load and deflection. The sequence of applied load and deflection was as follows: one full reversed cycle to 0.07% drift, one cycle to 80 kips, one half cycle to 100 kips, two cycles to 120 kips, one cycle to 0.17% drift, one cycle to 0.27% drift, one cycle to 180 kips, one cycle to 0.34% drift, one cycle to 0.5% drift, one cycle to 0.55% drift and one cycle to 0.6% drift. The load history is pictured in Figure 3.47.

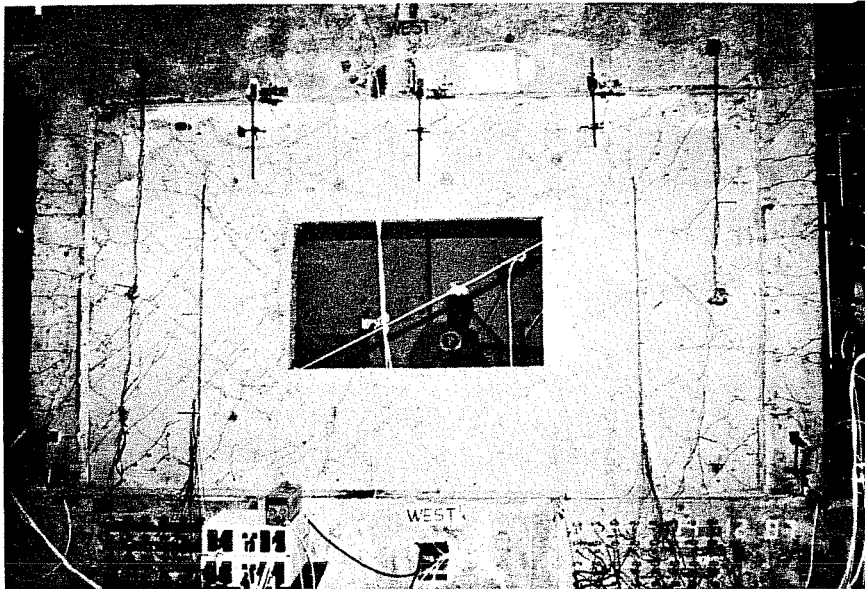


Fig. 3.41 Infill with Window at Failure, Elevation



Fig. 3.42 Upload Column at Failure



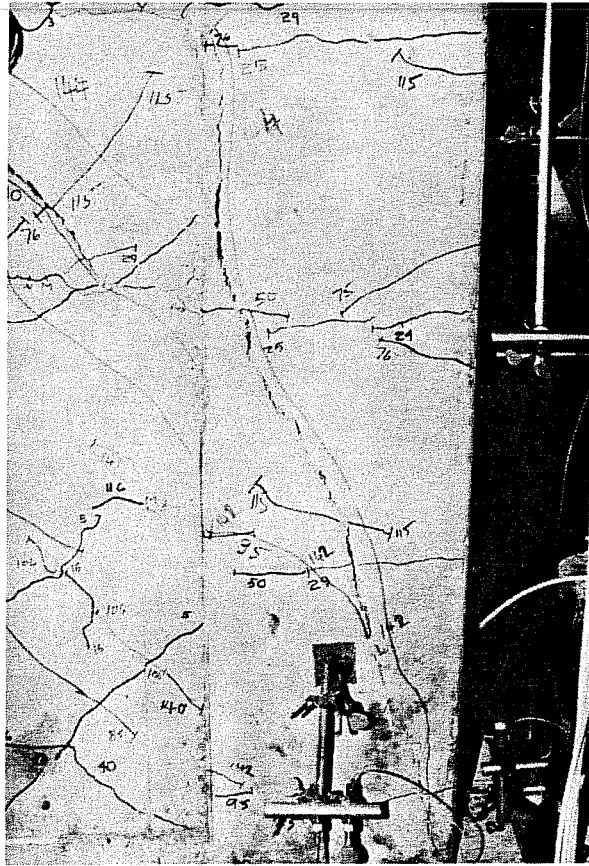


Fig. 3.44 Download Column at Failure

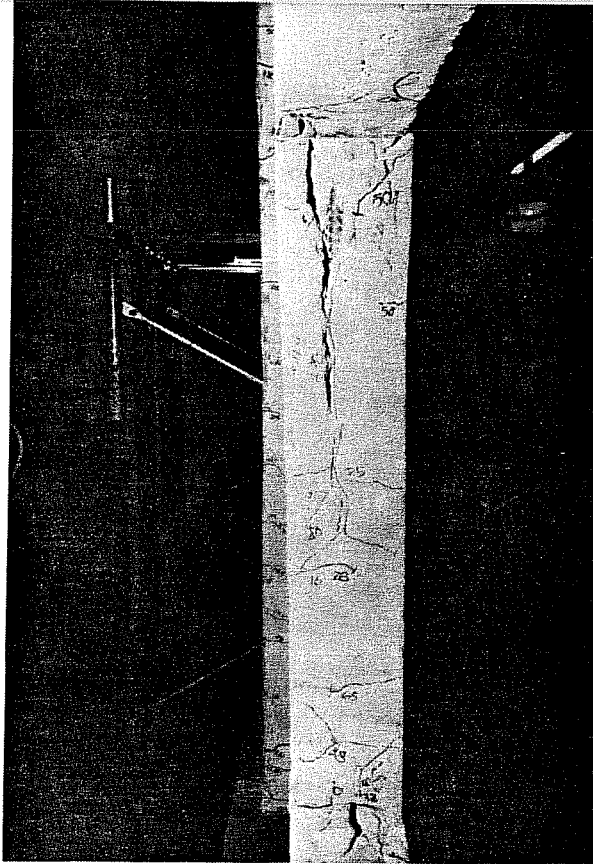


Fig. 3.45 Wall Splitting in Window Opening



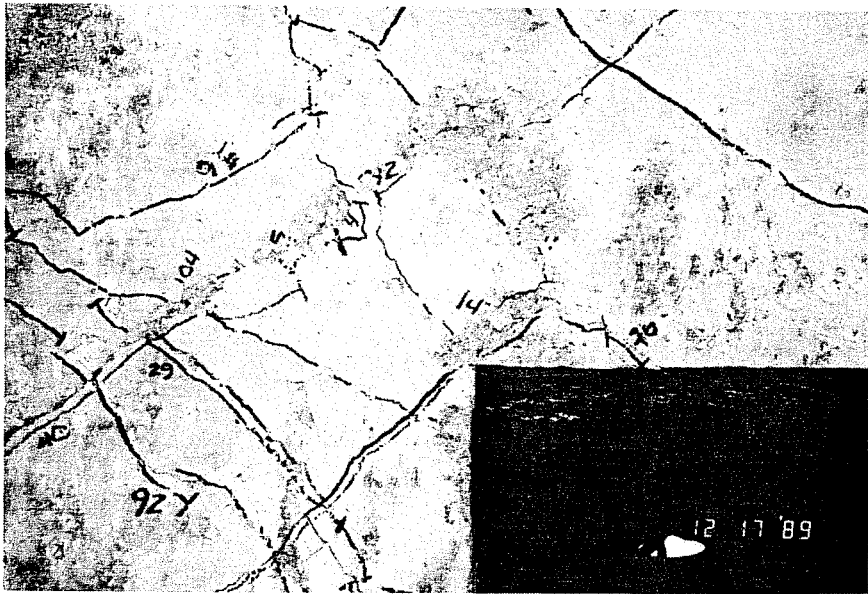
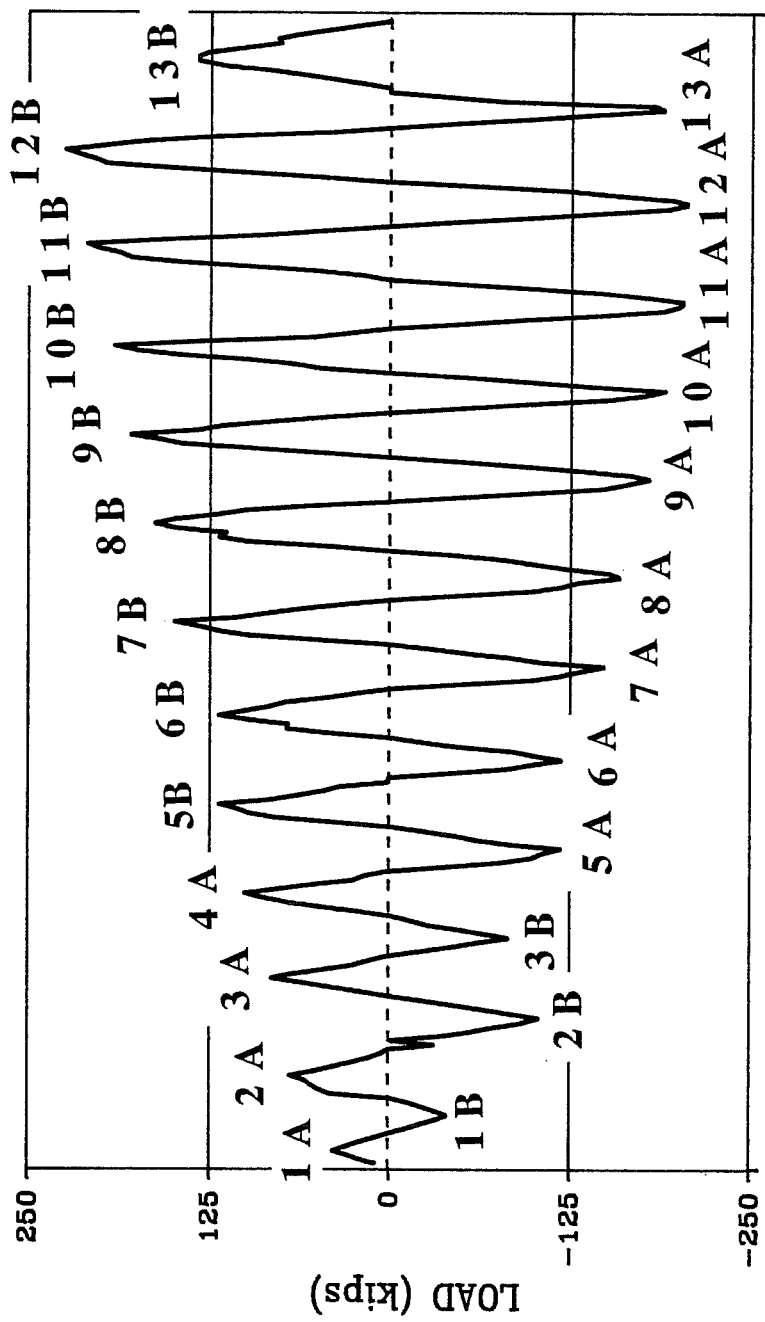


Fig. 3.46 Strut Crushing at Failure



LOAD STAGE

Fig. 3.47 Load History, Infill with Door

The load-deflection history is presented in Figure 3.48. Cracking was found in this panel prior to testing in corners around the opening, along dowels and trim steel and in the vicinity of large, epoxy repaired voids.

### 3.3.2 Response to Cyclic Loading

*Cycle to 0.07% Drift.* One cycle of drift to 0.07% was applied to the infill with the door opening. This drift limit was based on a comparison with the drifts exhibited by the full infill and the infill with the window opening. The load-deflection plot for this cycle is contained in Figure 3.49. An average drift of 0.06% was achieved in this cycle, however, the stiffnesses were different in the positive and negative directions. The stiffness in the negative direction was 75% of the stiffness in the positive direction. Difficulties with the X-Y plotter used to control deflection and load caused the specimen to be subjected to a much larger deflection in the negative direction than in the positive direction. Drift in the positive direction was 0.05% and 0.08% in the negative direction. The load reached in the positive direction was 69 kips and 104 kips in the negative direction. Inclined cracking in the panel was extensive. Four major cracks were found in the upload panel and three were found in the download panel under negative loads. These cracks indicated an attempt to mobilize most of the pier as they were well spaced. In this specimen, a "pier" was considered to be the column and the infilled wall sections on either side of the door opening. Horizontal cracks in the upload column appeared at the level of the first, third, fourth and seventh column ties from the bottom and at the base of the column. While loading in the positive direction, three major cracks were formed in the upload pier and one in the download pier. Horizontal cracks in the upload column formed only at the base. The specimen was pictured in Figure 3.50.

Strain distributions at the base of the specimen during this load cycle indicate areas of high tension in the upload column and in the download pier at the door opening. The download column was in net compression. A horizontal section at the level of the door opening indicated the top of the upload pier was in net tension and the top of the download pier was in net compression. The strain distributions are pictured in Figures 3.51 and 3.52. On a horizontal section

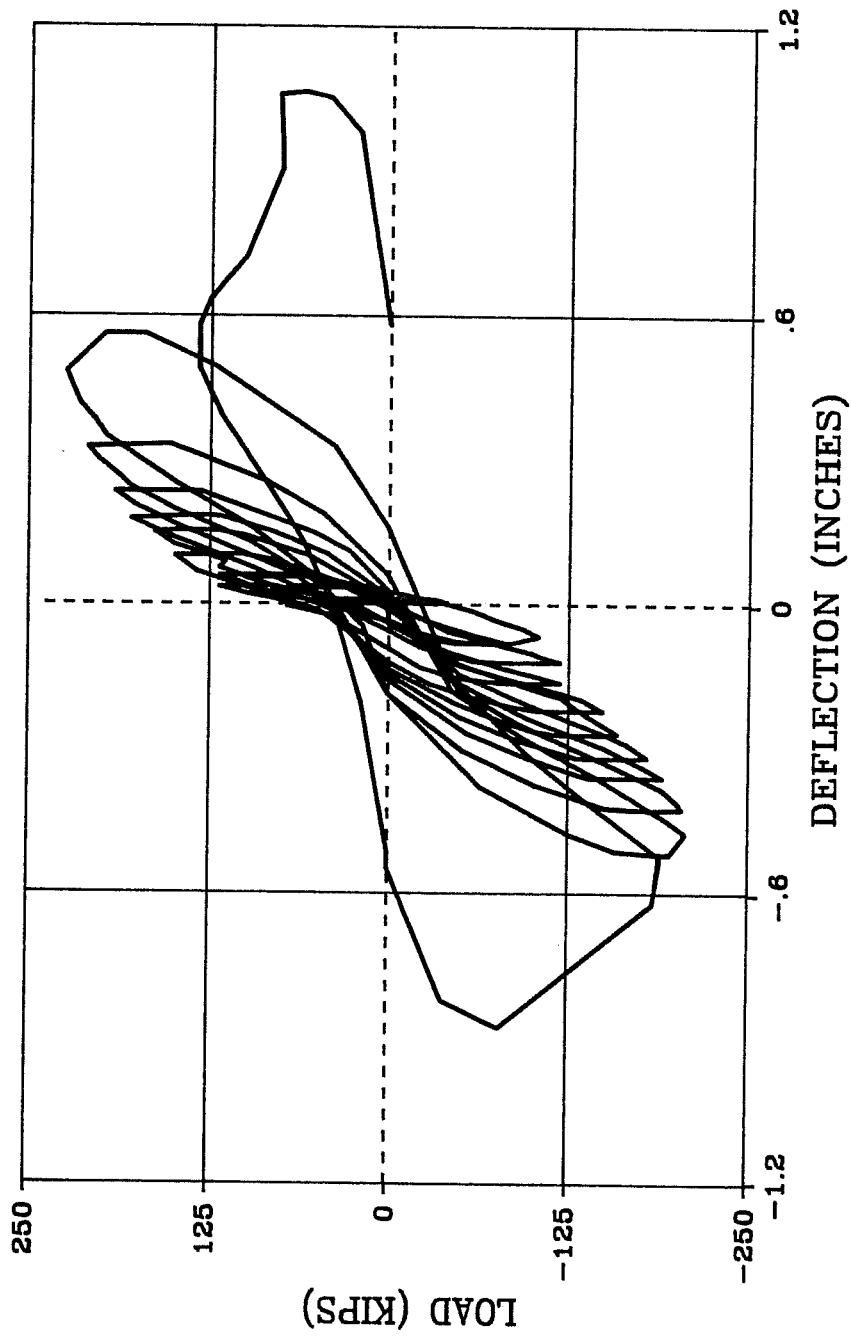


Fig. 3.48 Load-Deflection History, Infill with Door

# INFILL WITH DOOR

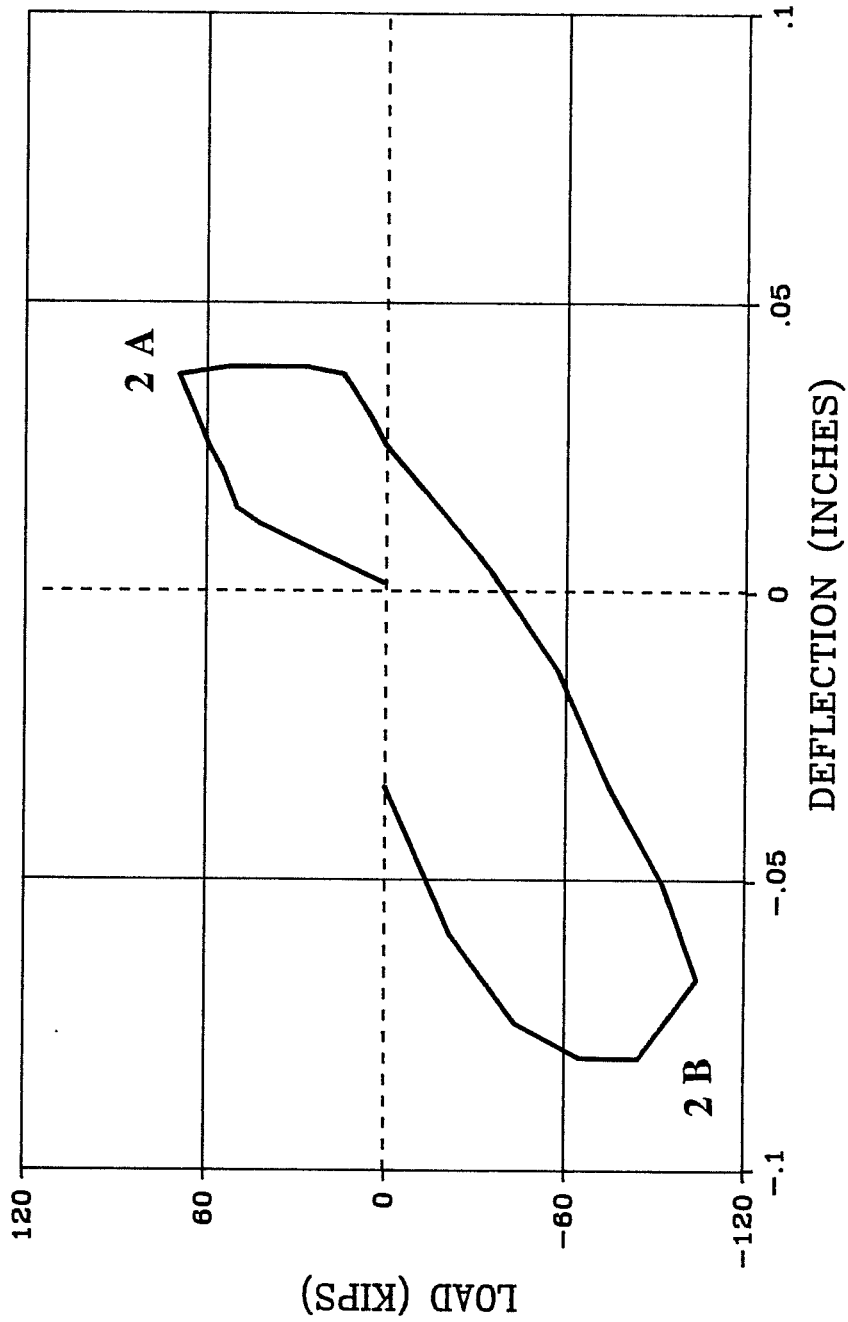


Fig. 3.49 Load-Deflection Response, Cycles to 0.07% Drift

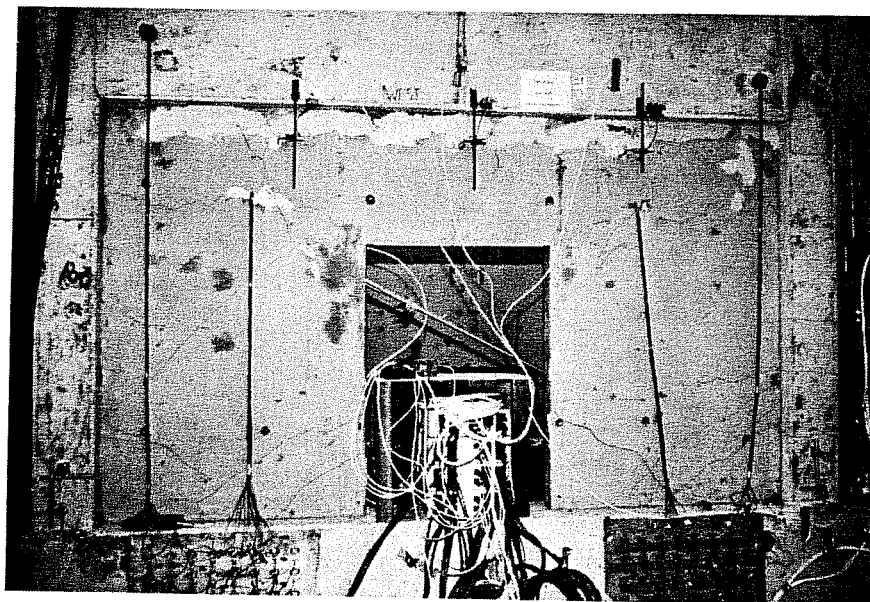


Fig. 3.50 Crack Patterns, Cycles to 0.07% Drift

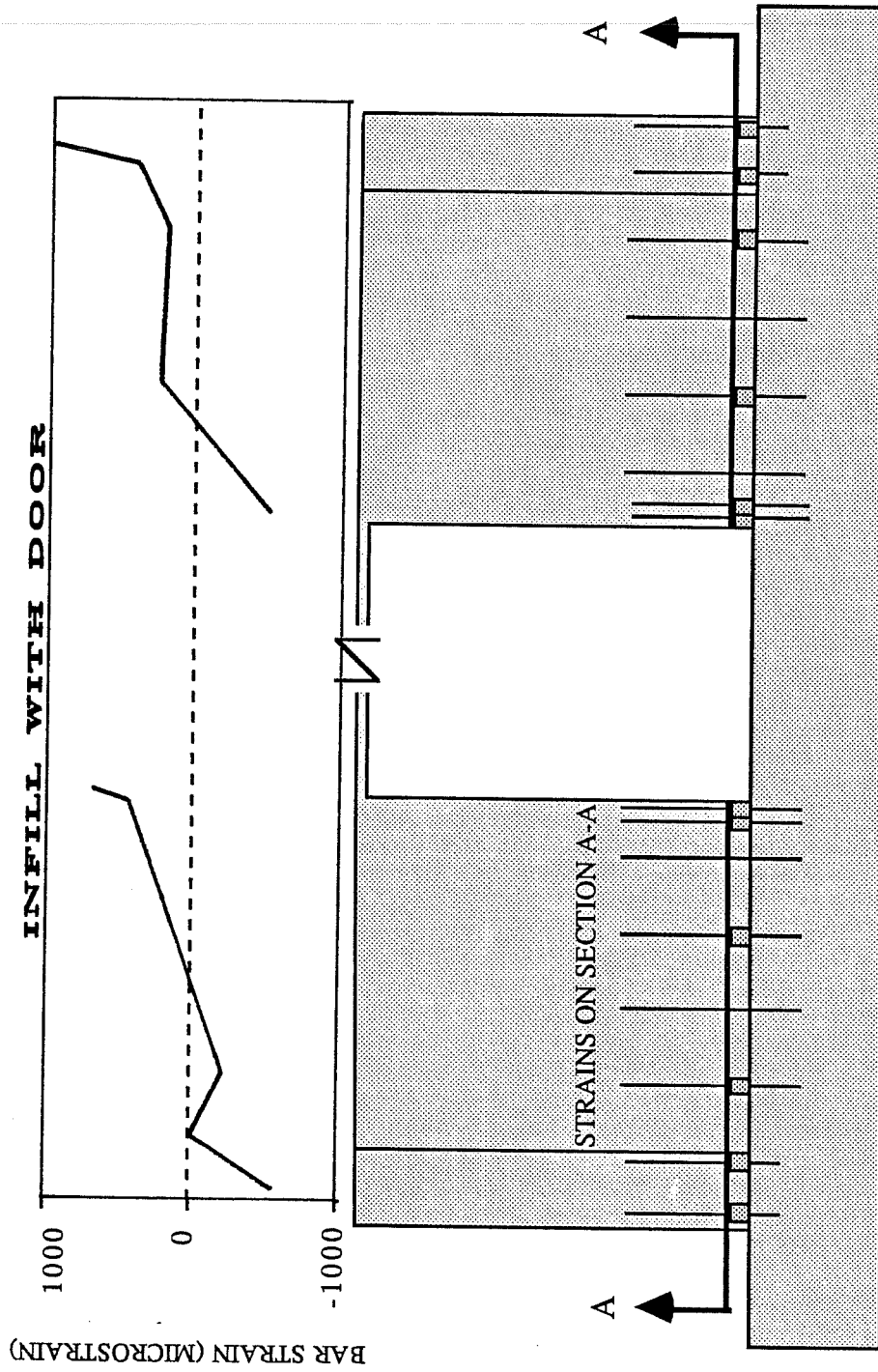


Fig. 3.51 Strain Profiles, Cycles to 0.07% Drift, Base of Wall

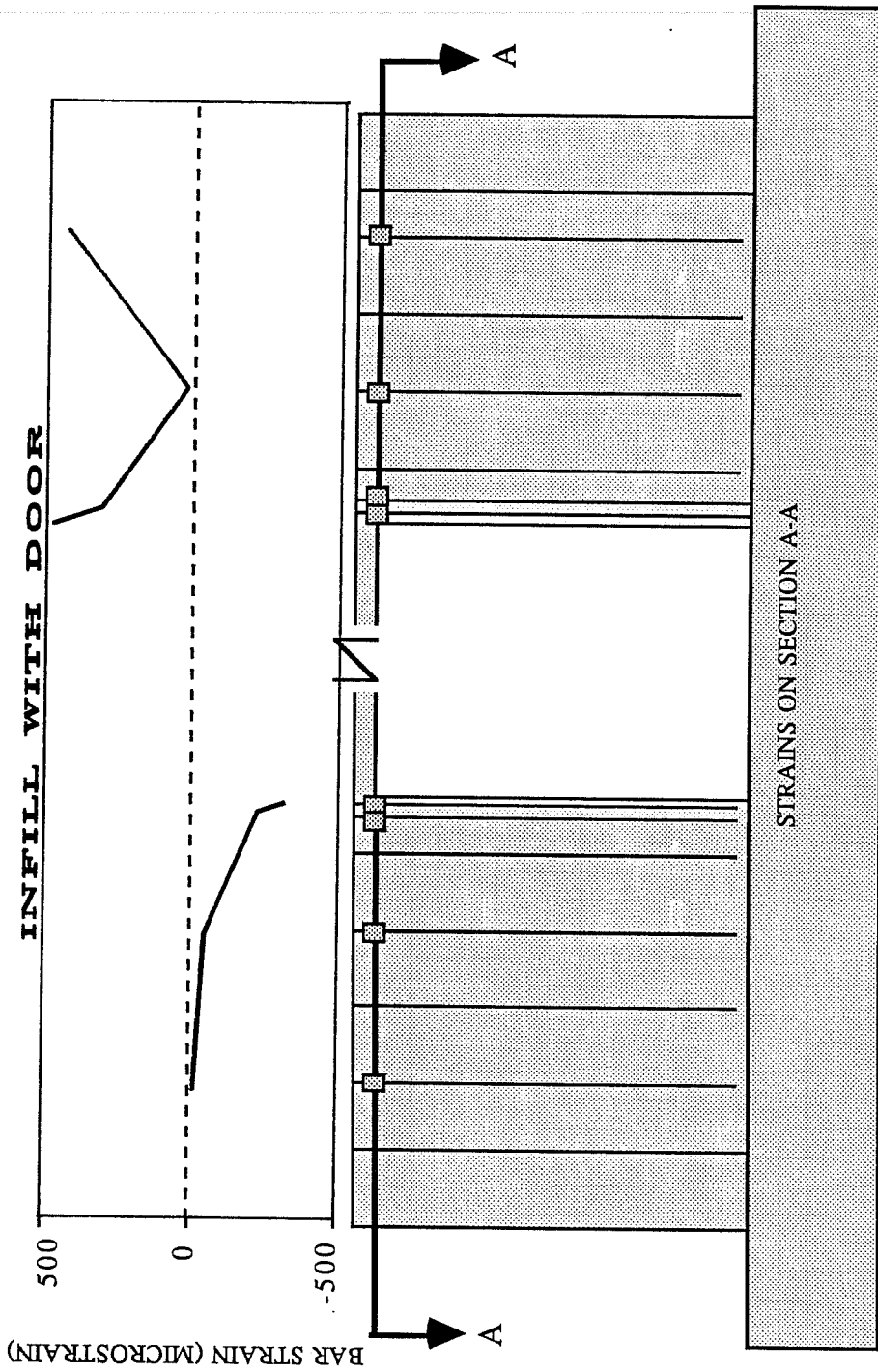


Fig. 3.52 Strain Profile, Cycles to 0.07% Drift, Top of Opening



at the top of the wall, strain histories revealed that the only location of distress was in the upload column bars closest to the infilled wall. Those bars reached a maximum tensile strain of greater than 75% of yield in the last two cycles. On vertical sections, dowels grouted into upload and download columns showed no significant strains for the duration of this test. Gages on horizontal trim bars on the upload side of the opening showed small strains in strain histories. On the download side of the opening, horizontal trim bar strains were compressive reaching a maximum compressive strain of greater than one half of the yield strain in the last three cycles.

*Cycles to 80K.* One cycle of load was applied to the infill with the door opening next. This load cycle was executed primarily to check out equipment problems. The load-deflection plot for this cycle is contained in Figure 3.53. The average drift in this cycle was 0.07% at an average load of 83 kips. The drifts in the two directions were significantly different reflecting a large residual deformation in the negative direction prior to and upon completion of the full reversed cycle. Stiffness in the negative direction was 81% of the stiffness in the positive direction. This difference in stiffness in the two directions was primarily attributed to damage resulting from the higher load and deflection applied in the negative direction in the previous cycle. The presence of epoxied voids in the upload upper joint for loading in the negative direction probably had some effect on stiffness as well. Stiffness in this cycle was 66% of the average stiffness in the previous cycle to 0.07% drift. While loading in the positive direction, horizontal cracks formed in the upload column at the location of the first four column ties from the bottom of the specimen. Some rather small inclined cracks formed in the upload panel at the height of the top of the door. A vertical crack formed on the vertical trim bar on the download side of the opening. This crack indicated the beginning of buckling in the trim bar, which was unconfined and in compression at the elevation of the crack. Loading in the negative direction led to horizontal crack formation in the upload column at the first and second column ties from the bottom of the specimen. Small extensions in inclined panel

# INFILL WITH DOOR

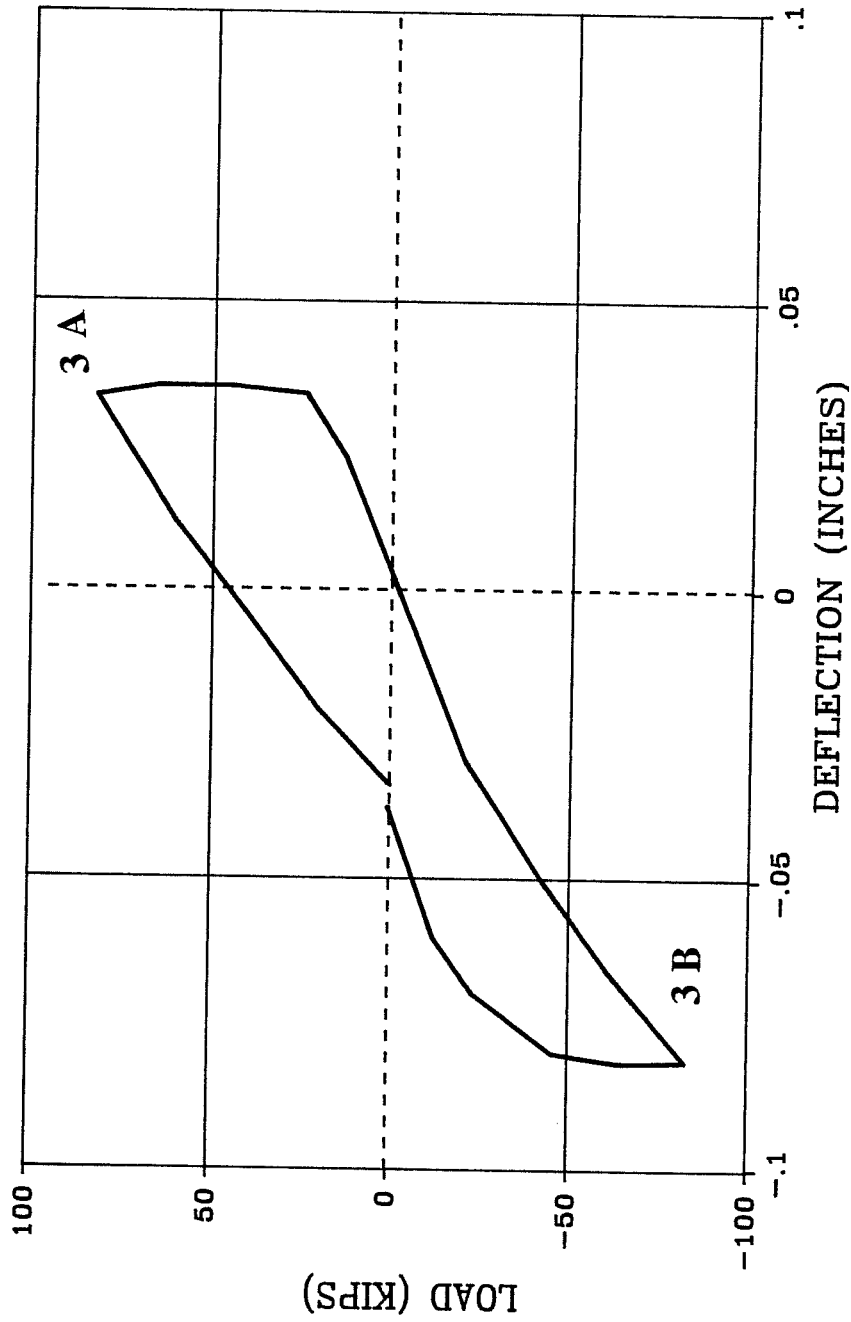


Fig. 3.53 Load-Deflection Response, Cycles to 80 K

cracks were found on the upload pier. Small new inclined cracks formed in the download pier in addition to some small extensions of cracks there.

Strain profiles at the base of the wall indicated that the extreme column bar in the upload pier yielded. The vertical trim bar on the download side of the door opening was about one half of the yield strain. Strains at the top of the door opening indicated net tension on the upload side and an increase in tensile strains across that section. The download section at this elevation also showed a decrease in compressive strains. These strain profiles are presented in Figures 3.54 and 3.55.

*Cycle to 100K.* At this stage in the test, it was decided to even out the damage in the two directions to bring absolute deflections to symmetry. To this end, one cycle of load to 100 kips was applied in the positive direction only. The load-deflection plot for this half cycle is contained in Figure 3.56. The drift reached in this cycle was 0.07%. The stiffness in this half cycle was 98% of the average stiffness in the previous cycle, 10% greater than the stiffness in the negative direction and 89% of the stiffness in the positive direction in the previous cycle. Thus, the stiffnesses in the two directions were essentially the same. In terms of damage as indicated by crack patterns, this attempt was successful. In this cycle, horizontal cracks in the upload column formed at the fifth and sixth column ties from the bottom of the wall. Inclined cracks in the joint at the top of the upload column also formed. One more major crack formed in the upload pier and a smaller crack formed in the download pier. A small positive residual deformation after this positive loading remained upon completion of this half cycle. This residual deflection was not large enough to bring deflections in the two directions to symmetry.

Strain profiles at the base of the specimen for this half cycle were essentially the same as in the previous cycle. Strains on a section at the level of the top of the door opening indicate that most of the action had taken place in the upload pier with significant increases in tensile strains there. Strains in the download pier at this elevation showed virtually no change.

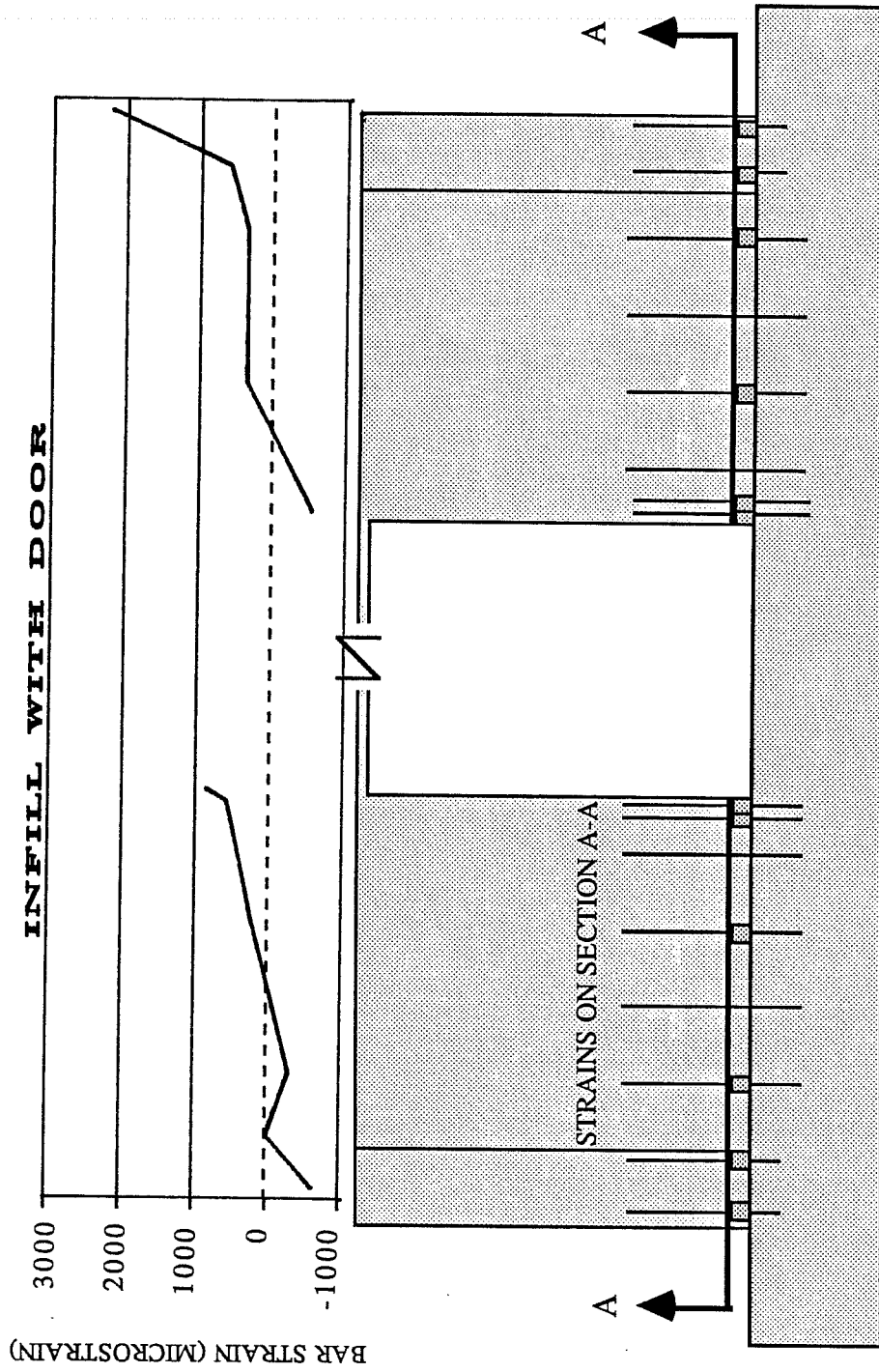


Fig. 3.54 Strain Profiles, Cycles to 80 K, Base of Wall

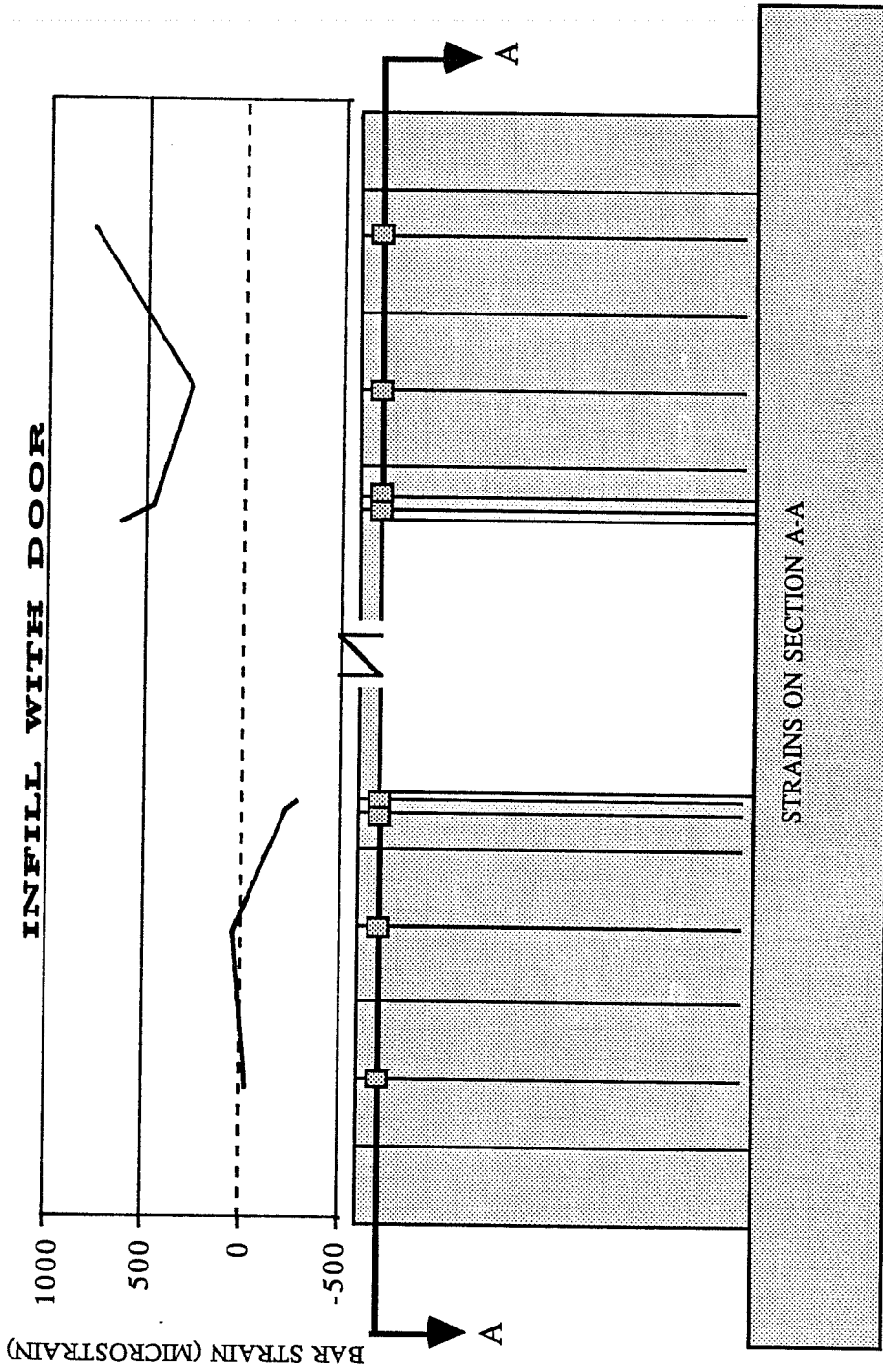


Fig. 3.55 Strain Profile, Cycles to 80 K, Top of Opening

# INFILL WITH DOOR

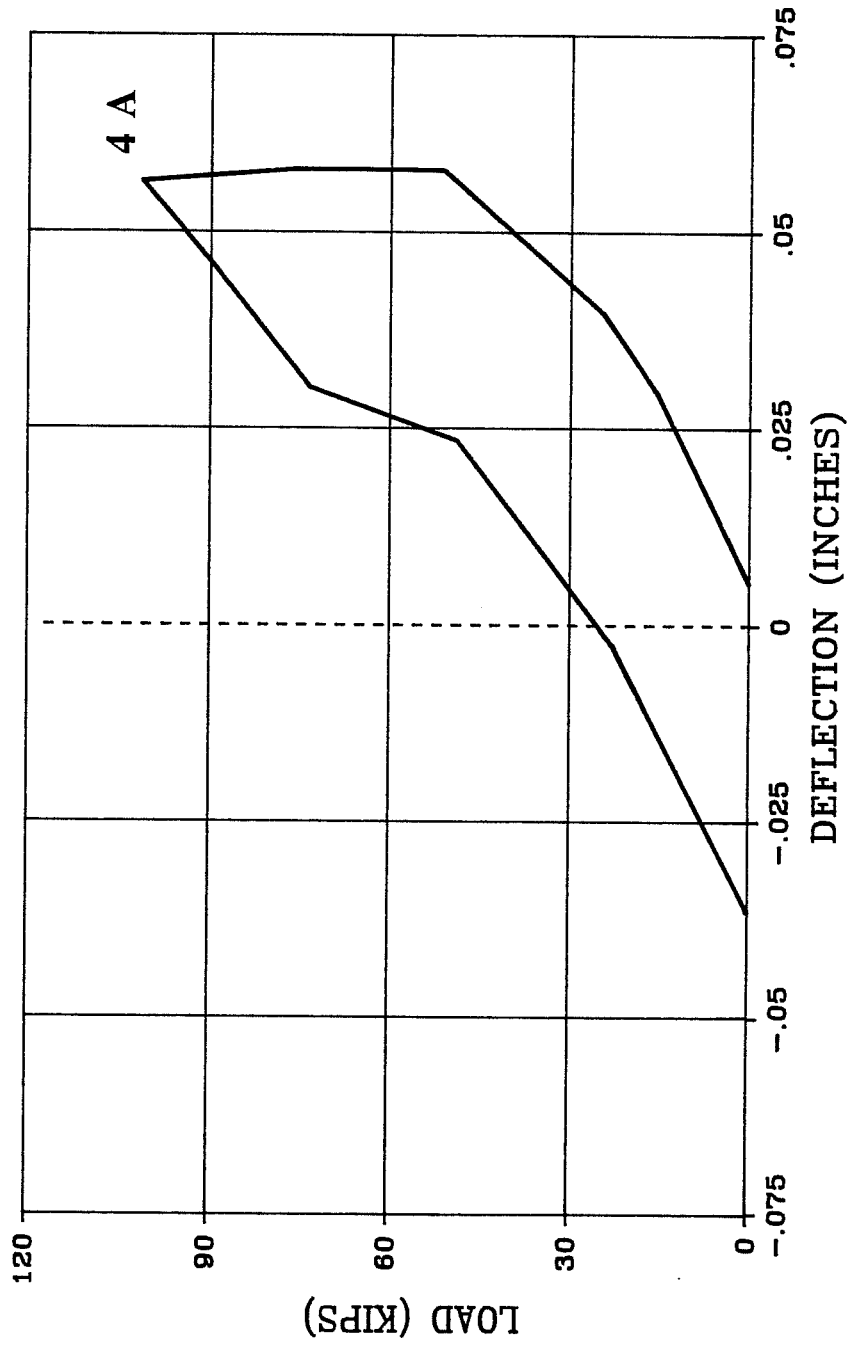


Fig. 3.56 Load-Deflection Response, Cycles to 100 K

*Cycles to 120K.* Two cycles of load to 120 kips were applied to the infill with the door opening. This load limit was chosen for comparison with the full infill and the infill with the window opening. The load-deflection plot for these two cycles is contained in Figure 3.57. Note that the negative peak is labelled "A" as the negative direction was the direction of first loading for this and all subsequent cycles.

Upon completion of the first cycle to 120 kips, there was a negative residual deflection after loading in the positive direction. This resulted in two very different drift levels in each direction with an average drift of 0.11%. The stiffness in the two directions was similar. The stiffness in this cycle was 92% of the stiffness in the previous half cycle. The closing of cracks produced the increase in stiffness with increasing load early in these cycles that was found in the previous tests. There was one major crack in this cycle in the download pier. Extensions of previous cracks formed in the upload joint at the top of the wall, in the upload and download piers and around column ties at the top of the column. Small inclined cracks occurred at the top of the wall on the upload side of the specimen.

Changes in the strain gradient at the base of the specimen were concentrated in the upload pier where increases in tensile strains were found. The interior column bar in the upload pier deformed to about one half of the yield strain in tension. Strains on this section in the download pier showed essentially no change except in the column where the value of the gradient almost doubles over the value in the previous cycle. These distributions do not change significantly with additional cycles to the same load. The strain profile on the horizontal section at the level of the top of the door opening showed slight increases in net tension in the upload pier and no change in the strains in the download pier. Comparisons of distributions on the section at this elevation revealed no change in the next cycle to the same load.

In the second cycle to 120 kips, drift level averaged 0.12% with large differences in the drift exhibited in the two directions. Stiffnesses in the two directions were, however, similar and constituted 96% of the stiffness exhibited

# INFILL WITH DOOR

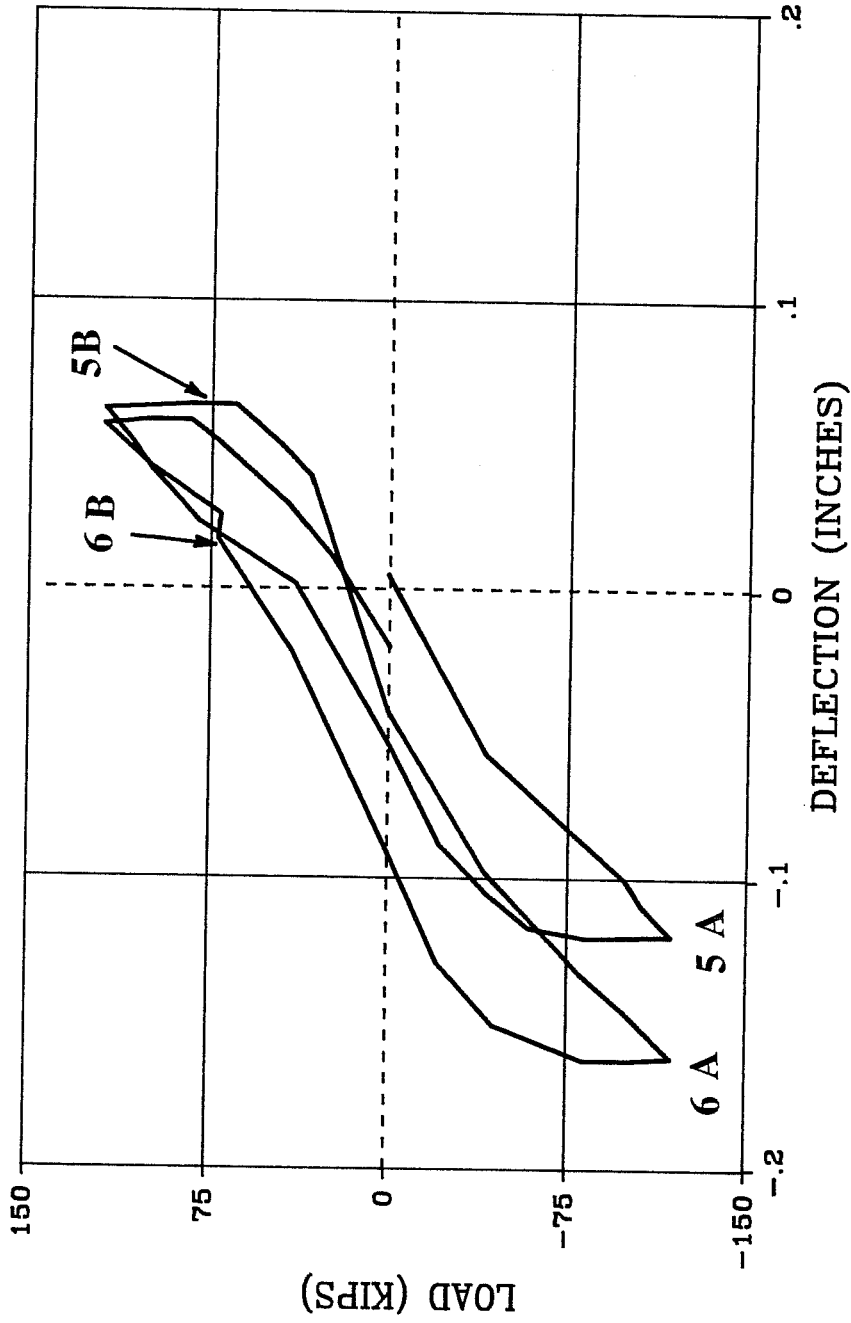


Fig. 3.57 Load-Deflection Response, Cycles to 120 K



in the previous cycle to 120 kips. No major cracking occurred in this cycle, rather small extensions of cracks were found near the top of the columns and in the upload and download piers. Small new inclined cracks formed at the top of the wall over the door opening and on the upload end of the wall.

*Cycles to 0.17% Drift.* One cycle of drift to 0.17% was applied to the infill with the door opening. This drift limit was exhibited in both the full infill and in the infill with the window opening. The load-deflection plot for this cycle is illustrated in Figure 3.58. The drifts in each direction were asymmetric with an average drift of 0.19%. Stiffnesses were not similar in the two directions with the stiffness in the positive direction totalling 83% of the stiffness in the negative direction. The average stiffness in this cycle was 78% of the average stiffness in the previous cycle to 120 kips. Damage occurred in both the upload and download piers in the form of new large cracks. Several new cracks formed on the upload side near the top of the specimen and at mid height of the door opening. Cracks in the download pier formed at about mid height of the door opening and ran down to the foundation girder. More horizontal cracks formed in the columns near the sixth and seventh column ties from the bottom of the specimen on the upload side. One large crack formed over the doorway. Crack patterns are pictured in Figures 3.59 and 3.60.

Strain profiles at the base of the specimen for this cycle indicate increases in tension in the two column bars of the upload pier and in the trim bars in the download pier. The gradient in the download column increases only slightly. The profile on the section at the door opening show slight increases in net tension across the upload pier and virtually no change in the distribution over the download pier.

*Cycles to 0.27% Drift.* One cycle of drift to 0.27% was applied to the infill with the door opening for comparison with behavior exhibited by the full infill and the infill with the window opening at the same drift. The load-deflection plot for this specimen is illustrated in Figure 3.61. The average drift obtained for this cycle was 0.25% with very different drifts in the negative and positive directions. Stiffness in the two directions was similar with an average loss of

# INFILL WITH DOOR

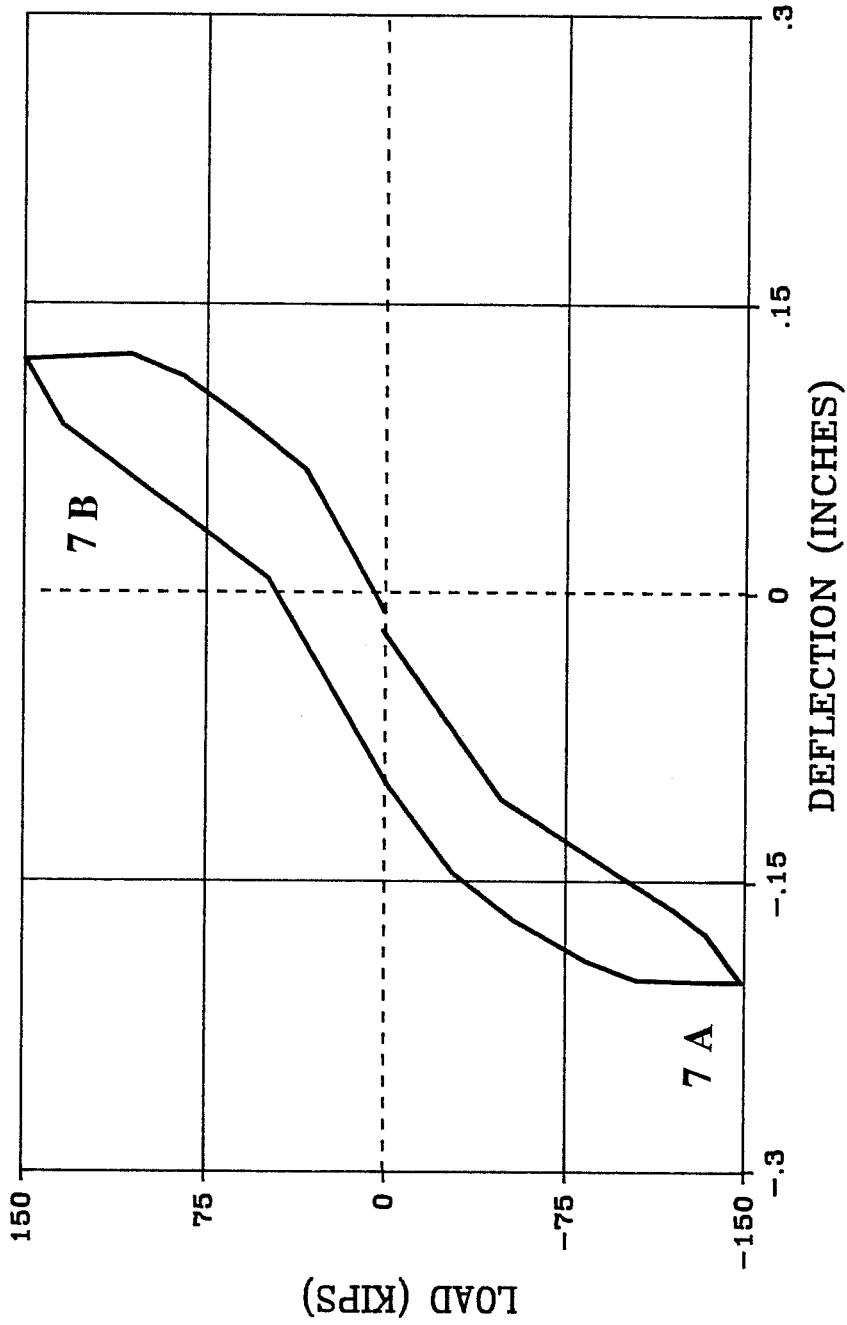


Fig. 3.58 Load-Deflection Response, Cycles to 0.17% Drift



Fig. 3.59 Crack Patterns, Cycles to 0.17% Drift, North Pier



Fig. 3.60 Crack Patterns, Cycles to 0.17% Drift, South Pier

# INFILL WITH DOOR

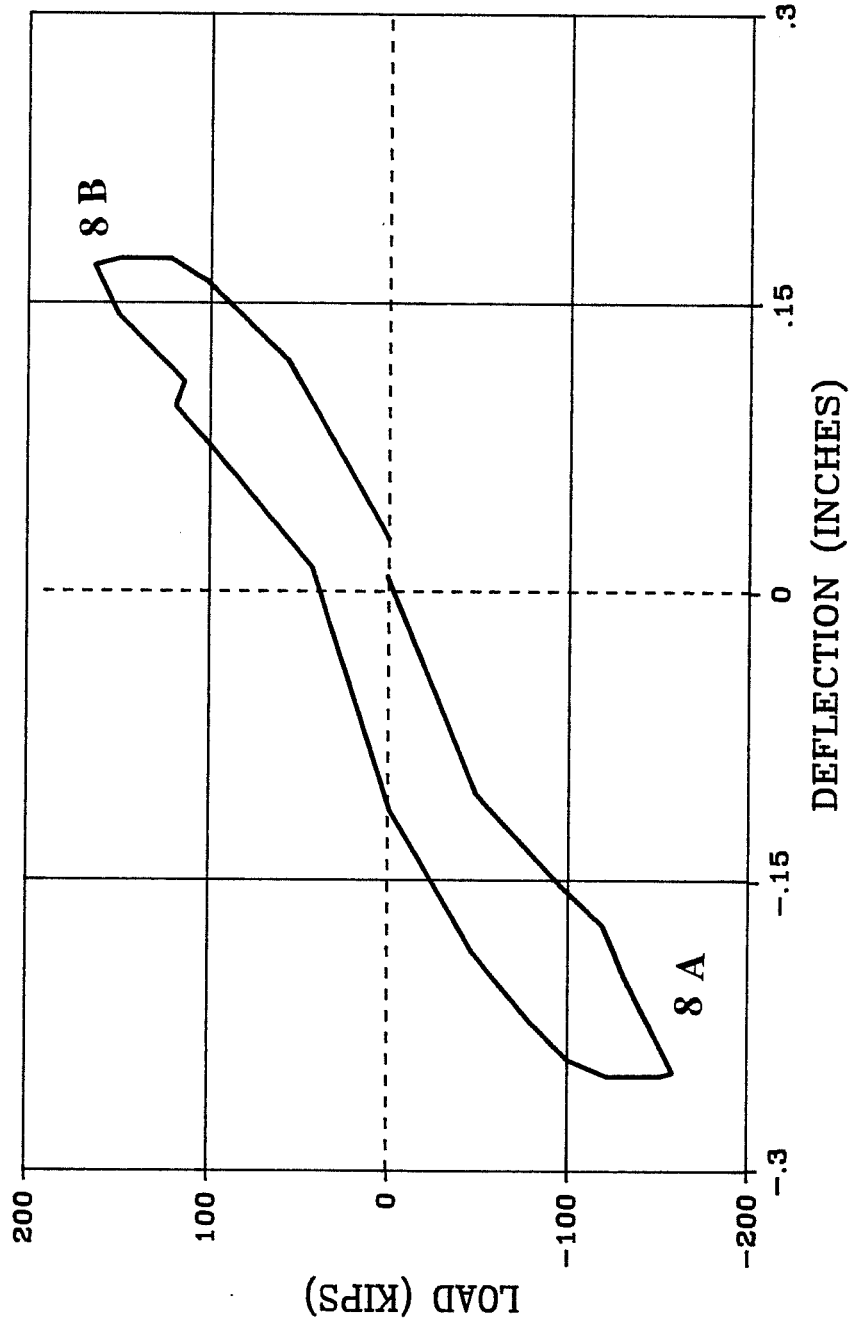


Fig. 3.61 Load-Deflection Response, Cycles to 0.27% Drift

17% of the stiffness in the previous cycle. Major cracking occurred in this cycle. Inclined cracks appeared in the middle of the upload pier between previously formed cracks. New horizontal cracks appeared in the upload columns at the first and seventh column ties. Vertical cracks near the corners of this column appeared in the splice region. A large inclined crack opened up on the download pier running from the top of the door opening to the face of the column. Damage in the download pier was remarkably symmetric. Cracks in the upload pier were in excess of 0.5 mm wide at the peak load. Cracks in the download pier were 0.4 mm wide. The damaged specimen is pictured in Figure 3.62. Strain profiles at the base of the wall indicated increases in tensile strain in the two column bars in the upload pier. The remainder of that pier exhibited almost no change of strain for this cycle. In the download pier, more tensile strains were found in the trim bars and an increase in the gradient in the two download column bars. The section at the top of the door opening on the download pier changed to net tension on that section. This change to net tension here indicated a shift in the orientation of the struts in the download pier. For the preceding cycles, the trim bars were in compression indicating that the compression strut passed through this location. A steeper angle of inclination of the strut forced the trim bars to provide the tensile tie required for equilibrium at the top of the opening. Increases in strain at this elevation in the upload pier were found. The vertical reinforcement in the panel at this elevation nearest to the column was within 10% of the yield strain. The profiles at these elevations for this cycle for loading in the positive direction are presented in Figure 3.63 and 3.64.

*Cycle to 180K.* One cycle of load to 180 kips was applied to the infill with the door opening. This load limit was chosen for comparison with the full infill and the infill with the window opening. The load-deflection plot for this cycle is pictured in Figure 3.65. The average drift exhibited in this cycle was 0.29%. Stiffnesses were similar in the two directions and constituted 93% of the stiffness exhibited in the previous cycle to 0.27% drift. New cracks appeared at the top of the wall near the download end of the opening and extended into the download pier. Small extensions of cracks were found in the download pier near the base of the specimen. In the upload pier, extensions of inclined cracks

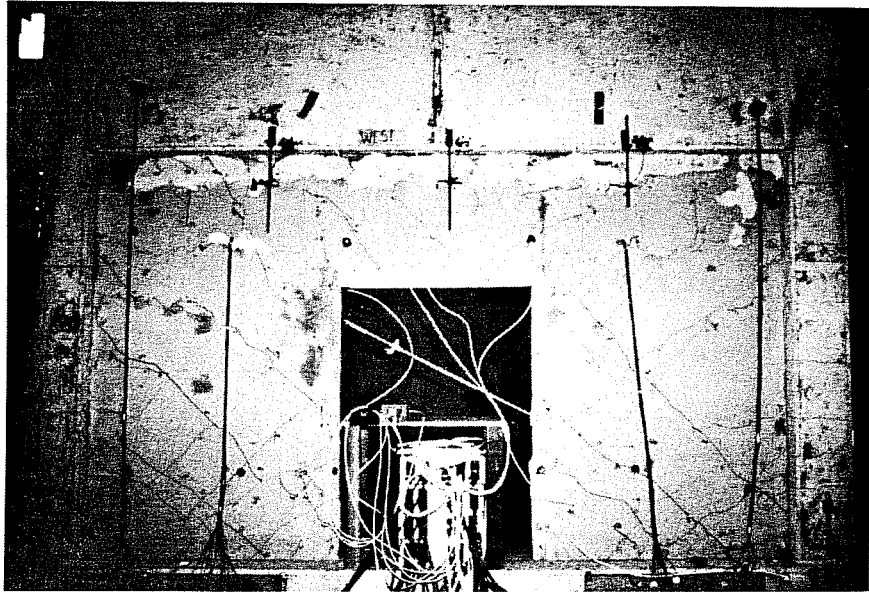


Fig. 3.62 Crack Patterns, Cycles to 0.27% Drift

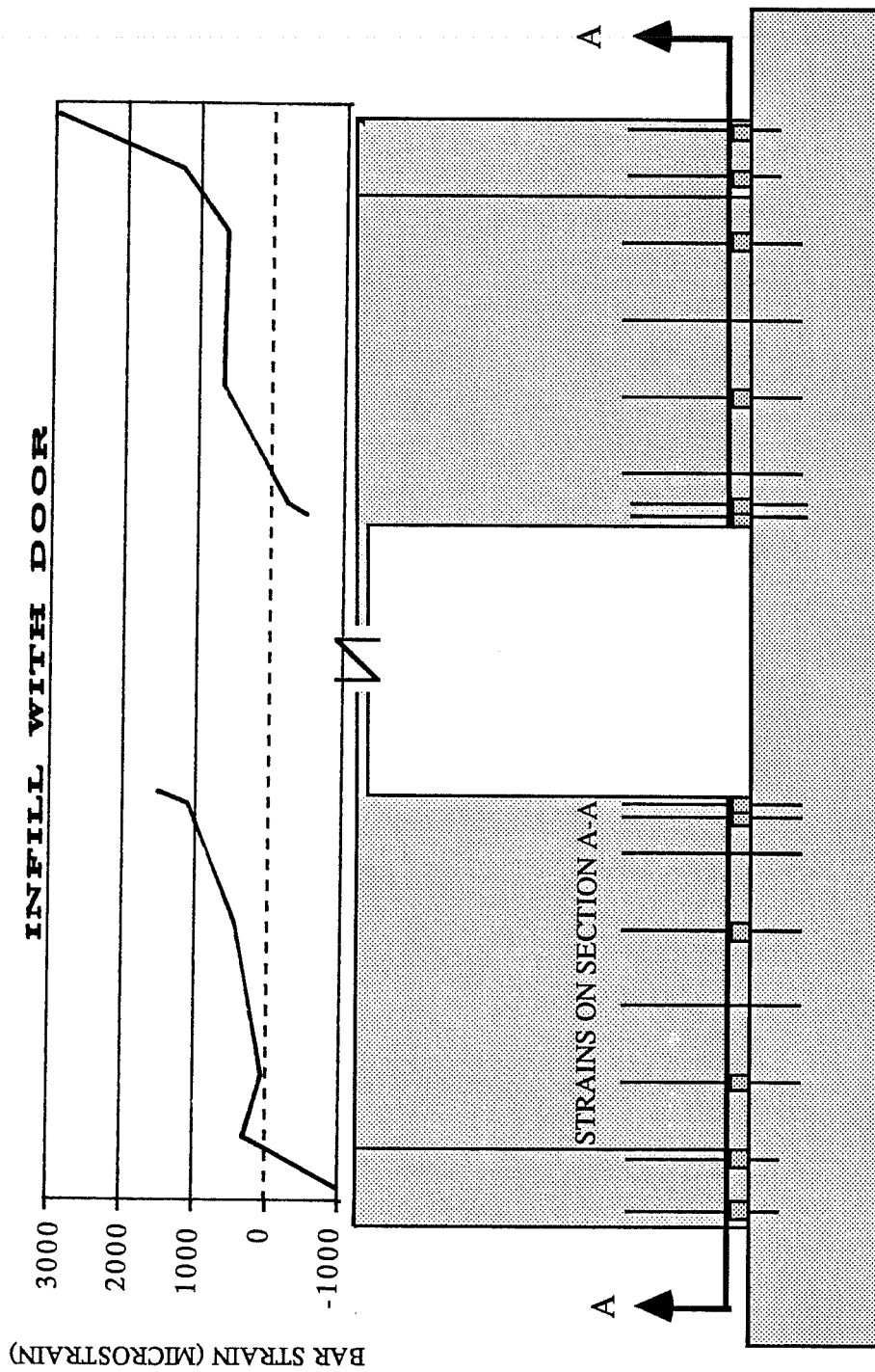


Fig. 3.63 Strain Profiles, Cycles to 0.27% Drift, Base of Wall



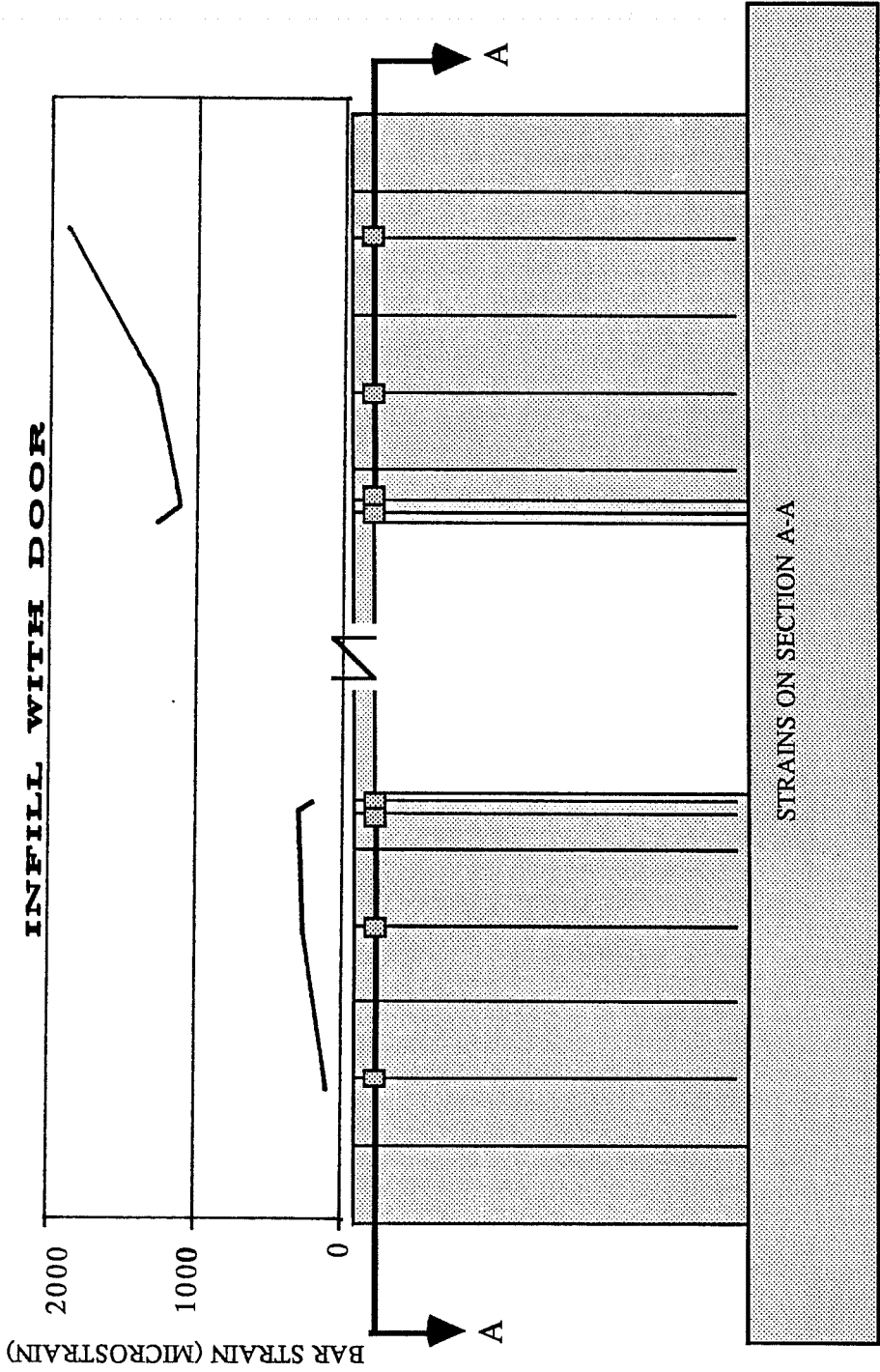


Fig. 3.64 Strain Profiles, Cycles to 0.27% Drift, Top of Opening

# INFILL WITH DOOR

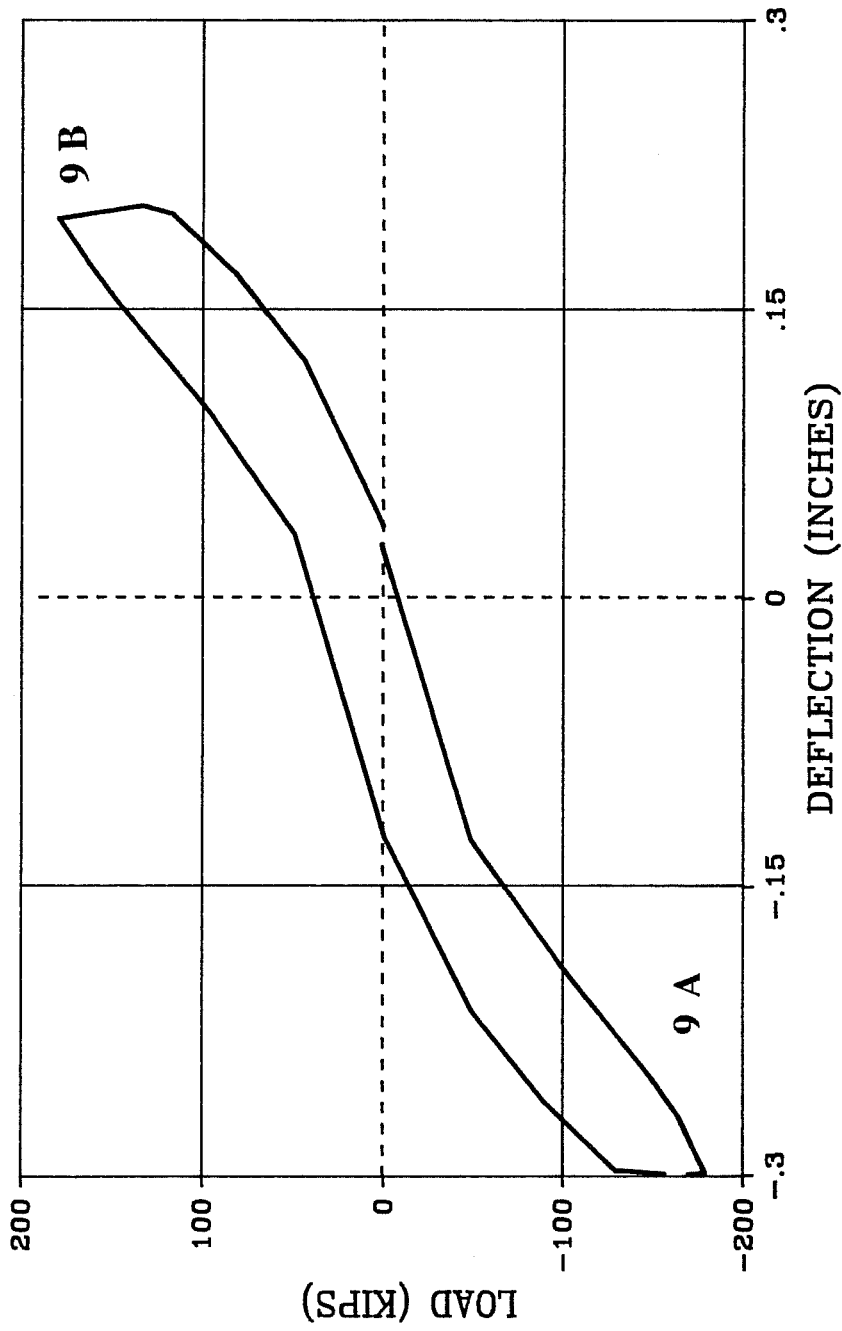


Fig. 3.65 Load-Deflection Response, Cycles to 180 K

occurred near the bottom of the pier and new cracks formed at mid height of the door opening and near the upload column at about the level of the seventh column tie. Inclined cracks in the upload column formed at the level of the fourth column tie and horizontal column cracks formed at the level of the seventh pier. Crack widths in the upload pier were in excess of 1.0 mm as were the crack widths in the download pier.

The strain profile at the base of the specimen showed the same trends of increasing tensile strains in the upload column bars and in the download trim bars and also the increase in the gradient in the download column bars. The extreme column bar in the upload pier was in excess of 3500 microstrain and the download trim bar was at about 75% of yield. On the section at the elevation of the door opening, nearly perfectly linear strains were found in both the upload and download piers. The trim bars in both piers were the exceptions. The trim bar closest to the opening in the upload pier showed an increase in tension as it bridges the horizontal cracks at that location. The trim bar closest to the opening in the download pier shows decreased tension.

*Cycles to 0.34% Drift.* One cycle of drift to 0.34% was the next cycle to be applied to the infill with the door opening. It was chosen as a comparison with the infill with the window opening, which exhibited this drift during its cycle to 180 kips. The load deflection plot for this cycle is illustrated in Figure 3.66. The average drift attained in this cycle was 0.35%. The stiffness in the two directions was similar. The loss of stiffness in this cycle over the stiffness achieved in the previous cycle was 10%. Extensions of inclined cracks formed in the download pier. Large extensions of inclined cracks formed in the upload end of the wall running from the upper joint to the level of the top of the door opening. More horizontal cracking was noted in the upload column at the level of the seventh column tie from the bottom of the specimen and at the level of the top of the door opening. Vertical cracks appeared in the upper joint and formed along the vertical trim steel on the download side of the door opening. The cracking along the trim steel was located near the top of the opening, where strain gages indicated compressive strains. Two cracks formed in the upload pier at the top of the door opening that were oriented at roughly 90° to all other

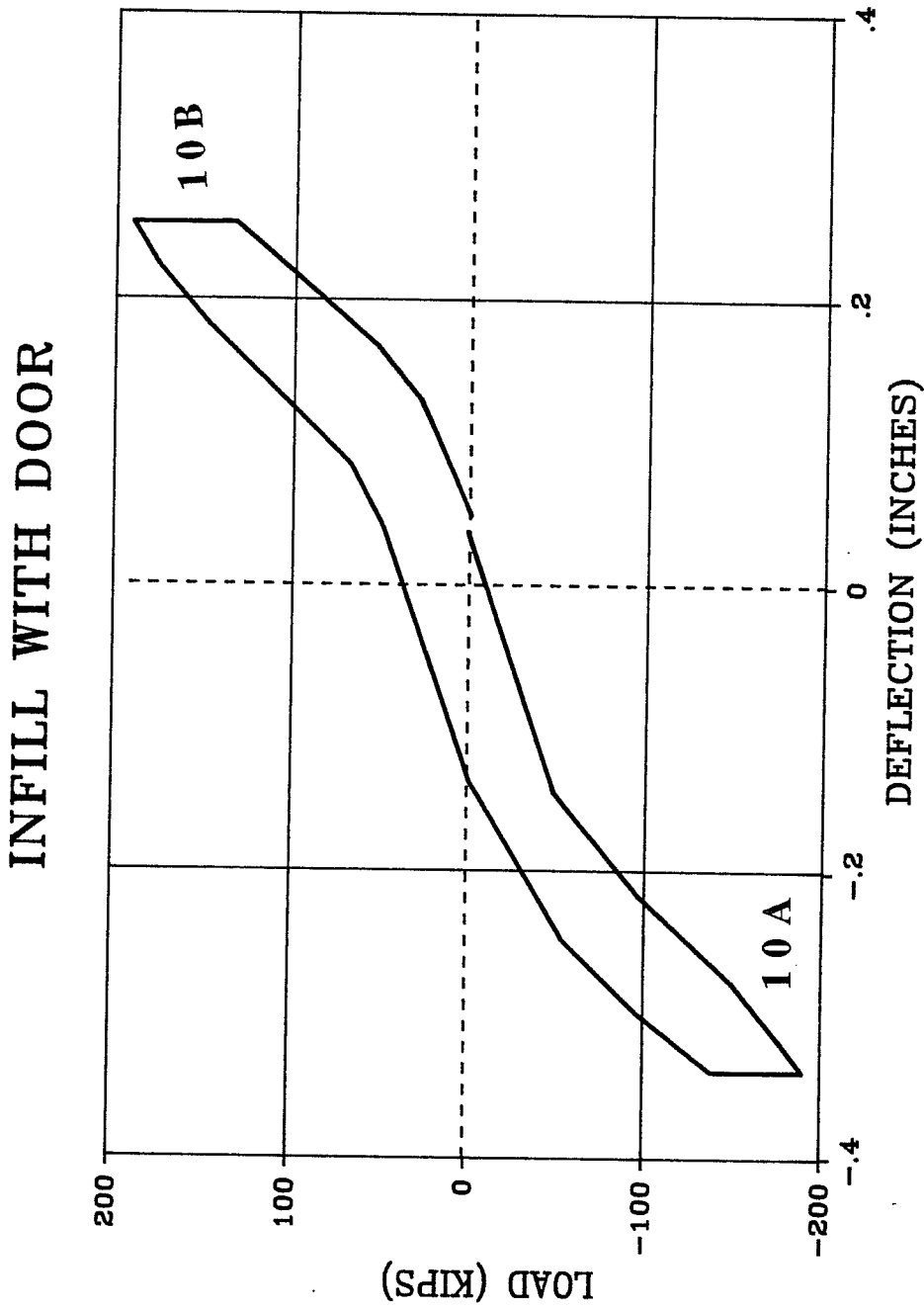


Fig. 3.66 Load-Deflection Response, Cycles to 0.34% Drift

cracks formed under loading in this direction. Crack widths in both sides of the opening ranged from 1.2 mm to 1.4 mm under sustained load.

Strain profiles at the top of the door opening showed no change in the distribution of strains over the upload section, only an increase in net tension on the section. Compressive strains in the trim bar closest to the opening in the download pier were found. This increase in compressive strain indicated an increase in the strut force passing over this location.

*Cycle to 0.5% Drift.* One cycle of drift to 0.5% was applied to the infill with the door opening. This drift limit was chosen for comparison with the full infill and the infill with the window opening. The load-deflection plot for this cycle is illustrated in Figure 3.67. The average drift exhibited in this cycle was 0.45%. The stiffness in this cycle was 86% of the stiffness noted in the previous cycle to 0.34% drift and stiffness was symmetric in the two directions. The damage in the specimen consisted of crack extensions in the upload pier. Large cracks and crack extensions formed in the download pier, some indicating the formation of a strut mobilizing a diagonal section with nodes at the top of the wall over the middle of the door and at the lower frame joint. Vertical cracks formed at the base of the download trim bars indicating distress in the splice. Crack widths in inclined cracks in the panel ranged from 1.4 to 1.8 mm under sustained load. The damaged specimen is pictured in Figures 3.68, 3.69 and 3.70. Strain profiles at the base of the specimen show the two column bars in the upload pier were in excess of the yield strain. Strains in the download pier were skewed with the cracking of that pier. This cracking released the forces in the download column. The download column strains no longer indicated independent bending, rather a flat strain gradient of about 1000 microstrain in tension. The spliced trim bars apparently slipped, as the tensile strains measured at the base decreased in magnitude. The profile at the level of the top of the door opening indicated yield in the two vertical panel reinforcing bars nearest the column. The compressive strains in the download trim bars increased while the strains in the remainder of the pier did not change. These profiles for this cycle for loading in the positive direction are presented in Figure 3.71 and 3.72.

# INFILL WITH DOOR

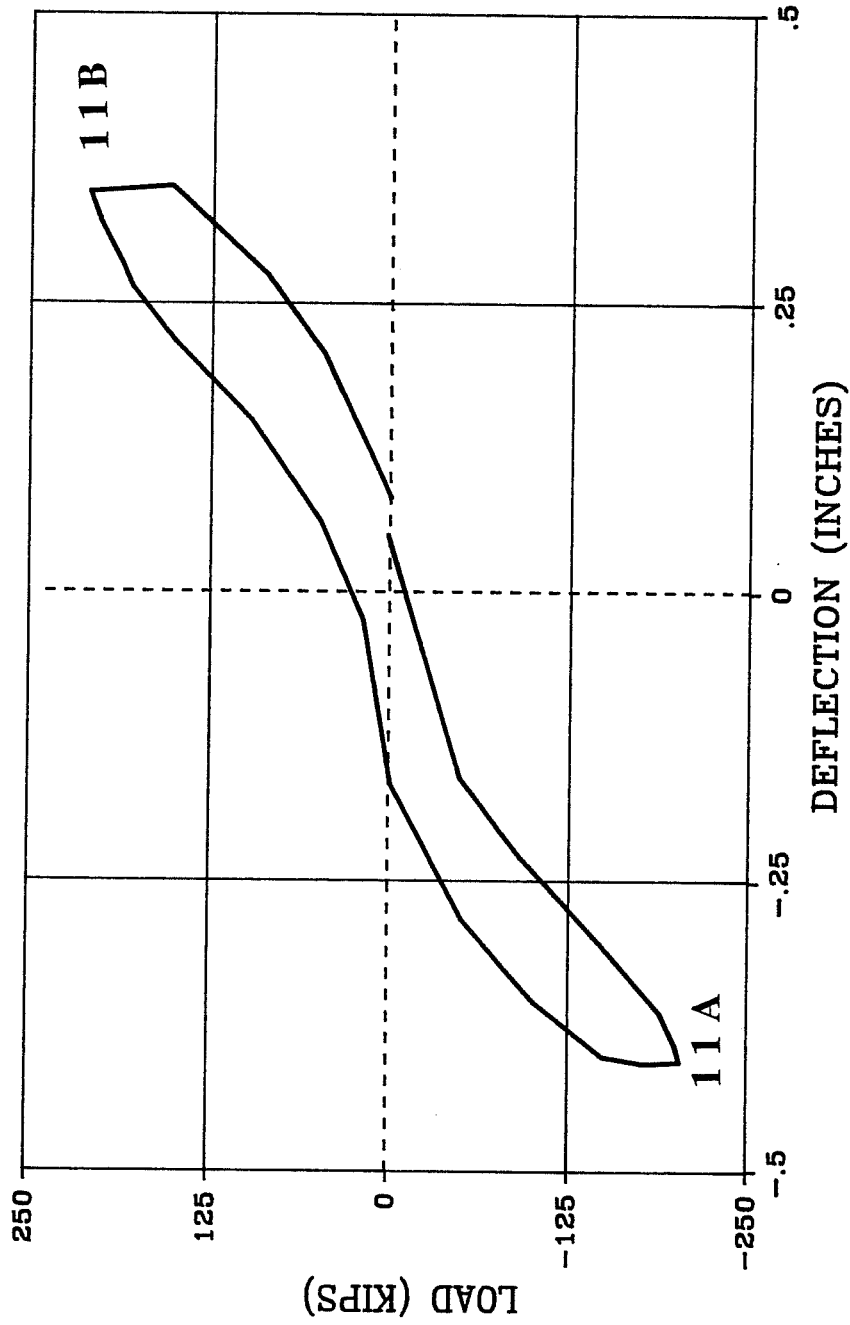


Fig. 3.67 Load-Deflection Response, Cycles to 0.50% Drift

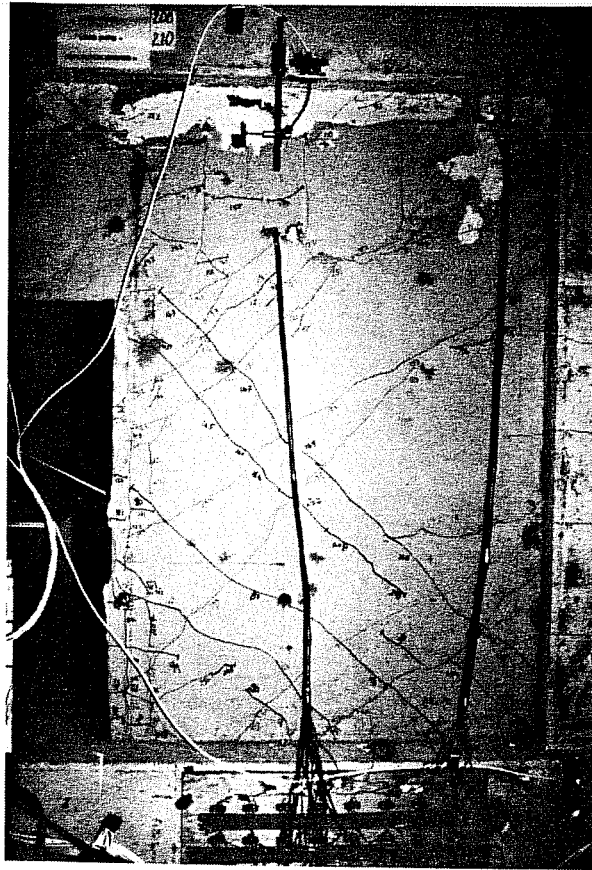


Fig. 3.68 Crack Patterns, Cycles to 0.50% Drift, South Pier

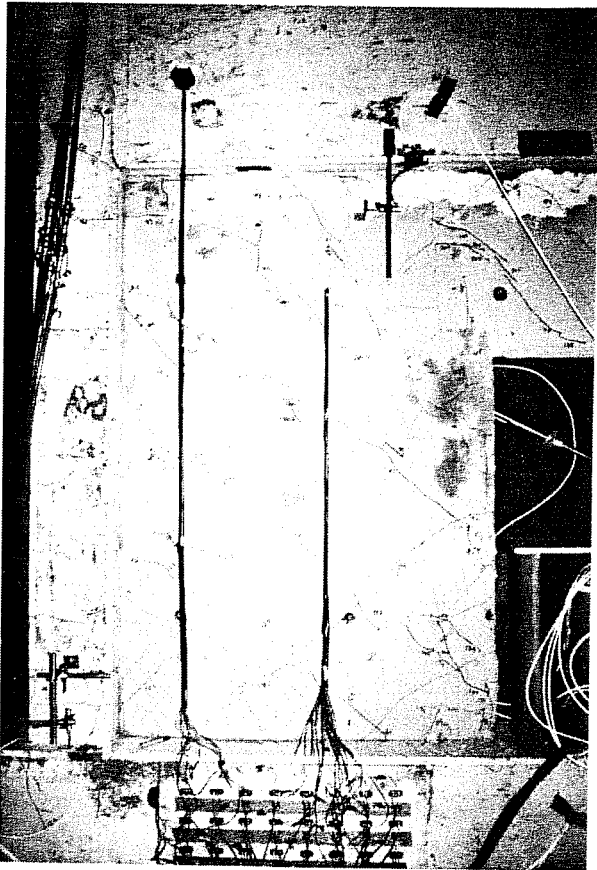


Fig. 3.69 Crack Patterns, Cycles to 0,50% Drift, North Pier



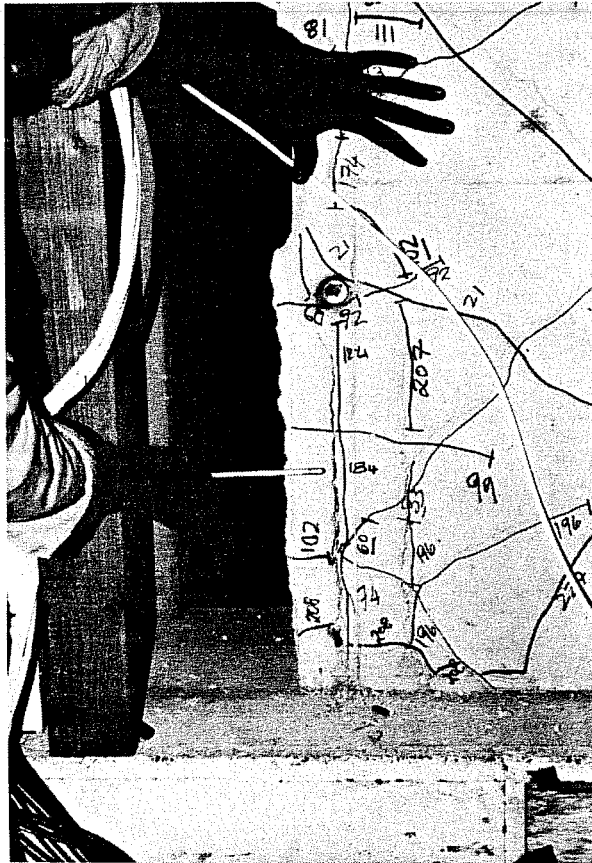


Fig. 3.70 Anchorage Failure of Vertical Trim Steel

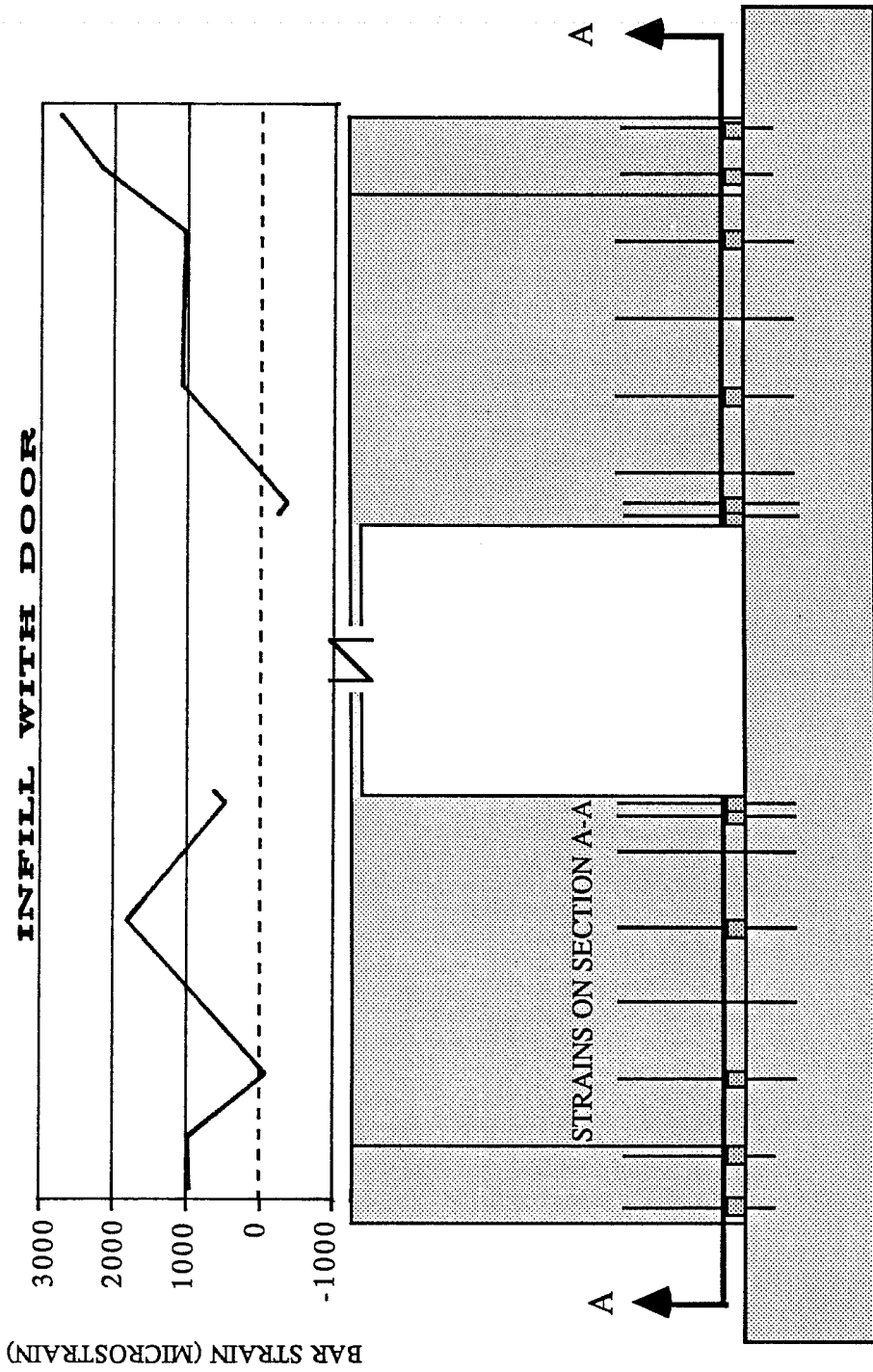


Fig. 3.71 Strain Profiles, Cycles to 0.50% Drift, Base of Wall

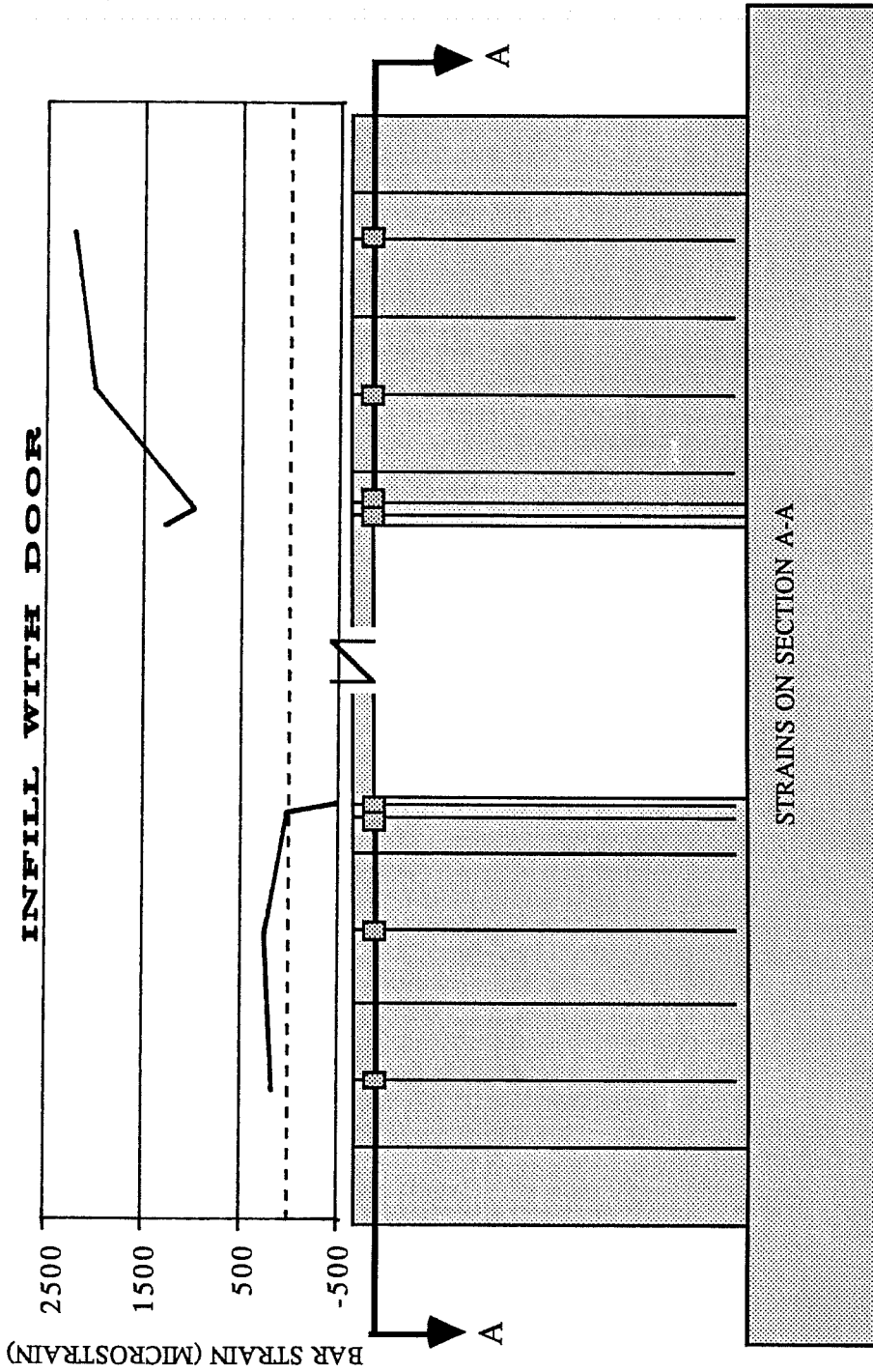


Fig. 3.72 Strain Profile, Cycles to 0.50% Drift, Top of Opening

*Cycle to 0.55% Drift.* The infill with the door opening was subjected to one cycle of drift to 0.55%. This limit represents the drift that the infill with the window opening exhibited under failure load. The average drift exhibited in this cycle was 0.57%. The peak load was reached in this cycle and was 225 kips in the negative direction and 206 kips in the positive direction. The load-deflection plot for this cycle is illustrated in Figure 3.73. The continuous load-deflection plot obtained during the test indicated flattening of the curve in this cycle, which indicated gross yielding of the specimen. The stiffness in this cycle was 84% of the stiffness in the previous cycle to 0.5% drift and the two directions were fairly symmetric. Small crack extensions formed in both piers. Cracks formed in the upload pier at the level of the door opening that were oriented at 90° to the majority of cracks that formed under loading in this, the negative direction. Crack widths in panel cracks exceeded 1.5 mm. The specimen under peak load is pictured in Figure 3.74. The strain profile on a horizontal section at the top of the door opening showed small increases in the tensile strains nearest the upload column. Compressive strains in the trim bars on the download side at this elevation increased. The strain in one of the panel bars in the download pier increased by one order of magnitude, from less than 500 microstrain to almost 5000 microstrain, as a large crack formed there.

*Cycle to 0.6% Drift.* The infill with the door opening was subjected to one cycle of drift to 0.6%. Failure occurred in this cycle. The drift in the negative direction was 0.54% and in the positive direction was 0.67%. Peak loads in this cycle were 189 kips in the negative direction and 134 kips in the positive direction.

The load-deflection plot for this cycle is pictured in Figure 3.75. The failure occurred through failure of the anchorage of the column steel in the upload piers. The failure plane opened at the level of the top of the compression splice and ran through the upload pier at the level where the steel dowelled into the foundation girder terminates in the wall. The cracks over the door opening also opened very wide under sustained load. The splice of the vertical trim bars in the download pier failed when the horizontal load was transferred from the upload pier to the download pier upon failure of the column splice. Failure of the trim

# INFILL WITH DOOR

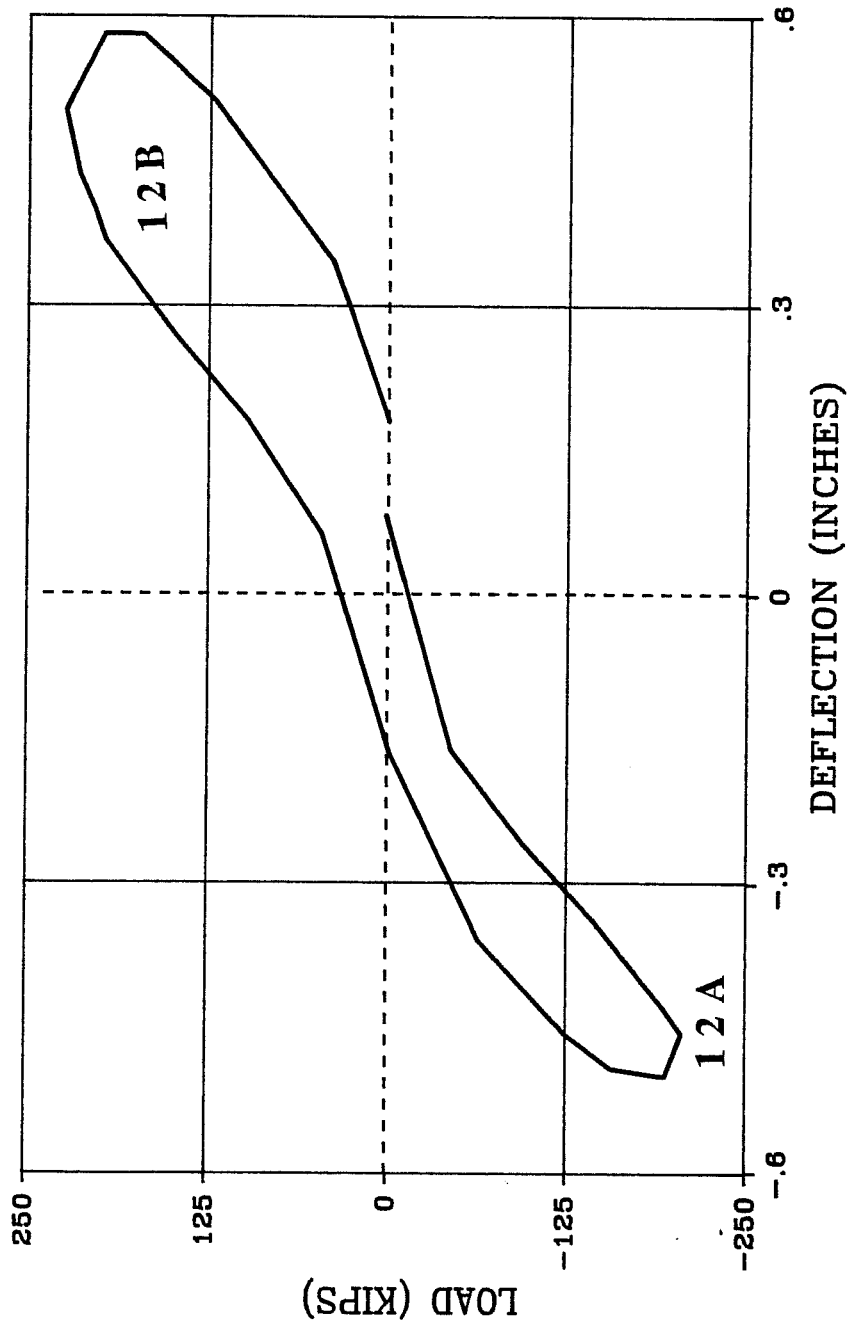


Fig. 3.73 Load-Deflection Response, Cycles to 0.55% Drift

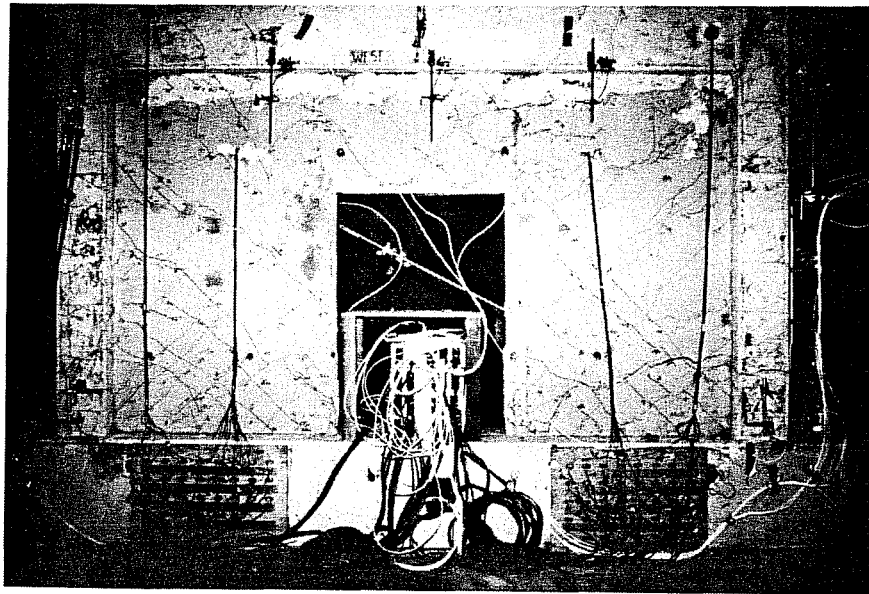


Fig. 3.74 Crack Patterns, Cycles to 0.55% Drift

# INFILL WITH DOOR

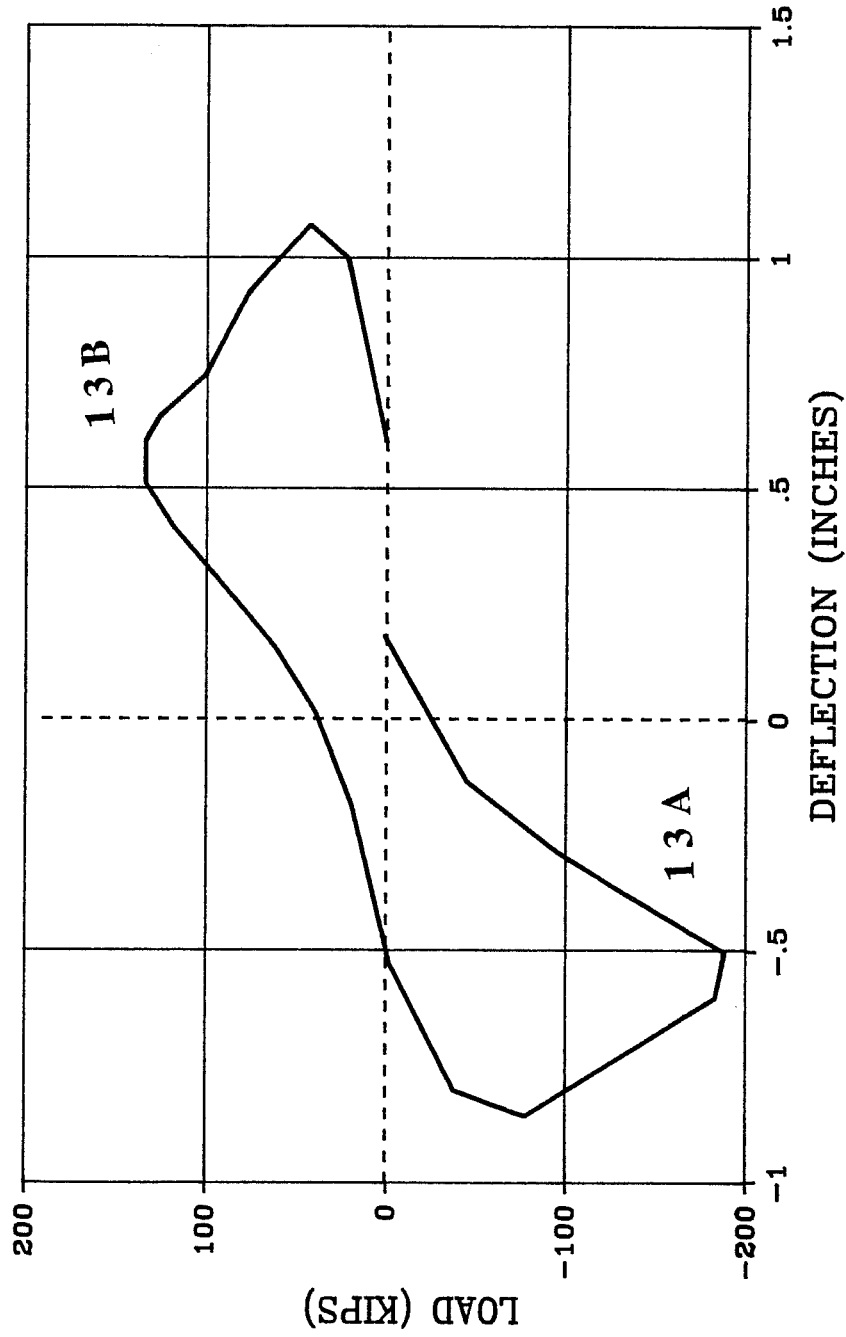


Fig. 3.75 Load-Deflection Response, Cycles to 0.60% Drift

bar splice occurred while loading in the positive direction. The damaged areas are pictured in Figures 3.76, 3.77 and 3.78.

The strain distribution at the base of the specimen showed the maximum strain reached in the extreme upload column bar to be more than 0.013 in./in. in the negative direction before the splice failure and 0.01 in./in. after. The interior column bar in the upload pier had a strain of 3400 microstrain before the splice failure in this direction and 7500 after. In the positive direction, the maximum strain in the extreme upload column bar before the splice failure could not be determined as the gage failed in the previous half cycle. The interior column bar in this column reached a maximum strain of 8600 microstrain. The only noteworthy changes in strain at the top of the door opening were more increases in compressive strains in the download trim bars.

### **3.4 Behavior of Epoxied Voids**

From these tests, it was apparent that the techniques of injecting cracks with epoxy and patching large voids with epoxy grout were successful. In all tests, the relative slip between the bottom of the first story girder and the top of the wall was recorded in several locations. The results of these tests revealed some interesting trends. The most noteworthy conclusion was that the magnitude of the slip recorded was small in all cases. The infill with the door exhibited the most slip at the joint and the other infills had similar slip magnitudes. Load slip plots for the full infill are contained in Figures 3.79 and 3.80. Results for the infill with the window are contained in Figure 3.81, 3.82 and 3.83. Load slip plots for the infill with the door opening are contained in Figure 3.84 and 3.85.

The appearance of the patched voids during the tests indicated that the epoxy grouted patches behaved very well. These patched areas showed no early signs of degradation nor was there any apparent distress in the concrete around these patches that might have arisen from concentrations of stress at patched locations. The epoxied patches cracked when the concrete panel cracked, thus indicating that there was composite action in these areas. Evidence of this is pictured in Figure 3.86. In no case was there evidence of spalling of the epoxy



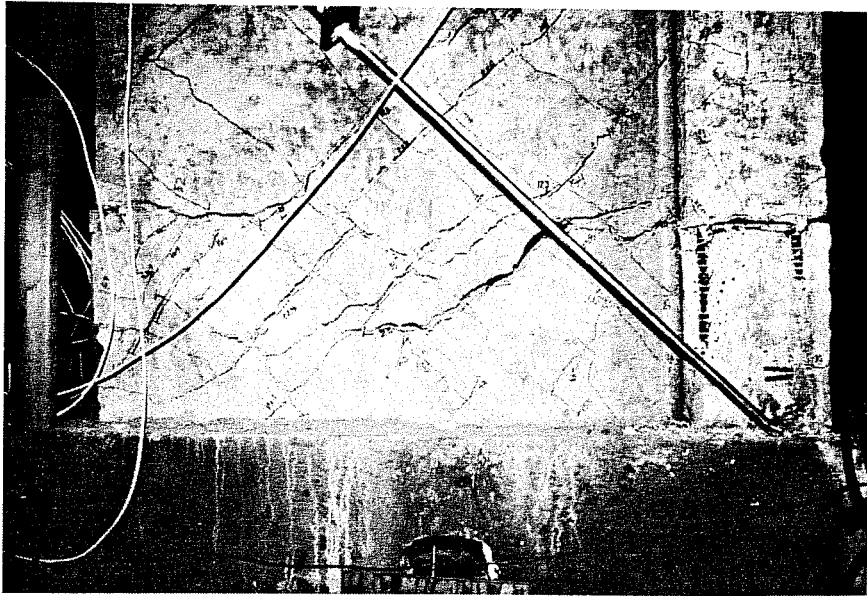


Fig. 3.76 Upload Pier Under Load at Failure

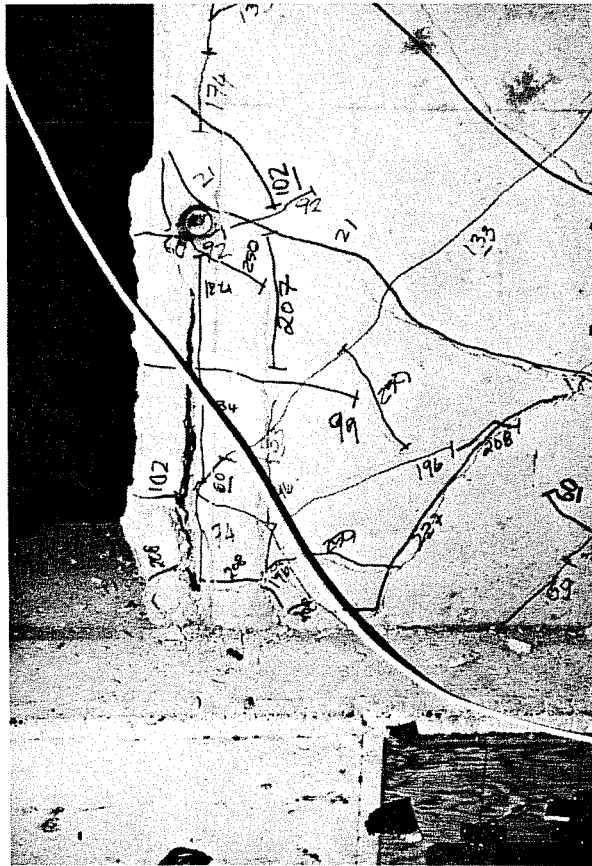


Fig. 3.77 Vertical Trim Steel at Failure

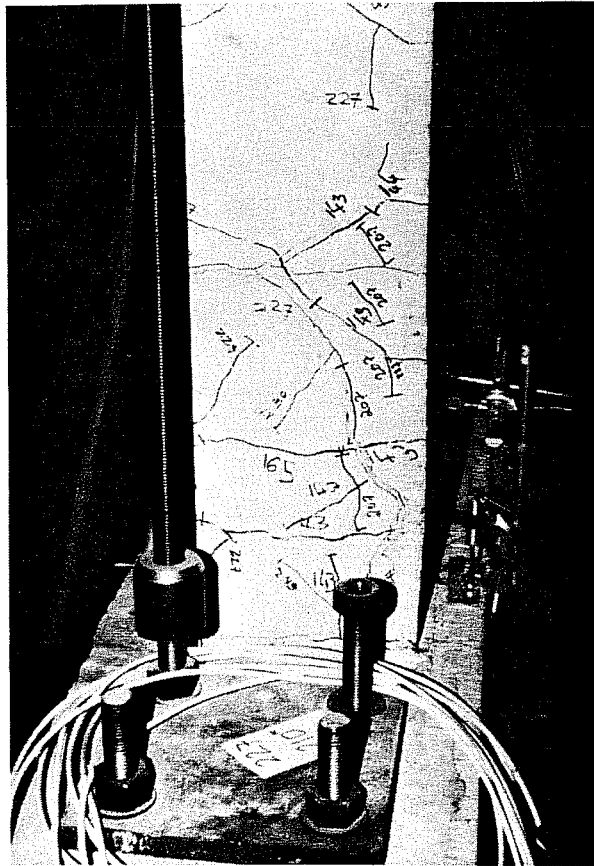


Fig. 3.78 Splice Failure in Upload Column

FULL INFILL

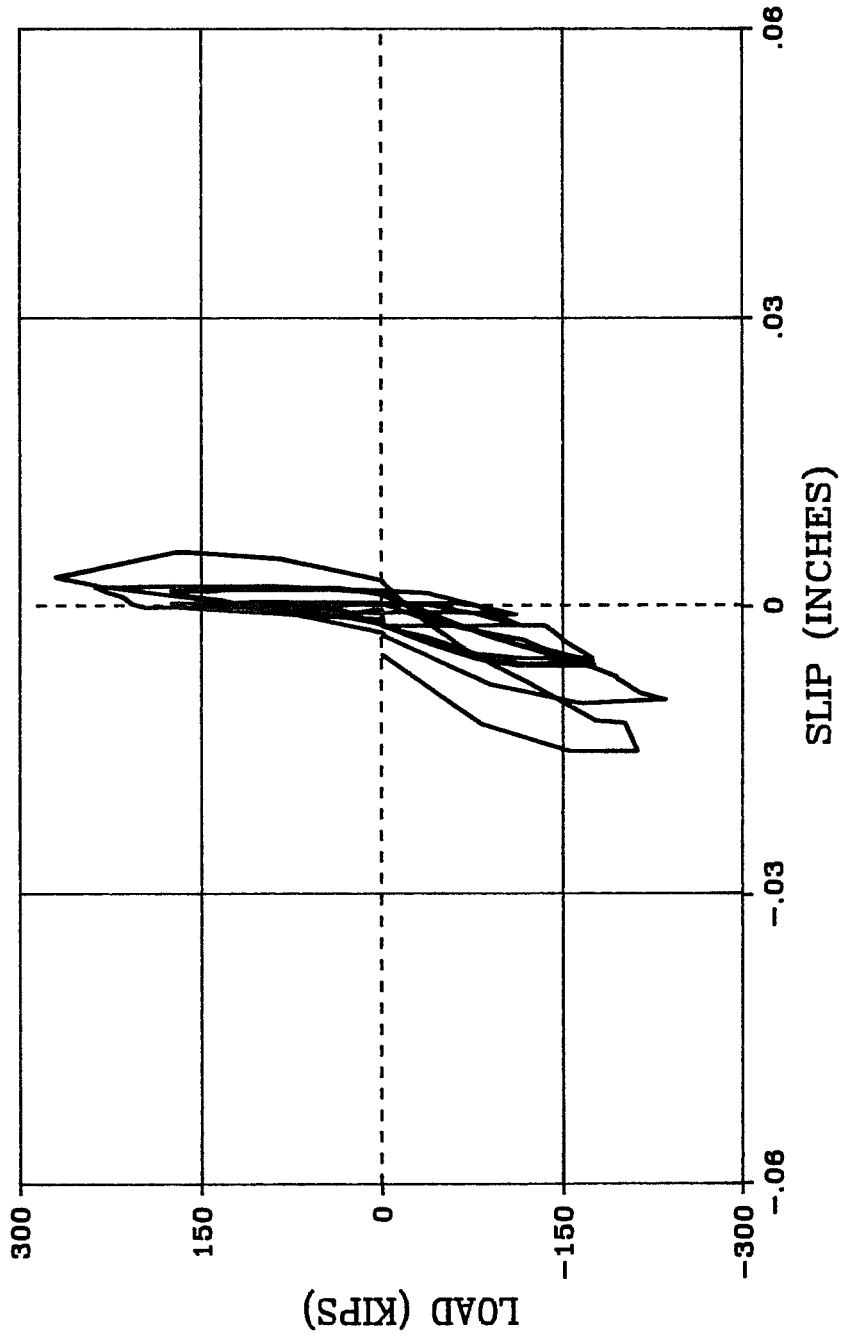


Fig. 3.79 Load-Slip Behavior, Positive Potentiometer

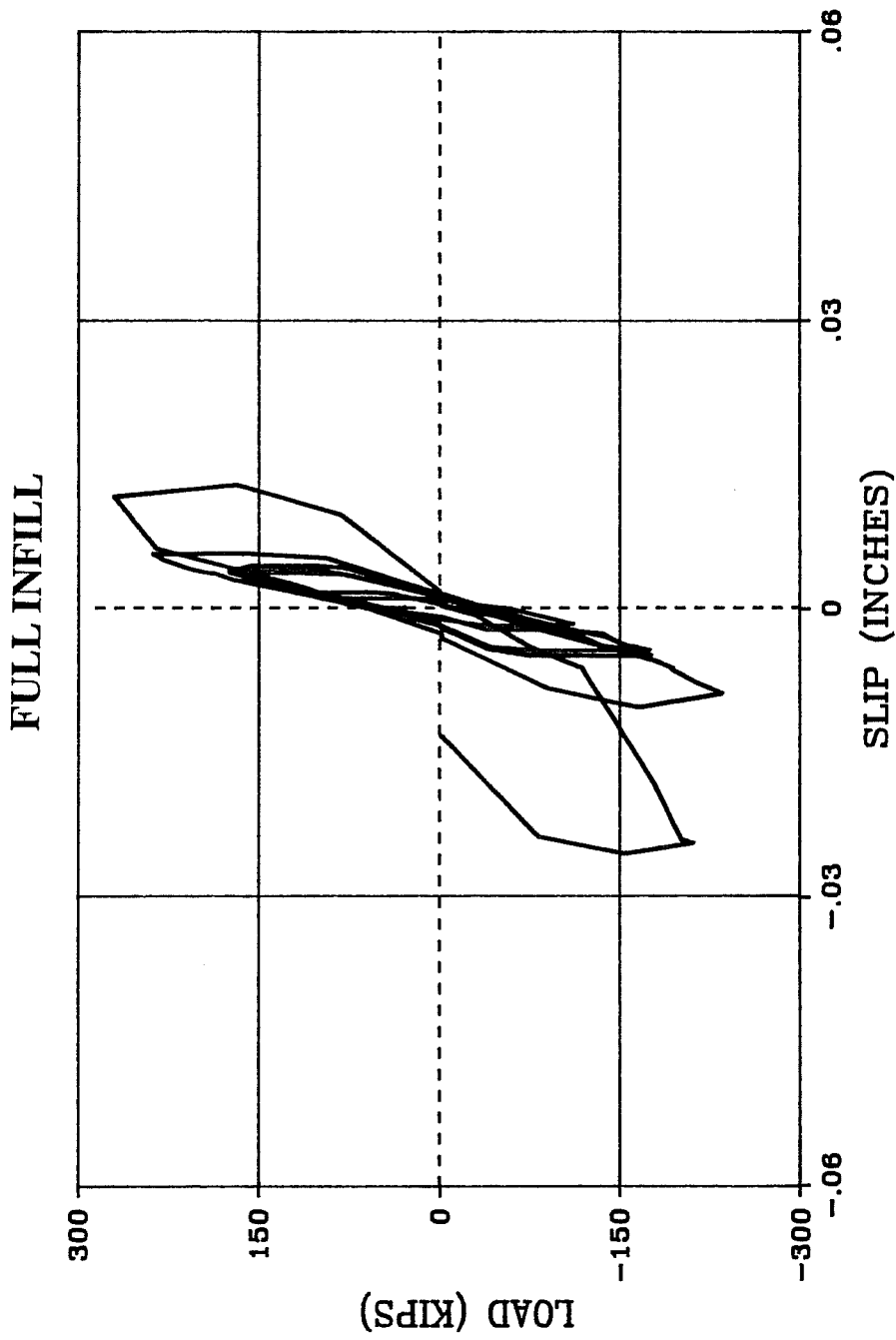


Fig. 3.80 Load-Slip Behavior, Center

INFILL WITH WINDOW

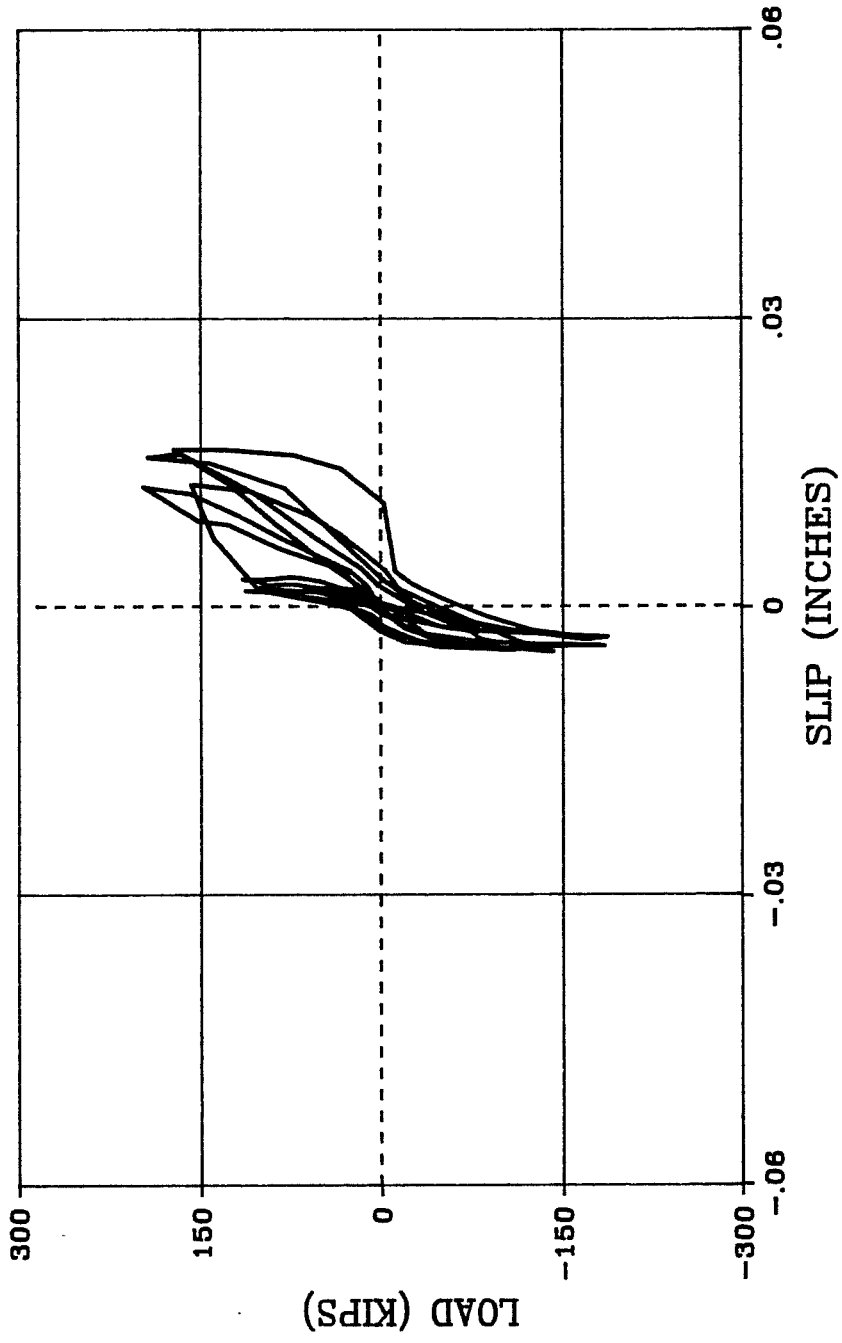


Fig. 3.81 Load-Slip Behavior, South Potentiometer

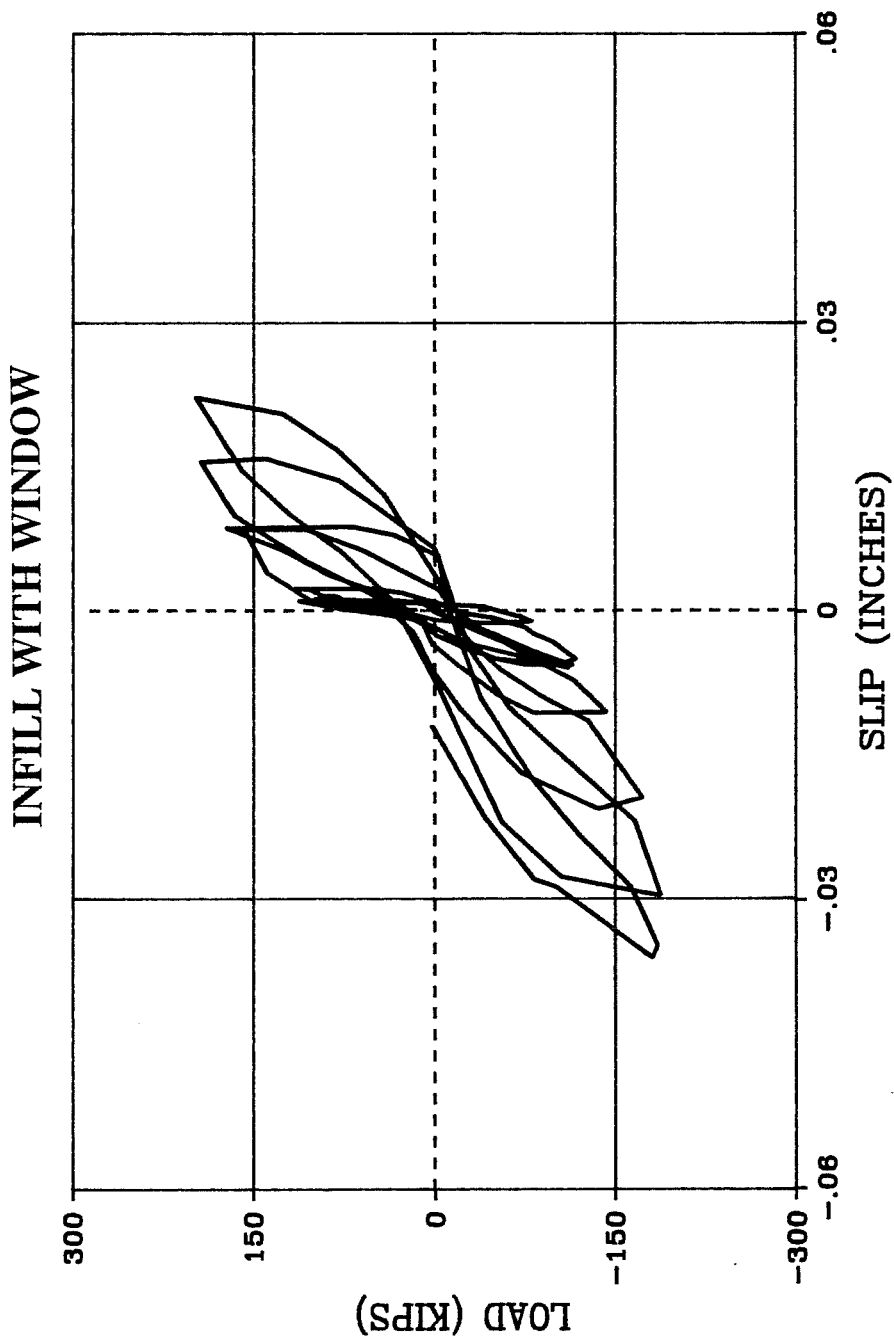


Fig. 3.82 Load-Slip Behavior, Center Potentiometer

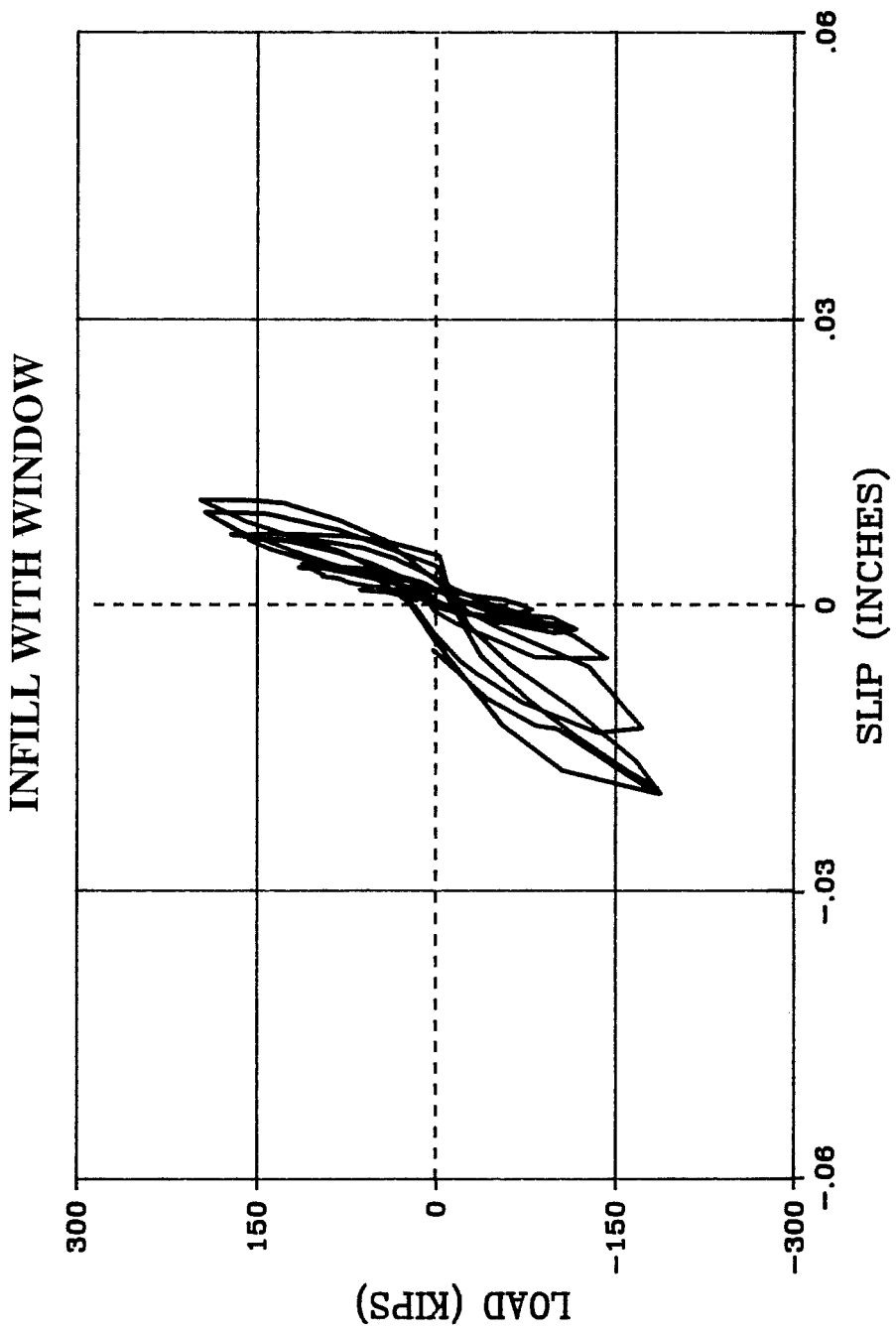


Fig. 3.83 Load-Slip Behavior, Positive Potentiometer



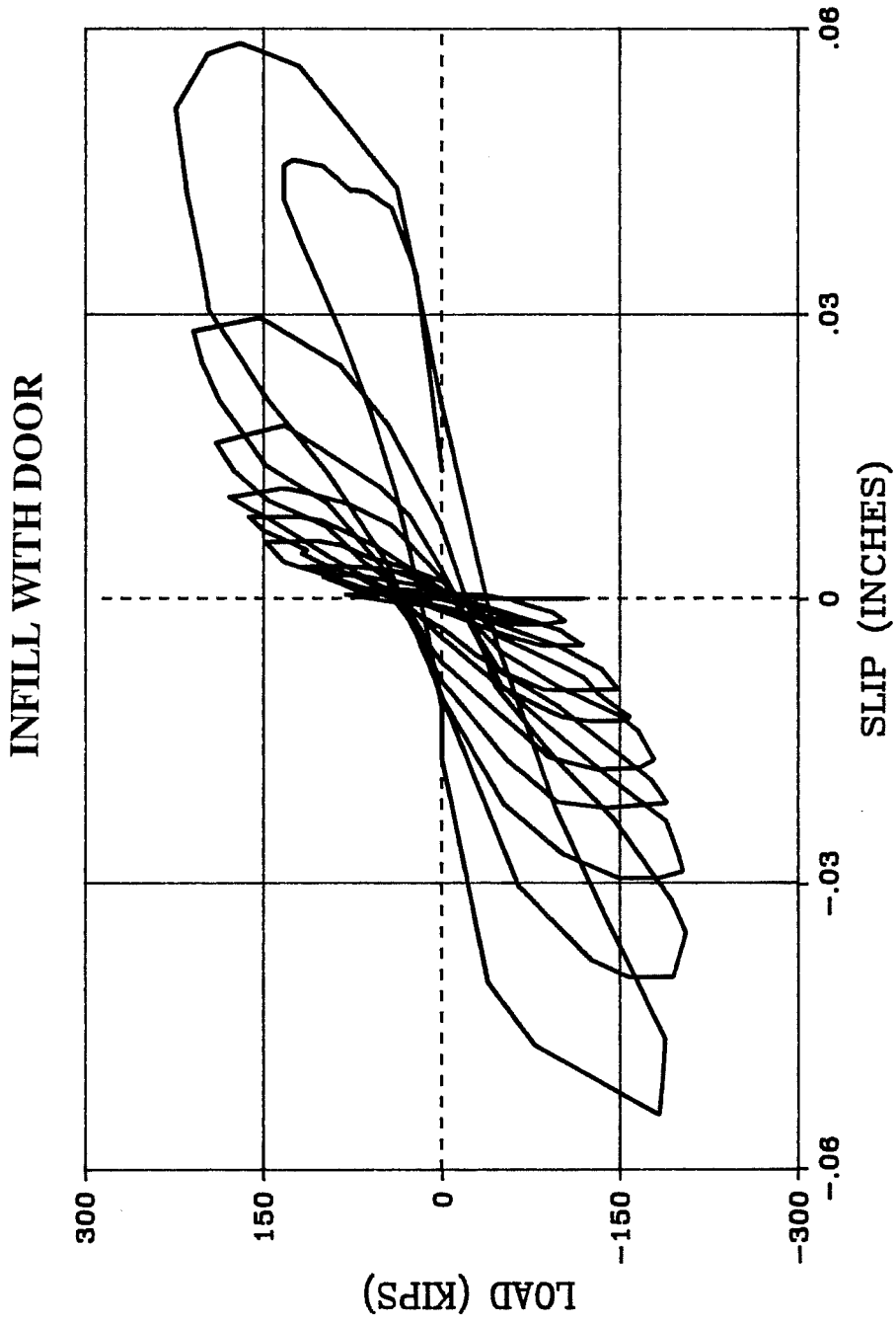


Fig. 3.84 Load-Slip Behavior, Center Potentiometer

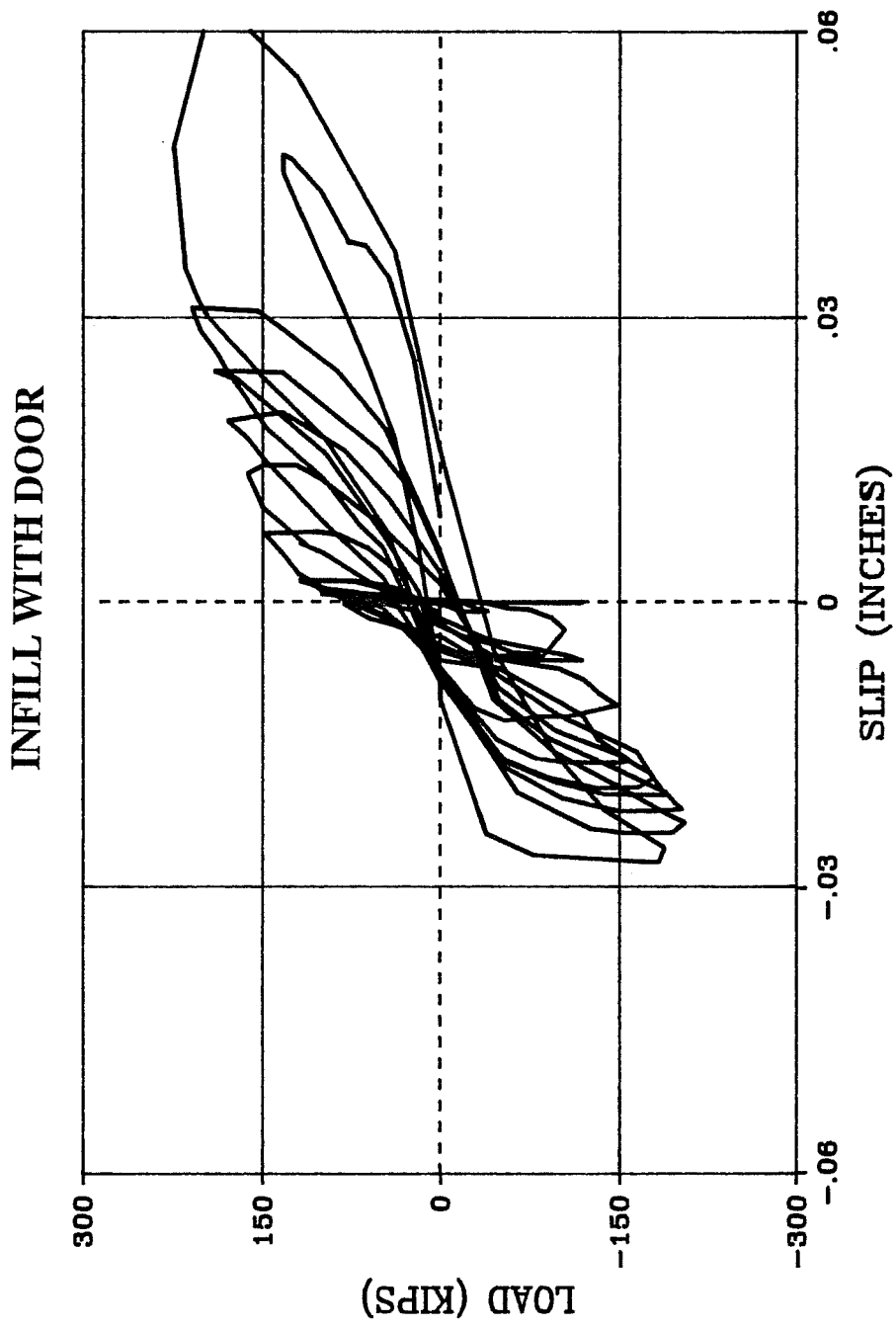


Fig. 3.85 Load-Slip Behavior, Negative Potentiometer

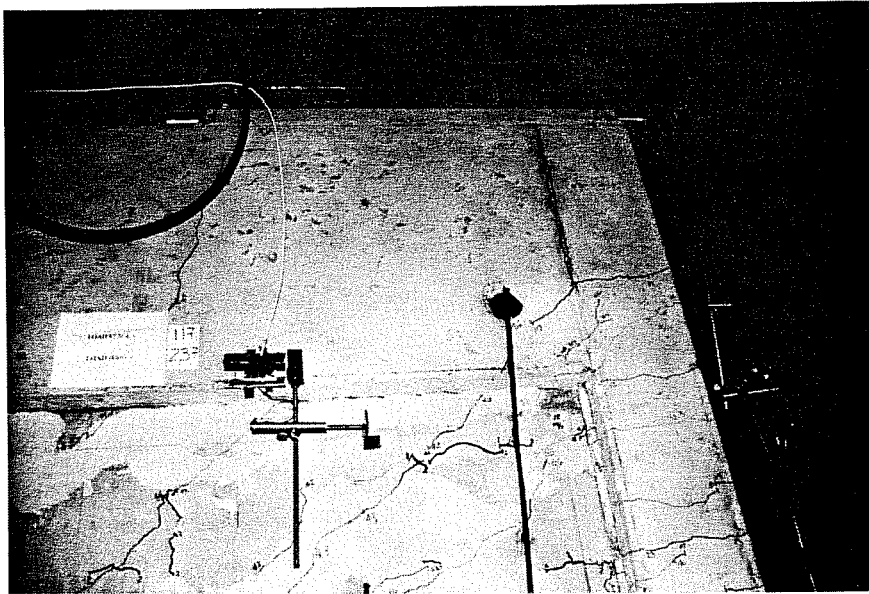


Fig. 3.86 Cracked Epoxy Under Load

grout patch. However, some expulsion of plain epoxy was found in the infill with the door opening where a crack, created by slumping of the plastic shotcrete from a point of restraint, was injected with plain epoxy only. The width of the crack was about 0.25 inches and was not, therefore, patched with epoxy grout. During testing, this crack was located where a large compression strut had formed and the epoxy showed signs of extension under load. This phenomenon is pictured in Figure 3.87. As mentioned previously, some loss of stiffness occurred where patched areas were located in strut paths however, the loss was less than 15% of the stiffness in the other direction and apparently had no effect on residual deformations or drifts. Thus, the patched areas responded elastically under reversed cyclic loads until they cracked. Furthermore, the trends noted in cycles in which stiffness differences were attributed to the presence of epoxied voids generally did not carry over into subsequent cycles. That is, the stiffnesses in the two directions of loading were symmetric in later cycles of loading.

There were several trends that emerged from the data that was taken at the joint at the top of the wall and the bottom of the first story girder. The relative slip measured by one potentiometer at either the negative or the positive quarter point was largest under loads in the direction that made the potentiometer's location on the upload end of the specimen. For example, the positive potentiometer read the largest slip when loading in the negative direction and vice versa. The magnitude of the slip measured on the upload side was roughly equal to the magnitude of the slip measured in the center of the wall, though often, the slip was largest in the center of the wall. The magnitude of the slip measured in the center of the wall was approximately equal in the two directions of loading. These trends were most clearly demonstrated at the higher levels of applied load and drift during a test. The magnitude of slip among the specimens at a given load were roughly equal. The plots showed the same tendency found in the load-wall deflection plots of a low initial "stiffness" that increased with increasing load. This trend indicated that the joint slipped until a strut could form in the upload corner of the wall, at which point, the "stiffness" increased. Thus, most of the applied shear was distributed into the wall through the upload half of the specimen. The slip measured by the upload

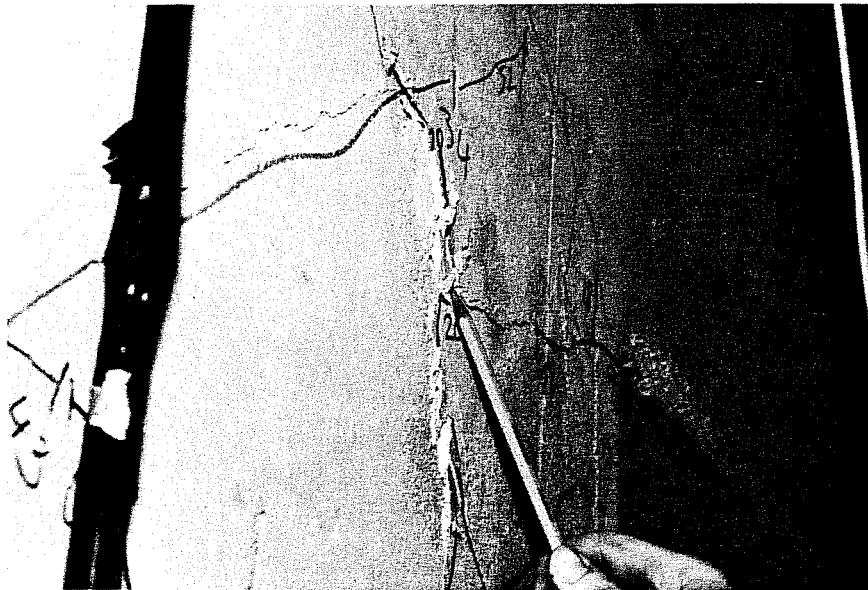


Fig. 3.87 Crushing of Plain Epoxy

potentiometer was generally less than 5% of the total lateral deflection in the all of the specimens.

## **CHAPTER 4**

### **ANALYSIS**

#### **4.1 Linear Elastic Response**

“Elastic” stiffness generally refers to the initial linear response of a system. Theoretically, the elastic response can be calculated using classical mechanics or other analysis techniques. Theoretical elastic stiffnesses are readily comparable because they can describe the linear response of a reinforced structure in either the pre-cracking or post-cracking range. In the experimental program, the pre-cracking range is relatively small and the test specimens are very stiff. The elastic stiffness of the test specimens is reported using several different techniques. For comparison with other tests or analysis, careful attention must be paid to the assumptions used in determining the various stiffness values.

**4.1.1 Measured Elastic Stiffness.** The measured elastic stiffnesses presented in this section are taken from the first half cycle of load applied to each test specimen. The load-deflection curve for the first half cycle represents the virgin state of the test specimens and no residual deflection is present until the second half of loading is applied. The load-deflection curves for the first cycle of loading are presented in Figures 4.1–4.3. Measured stiffnesses are tabulated for the secant stiffness at equal load, the secant stiffness at equal drift and the secant peak stiffness.

The peak secant stiffness is the secant between the origin and the peak load and peak deflection exhibited in the first half cycle of loading as illustrated in Figure 4.1–4.3. The values of peak secant stiffness are listed in Table 4.1. The full infill exhibits the greatest stiffness, followed by the infill with the door opening. The infill with the window opening is the least stiff specimen at the peak. The initial cycle for the infill with the door (Figure 4.3) shows no recovery of deflection on unloading in the first half cycle. This is due to instrumentation insensitivity under low deflection. The stiffness in the first half cycle is representative because the specimen recovers nearly the same deflection upon loading in the negative direction.

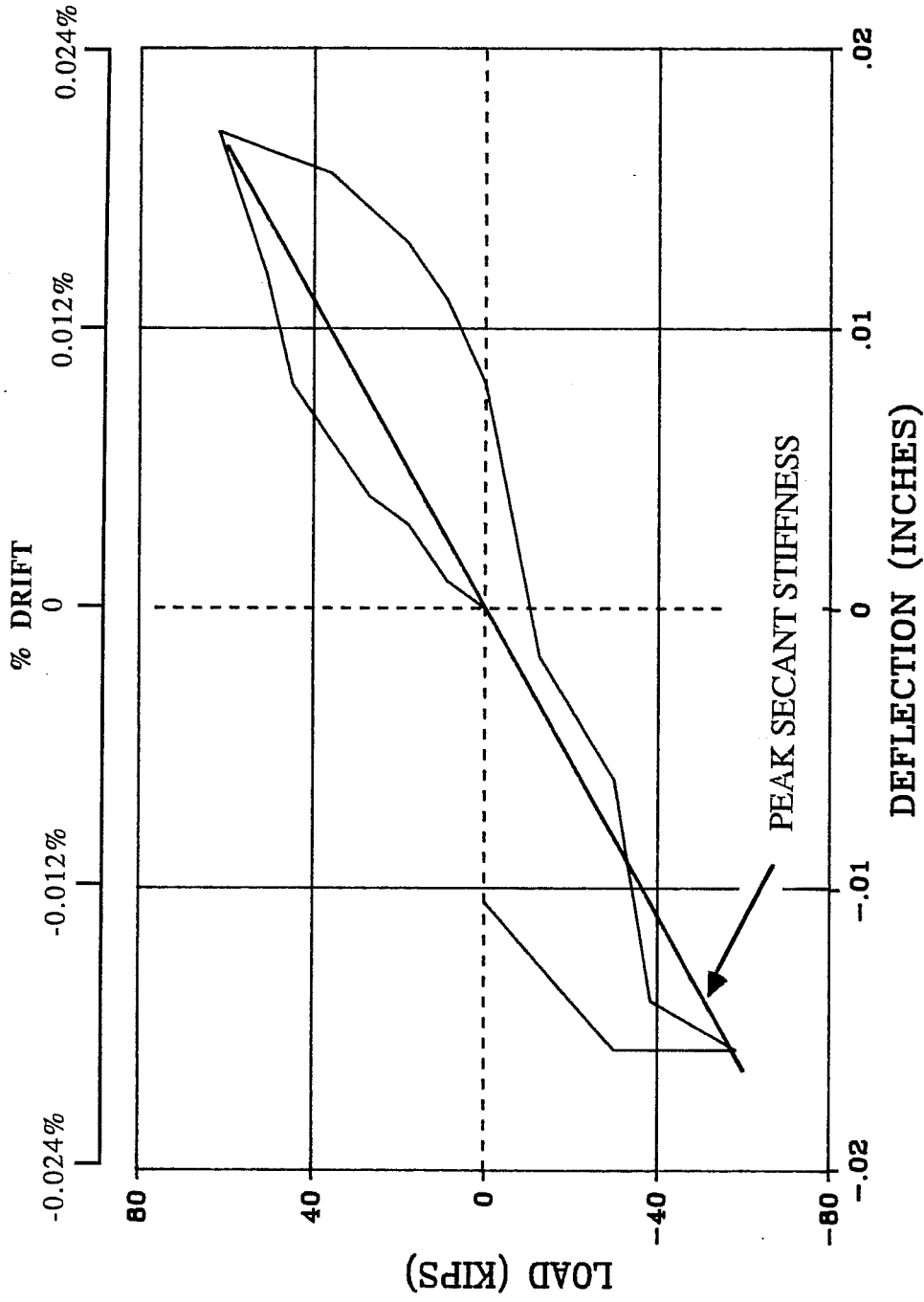


Fig. 4.1 Load-Deflection Response, Initial Cycle, Full Infill



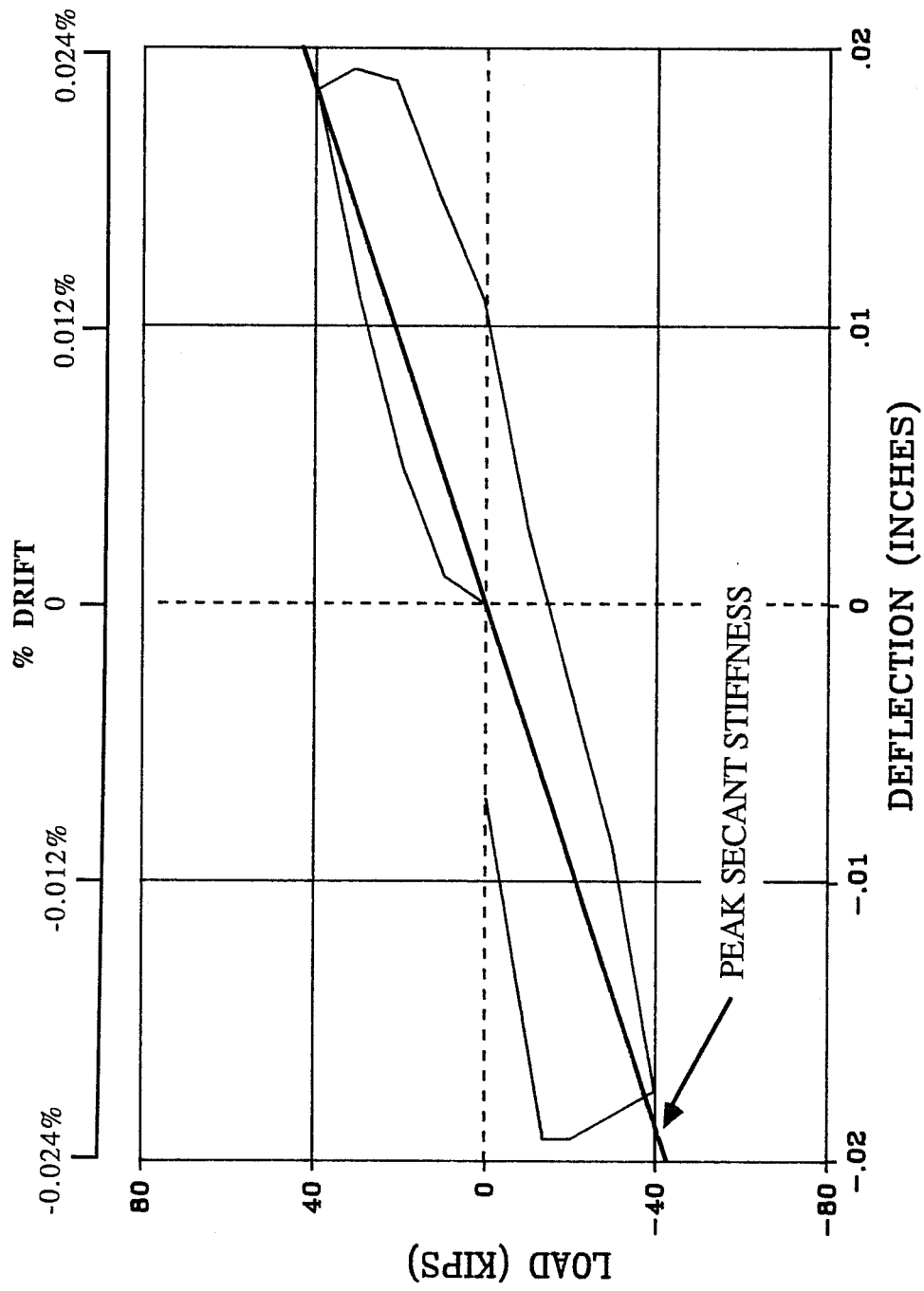


Fig. 4.2 Load-Deflection Response, Initial Cycle, Infill with Window

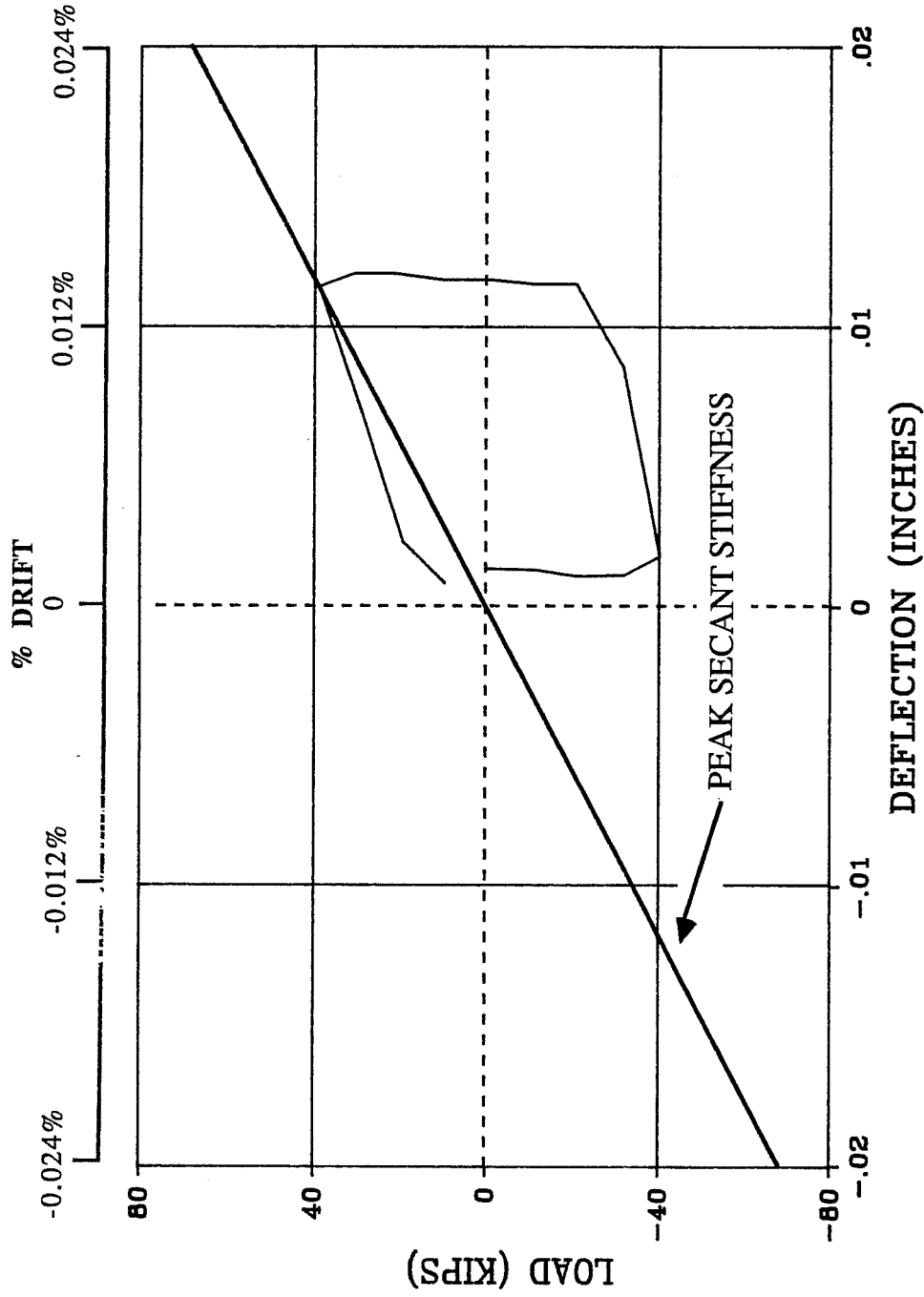


Fig. 4.3 Load-Deflection Response, Initial Cycle, Infill with Door

**TABLE 4.1**  
**Initial Stiffnesses**  
**(kip/in.)**

	Full Infill	Infill With Window	Infill With Door
<b>Measured</b>			
Peak Secant	3600	2100	3400
Equal Load	5800	2100	3400
Equal Drift	5900	3000	3800
<b>Calculated</b>			
Sidesway	10400	10700	10100
Coupled	10400	7300	6000
Finite Element	11000	7300	7200

The secant stiffness at equal load is the secant between the origin and a load of 40 kips in the first half cycle of loading. The value of 40 kips is the peak load in the first half cycle for the infills with openings. From Table 4.1, it can be seen that the same relationships among the stiffnesses of the specimens, although actual values differ slightly.

The secant stiffness at equal drift was calculated as the secant between the origin and a drift of 0.01%. The 0.01% drift is the median exhibited by the three test specimens in the initial cycles. The values listed in Table 4.1 indicate that the full infill is the stiffest and the infill with the window is the least stiff.

Comparisons of the three experimental stiffness values reveal different stiffnesses in the first half cycle of load. The infill with the door is stiffer than the infill with the window by any estimate of stiffness. The full infill is stiffest in the elastic range. The secant between the origin and the first load stage in the first half-cycle of load indicates very high initial stiffnesses for all three specimens. The deflections read in the first loading stage were small, especially compared to the accuracy of the potentiometers. For this reason, the initial stiffness values resulting from small deflections are not considered reliable enough to report in this chapter. All three specimens continuously degrade in the first half cycle. The range over which any of the test specimens exhibit stiffnesses on the order of the stiffnesses presented above is limited to the first cycle. In order to quantify stiffness in a given half-cycle, the secant stiffness was calculated between successive load stages in half-cycle of the entire load- deflection history. The results indicate that the slope of the secants between successive load stages in any cycle after the first is less than 75% of any of the first cycle values presented above. There were several isolated increments where more than 75% of the first cycle stiffness values were found. This usually occurred when loading to new peak loads, near the peak load. However, these high secant values were by no means representative of cyclic response.

**4.1.2 Classical Theory.** The uncracked stiffness of the infilled assemblages was calculated using classical elastic theory. The elastic stiffness of the specimens is obtained by summing up lateral displacements in portions of

the wall with constant cross-section. The lateral displacement consists of deformations due to flexure and shear. The elastic stiffness was calculated using two different assumptions regarding the behavior of the piers (the portions of the wall on either side of the openings). In the first method, the piers were assumed to be fixed at both ends with no net rotation of the specimen due to flexure in the piers. In other words, a sidesway mechanism was assumed. In the second method, the piers were assumed to be coupled by the deep beam over the opening so that the piers act as one section in cantilever bending. The deflections on which the stiffnesses are based are pictured in Figures 4.4 and 4.5 and are listed in Table 4.2. It was anticipated that the actual test specimen boundary conditions would fall somewhere between coupled and sidesway behavior in the piers. Thus, each was calculated separately. The results are compared at the end of this section. The values of stiffnesses determined using sidesway and coupled behavior are listed in Table 4.1.

The piers used in the classical analysis consist of the column and a section of the infill wall. It was assumed that no slip occurred on the boundary between the existing frame and the infill wall. Uncracked, plain concrete sections were used. The modulus of elasticity,  $E$ , was assumed to be:

$$57\sqrt{4000} \text{ (ksi)}$$

The shear modulus,  $G$ , was calculated as:

$$\frac{E}{2(1 + .17)} \text{ (ksi)}$$

The results of the analysis assuming a sidesway mechanism in the piers indicate very high stiffnesses for all three specimens that are virtually identical. The components of the total lateral deflection vary for each specimen. Flexural deformations comprise over 30% of the total lateral deflection of the full infill, approximately 5% for the infill with the window and 13% for the infill with the door. The contribution of flexural rotation in the wall sections over and under

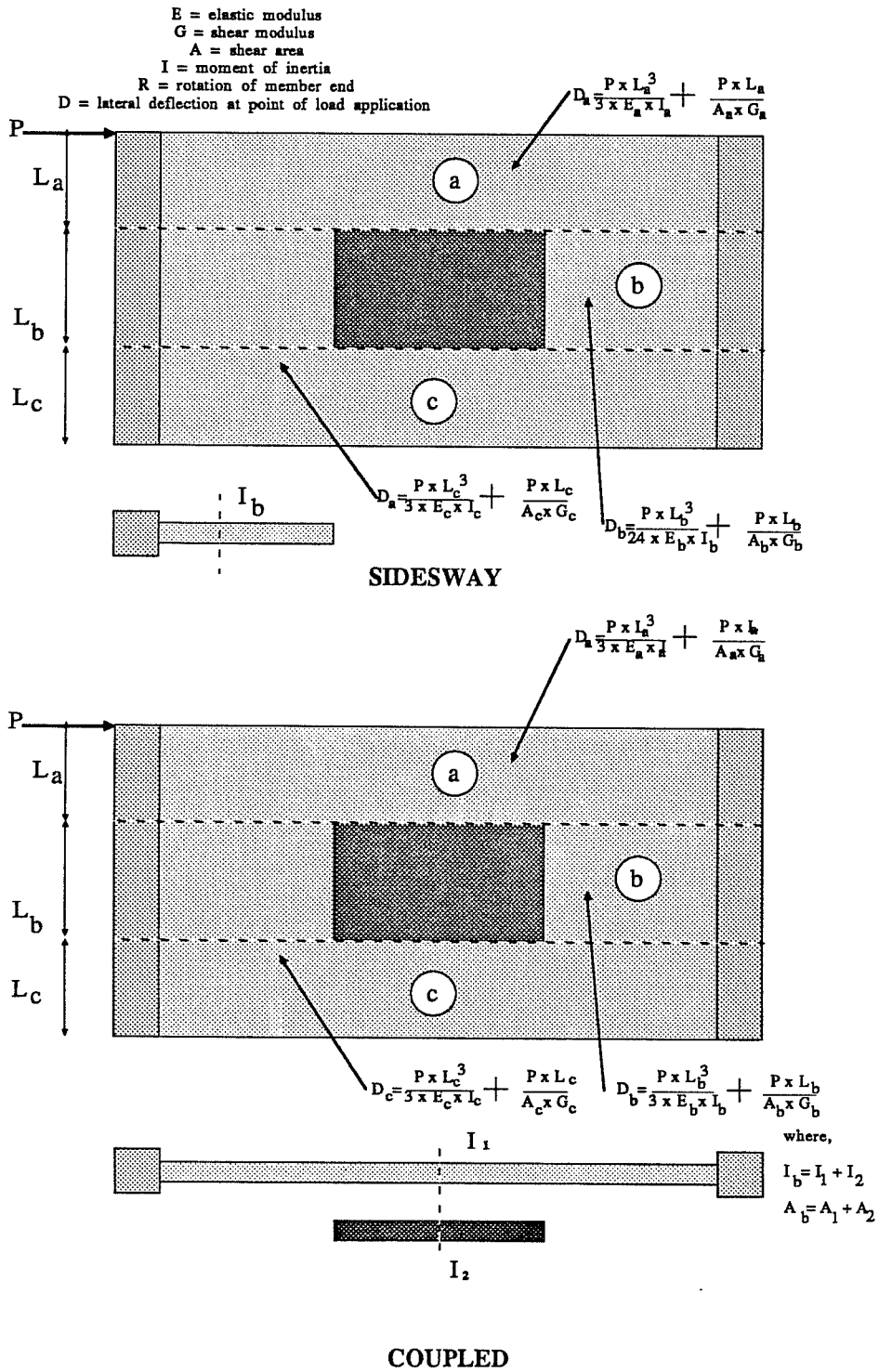


Fig. 4.4 Classical Deflections, Infill with Window

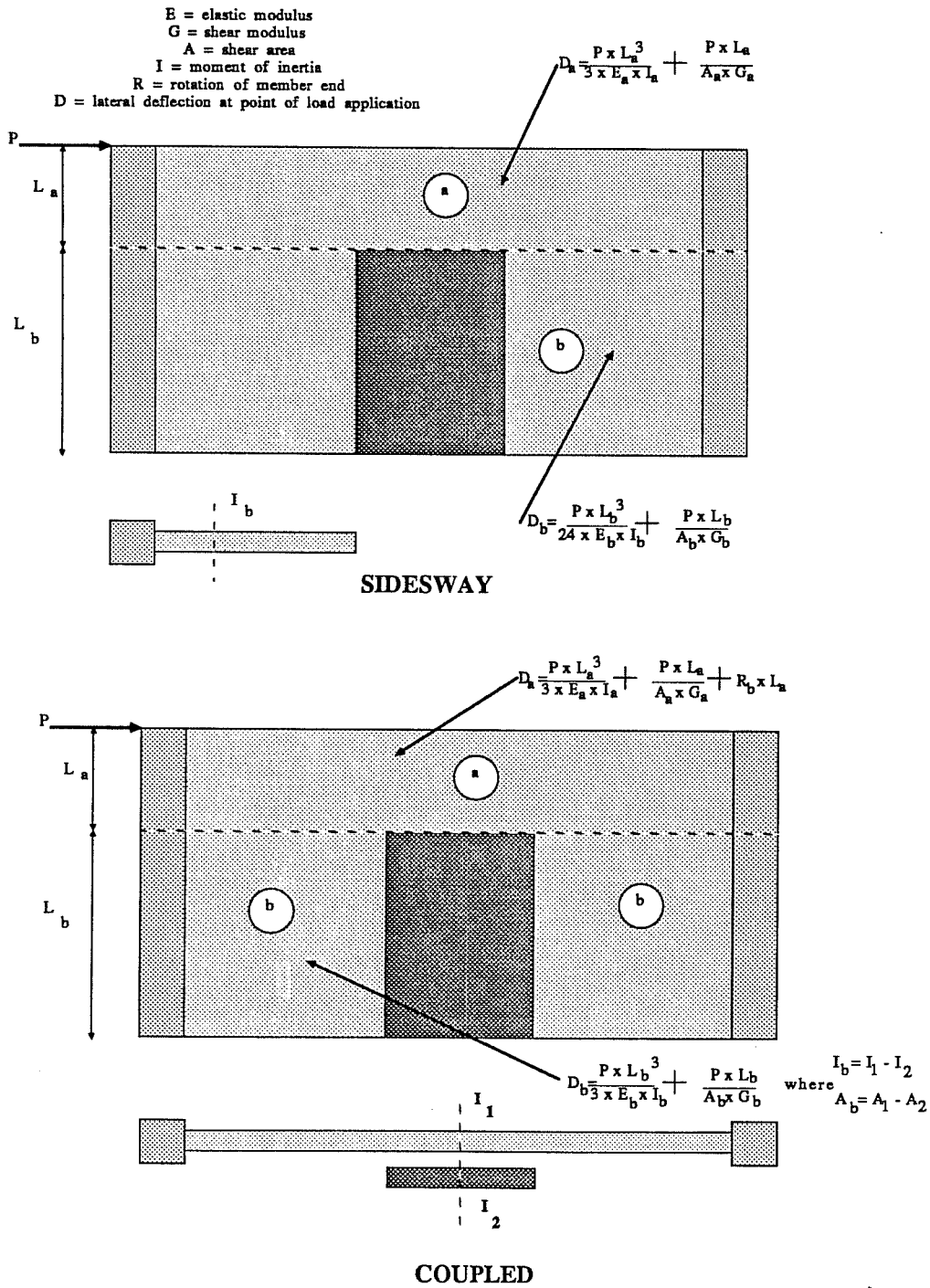


Fig. 4.5 Classical Deflections, Infill with Door

**TABLE 4.2**  
**Deflections Under Unit Load**

**Sidesway**

Specimen	Section	Flexural Deformation	Shear Deformation	Rotational Deformation	Total Deflection
Door	A	1.16	6.44	0	9.89
	B	0.11	2.17	0	
Window	A	0.09	2.02	0	9.32
	B	0.32	4.32	0.17	
	C	0.09	2.02	0.30	
Full	A	3.06	6.52	0	9.58

**Coupled**

Door	A	0.90	12.9	0	16.8
	B	0.11	2.17	0.69	
Window	A	0.09	2.02	0	13.7
	B	0.18	8.64	0.17	
	C	0.09	2.02	0.52	
Full	A	3.06	6.52	0	9.58

NOTE: Units are inches x 10<sup>-5</sup>



openings to the total lateral deflection is insignificant in all of the specimens. The shear component is the largest contributor, comprising nearly 90% of the total lateral deflection for the infills with openings and 70% for the full infill.

The assumption of coupled bending of the piers results in significant differences in the stiffnesses among the three specimens. The full infill is expected to be the most stiff and the infill with the door is expected to be the least stiff. The ratio of stiffnesses of the infills with openings to the full infill is of interest. The relative stiffness is 0.57 for the infill with the window and 0.70 for the infill with the door. The dominant term in the deflection calculation is again the shear component. Under assumptions of coupled bending, the shear component contributes 90% of the total lateral deflection for the infills with the openings.

**4.1.3 Finite Element Analysis.** A simple finite element study was undertaken to clarify unusual trends found in the data, as well as to help explain some of the behavior observed during the tests. It was not intended to provide stresses directly. The results are presented in this section and compared to experimental values in this and later sections.

A commercial computer program was used to model and analyze the test specimens. The models were constructed primarily of planar finite elements on a four inch square grid. The models were uncracked, plain concrete models. The materials were assumed to be homogeneous throughout the specimen. No attempt was made to include the reinforcement. No differentiation was made between the concrete in the frame and the concrete in the walls. The boundary condition at the interface of the wall and the bounding frame was not modelled. The elements in the openings were given zero thickness. The models are pictured in Figures 4.6 - 4.8. The nodes at the base were fixed. The horizontal load was applied to nodes at the top of the wall, modelling load application in the real structure.

**4.1.3.1 Stiffness.** The stiffness of each specimen is listed in Table 4.2. The results indicated that the infills with openings were less stiff than the full infill, with a relative stiffness of approximately 0.65 for both.

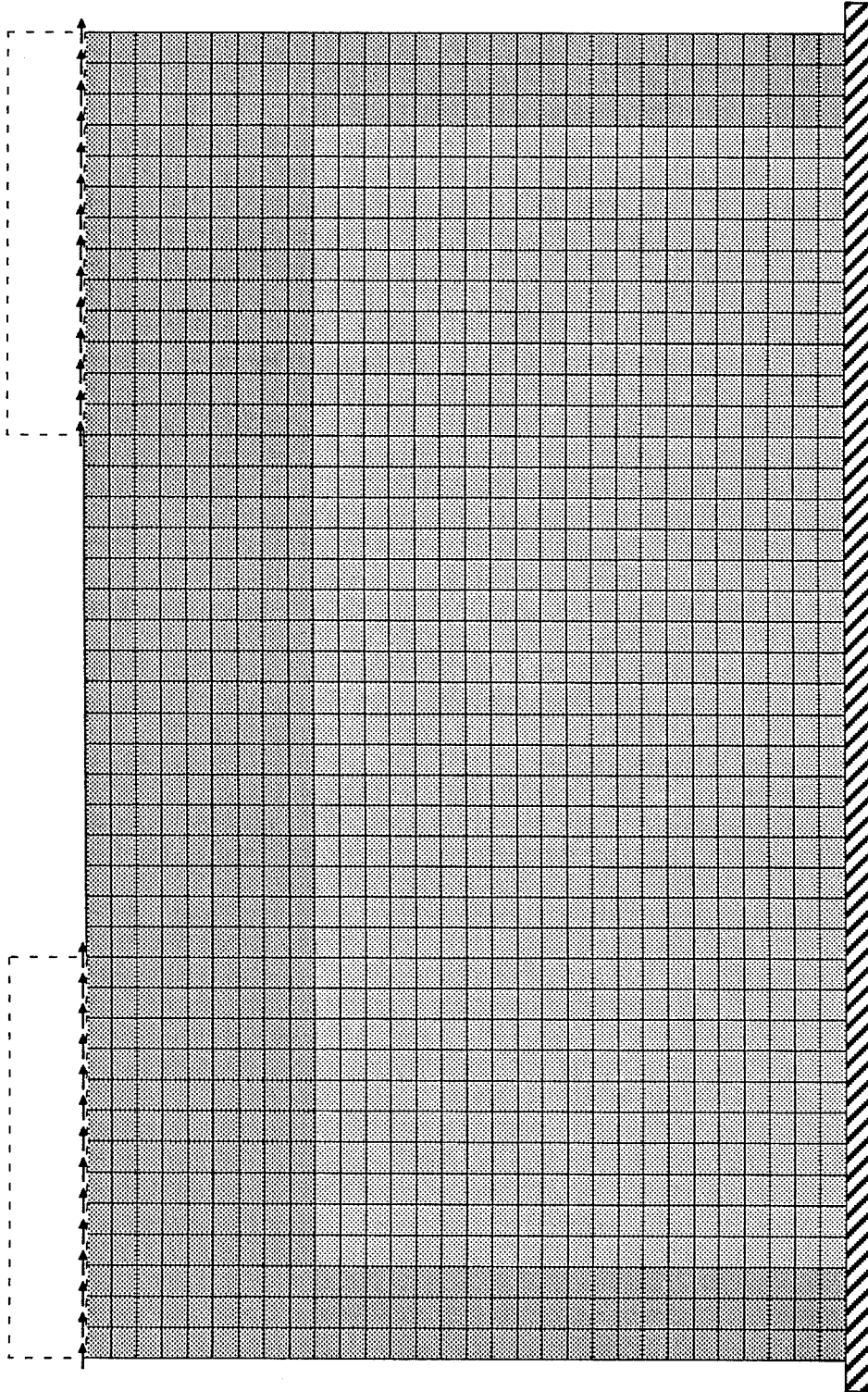


Fig. 4.6 Finite Element Model, Full Infill

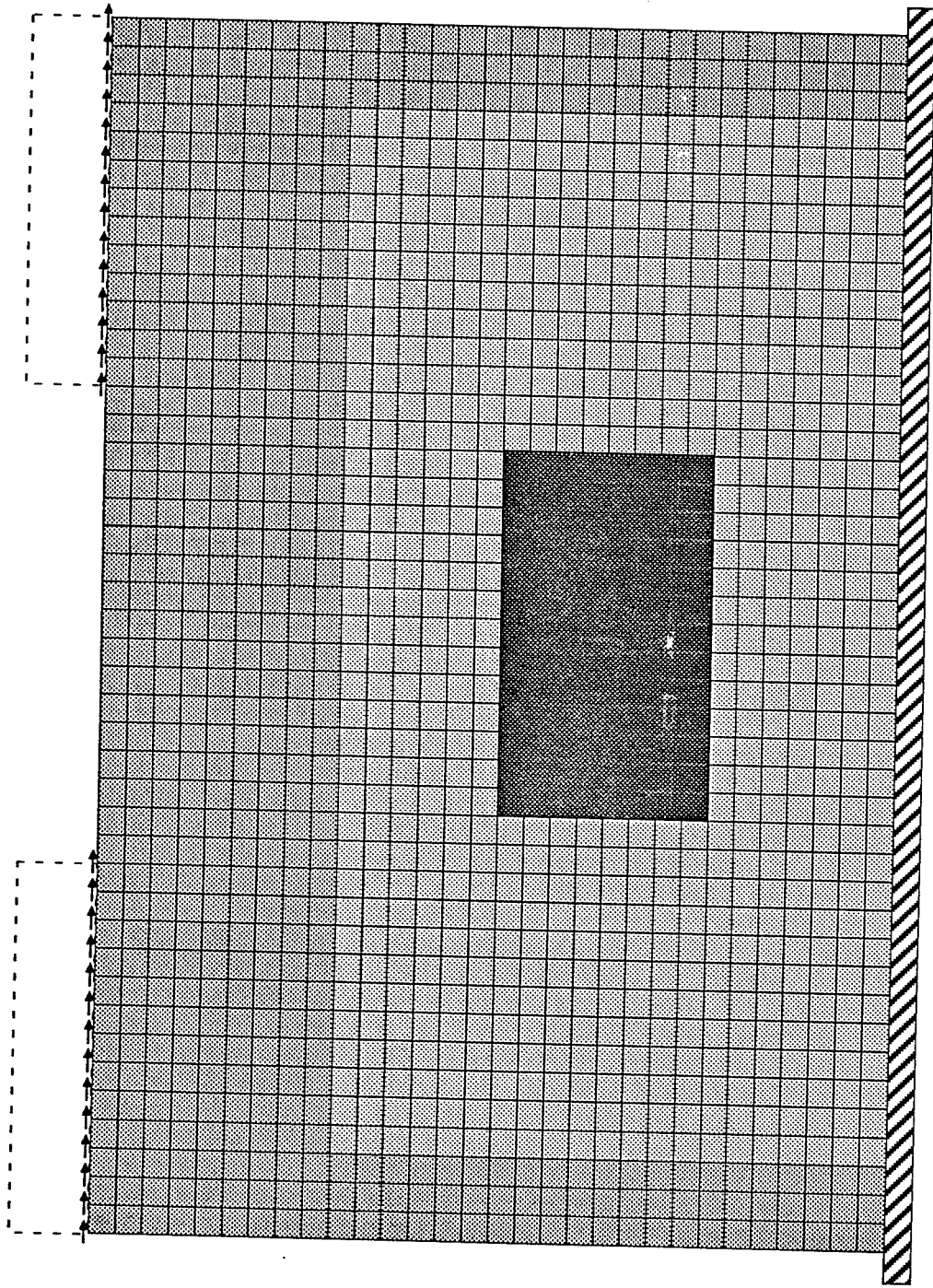


Fig. 4.7 Finite Element Model, Infill with Window

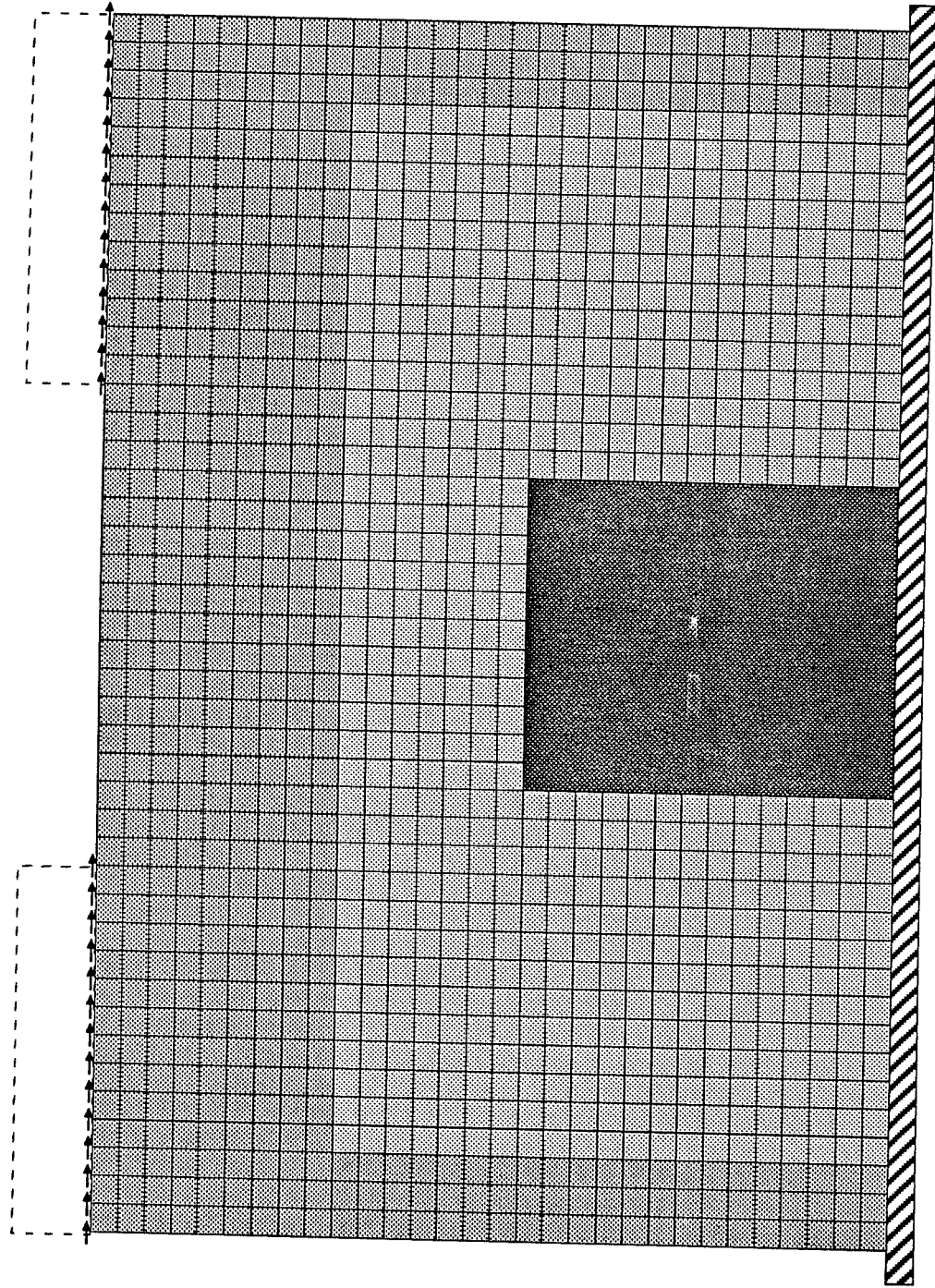


Fig. 4.8 Finite Element Model, Infill with Door

**4.1.3.2 Strain Profiles.** The normalized strain profiles from the finite element analysis for the infills with openings are presented in Figures 4.9 and 4.10. These figures represent strains that act on the horizontal section at the base of the specimen. The strain is computed from element stresses, and normalized for each specimen. The two figures are superimposed and normalized for the maximum value of strain found in the data for both infills with openings (Figure 4.11). This figure indicates that for a given load, the presence of the door opening produces the most severe condition on the extreme download fiber. Comparison of Figures 4.9 and 4.10 with strain profiles presented in Chapter 3 for the infills with openings indicates that the analysis and the experimental values are qualitatively similar to measured strain distributions. The boundary condition at the joint between the bounding frame and the infilled wall is assumed to have no slip in the finite element study. However, composite behavior was not observed in the download columns where the column deformed independently and slip occurred at the interface. Such behavior was indicated by both tensile and compressive strains in the column longitudinal bars.

**4.1.3.3 Deflection Modes.** The deflection modes for the infills as predicted by the finite element analysis are presented in Figures 4.12 - 4.14. The openings appear to "deform" in a shear mode while the specimen deflects in a cantilever mode. The corners of the openings that open under applied horizontal load correspond to the locations where unusual inclined cracking is present in the wall. As discussed in Chapter 3, these cracks are unusual because they were oriented at  $90^\circ$  to all other inclined panel cracks that formed under loading in a given direction. The corner that closes under load and is located over the opening corresponds to locations where concentrations of compression produced spalling and rapid degradation. Furthermore, the shape of the opening is trapezoidal. This indicates that significant shear deflections take place in the piers. Superposition of the diagrams reveals that the deflected shapes of the specimens with openings are qualitatively similar to the behavior of the full infill (Figure 4.15).

**4.1.4 Comparisons Of Measured and Theoretical Stiffnesses.** Some interesting trends are found when comparing the theoretical stiffnesses

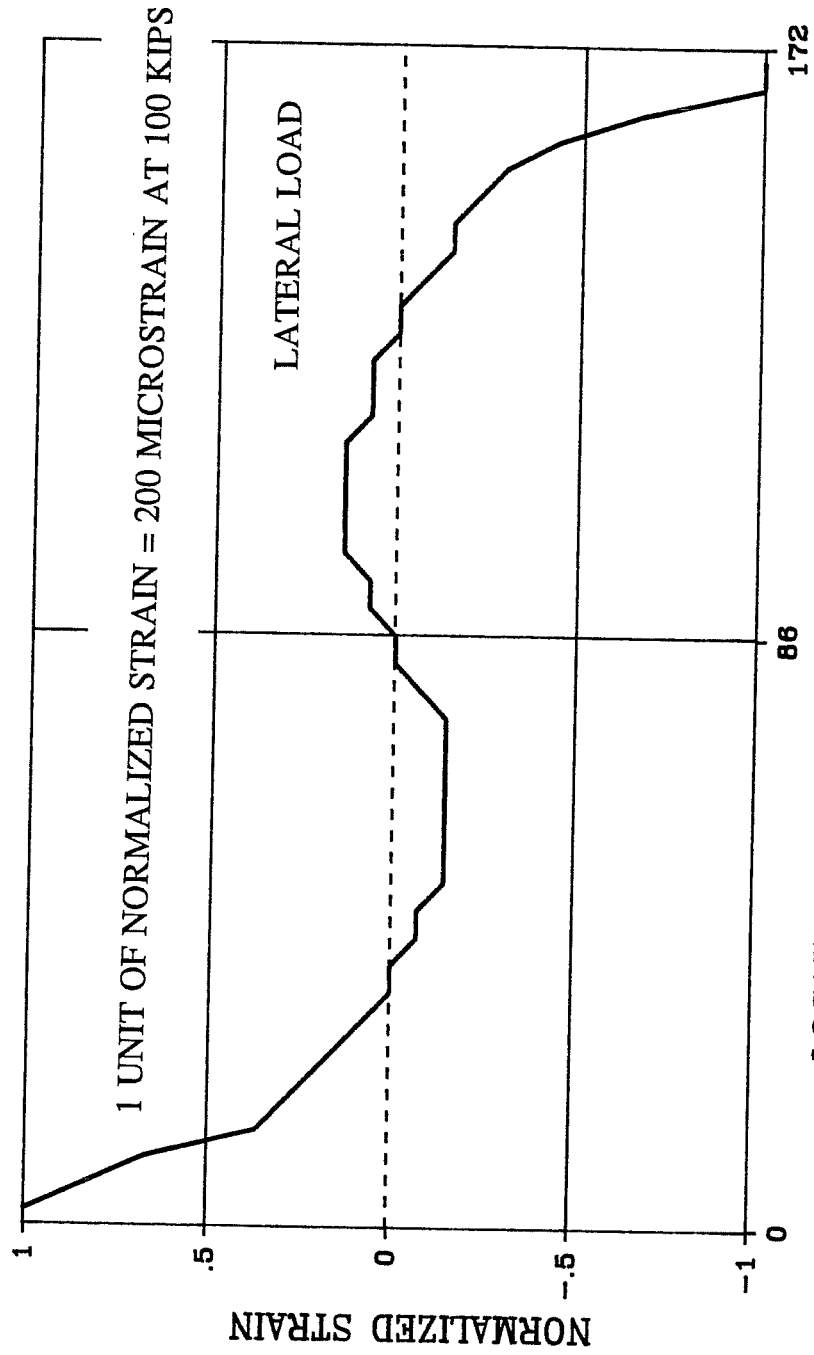


Fig. 4.9 Strain Profile, Finite Element Model, Infill with Window

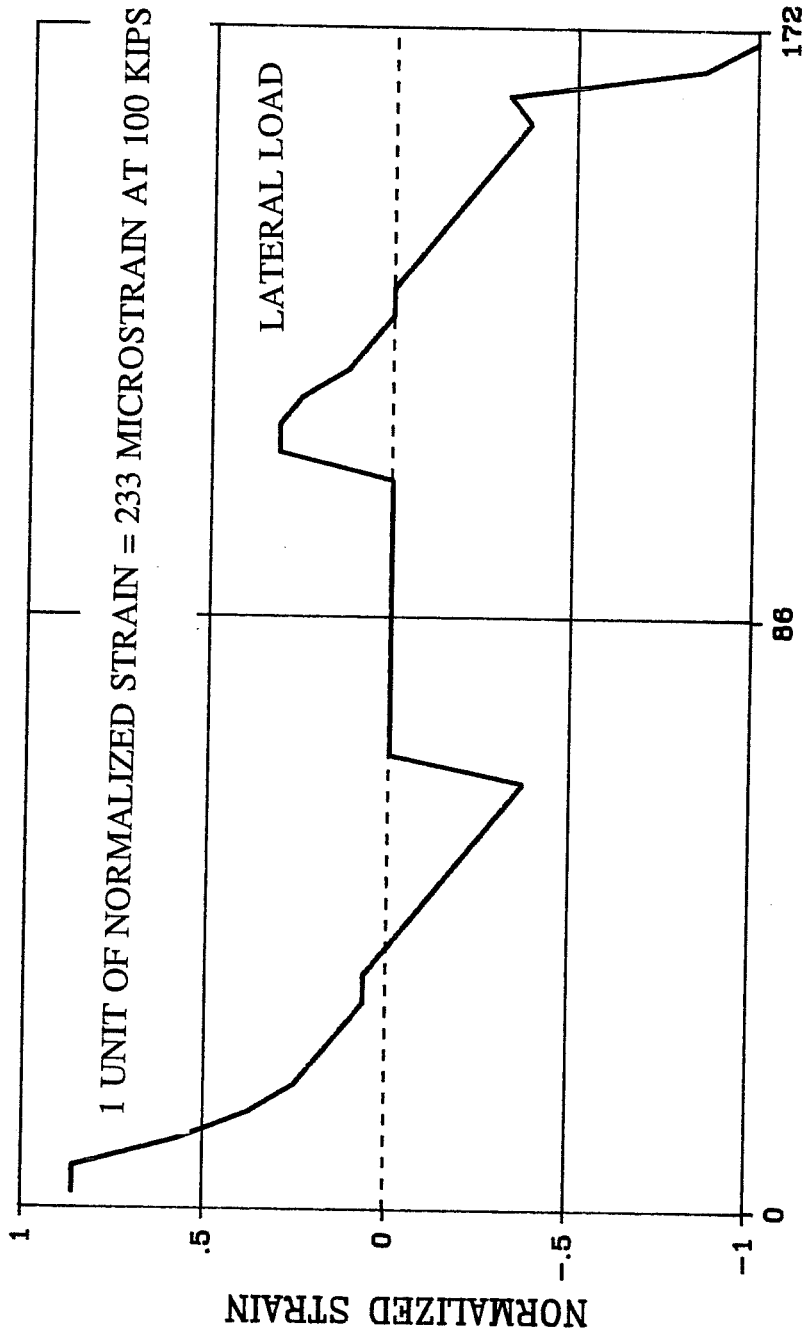


Fig. 4.10 Strain Profile, Finite Element Model, Infill with Door

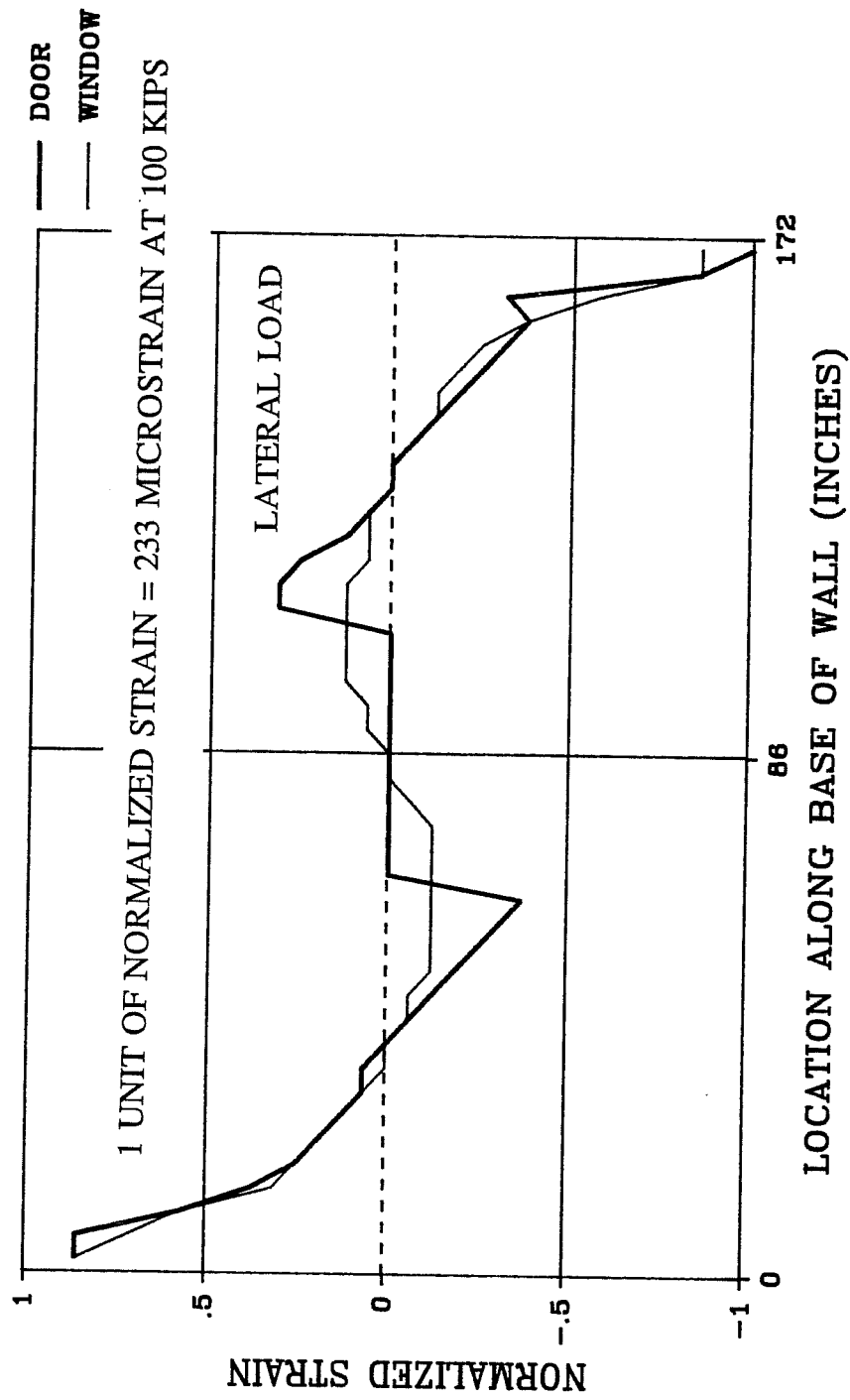


Fig. 4.11 Superimposed Finite Element Profiles



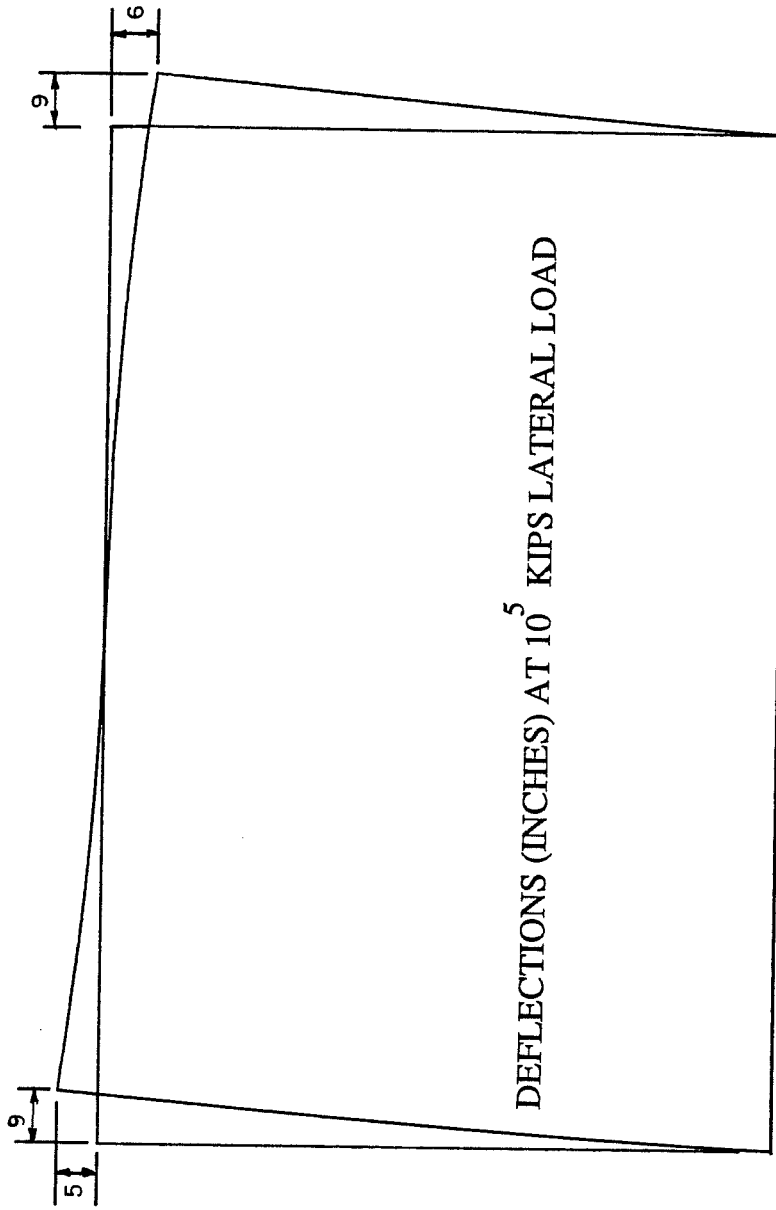


Fig. 4.12 Lateral Deflection Profile, Finite Element Model, Full Infill

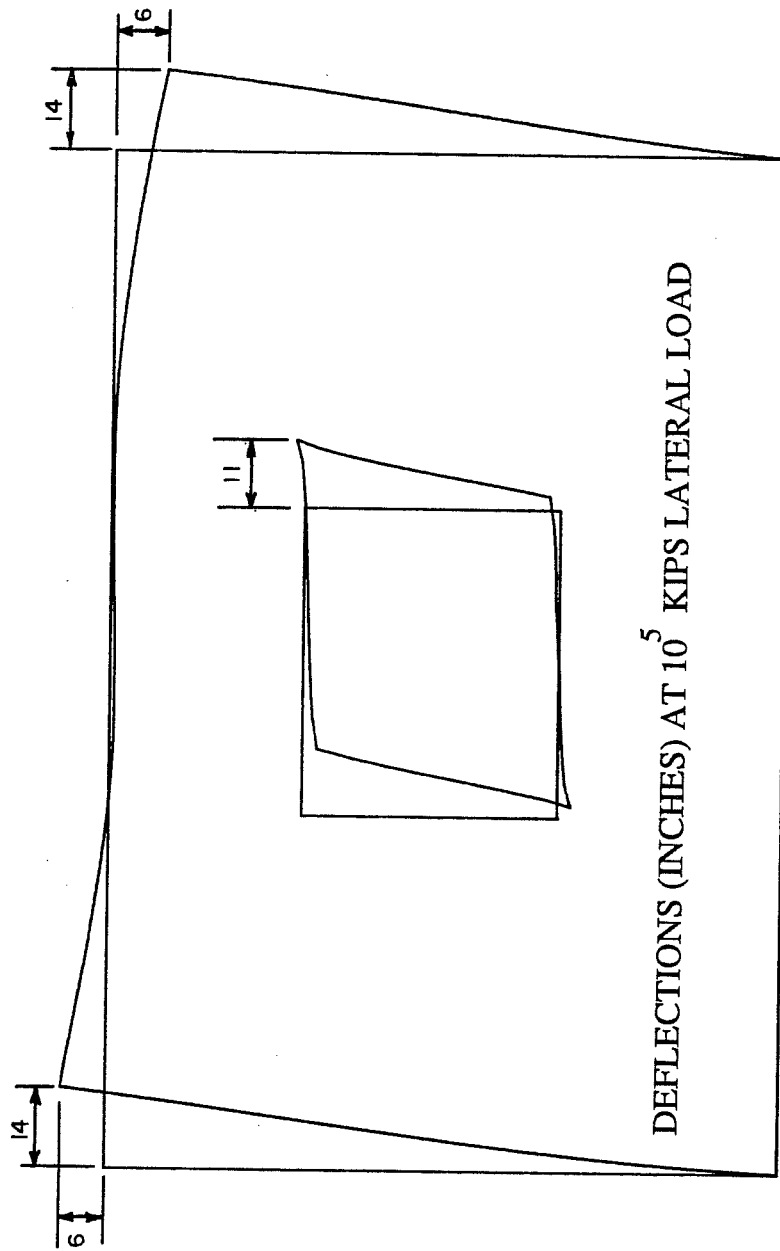


Fig. 4.13 Lateral Deflection Profile, Finite Element Model, Infill with Window

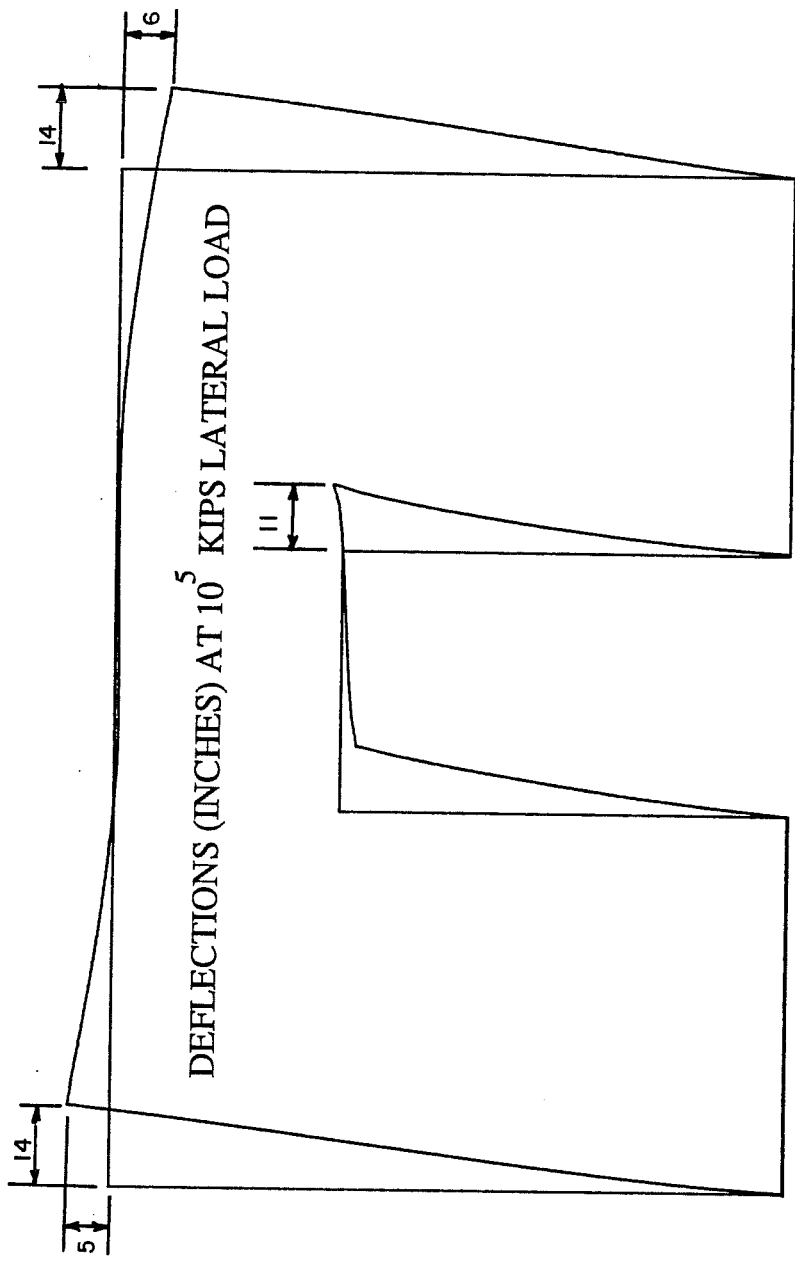


Fig. 4.14 Lateral Deflection Profile, Finite Element Model, Infill with Door

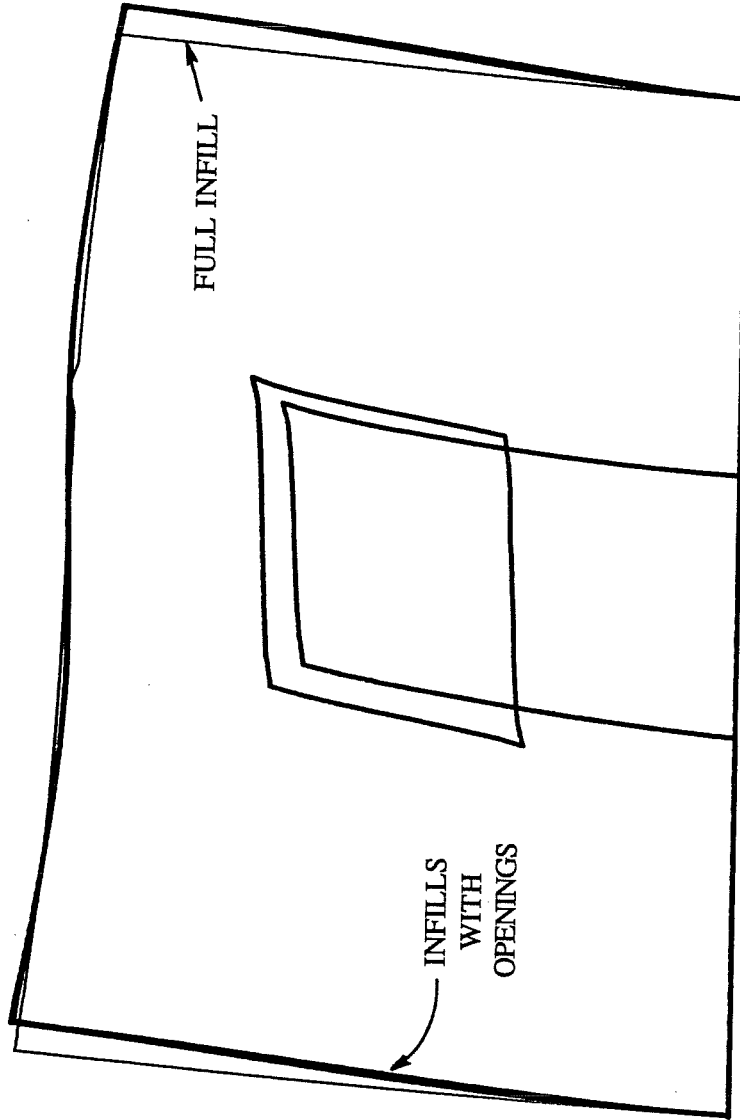


Fig. 4.15 Superimposed Lateral Deflection Profiles, Finite Element Models

for the test specimens. All of the techniques used predict essentially the same stiffness for the full infill. However, the assumption of sidesway in the window piers is not justified in view of the equivalent stiffnesses predicted by both the finite element analysis and the assumption of coupled bending using classical methods of analysis. Theory would indicate that the infill with the window would act as a coupled system, bending like a single vertical cantilever. The infill with the door is predicted to behave in a manner somewhere between that of a frame in sidesway and that of a coupled wall system, as the finite element stiffness falls between these two values.

Comparisons among theoretical stiffness predictions and experimentally obtained values indicate that classical theory predicts high stiffnesses for the test specimens. The experimental elastic response is not accurately predicted by any of the theoretical tools used here. This is likely the result of several factors. One reason for the high stiffness is that the theoretical models did not attempt to incorporate the boundary condition that exists between the bounding frame and the infill wall. Evidence of the unique boundary condition is obtained in the strain profiles at the base of the infills that are presented in Chapter 3. The independent bending of the download column indicates that discontinuity exists at the joint between the column and the infill wall. The crack patterns observed also support the concept of independent column bending. The occurrence of slip along the interface provides a more flexible mechanism than the ideal conditions modelled in the analyses. Secondly, temperature and shrinkage cracking is located in critical regions. Lastly, the modulus of elasticity is probably overestimated in the theoretical analysis.

## 4.2 Inelastic Response

**4.2.1 Stiffness.** In describing inelastic response, the peak secant stiffness (detailed in the previous section) will be used. The "average stiffness" is the average of the stiffnesses in the two directions of loading in a given cycle.

The load-deflection curves for the three test specimens at various levels of load and deflection are presented in Figures 4.16 - 4.20. As previously discussed, the measured load response curves for the infill with the door which were

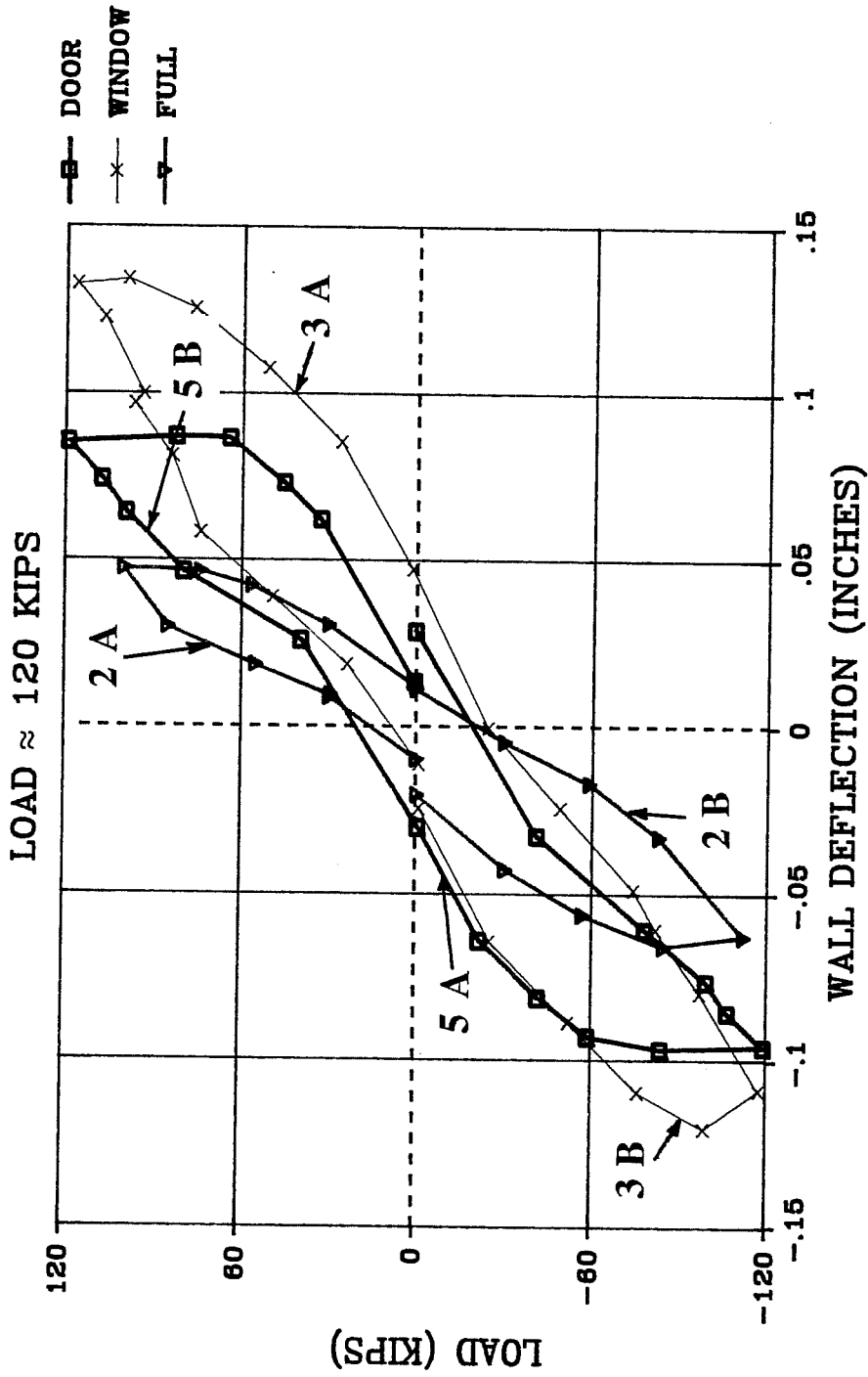


Fig. 4.16 Load-Deflection Response, 120 K

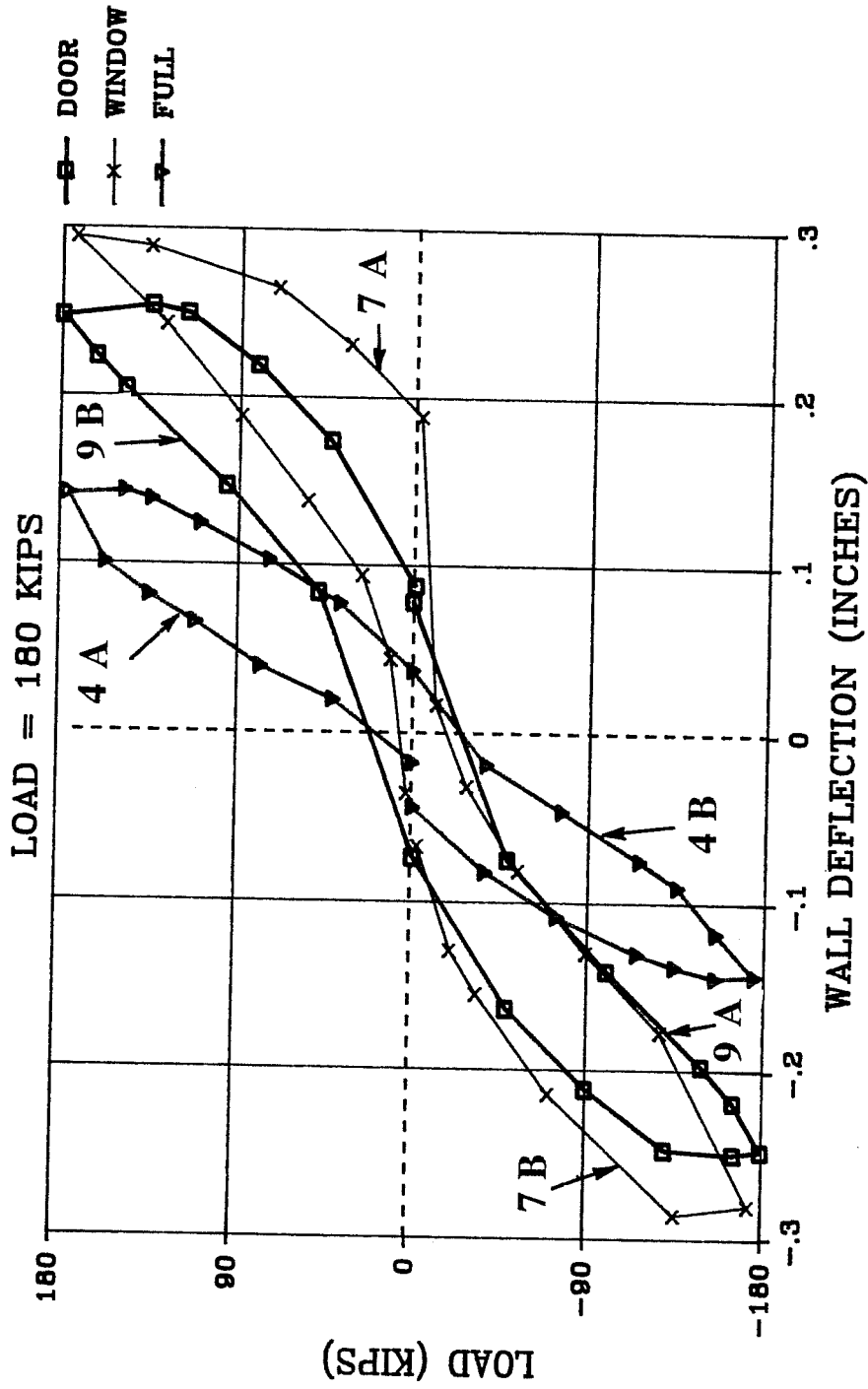


Fig. 4.17 Load-Deflection Response, 180 K

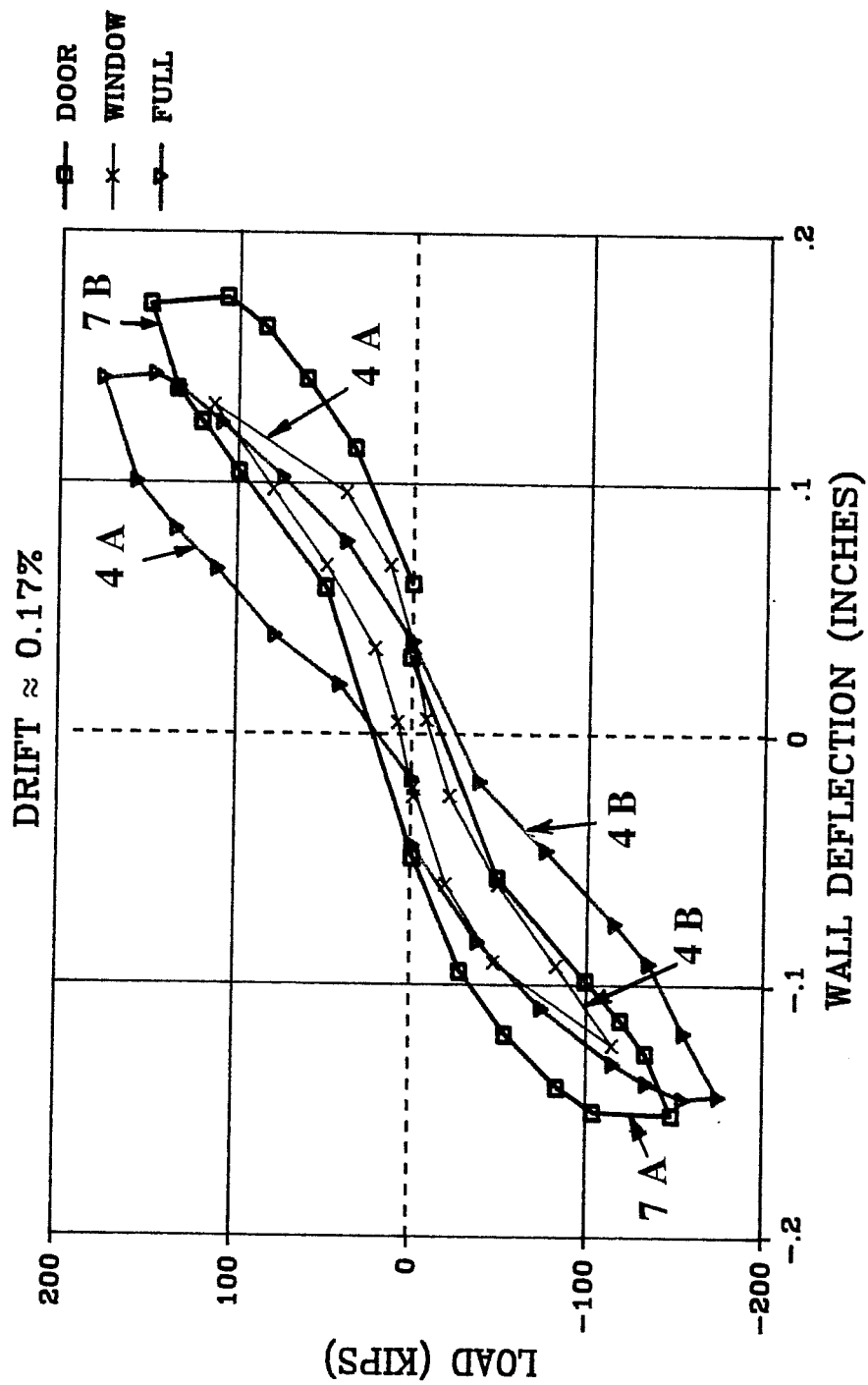


Fig. 4.18 Load-Deflection Response, 0.17%



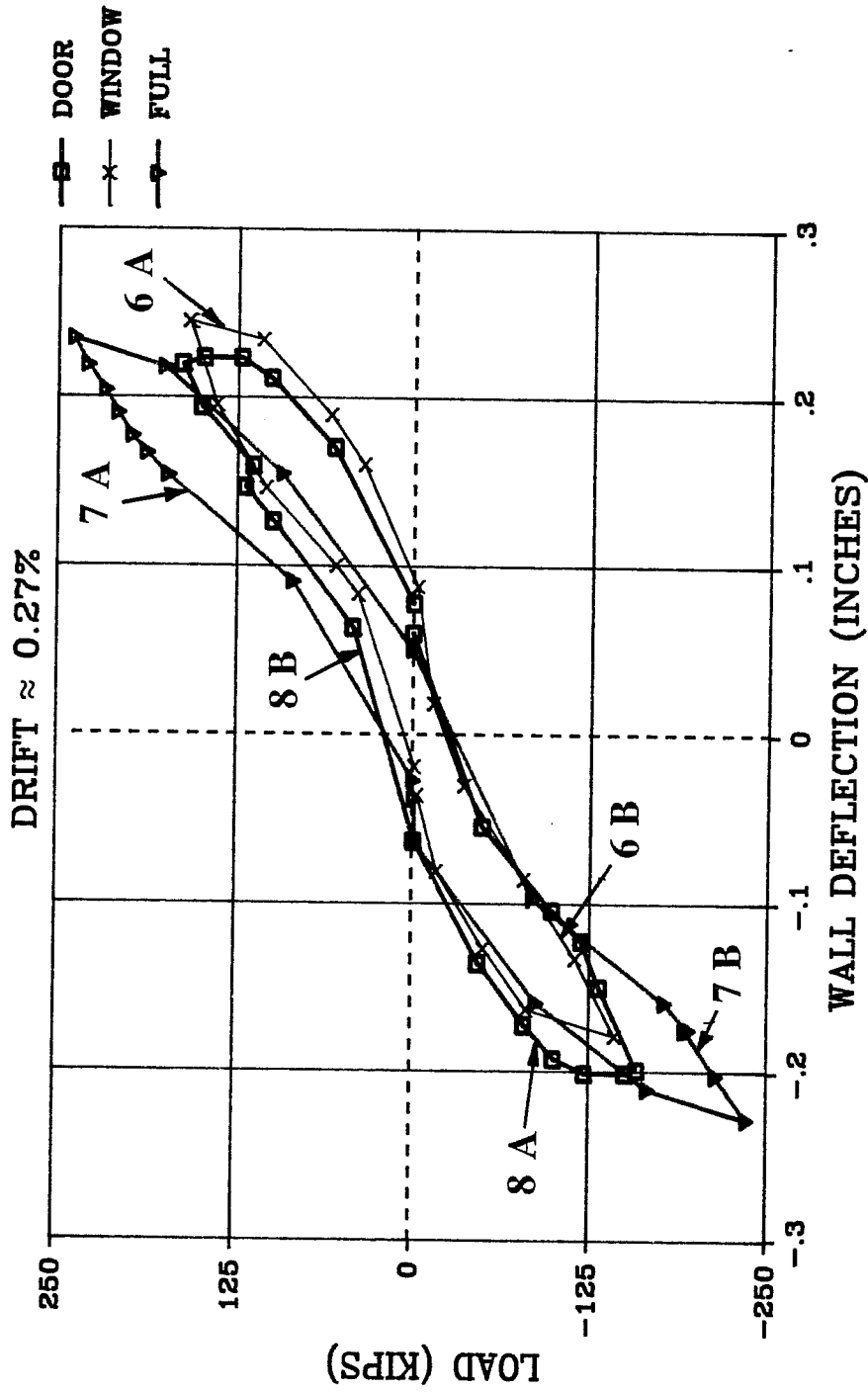


Fig. 4.19 Load-Deflection Response, 0.27%

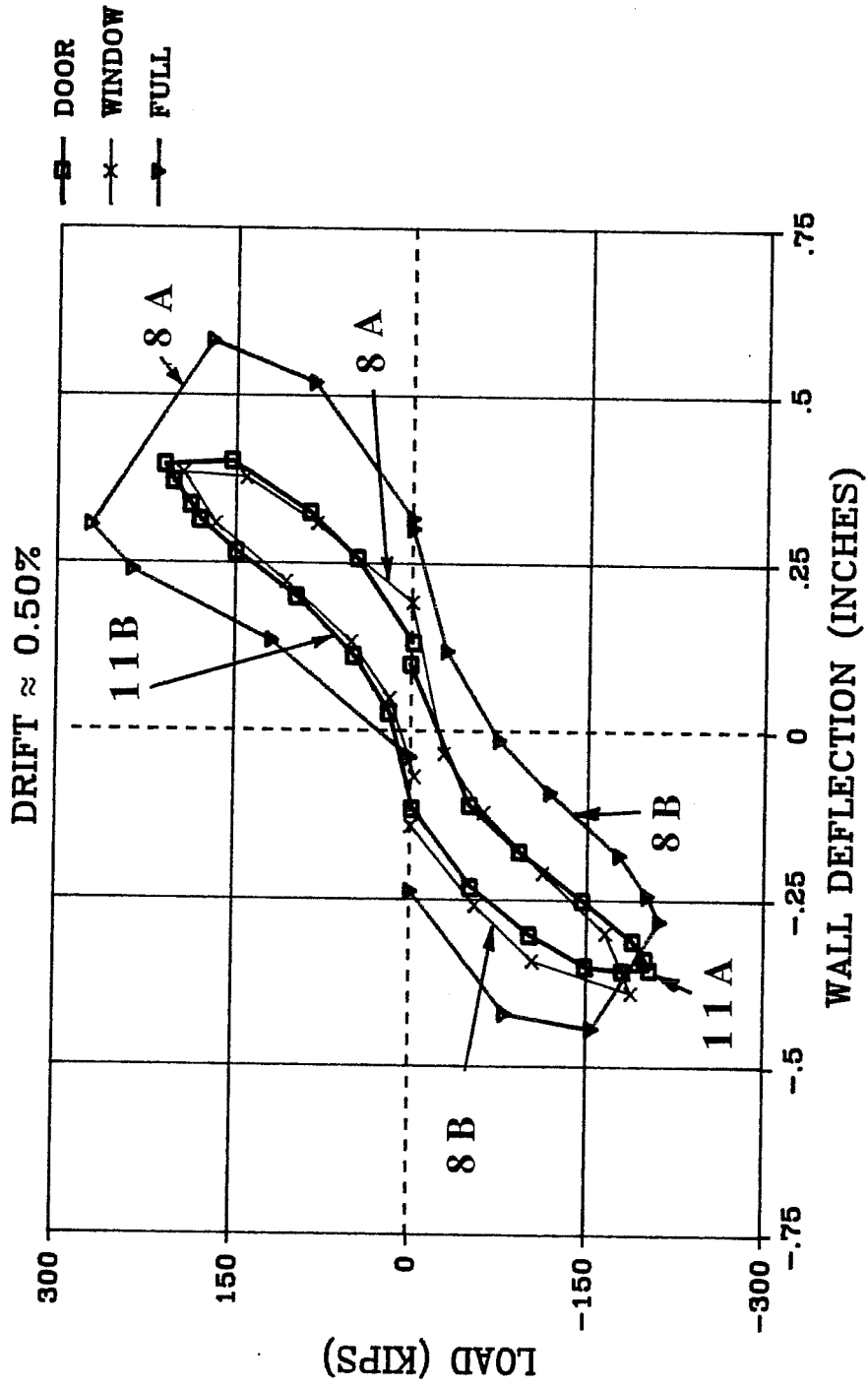


Fig. 4.20 Load-Deflection Response, 0.50%

presented in Chapter 3 indicate asymmetric deflections about the origin. For comparisons of behavior with other specimens, the offset was adjusted to produce symmetrical response about the origin for the infill with the door. Similar load-deflection behavior in the two directions of loading is shown in Figure 4.21. The load-deflection plots for the two halves of a given cycle are superimposed. The behavior is nearly identical.

In every cycle to a given load or deflection level, the full infill exhibits the greatest stiffness. Generally, the infill with the door exhibits considerably less stiffness than the full infill and more than the infill with the window. The relative stiffness (average measured stiffness of the infill with an opening divided by the average measured stiffness of the full infill) of the infills with openings in comparable cycles is illustrated graphically in Figure 4.22. The theoretical relative stiffness calculated using classical mechanics and assuming coupled bending of the piers was presented in the previous section. The values were 0.57 for the infill with the door and 0.70 for the infill with the window. Comparing the theoretical values with the experimental ones indicates that the infill with the window ranges from 45% to 54% with respect to the full infill. The infill with the door opening ranges from 55% to 75%. Thus the measured relative values are comparable to the theoretical ones. For the most part, the stiffness of the infill with the window at equivalent load or drift is comparable to that of the infill with the door.

The degradation of stiffness in a specimen may be described by the ratio of the stiffness in any cycle to the stiffness exhibited in the first cycle of load. This ratio is referred to as the "relative stiffness." Figure 4.23 contains relative stiffnesses at selected drift levels for the three specimens. The relative stiffness at yield of the extreme column longitudinal bars is 0.33 for the infill with the door, 0.23 for the full infill and 0.15 for the infill with the window. Figure 4.23 also indicates that at ultimate, the infills with openings have degraded equally with respect to their initial values, yet the infill with the door opening was subjected to many more cycles than the infill with the window. The infill with the door generally retained less of its initial stiffness at any level of drift. The infill with the window retained the most, however, the differences among specimens are

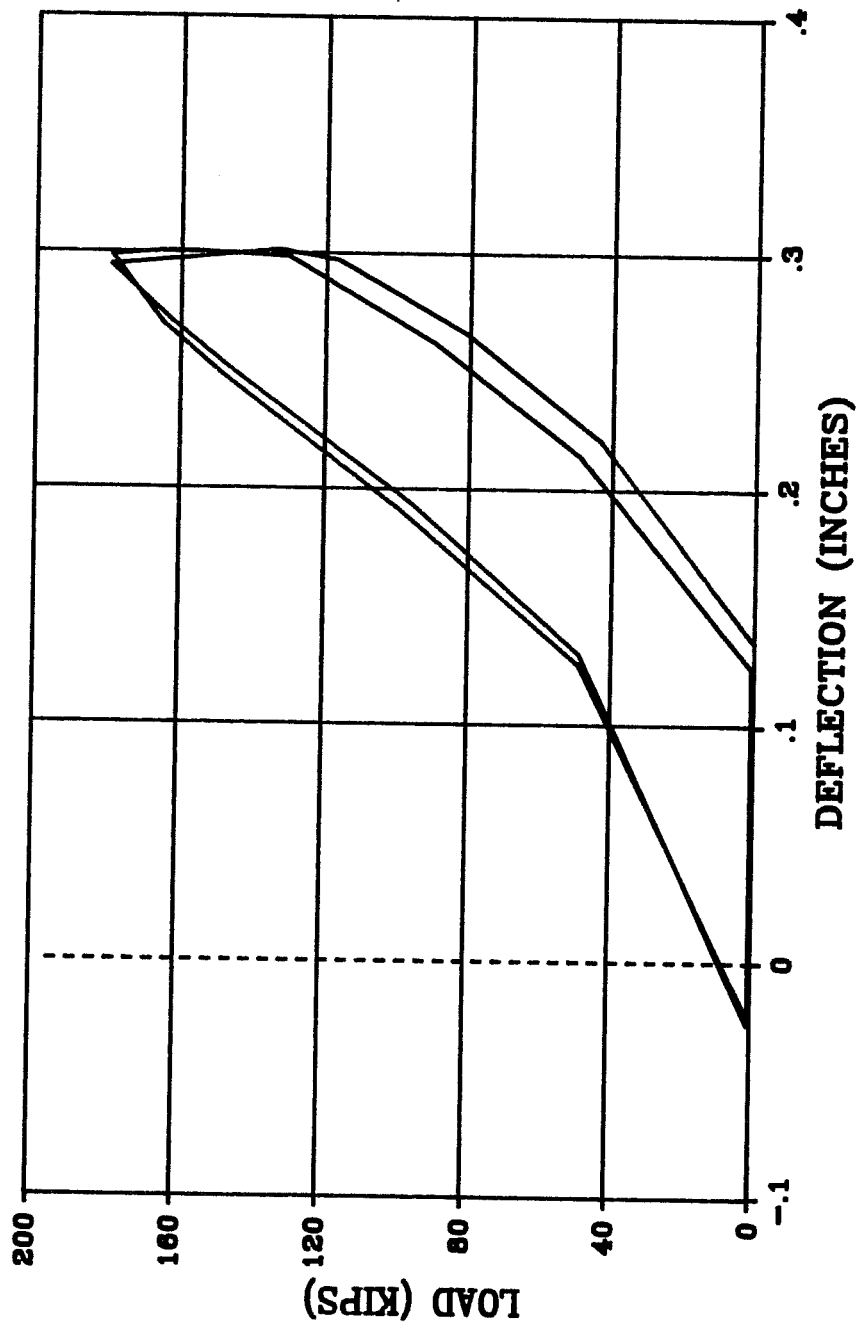


Fig. 4.21 Superimposed Half-Cycles, Infill with Door

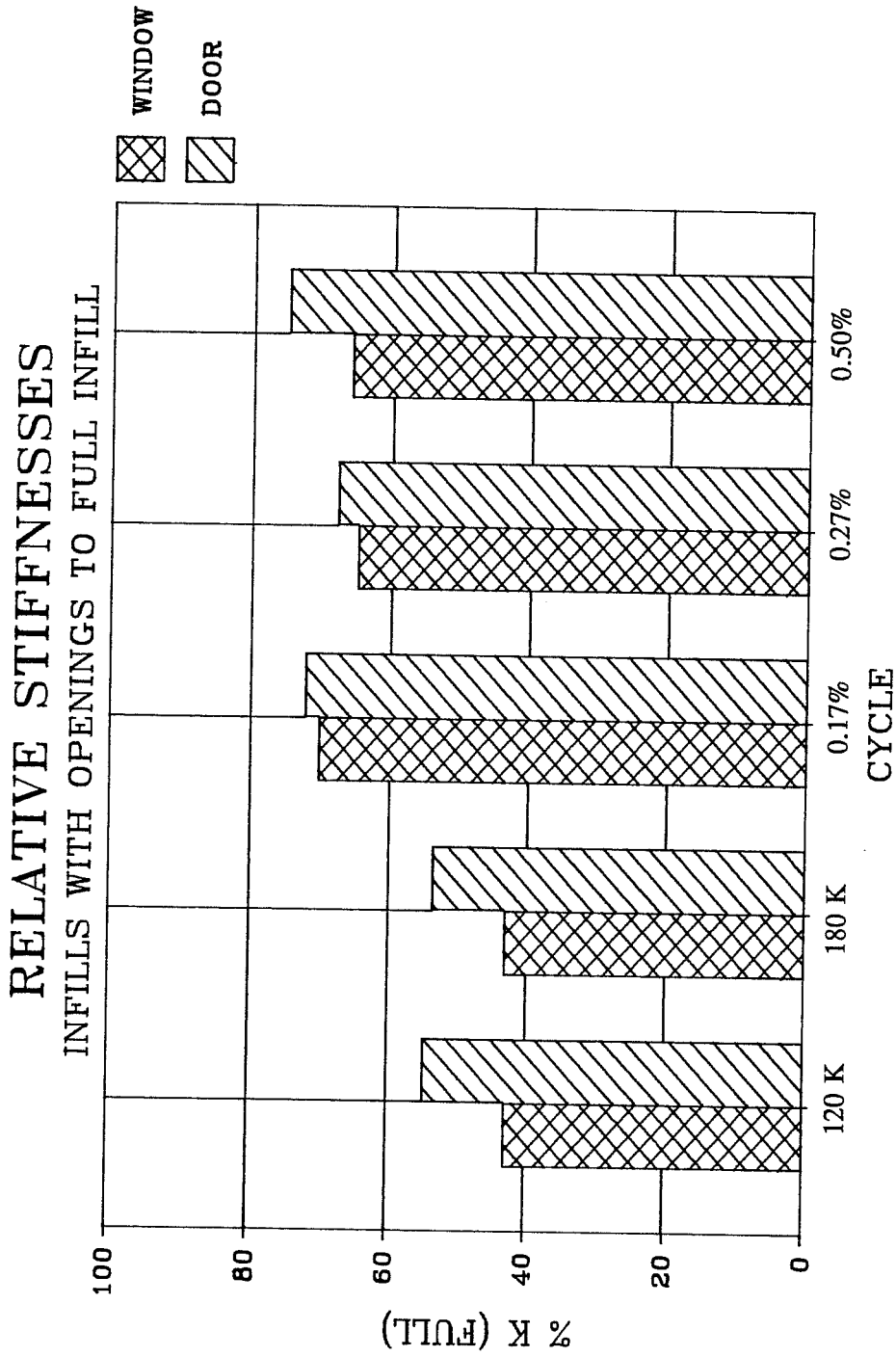


Fig. 4.22 Measured Relative Stiffness

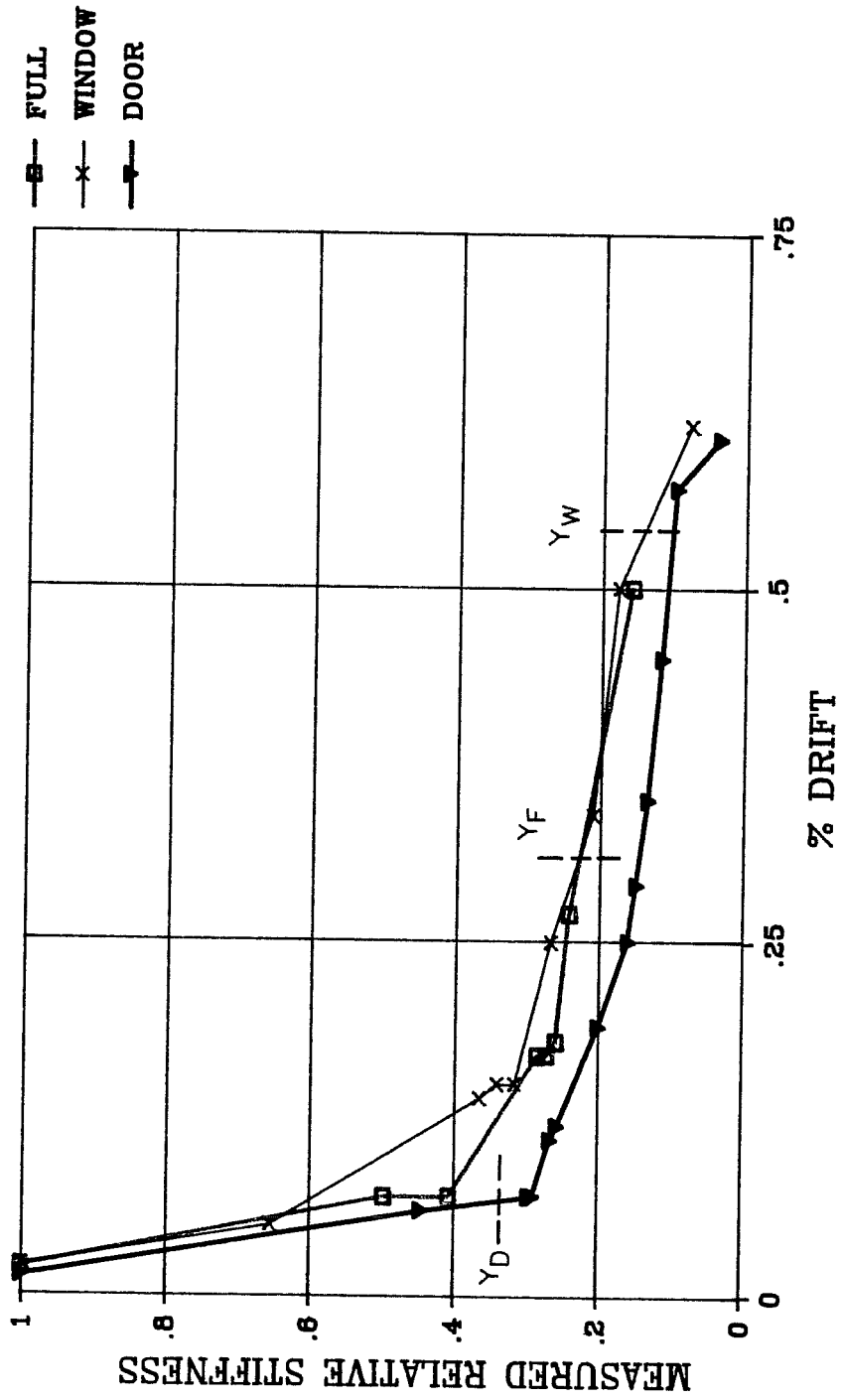


Fig. 4.23 Measured Relative Stiffness vs. Drift

small. The infills exhibit less than 40% of their relative stiffnesses at drifts in excess of 0.2%. At ultimate, less than 10% remains in the infills with openings.

The values of relative stiffness at initial yielding of the column longitudinal bars have particular significance for the infills with openings. Although the infill with the door began to yield at less than one half of the load at which the infill with the window yielded, it retained nearly the same amount of its initial stiffness at every load than did the infill with the window. The retention of large relative stiffness values after yielding of the column longitudinal still indicates that the shear behavior is the dominant action for the infill with the door.

The measured stiffnesses were divided by the theoretical stiffness of the full infill using classical techniques. The results are illustrated in Figure 4.24. Generally, at drift levels in excess of 0.10%, the infills exhibit less than 20% of the theoretical stiffness of the full infill. Again, the differences among the specimens are small yet, the infill with the door exhibits greater stiffnesses at any drift than the infill with the window. Degradation is also indicated by "pinching" of the load-deflection curves. Pinching of the hysteretic loops is most severe for the infill with the window and least evident in the response of the full infill (Figures 4.16 -4.20).

#### 4.2.2 Deflection Components

*4.2.2.1 Shear Component of Lateral Deflection.* The total lateral deflection was assumed to be comprised of deformation due to flexural action and deformation due to shear. In the experimental program, shear deformations were measured with potentiometers that spanned the diagonal of each specimen (see Figure 2.25). The potentiometers measured the change in length of the diagonal. The lateral component of the change in length of the diagonal is considered to be shear deformation only. This assumption is justified because the change in length of the diagonal was isolated from deflections due to flexural rotation that occur cracks that open at the base. The change in length of the diagonal was isolated experimentally by placing the anchor pin for the instrumentation 1 in. above the base of the column, as illustrated in Figure 4.25. Flexural cracks opened at the joint between the column and the foundation girder and contributed to

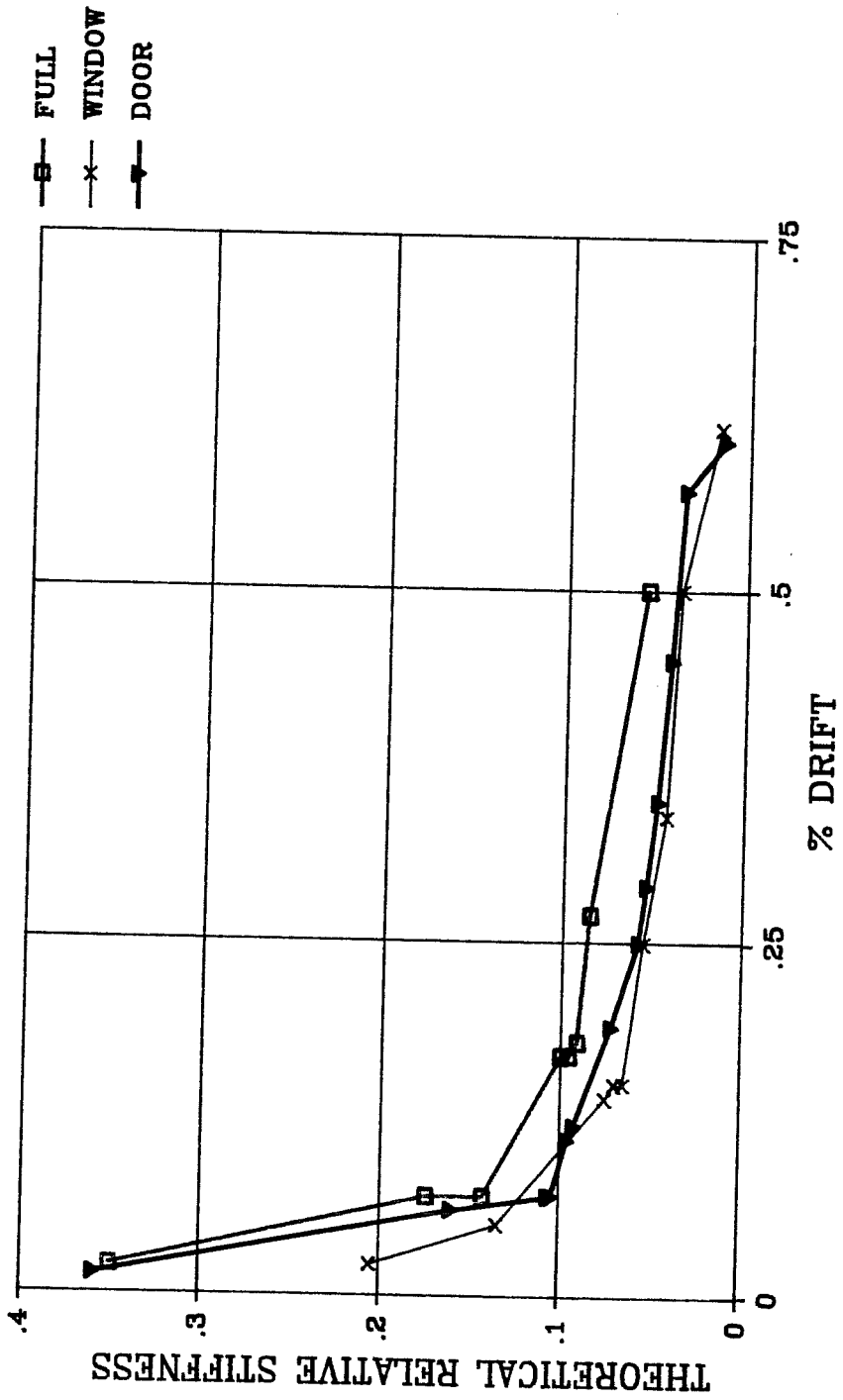
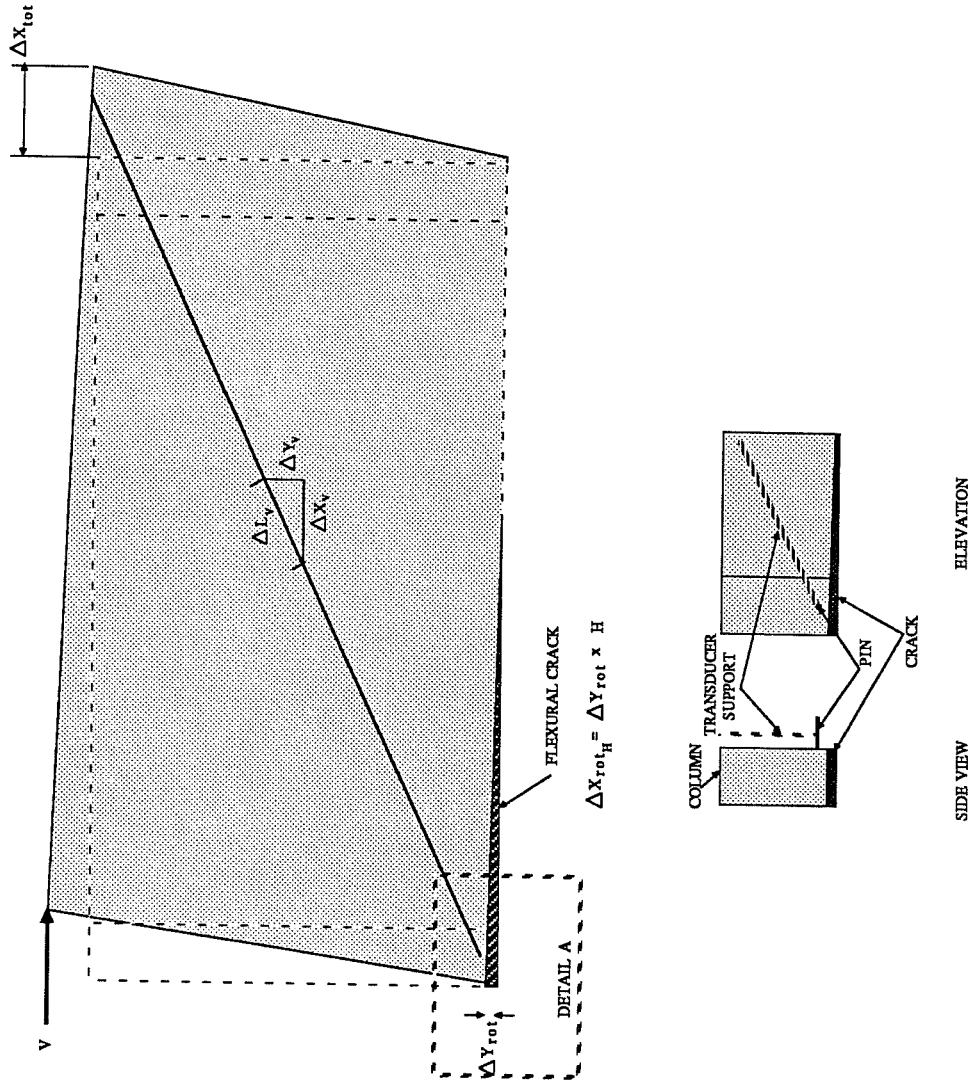


Fig. 4.24 Theoretical Relative Stiffness vs. Drift





DETAIL A  
 Fig. 4.25 Shear Deformations in Walls

the deflection at the top of the wall through rotations at the base. The flexural deformation was the difference between the total measured lateral deformation at the top of the wall less the lateral shear deformation.

The content of the total lateral deflection may be described through the use of a ratio of the measured lateral shear component to the total lateral deflection at the top of the wall. This quantity is referred to as the "shear component ratio." Figure 4.26 contains plots of the load-shear component ratio envelopes for the specimens. From these plots, it is apparent that at all loads, the shear component ratio is significantly larger in the full infill than for the infill with the door opening. The shear component ratio exhibited by the full infill is greater than that for the infill with the window for virtually the entire load history of the infill with the window. The shear component ratio for the full infill becomes constant at approximately 48%. This indicates that the specimen no longer degrades in shear, rather, some other deformation becomes dominant. The shear component ratio may be theoretically determined using classical mechanics. Under the assumptions discussed in the previous section on linear elastic behavior, the predicted shear component ratio for the full infill is 0.68 which is significantly larger than the experimentally observed range of 0.35 to 0.45. The difference between the theoretical and experimental values indicate that flexure contributes significantly to lateral deflection.

The infill with the window exhibited a larger shear component ratio through its entire load history than did the infill with the door opening. The shape of the load-shear component ratio curves suggest that the relationship between applied load and shear component ratio is linear and that the shear component increases with load. The evidence suggests that the infills deteriorate in shear. In other words, the influence of cracking on the flexural stiffness of the specimen was apparently, not as significant as the influence of cracking on the shear stiffness. The theoretical shear component ratio calculated for the infill with the window using classical mechanics and assuming coupled behavior of the piers is 0.93. This, again, is greater than the experimentally observed range of 0.10 to 0.60. The low experimental values indicate that deflections due to rotation are significant.

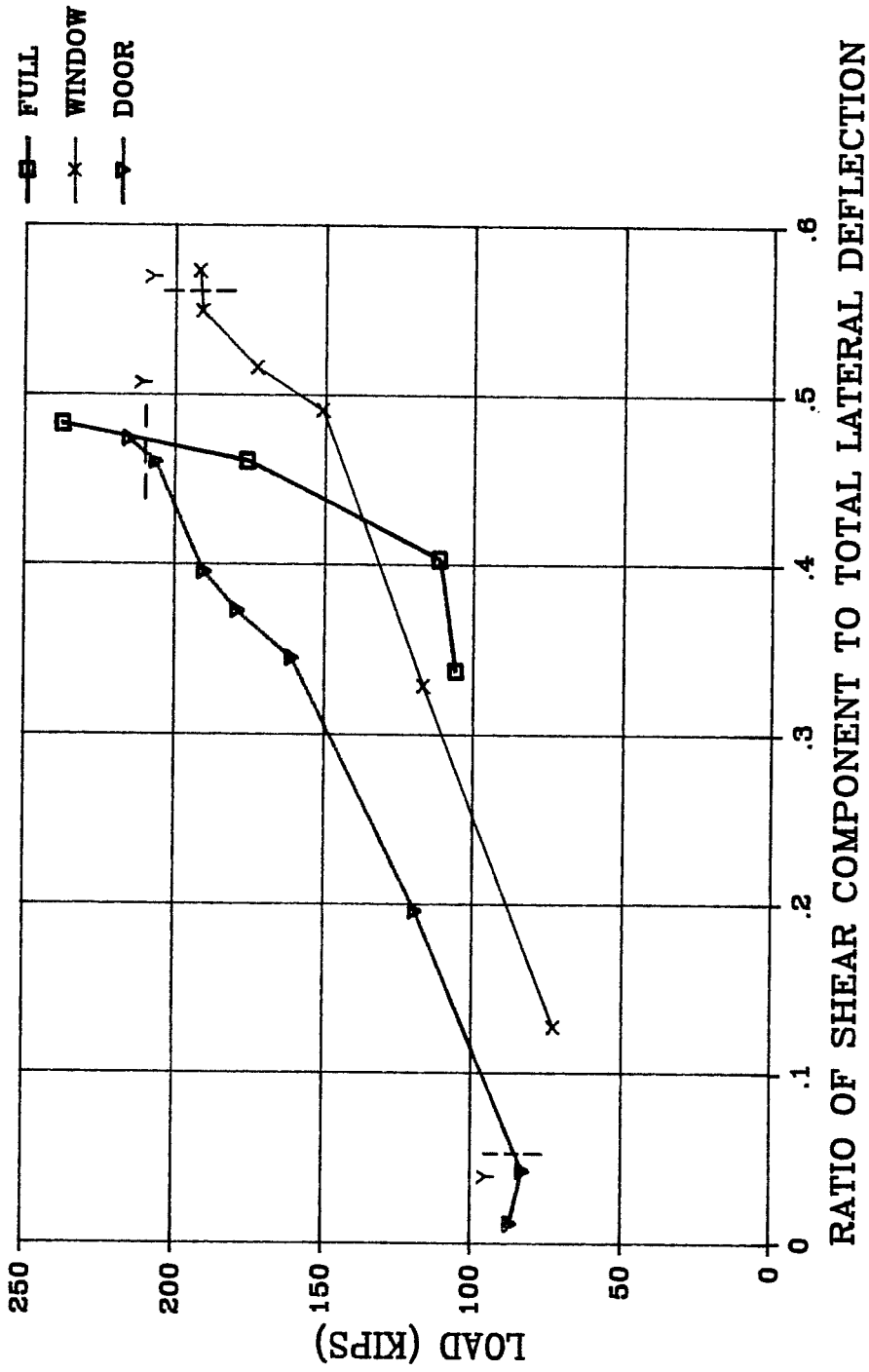


Fig. 4.26 Load-Shear Component Ratio Envelopes

The infill with the door opening exhibited the lowest shear component ratio compared to the other two specimens at every load. The relationship between applied load and shear component ratio is nearly linear. A linear relationship between load and shear component ratios for both pre-yield and post-yield loads was observed for the infill with the door. The theoretical shear component ratio for the infill with the door was 0.90 which is greater than the maximum value prior to yield. The theoretical value of 0.90 exceeds the maximum value of 0.45 at ultimate. The difference between the theoretical and experimental values is due to flexural rotation.

From the deflections measured, it appears that the effect of openings is to reduce the shear component of the lateral deflection. Intuition suggests that the reduced shear stiffness produces higher shear deflections at a given load and therefore, would increase the shear component of the lateral deflection. Second, the behavior in these tests is clearly more affected by the configuration of the openings than by the size of the openings. The door opening constituted the largest opening and yet had the lowest shear component ratios. This is true because the infill with the door has a greater shear area in the piers than the infill with the window and higher flexural deformations in the piers. Shear component ratios increase linearly with load in both the pre-yield and post-yield ranges. Finally, the shear component ratios are considerably overestimated by the classical methods employed here.

*4.2.2.2 Lateral Deflection Profiles.* The measured lateral deflection over the height of the infills are pictured in Figures 4.27 - 4.29. The measured deflections are based on horizontal deflection data which was acquired through the use of potentiometers on one end of the specimen (Figure 2.25). All deflections are magnified by a constant factor for clarity. The deflection profiles are superimposed on the deflections from the finite element analysis. The finite element deflections are normalized to the peak measured lateral deflection at the top of the wall.

From the measured deflections, it is apparent that the presence of openings influences deflections significantly. The measured lateral deflection profile

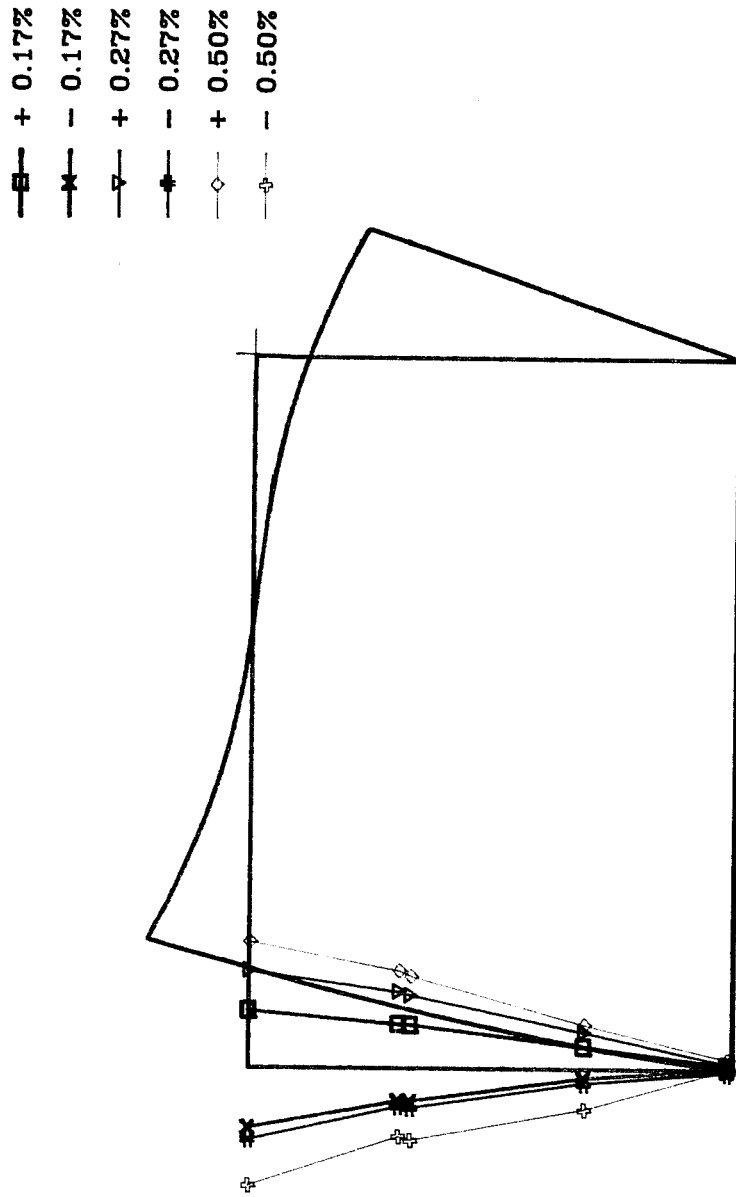


Fig. 4.27 Lateral Deflection Profile, Full Infill

- + 0.17%
- ×— - 0.17%
- ▽— + 0.27%
- ◆— - 0.27%
- ◇— + 0.50%
- ⊕— - 0.50%

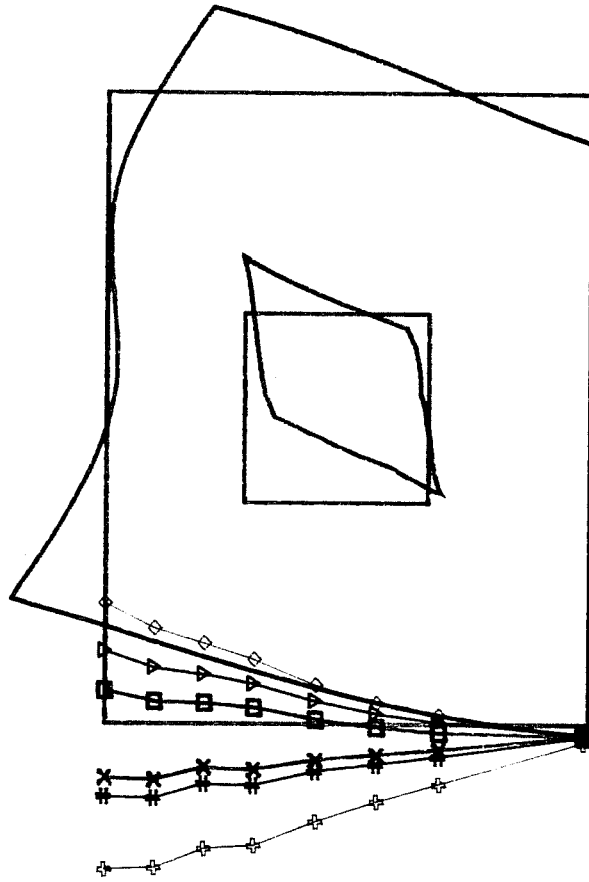


Fig. 4.28 Lateral Deflection Profile, Infill with Window

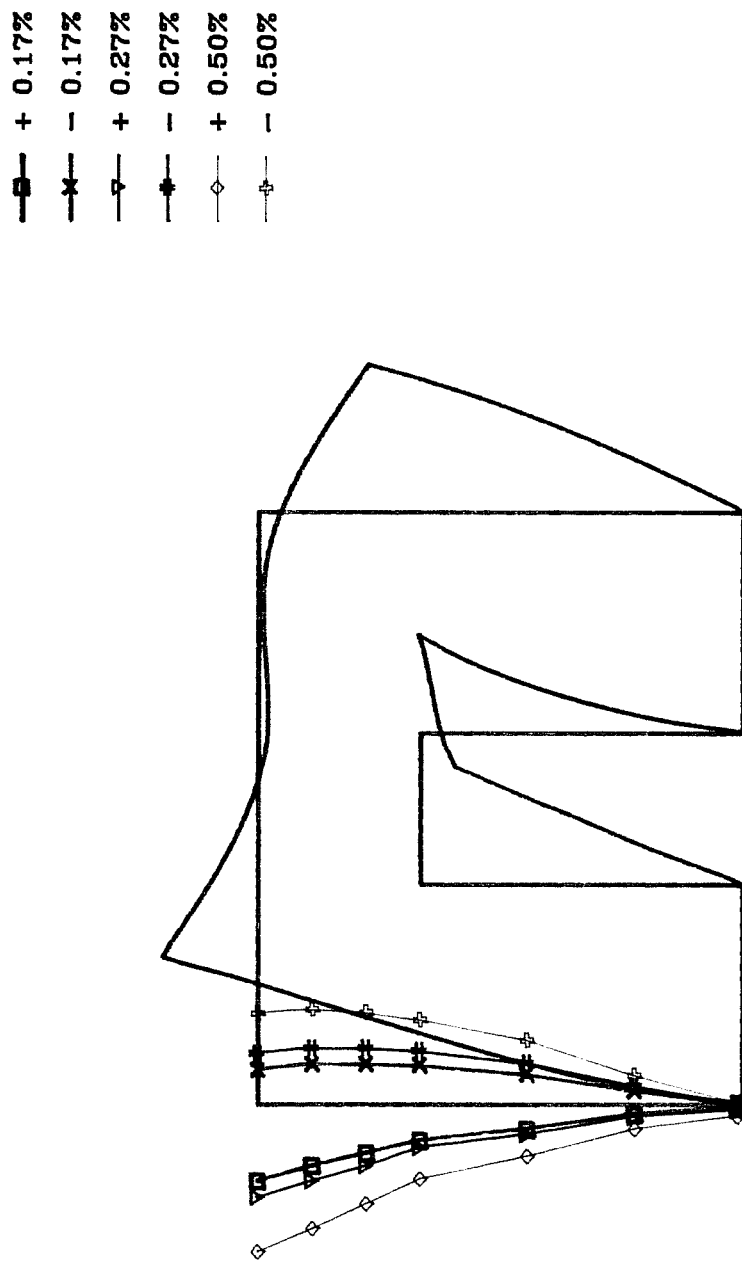


Fig. 4.29 Lateral Deflection Profile, Infill with Door

is virtually linear for the full infill. A linear deflection profile is indicative of dominant shear action. The measured deflections in the piers of the infills with openings show more curvature, particularly in the infill with the door opening. The lintel beams in the specimens with openings exhibit linear deflection profiles. Visual inspection of the deflection plots indicates that deflections in the opening are largest contributors to the total lateral deflection at the top of the wall. For the infills with openings, the deflections indicate that the openings produce coupled wall behavior.

**4.2.3 Coupled Wall Behavior.** The degree of coupling is a function of the relative stiffness of the coupling beams to the pier sections they connect. In the specimens constructed for this investigation, the coupling beam cross-section consisted of a section of the wall and the deep first story girder used to distribute load. The uncracked moments of inertia of the sections between the piers and the coupling beams are listed in Table 4.3. From this comparison, it is apparent that the degree of coupling was fairly light as the moments of inertia are of the same order of magnitude for both infills with openings.

More refined analysis of coupling involves the determination of a parameter,  $\alpha$ , which gives an indication of the degree of coupling in a system. Beck [21] derived a method for determining the response of pierced shear walls to lateral load using a laminar analysis discussed in Chapter 1. From this analysis, a parameter,  $\alpha$ , is determined to indicate the degree of coupling in a pierced shear wall system.

$$\alpha = \sqrt{\frac{6 \cdot a_1^2 \cdot l_2 \cdot I_2}{a_2 \cdot l_2^3 \cdot I_1}}$$

The variables are illustrated in Figure 4.30 and the results of this analysis are presented in Table 4.4. As  $\alpha$  increases, so does the degree of coupling in a given system. As coupling increases, the behavior of the shear walls systems progresses from that of two linked walls to that of composite action of the two piers. The formula is predicated upon frame action and indicates that coupling



**TABLE 4.3**  
**Member Moments of Inertia, Coupling Beam Analogy**

Assumption	Moment of Inertia (in. <sup>4</sup> )	
	Beam	Pier
<b>Window</b>		
Uncracked, transformed	171000	136000
Uncracked, plain concrete	154000	120000
<b>Door</b>		
Uncracked, transformed	182000	197000
Uncracked, plain concrete	169000	175000

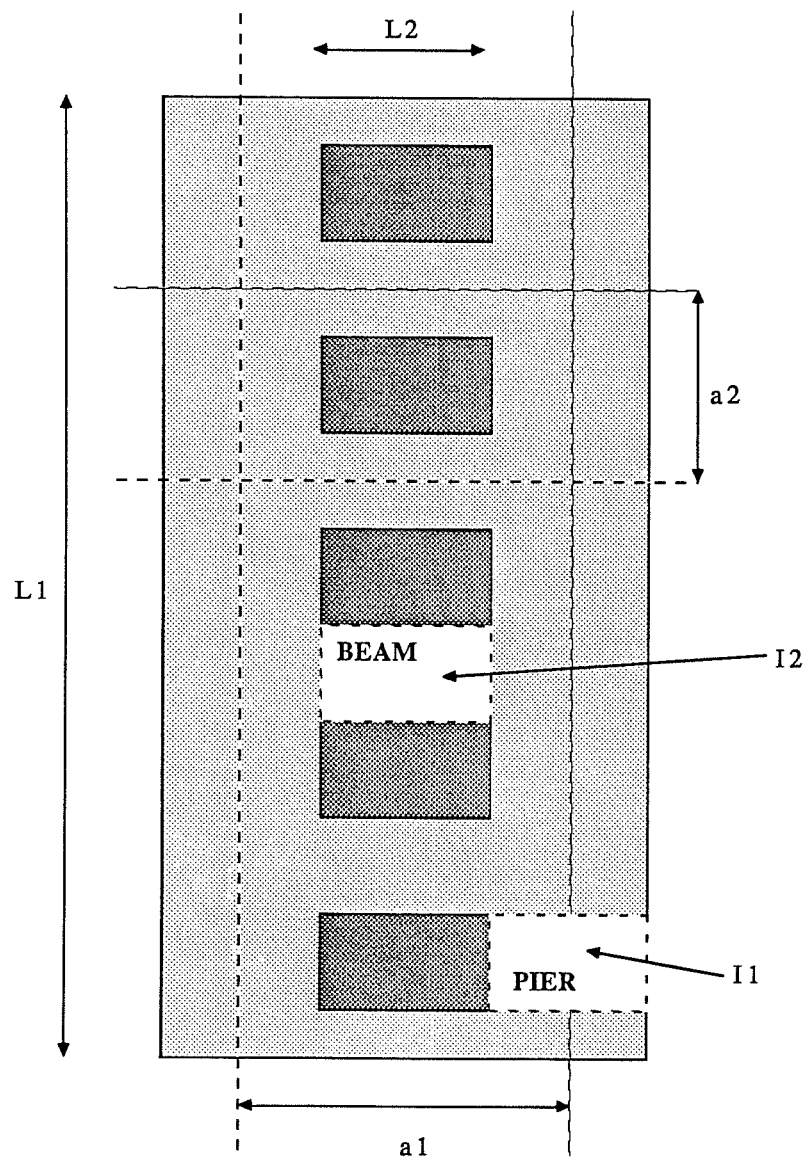


Fig. 4.30 Geometric Parameters for Coupling Factor

**TABLE 4.4**  
**Alpha Parameters and Values**  
**Infills with Openings**

Parameter	Window Value (inches)	Door Value (inches)
$a_1$	124	116
$a_2$	82	93
$l_1$	120	120
$l_2$	56	40
$I_1$	120000	175000
$I_2$	154000	169000
$\alpha$	11	14

increases with parameters that increase overturning forces in the piers. Overturning forces in the piers arise from the end shear of the coupling beams. Hence,  $\alpha$  increases with increasing height of the assemblage, increasing distance between the piers and increasing flexural inertia of the coupling beams. The resulting values of alpha indicate that the degree of coupling is moderate to high [5], which suggests that in any case, the system will exhibit behavior approximating that of a vertical cantilever.

The degree of coupling exhibited by the infills with openings is most clearly shown in the strain profiles on various horizontal sections. In a heavily coupled system, the strain profile across the critical section would be approximately linear from extreme upload fiber to extreme download fiber of the assemblage. The individual piers are subject to both moment and axial force due to overturning. The finite element model shows very little coupling for both of the infills with openings, based on the strain profile at the base of the wall (Figures 4.9 and 4.10). The computed strain profiles indicate essentially independent action of the two piers and very little overturning effect. Review of the strain profiles presented in Chapter 3 for the infill with the openings confirms the finite element predictions. Furthermore, there is virtually no damage to the coupling beams over the openings as expected in coupled assemblages.

The strain data and crack patterns of the infills with openings do not suggest a large degree of coupling between the two piers. This is due to several factors. First, the assemblages are single story and this limits the amount of axial force induced in the piers due to overturning. The horizontal distance between the centroids of the two piers is relatively small and further limits overturning axial forces. Finally, the stiffness of the coupling beams are of the same order of magnitude as the stiffness of the piers.

### 4.3 Strength

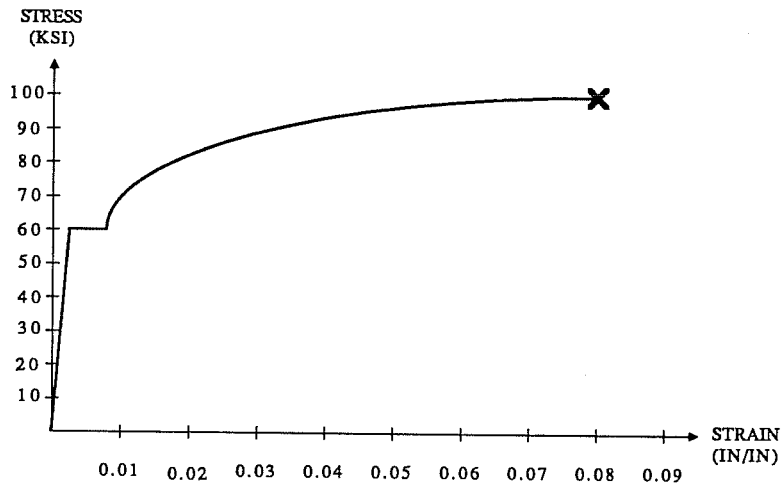
**4.3.1 Comparative Strength and Deformation Capacity of Infills.** In the three specimens tested, failure was brittle. In the full infill and in the infill with the door opening, column splices failed and triggered a tension failure

along the length of the wall. In both of these specimens, significant cracking had occurred prior to failure. In the infill with the window, the infill failed in diagonal tension. Significant cracking occurred in the panel, but there was little evidence of flexural distress.

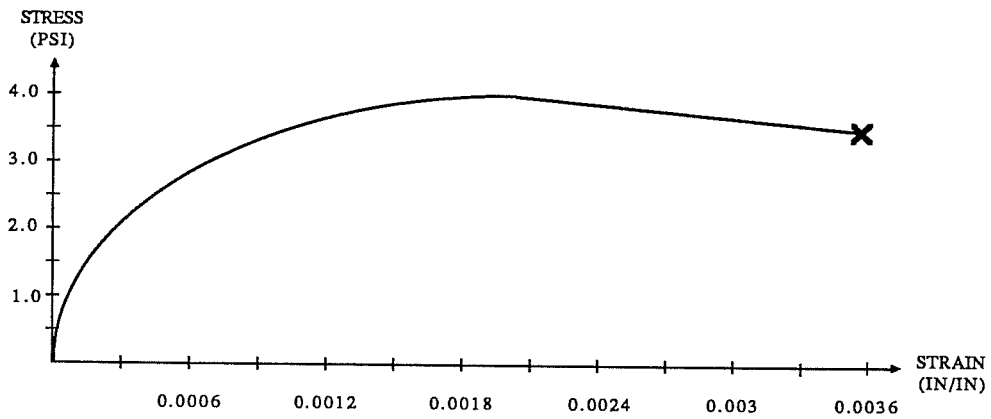
The infills with openings showed greater drift capacity than did the full infill. The full infill had higher load carrying capacity than either of the infills with openings. The infill with the door opening had a higher strength and sustained higher drift levels than the infill with the window. It also exhibited a more ductile failure mode than the infill with the window.

**4.3.2 Flexural Strength.** The flexural capacity of a low rise shear wall may be determined through the use of a moment-axial force interaction diagram. In this procedure, the forces and moments on the section are equilibrated, resulting in an equation with one unknown. The unknown quantity is the depth of the neutral axis. The assumption of linear distribution of strain across the section is made along with assumptions about material stress-strain behavior. The forces on the cracked section are then determined iteratively.

A microcomputer version of the program RCCOLA was used to analyze the various sections. The assumed stress-strain characteristics for the concrete and steel in this section are illustrated in Figure 4.31. The value of moment at zero axial load was chosen as the flexural capacity of the infills. This moment corresponded to a maximum concrete strain of 0.003 in./in. in compression. The value  $V_{M_{ult}}$  is the shear consistent with the development of the flexural capacity and is listed in Table 4.5. Specifically, for the full infill and the infill with the window opening, the value of  $V_{M_{ult}}$  is the flexural capacity divided by the distance between the point of application of load and the base of the wall. For the infill with the door opening, the value of  $V_{M_{ult}}$  is based on the flexural capacities of the pier sections on each side of the door considered as individual wall units. A sidesway mechanism was assumed for the piers. The critical section was at the top of the piers. It is apparent that the shear associated with the flexural capacity of low rise shear walls is very large.



STRESS-STRAIN RELATIONSHIP FOR STEEL REINFORCEMENT



STRESS-STRAIN RELATIONSHIP FOR CONCRETE

Fig. 4.31 Stress-Strain Relationship for Concrete and Steel

**TABLE 4.5**  
**Flexural Strength of Infilled Walls**  
**from Interaction Analyses and Experimental Data**

	Full Infill	Infill With Window	Infill with Door
$V_{M\text{ult}}$	487	487	435
$V_{M\text{y}}^*$	275	275	254
$V_{\text{ult exp}}$	271	198	225
$V_{\text{y exp}}^*$	214	191	80

NOTE: Units are kips

\* first yield in column bars

The capacity at first yield of the section was also calculated to determine the shear associated with development of yield in the spliced column bars. Because the splice was designed for compression only, it was considered unlikely that large inelastic strains could be developed. The moment at first yielding is considerably lower than  $M_{ult}$  and has a correspondingly lower shear associated with it,  $V_{M_y}$ .

The results in Table 4.5 indicate that the calculated flexural capacities were greater than measured values. The difference was greatest in the specimen with the door opening. A general frame analysis was performed taking into account the shear stiffness of the members. The results were not significantly different. Clearly, frame analysis will not provide an adequate means for assessing the response of a low rise wall with a door opening to lateral load.

The ratio of the observed yield force and the theoretical yield force for the infill with the window opening and the full infill were 0.70 and 0.77 respectively. The results of the strength analysis are not greatly affected by the material properties such as the concrete stress-strain characteristics assumed. The post elastic stress-strain characteristics of the reinforcing steel had only a slight affect on the calculated strength. The differences between experimental and theoretical strengths indicate that the use of the moment-axial force interaction techniques for these low rise reinforced concrete infilled walls is not justified.

**4.3.3 Shear Strength.** The measured maximum shears are listed in Table 4.6. The maximum shears for the full infill and the infill with the door are not indications of the shear capacity of those specimens, but rather, the strength of the column splice. Four methods were used to evaluate the shear capacity of the infilled walls. In one method, the shear capacity of the full infill was determined and the strength of the infills with openings were assumed to be in the same proportion as the relative stiffness of the infill with respect to the full infill. The relative stiffness was calculated as the ratio of stiffness of the infill with the opening to the stiffness of the full infill. Classical methods assuming coupled behavior were assumed as discussed in the previous section on linear elastic behavior. Current provisions in Appendix A of ACI 318-86, Building Code



**TABLE 4.6**  
**Shear Strength Predictions and Experimental Values**

	Full Infill	Infill With Window	Infill With Door
$f'_c$	3200 psi	3600 psi	3400 psi
Experimental Value	271 [303]	198 [209]	225 [244]
Relative Rigidity	319 (303)	223 (215)	182 (178)
ACI Shear Provisions	319 (303)	207 (200)	238 (233)
AIJ Provisions	156 (152)	101 (107)	96 (99)
Combined Reduction	319 (303)	207 (200)	197 (192)

( ) values for measured concrete strengths

[ ] measured strength normalized by  $\sqrt{\frac{4000}{f'_c}}$

NOTE: Units are kips

Requirements for Reinforced Concrete, limit the maximum concrete contribution to shear capacity on the basis of the aspect ratio of the wall. Specifically, the shear capacity of a wall with an aspect ratio of less than 2 is calculated as:

$$V_n = A_{cv} \cdot \left( \alpha_c \cdot \sqrt{f'_c} + \rho_n f_y \right)$$

where,

$A_{cv}$  = net section area

$\rho_n$  = ratio of steel area to  $A_{cv}$

$f_y$  = yield strength of reinforcement

$\alpha_c$  = 3.0 for aspect ratios of 1.5 or less

The results of this analysis are presented in Table 4.6 under the heading of “relative rigidity” based on nominal and actual concrete strengths. The actual strength is listed in parenthesis next to the nominal value.

The procedure wherein the shear capacity of the infills with openings was determined by its relative rigidity with respect to the full infill was does not appear to be appropriate for the tests reported here.

In the second method, the strength of the infills with openings was assumed to be limited by the strength of the piers located on each side of the opening. The strength of that pier was calculated using Appendix A of ACI 318-86, Building Code Requirements for Reinforced Concrete, and resulted in the same nominal stresses as were used for the full infill, although the aspect ratio of the pier rather than the aspect ratio of the entire wall, was used to compute the coefficient of the concrete contribution. The results of this analysis are presented in Table 4.6 under the heading of ACI Shear Provisions for both nominal and actual concrete strengths. Listed in parenthesis next to the nominal capacity using this method is the capacity using the measured concrete strength.

The value of the shear capacity calculated using ACI shear provisions based on the pier sections was reached in test of the infill with the window. The

extent of degradation as indicated by the load-deflection response near failure of the full infill at failure indicates that it probably would have been able to carry the additional shear required to develop at the nominal shear capacity had the splice not governed the failure. The load-deflection response of the infill with the door indicated that it also probably would not have failed in shear before reaching the computed strength using actual material properties. The maximum applied load applied to each of the specimens corresponded to an average shear stress on the net area (excluding openings) of  $5.5\sqrt{f'_c}$  (0.32 ksi) irrespective of the failure mode. The ACI shear provisions are conservative and quite reliable for estimating the capacity of infilled walls.

The third technique used to evaluate the shear capacity of the infills with openings was taken from the Architectural Institute of Japan Standard for Structural Calculation of Reinforced Concrete Structures, 1979. In this method, the shear capacity of an equivalent infill with no openings is determined and then reduced by a factor that relates the geometry of the opening to the geometry of the wall. The shear capacity of the full infill is governed by the larger of the following equations:

$$Q_1 = r \cdot t \cdot l \cdot f_s$$

and

$$Q_2 = r \cdot (Q_w + \sum Q_c)$$

where,

$r$  = reduction factor that is the smaller value of

$$r_1 = 1 - l_o/l$$

and

$$r_2 = 1 - \sqrt{\frac{(h_o \cdot l_o)}{(h \cdot l)}}$$

The quantity,  $f_s$ , is a temporary allowable concrete stress that is the allowable permanent concrete stress magnified by a factor of 1.5. Specifically,  $f_s$  is the smaller of:

$$1.5 \cdot F_c / 30$$

and

$$1.5 (5 + F_c / 100)$$

The geometric variables are illustrated in Figure 4.32. The quantity,  $Q_1$ , is a capacity based entirely on concrete strength. The capacity,  $Q_2$ , is the sum of the shear strength of the wall and the sum of the strength of boundary columns reduced by the governing reduction factor. The capacity of the wall is based solely on a steel contribution and neglects any concrete contribution to strength. The capacity of the boundary columns consists of contributions due to both concrete and steel. Specifically,

$$Q_w = \rho_s \cdot t \cdot l' \cdot f_t$$

where

$$\rho_s = A_s / (b \cdot s)$$

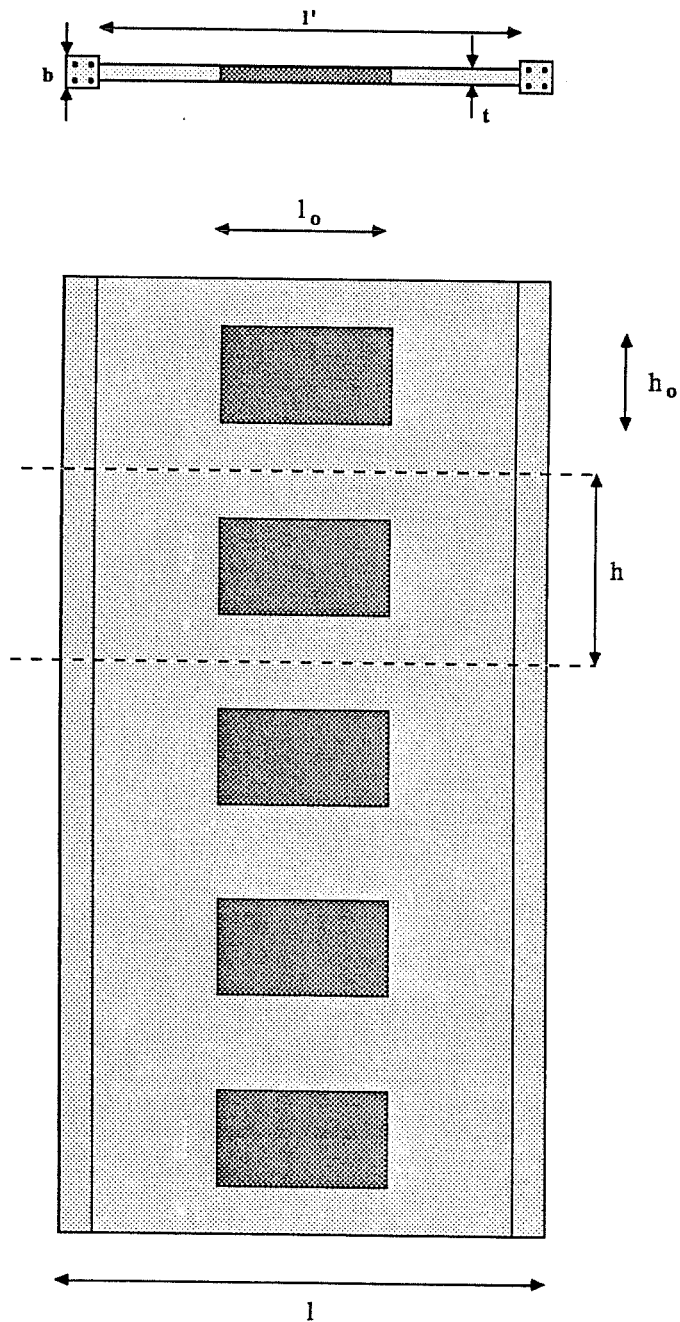
$A_s$  = area of orthogonal steel.

$s$  = spacing of orthogonal steel.

$f_t$  = allowable tensile stress of the reinforcement.

The geometric parameters are illustrated in Figure 4.32. The capacity of the boundary columns is described by:

$$Q_c = b \cdot j \left( 1.5 f_s + 0.5 f_t (\rho_w - 0.002) \right)$$



GEOMETRIC PARAMETERS FOR  
AIJ STANDARDS

Fig. 4.32 Geometric Parameters for AIJ Standard

where,

$$j = 7/8 \cdot d$$

$f_c$  = the temporary allowable stress in the concrete

$f_t$  = the temporary allowable stress in the ties

$d$  = the effective depth of the column

$$\rho_w = A_w / (b \cdot s)$$

$A_w$  = area of tie steel in a spacing,  $s$

The units in these equations are kg and cm. The analysis was performed using nominal and actual concrete properties and the results are listed in Table 4.6 under AIJ Provisions. The strength based on actual material strengths are listed in parenthesis next to the nominal capacity. The temporary allowable stresses for reinforcement is generally the yield strength of shear reinforcement, although an upper limit of 3000 kg/cm<sup>2</sup> is prescribed in the AIJ document. This value was used in the both the nominal analysis and the "actual" analysis although Grade 60 steel is considerably stronger than that. The AIJ standard limits the value of the reduction factor,  $r_2$  to be greater than or equal to 0.60 by limiting the area ratio. Both reinforcement ratios are also limited to 1.2% in the analysis.

The results indicate that the larger strength is predicted by  $Q_2$  and so, governs the strength for all of the test specimens. The predicted ultimate load using the AIJ standard is approximately 50% of the experimental ultimate exhibited by the infill with the window. Shear capacities predicted for both the full infill and the infill with the door opening are less than the AIJ values by a similar margin. The shear capacities as predicted by the AIJ standard result in average shear stresses on the net section of  $3\sqrt{f'c}$  at ultimate for the full infill and  $2\sqrt{f'c}$  for the infills with openings. The strength predicted by  $Q_1$  is much lower than the value of  $Q_2$  and is less than the shear capacity by an even larger margin. The AIJ predictions are very conservative.

The fourth technique used to predict the shear strength of shear walls with openings was based on the combined recommendations of the Architectural Institute of Japan and the American Concrete Institute. In this technique, the strength of the full infill was computed using the above mentioned ACI recommendations. The shear capacity of the infills with openings was then calculated as the capacity of the full infill reduced by the same reduction factor used in the AIJ method above. The results are tabulated in Table 4.5 under the heading of Combined Reduction Factor method. The actual value in parenthesis is the shear capacity of the full infill using the concrete strength of the respective infill reduced by the correct reduction factor.

The Combined Reduction Factor method most accurately estimates the strength of the infill with the window opening. However, the method proves to be conservative for the infill with the door opening. The combined reduction factor method and ACI approach are exactly the same for the infill with the window because the reduction factor,  $r_1$ , is equivalent to the net area of the piers. The reduction factor for the infill with the door,  $r_2$ , does not relate directly to net area. As discussed in Chapter 1, the research on which this is based consisted of tests of [27] three story shear walls with window openings of various sizes. Thus, this reduction factor method is applicable to shear walls with window openings of various sizes in assemblages of various heights and may be conservatively applied to shear walls with door openings. The source of the differences between AIJ and those calculated using the Combined Reduction Factor method is clearly the strength of the full wall. ACI strength predictions based on the sum of this concrete and steel contributions of a wall (of constant thickness and a length that spans the center to center distance of the columns) is more accurate than the AIJ method. ACI methods appear to be are also more rational than a procedure that uses the sum of the concrete plus steel contribution for the columns and the steel contribution of the wall.

From this analysis, it is clear that in these tests of low rise systems, the effect of the size of an opening in a reinforced concrete infilled shear wall is reflected in the shear strength. The research results reported here concur with previous studies that indicate that the capacity in shear of infills with openings is

determined by the strength of the wide piers opposite the openings [14]. Current ACI methods for determining the shear strength of walls are conservative when applied to the wide piers opposite openings in these infilled walls. From this shear strength evaluation, it can be stated that the accuracy of the ACI prediction of shear strength is more influenced by the configuration of the opening and therefore the piers rather than the size of the opening. Using the combined reduction factor and the relative rigidity methods, the strength of an infill with a centrally located window is more accurately predicted than the strength of a centrally located door. Thus, methods where the shear capacity of an infilled system is determined using a reduction factor based solely on the relative size of the opening without regard for its location may not be accurate and may be unconservative in some cases.

**4.3.4 Anchorage of Reinforcement.** The length of the splice in the vertical reinforcement in the column was dictated by provisions in the 1955 edition of the Uniform Building Code. Splice lengths were a function of the working stress of the bar and were specified in terms of the diameter of the bar for a minimum concrete strength of 3000 psi. The resulting length of the lap splice was 24 bar diameters or 21 inches. The current requirements for a tension lap splice are approximately 39 inches. The length of the splice provided was 54% of current requirements.

The deficient splice provided sufficient anchorage to enable the reinforcement to yield, however, the column in the splice region showed signs of distress at roughly 75% of the yield strain. The compression splice developed the strength of the bar in tension but was unable to allow any significant inelastic strain to develop. Horizontal and vertical cracking in the columns was concentrated in the bottom 2 ft. of the column which further reduced bond at that location. The largest bar strain recorded was in one extreme column bar and was in excess of 0.013 in./in. which represented roughly 30% of the fracture strain of the material. The maximum bar strains in the extreme column bars were generally about 0.007 in./in.



It is clear from the results obtained in tests of the infill with the door and the full infill that in a situation where a deficient splice exists in a column, some provision must be made to avoid the failure of the splice if a brittle failure of the wall is to be avoided. When the vertical load carrying capacity of the columns is entirely destroyed, the vertical loads must be transferred entirely to the walls. If the splice is allowed to fail, provision must be made in the retrofit scheme to allow the transition of vertical load to occur without endangering other members of the building and to arrest propagation of the failure plane into the wall. This can be accomplished in several ways. Vertical reinforcement may be placed in the infill wall at the column face to receive the load when the splice fails. This reinforcement must be carefully detailed to prevent buckling and the subsequent splitting of the wall. Another retrofit scheme which could be used in conjunction with infilling is column encasement. In this case, the existing columns are jacketed with a sufficient amount of well anchored longitudinal steel and confined with closely spaced ties. In this manner, anchorage failure may be avoided.

#### **4.4 Strength of Low Rise Infilled Systems with Openings**

The evidence obtained from the experimental investigation of infills with openings in conjunction with the finite element and strength analyses suggest that bending of the piers does not govern the strength of low rise assemblages. The walls with openings do not appear to behave as coupled systems either, in spite of the high degree of coupling predicted. The frame analysis performed for the infill with the door used in conjunction with the flexural strength analysis does not predict the yield point accurately and is unconservative. Research suggests that bending behavior occurs and can be accurately predicted in pierced shear wall systems with a larger aspect ratio. Clearly, the single most influential parameter for determining elastic and cracked behavior and strength of these infills is the aspect ratio of the system.

The infilling techniques employed in the design and construction of these specimens provided an adequate, but not absolute means for interface shear transfer between the existing bounding frame and the new shear walls.

Crack patterns in the infill indicated the formation of large, well distributed compression struts, the orientation of which are dependent upon the configuration of the opening or upon the aspect ratio of the solid wall. Cracking in the columns consisted primarily of horizontal cracks that formed on the upload side of the specimen. Thus, the upload column acts essentially as the tension tie for the strut that forms along the diagonal. The orientation of the struts varies the most on the upload side of the specimen, seeking the most efficient orientation for transfer of the horizontal loads. In the earliest load stages, the struts tended toward the horizontal and inclined to the vertical as damage progressed (see figures in Chapter 3). The more vertical the orientation of the strut, the larger the strut force must be to transfer the same horizontal load. The damage to the specimen is more extensive on the upload side of the specimen, indicating that the upload side of the specimen receives a majority of the applied shear. This concentration of shear on the upload side of the specimen is coherent in the light of the mechanisms that form on the download end of the specimen as indicated by the strain profiles at the base of the wall. On the download side of the specimen, many of the struts span between the top of the opening and the bottom, download corner of the wall. The vertical trim steel in the opening acts as the tension tie for the struts that form on the download side of the specimen. The download column bends independently of the infilled wall section. The combination of strut formation in the wall and bending in the column forms a less efficient mechanism for shear transfer than is realized in the upload side of the specimen.

The analysis technique to determine the strength of a low rise infilled wall with openings suggested by this research is one that is based on a strut and tie concept. In this model, concrete struts form in the piers of the infill walls at orientations are governed by the size and location of the opening. Figure 4.33 illustrates the orientations that are suggested by the crack patterns in the infills with openings. The geometry of the piers suggests that the vertical and panel trim steel will work most efficiently to provide tie forces for struts in the download pier in the infill with the door opening. The struts in the infill with the window may be efficiently tied by vertical or horizontal trim steel, as the strut

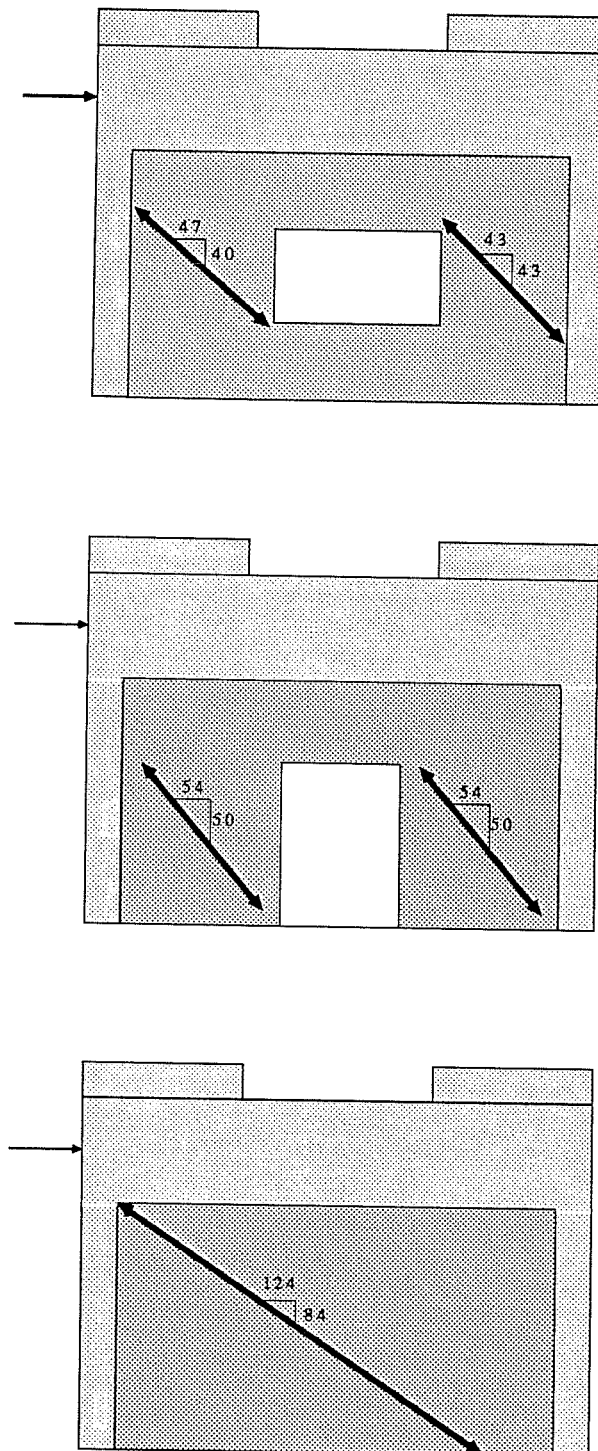


Fig. 4.33 Strut Models for Infills

inclination is approximately  $45^\circ$ . These observations are supported by strain data taken from the trim steel. The tie forces are provided solely by longitudinal reinforcement in the bounding frame members and by the trim steel in the infill near the opening. In other words, a cracked section is assumed. The tie force required at a node is determined from equilibrium. Unequal load sharing between the upload and download piers may be investigated using this method.

**4.4.1 Strength Analysis Using the Strut Model.** The method was used to predict the initial yield of the two extreme column longitudinal bars and another point near ultimate for the infills with openings. In the following analysis, a load stage was chosen either at initial yielding of the column bars or near ultimate. The strains in the four column longitudinal bars were extracted along with strains in the relevant trim bars. Strain data was taken from the base of the column for the upload pier tie force. Strains in the horizontal trim steel were taken from a download corner of the opening. The force in each bar was determined and the tie force,  $T$ , in the upload and download piers was established using the column and trim bars, respectively. From strut equilibrium, the horizontal force associated with the tie force,  $H$ , was determined. For example, in the upload pier of the infill with the door, the horizontal force is (refer to Figure 4.33)

$$H_U = \left(\frac{54}{50}\right)T_U$$

In the download pier, the horizontal force is

$$H_D = \left(\frac{54}{50}\right)T_D$$

The sum of these horizontal pier forces,  $H_T$ , is compared to the total measured force applied to the specimen. For the infill with the window opening, the horizontal pier forces in the upload pier are described by

$$H_U = \frac{47}{40}T_U$$

The horizontal force in the download pier tied by vertical trim steel is

$$H_D = \frac{43}{43} T_D$$

The total horizontal force is

$$H_T = H_U + H_D$$

The technique outlined above was applied to all of the test specimens. For the full infill, the upload column was the only tie for the strut that spanned the diagonal. In the infill with the door the vertical trim steel formed the tie on the download end of the specimen. Strains in the infill with the window indicate the download tie force was formed by the vertical trim steel under positive load and the horizontal trim steel under negative load. The equilibrium of a strut is illustrated in Figure 1.2.

The results of this analysis are presented in Table 4.7.  $H_{exp}$  is the actual applied load. %U and %D are the ratios of  $H_U/H_T$  and  $H_D/H_T$ , respectively. This method closely estimates the various strengths of the infills with openings. The strength of the infill with the door is overestimated by the method. The source of the difference is that several of the vertical panel bars act as ties for struts instead of the larger trim bars. The method more closely predicts the strength of the infill with the window and the full infill. The predicted strength of the full infill is less than the actual strength because other smaller struts act as well as the main one. The contribution of the smaller struts is neglected in this method.

The values of %U and %D reveal that in both the infills with openings, the upload pier is estimated to carry approximately 75% of the applied shear. The download pier is predicted to carry nearly 25% of the applied force. The unequal load sharing has significance for shear design of walls. The individual piers should be designed to handle at least 75% of the applied load. Both piers

**TABLE 4.7**  
**Strength Analysis Using Strut Model**

	Full		Door		Window	
	First Yield	Near Ult.	First Yield	Near Ult	First Yield	Near Ult
$T_U$	133	140	70	144	128	132
$H_u$	196	207	76	156	148	152
$T_D$	—	—	19‡	44‡	53*	40‡
$H_D$	—	207	20	48	53	40
$H_T$	196	236	96	204	201	192
$H_{exp}$	212	—	80	190	188	198
%U	—	—	79	76	74	79
%D	—	—	21	24	26	21

\* Based on horizontal trim bar strains

‡ Based on vertical trim bar strains

NOTE: Forces are in kip units

should be assumed to handle this proportion of the applied load because of load reversal.

If lateral forces in the download pier are tied with horizontal trim steel as in the negative direction for the infill with the window opening, piers should be designed to carry 100% of the applied load in each pier at ultimate. From equilibrium, the force in the horizontal trim bar winds up in the upload pier, as illustrated in Figure 4.34. This phenomenon was clearly illustrated in the failure of the infill with the window under negative load. The failure plane in the upload wall segment under negative load opened near the end of the anchorage zone of the horizontal trim bar (see Figure 3.43) where the horizontal force was transferred to the upload pier.

**4.4.2 Design Techniques Using the Strut Model.** This analysis was applied to the infills with openings required to develop the ACI strength of the panel in shear. The shear capacity of the infill was the horizontal load applied. The tie forces required to equilibrate the vertical component of the strut force that must develop to carry the shear capacity were calculated. The upload pier was assumed to carry 75% of the applied load in the infill with the door and 100% in the infill with the window. The required area of steel was determined assuming 60 ksi steel. The strut orientations are pictured in Figure 4.33. Specifically, for the infill with the door, the column tie force is

$$0.75 \cdot 238 \cdot \frac{50}{54} = 165 \text{ kips}$$

The required steel area is

$$\frac{165}{60} = 2.75 \text{ in.}^2$$

which is 5 - #7 bars. the original design called for 4 - #7 bars and so the increase is moderate. The tie force provided by the vertical trim steel is

$$0.25 \cdot 238 \cdot \frac{50}{54} = 55 \text{ kips}$$

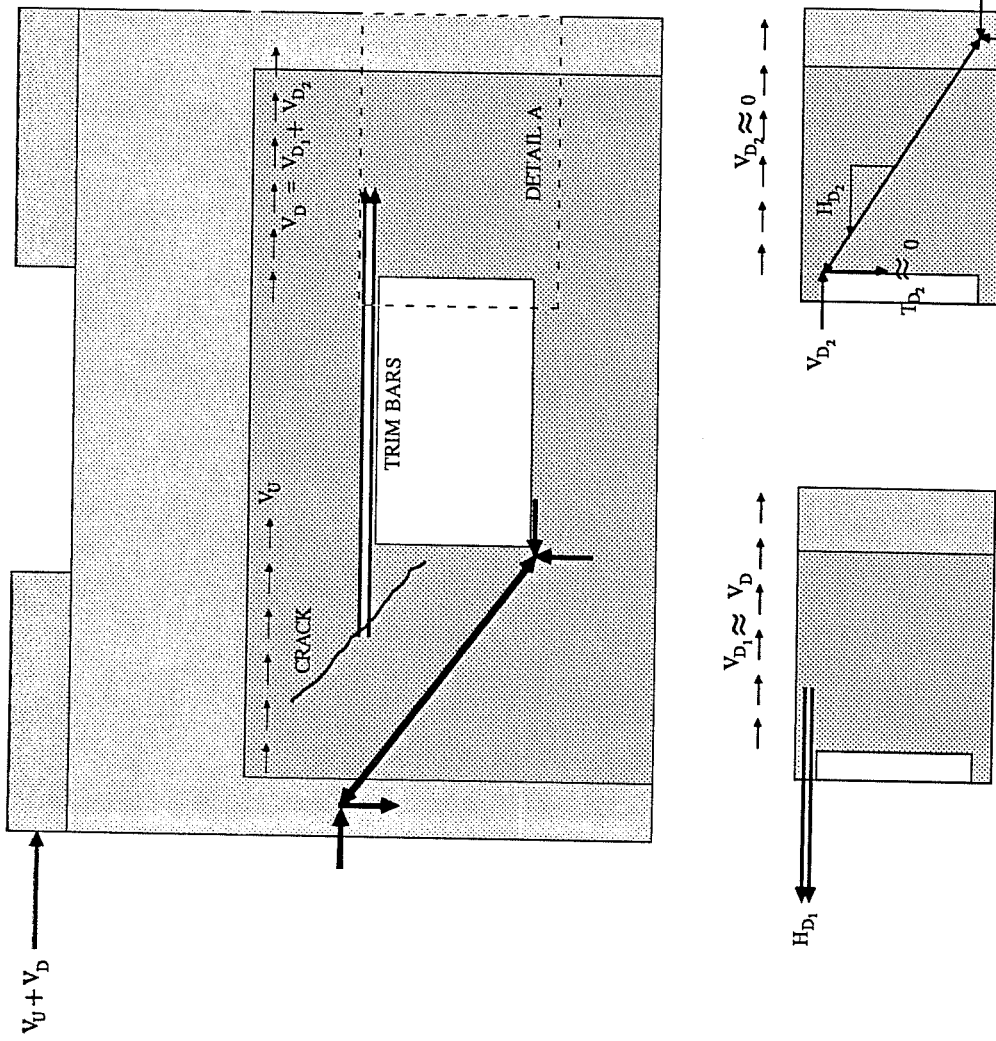


Fig. 4.34 Download Pier Mechanism, Infill with Window



which requires

$$\frac{55}{60} = 0.92 \text{ in.}^2$$

which is essentially provided by the 2 - #6 bars called for in the wall design. The horizontal trim bars are designed to transfer the horizontal force assigned to the download pier, specifically,

$$0.25 \cdot 238 = 60 \text{ kips}$$

which requires

$$\frac{60}{60} = 0.99 \text{ in.}^2$$

This may be provided by 3 - #5 bars and is a moderate increase over the 2 - #5 bars provided. The column tie force for the infill with the window is

$$1.00 \cdot 207 \cdot \frac{40}{47} = 176 \text{ kips}$$

The required area of steel is

$$\frac{176}{60} = 2.9 \text{ in.}^2$$

which requires 7 - #7 bars. This is a fairly significant increase over the amount of steel provided. The horizontal and vertical trim steel was based on 25% of the applied load. Specifically, for vertical steel, the tie force is

$$.25 \cdot 207 \cdot \frac{43}{43} = 52 \text{ kips}$$

which required an area of steel of

$$\frac{52}{60} = .86 \text{ in.}^2$$

which is provided by the 2 - #6 bars in the original design. For horizontal steel, the tie force is the shear in the download pier or

$$.25 \cdot 207 = 52 \text{ kips}$$

which is also provided by the 2 - #6 bars in the original design.

The results of the design indicate moderate increases in the column steel are necessary. The trim steel provided is nearly adequate. The most significant difference is reflected in the higher shear demand on the individual piers. Using the ACI techniques described previously for nominal concrete strengths, the spacing of reinforcement required is four inches for the infill with the window and six inches for the infill with the door. The contribution from the concrete was unchanged. The reinforcement was assumed to pick up the additional shear. The size of the bars was #4 bars, the same size used in the test specimens. Thus, 2 and 3 times the amount of reinforcement is required for shear ( $s = 12$  in. in the test specimens) using this model.

**4.4.3 Conclusions.** For infills with openings where the aspect ratio of the pier is greater than 1, longitudinal steel in the bounding frame members should be able to provide enough tie force at every section along the vertical length to carry at least 75% of the applied shear in the upload column at a strut orientation of approximately 45°. Vertical and horizontal trim steel around the openings may be conservatively designed to provide a tie force for 25% of the applied shear. For infills where the aspect ratio of the piers is 1 or less, the column tie forces should be based on 100% of the applied lateral load. The trim steel may be designed to carry 25% of the lateral load. A strut orientation of 45° is also close to the observed inclinations and may be used for these piers. Accordingly, the shear capacity of the infill should be based on current ACI specifications for walls. The above mentioned technique implies that each pier

should be designed to carry the proportion of the applied shear that is assigned to it.

In new construction of low rise shear walls with openings, the tie steel should be placed in a tighter grouping than the 10 in. square grid that was available in the columns of the bounding frame. In this manner, the strength of the tie may be more accurately assessed. In the case of retrofit construction, it is probably best to group tie steel in the wall at the column face, irrespective of the anchorage of the existing column steel. This is a means of more clearly providing adequate steel where it is needed and reduces uncertainty. Clearly, more research is needed on this topic to determine precisely the effect of a wide grouping of tie steel on ultimate strength.

The strut and tie analysis provided a more rational method for determining the strength of low rise infilled assemblages studied. It resulted in higher requirements for panel and boundary steel in some cases.

## CHAPTER 5

### SUMMARY, CONCLUSIONS AND RECOMMENDATIONS

#### 5.1 Summary

This research program was undertaken to investigate the performance of infilled reinforced concrete shear walls with openings subjected to earthquake ground motions. The detailing and retrofitting techniques were of particular interest. To that end, three large scale reinforced concrete shear walls with openings were constructed using current retrofitting methods and with weaknesses inherent in construction of the 1950's. One infill had a window opening, one infill had a door opening and one infill was constructed without openings for comparison. The specimens were subjected to in-plane lateral reversed cyclic loads. Failure of two models was governed by deficient anchorage of the longitudinal steel in the columns, a detail typical of the construction of the 1950's. The third specimen failed in diagonal tension at a load predicted by ACI specifications.

#### 5.2 Conclusions and Recommendations

The conclusions and recommendations drawn from this research are grouped here into four major categories; behavior, construction techniques, details and design procedures.

##### *5.2.1 Behavior of Shear Walls.*

- 1) The behavior of shear walls with openings is governed by the aspect ratio of the system.
- 2) Low rise shear walls with openings formed compression struts in the piers located on either side of the openings and the piers do not bend near ultimate.
- 3) The effect of the size of an opening was reflected in the strength of the system.

- 4) The configuration of the opening represented a greater influence on stiffness and strength than does size of the opening.
- 5) The dowelling technique employed here was adequate to transfer the applied shear across the joint between the bounding frame and the infilled wall. The behavior obtained from these specimens was nearly the behavior predicted by the finite element study for a monolithically cast specimen.
- 6) Unequal load sharing occurred between the upload and download piers. This resulted in higher shear demands on piers than currently assumed.

#### *5.2.2 Construction of Reinforced Concrete Infilled Shear Walls*

- 1) The use of shotcrete was an efficient method of construction.
- 2) Some difficulty was observed because the shotcrete slumped and resulted in large voids and wide cracks along horizontal surfaces.
- 3) Epoxy injection and patching with epoxy grout were very effective repairs for filling the voids after shotcreting. The performance of repaired areas was excellent under reversed cyclic loads.
- 4) Rather extensive thermal cracking in the shotcrete was observed prior to testing.

#### *5.2.3 Detailing of Shear Walls*

- 1) The columns with deficient anchorages failed in a brittle manner. Such must be compensated for in the design of a retrofit structure.
- 2) Compression splices designed using 1950's standards developed the yield strength of reinforcement in tension, but displayed no significant ductility.
- 3) Vertical trim steel must be confined to be effective. Small bars should be used for trim steel.

- 4) Horizontal trim steel placed around openings created a plane of weakness in the concrete wall. If horizontal trim steel crossed the path of a compression strut, the area degraded rapidly under cyclic shear. An attempt should be made to anchor the horizontal reinforcement in locations that are far away from the paths of compression struts.
- 5) Providing ample space between formwork and reinforcement is recommended to improve shotcrete consolidation, particularly for trim steel around openings. One curtain of reinforcement is also recommended for shotcrete construction.

#### *5.2.4 Design Procedures for Infilled Shear Walls with Openings*

- 1) Flexural strength analysis techniques did not accurately predict the strength of these low rise infilled systems with openings and were unconservative.
- 2) Frame analyses were not suitable for the analysis of the shear walls with openings.
- 3) ACI specifications for the shear strength of walls accurately predicted the strength of the walls with openings when the strength was based on the weak section (i.e., the shear area of a full infill less the area of the openings).
- 4) The yield strength of shear walls with door openings was more accurately predicted by a strut model. The strut model conservatively estimated the yield strength of shear walls with openings.
- 5) The secant stiffness of infills with openings was less than 20% of the theoretical stiffness of a plain concrete infill with no openings.
- 6) Simple finite element models accurately predicted the strain distributions in shear walls with openings.

### **5.3 Research Recommendations**

There are several areas that need further investigation. They include the following:

- 1) Ductile details must be developed for confinement of trim steel.
- 2) Alternate force paths must be provided in shear walls with deficient anchorages in the boundary elements.
- 3) The phenomenon of independent downwind column bending bears further investigation to determine what can be done to produce more efficient composite action in the downwind pier.
- 4) If independent leeward column bending is characteristic of infilled systems and cannot be eliminated, its role in a more ductile ultimate limit state must be clarified.

## REFERENCES

1. L.F. Kahn, "Reinforced Concrete Walls for Aseismic Strengthening," unpublished Master's thesis, University of Michigan, January, 1976.
2. W.J. Goodsir, T. Paulay, A.J. Carr, "A Design Procedure for Interacting Wall-Frame Structures Under Seismic Actions," *Eighth World Conference on Earthquake Engineering*, San Francisco, 1984, Vol. 5, pp. 621-628.
3. V.V. Bertero, "State of the Art and Practice in Seismic Resistant Design of Reinforced Concrete Frame-Wall Structural Systems," *Eighth World Conference on Earthquake Engineering*, San Francisco, 1984, Vol. 5, pp. 613-620.
4. F.R. Khan, J.A. Sbarounis, "Interaction of Shear Walls and Frames," *Journal of the Structural Division*, ASCE, Vol. 90, No. ST3, June 1964, pp. 285-335.
5. American Concrete Institute, Committee 442, "Response of Buildings to Lateral Load," *ACI Manual of Concrete Practice*, Part 4, American Concrete Institute, Detroit, Michigan, 1987.
6. R. Park, T. Paulay, "Shear Walls of Multistory Buildings," *Reinforced Concrete Structures*, John Wiley and Sons, New York, 1975, pp. 610-662.
7. J.R. Benjamin, H.A. Williams, "The Behavior of One-Story Reinforced Concrete Shear Walls," *Journal of the Structural Division*, ASCE, Vol. 83, No. ST3, May 1957, pp. 1254-1 through 1254-49.
8. American Concrete Institute, Committee 318, *Building Code Requirements for Reinforced Concrete (ACI 318-83)*, American Concrete Institute, Detroit, Michigan, 1983.
9. T. Paulay, M.J.N. Priestley, A.J. Synge, "Ductility in Earthquake Resisting Squat Shearwalls," *ACI Journal*, Vol. X, No. X, July-August 1982, pp. 257-269.



10. T.C. Liauw, "An Effective Structural System Against Earthquakes - Infilled Frames," *Proceedings of the Seventh World Conference on Earthquake Engineering*, Vol. 4, Part 1, Istanbul, Turkey, September, 1980, pp. 481-485.
11. D.V. Mallick, "Infilled Frame Construction in Seismic Regions," *Proceedings of the Seventh World Conference on Earthquake Engineering*, Vol. 4, Part 1, Istanbul, Turkey, September, 1980, pp. 486-492.
12. S. Sugano, M Fujimura, "Aseismic Strengthening of Existing Reinforced Concrete Buildings," *Proceedings of the Seventh World Conference on Earthquake Engineering*, Vol. 4, Part 1, Istanbul, Turkey, September, 1980, pp. 449-456.
13. R.E. Klingner, V.V. Bertero, "Infilled Frames in Earthquake Resistant Construction," EERC 76-32, Earthquake Engineering Research Center, Berkeley, California, December, 1976.
14. J.R. Benjamin, H.A. Williams, "Behavior of One-Story Reinforced Concrete Shear Walls Containing Openings," *ACI Journal*, Vol. 30, No. 5, November, 1958, pp. 605-618.
15. Y. Higashi, T. Endo, Y. Shimizu, "Effects on Behaviors of Reinforced Concrete Frames By Adding Shear Walls," *Proceedings of the Second Seminar on Repair and Retrofit of Structures*, US/Japan Cooperative Earthquake Engineering Research Program, Ann Arbor, Michigan, May, 1981, pp. 265-290.
16. T.C. Liauw, S.W. Lee, "On the Behavior and the Analysis of Multi-story Infilled Frames Subject to Lateral Loading," *Proceedings of the Institution of Civil Engineers*, Part 2, No. 63, September 1977, pp. 657-671.
17. B. Stafford Smith, C. Carter, "A Method of Analysis for Infilled Frames," *Proceedings of the Institution of Civil Engineers*, Vol. 44, September 1969, pp. 31-48.

19. S.V. Polykov, "Some Investigations of the Problem of the Strength of Elements of Buildings Subjected to Horizontal Loads," *Tall Buildings*, Pergamon Press Limited, London, 1967, pp. 465-480.
20. K.N. Shiu, T. Takayanagi, W.G. Corley, "Seismic Behavior of Coupled Wall Systems," *Journal of Structural Engineering*, ASCE, Vol. 110, No. 5, May 1984, pp. 1051-1066.
21. H. Beck, "Contribution to the Analysis of Coupled Shear Walls," *ACI Journal*, Vol. 59, No. 8, August, 1962, pp. 1055-1070.
22. I.A. MacLeod, "Lateral Stiffness of Shear Walls with Openings," *Tall Buildings*, Pergamon Press Limited, London, 1967, pp. 223-244.
23. B.S. Smith, A. Girgis, "Simple Analogous Frames for Shear Wall Analysis," *Journal of Structural Engineering*, ASCE, Vol. 110, No. 11, November 1984, pp. 2655-2666.
24. P. Govindan, M. Lakshmi pathy, A.R. Santhakumar, "Ductility of In-filled Frames," *ACI Journal*, Vol 83, No. 4, July- August, 1986, pp.567-576.
25. D.V. Mallick, R.P. Garg, "Effect of Openings on the Lateral Stiffness of Infilled Frames," *Proceedings of the Institution of Civil Engineers*, Paper No. 7371, Datekernpp. 193-209.
26. F. Braga, M. Dolce, "Earthquake Resistant Design of Shear Walls with Several Rows of Openings," *Eighth World Conference on Earthquake Engineering*, Vol. 5, San Francisco, 1984, pp. 533-540.
27. H. Adachi, N. Shirai, M. Nakanishi, "Experimental Study on Reinforced Concrete Shear Walls With Openings," *Transactions of the Japan Concrete Institute*, Vol. 3, Tokyo, Japan, December, 1981, pp. 407-414.

## VITA

Patricia Jean Gaynor was born in Washington, D.C. on September 18, 1961, the daughter of Margaret Jane Bowers Gaynor and Richard Dana Gaynor. She received her high school diploma from Paint Branch High School, Burtonsville, Maryland, in 1979. She enrolled in the engineering curriculum of Montgomery College, Rockville, Maryland in September, 1980. She entered the College of Engineering at the University of Maryland, College Park in 1982. She graduated from the University of Maryland with a Bachelor of Science in Engineering in December, 1985. She entered the Graduate School of the University of Texas in January of 1986.

Permanent Address: 2433 Countryside Drive  
Colesville, Maryland

This thesis was typed by Patricia Gaynor